DETECTING *O*-GLCNAC AND UNDERSTANDING ITS ROLE IN INSULIN ACTION

by

CHIN FEN TEO

(Under the Direction of Lance Wells)

ABSTRACT

O-linked β-*N*-acetylglucosamine (*O*-GlcNAc) modification is a ubiquitous glycosylation found on the serine and threonine side chains of intracellular proteins. The spatial and temporal distribution of *O*-GlcNAc is orchestrated by a pair of cycling enzymes, *O*-GlcNAc transferase (OGT) and β-*N*-acetylglucosaminidase (OGA), in response to a variety of cellular and environmental stimuli. Given that UDP-GlcNAc, the end product of the hexosamine biosynthetic pathway (HBP), is an obligatory donor substrate of OGT, *O*-GlcNAc is posed as an effector of excessive glucose flux through the HBP which in turn can lead to the development of insulin resistance, a hallmark of type 2 diabetes. In this dissertation, we have studied the impact of *O*-GlcNAc modification on insulin signaling, as well as its implication in the development of insulin resistance. Specifically, given that glucosamine inhibits the anti-apoptotic action of insulin, we wanted to evaluate whether this occurs via an *O*-GlcNAc-dependent mechanism. By comparing different OGA inhibitors to modulate intracellular *O*-GlcNAc levels, I found that increases in global *O*-GlcNAc levels do not correlate with inhibition of the anti-apoptotic action of insulin and demonstrated that PUGNAc, a non-selective but commonly used OGA inhibitor, has off-target effects that influence insulin signaling. We also characterized three pan-*O*-GlcNAc specific monoclonal IgG antibodies using a panel of biochemical and mass-spectrometry (MS) based approaches and identified 215 *O*-GlcNAc modified proteins, 140 of which for the first time. Lastly, I devised a novel

workflow combining metabolic labeling, click chemistry, ammonia-based β-elimination (ABBE) and tandem MS for *O*-GlcNAc site determination. Thus, my work has established novel tools for the study of *O*-GlcNAc and disproved the hypothesis that elevated *O*-GlcNAc levels inhibit the anti-apoptotic action of insulin.

INDEX WORDS: β-*O*-linked *N*-acetylglucosamine (*O*-GlcNAc), OGT, OGA, insulin signaling, hexosamine biosynthetic pathway (HBP), *O*-GlcNAc specific antibodies, ammonia-based β-elimination (ABBE), mass spectrometry (MS)

DETECTING *O*-GLCNAC AND UNDERSTANDING ITS ROLE IN INSULIN ACTION

by

CHIN FEN TEO

B.S., National Taiwan University, Taiwan, 2001

Sc.M., Johns Hopkins University, 2005

A Dissertation Submitted to the Graduate Faculty of The University of Georgia in Partial Fulfillment of the Requirements for the Degree

DOCTOR OF PHILOSOPHY

ATHENS, GEORGIA

2013

DETECTING *O*-GLCNAC AND UNDERSTANDING ITS ROLE IN INSULIN ACTION

by

CHIN FEN TEO

Major Professor:	Lance Wells
Committee:	J. Michael Pierce
	Kelley W. Moremen
	Michael Tiemeyer

Electronic Version Approved:

Maureen Grasso

Dean of the Graduate School

The University of Georgia

August 2013

DEDICATIONS

For Sami, who gives me strength to carry on.

For my parents and siblings, who shapes me into who I am.

ACKNOWLEDGEMENTS

To everyone who has given me helps and hopes over the years, I am deeply indebted to you and sincerely thank you, forever.

TABLE OF CONTENTS

LIST OF TABLES

Page

LIST OF FIGURES

Page

CHAPTER 1

O-GLCNAC BIOLOGY: AN OVERVIEW

1. Introduction

Post-translational modifications (PTMs) on the amino acid side chains are non-template driven mechanisms utilized by biological system to increase the functional diversity of proteins. Of all the PTMs discovered in mammals, glycosylation is by far the most complex [1] because (i) the structural diversity of glycans is created from a combination of several carbohydrate building blocks, linkage positions and anomeric conformations, leading to glycan microheterogeneity, (ii) various amino acids in varying sequence contexts can be chosen for glycosylation, (iii) the site-occupancy of a particular glycosylation site can vary, and (iv) the machinery involved to maintain the glycosylation status spans multiple organelles [2, 3]. Until the early 80s, the field of glycobiology was associated with glycans or glycoconjugates destined to the secretory pathway, since all of the glycoproteins indentified at that point were either membrane-bound or extracellular proteins. Extensive chemical and biochemical studies allowed researchers to categorize most of the glycosylations according to their glycosidic bonds and sugar types into three major types, *N*-linked glycans (added to asparigine residue), *O*-linked glycans (added on mostly serine or threonine residues) or glycosaminoglycans (GAGs, can either exist as free polymers or be bound to serine or threonine of polypeptides), although other of types glycosylations such as *C*-mannosylation (on tryptophan) or glycophosphatidylinositol (GPI anchor, no strict requirement for amino acid residue) also exist [2, 3]. Furthermore, some of the glycans can be further

decorated by acetylation [4], phosphorylation [5] or sulfation [6], which, in turn, expands the complexity of the glycan structures. Dysregulation in either the biosynthesis or degradation of glycans have been linked to genetic and chronic illnesses, including the congenital disorders of glycosylation (CDGs), various cancers, as well as metabolic, neurodegenerative and autoimmune diseases [7, 8]. Glycosylation has also been shown to play an integral part in infectious diseases, since many pathogens, ranging from viruses and bacteria to fungi and parasites, utilize glycans to gain entry into host cells or mimic the glycosylation profiles on the host cells to evade immune response [9-13].

The early central dogma of glycobiology, in which glycans are added only in the secretory pathway and ended up in the extracellular milieu, was challenged and revised via a serendipitous discovery from the Hart group as reported in a series of papers starting from the mid 80s. Using radiolabelled UDP-[^{3}H]galactose and bovine β1,4-galactosyltransferase to probe for terminal GlcNAc-containing complex glycans on the surface proteins of mouse lymphocytes, Torres and Hart detected a population of alkali-sensitive β-*O*-linked *N*-acetylglucosamine monosaccharide (*O*-GlcNAc, Figure 1-1A) that is not only found the cell surface but also curiously resides inside the cells [14]. In follow-up papers, further biochemical evidence revealed that majority of the *O*-GlcNAc modified proteins are indeed localized to nuclear and cytosolic fractions [15] and that the attachment of *O*-GlcNAc is inducible upon T cell activation [16]. Additionally, utilizing pulse-chase experiments selectively labeling αB-crystalline either on the protein backbone ([^{3}H]leucine) or the GlcNAc moiety ([^{3}H]glucosamine), Roquomore *et al.* observed that the turnover of GlcNAc is much faster than that of the degradation of the polypeptide backbone, indicating the dynamic nature of *O*-GlcNAc modification [17]. Collectively, these studies illustrated the non-extended, nucleocytoplasmic, inducible and dynamic features of *O*-GlcNAc modification, that challenged what was known at that time in the field of glycobiology.

In the past three decades, many groups have advanced our knowledge of *O*-GlcNAc modification and its role in the biological systems. We now know that, with the exception of *Saccharomyces cerevisiae*, *O*-GlcNAc is prevalent in eukaryotic organisms and has been reported in many species, from single cellular pathogenic parasites, such as *Plasmodium falciparum* [18] and *Toxoplasma gondii* [19], to multicellular organisms, including nematodes, flies, mammals and plants [20, 21]. Major breakthroughs that contributed to our current understanding of *O*-GlcNAc biology involve (i) identification, characterization and cloning of the *O*-GlcNAc cycling enzymes [22-25]; (ii) animal models with transgenic expression or genetic knockout of the *O*-GlcNAc cycling enzymes [26-33]; (iii) pharmacological inhibitors against the *O*-GlcNAc cycling enzymes to manipulate global *O*-GlcNAc levels [34]; and (iv) ongoing efforts to generate biochemical and analytical tools for *O*-GlcNAc detection and site mapping [35]. Comprehensive structural and biochemical (enzyme kinetics) aspects of OGT and OGA have been reviewed elsewhere [36, 37]. In this chapter, I will provide a brief overview of *O*-GlcNAc biology focusing on major findings and outstanding questions in the *O*-GlcNAc field.

2. The O-GlcNAc cycling enzymes

The regulatory features of *O*-GlcNAc are achieved by a pair of *O*-GlcNAc cycling enzymes, *O*-linked GlcNAc transferase (OGT) and neutral β-*N*-acetyl-glucosaminidase (OGA), for the attachment and removal of the GlcNAc moiety, respectively [Figure 1-1B; Figure A-1]. Unlike complex glycan processing glycosyltransferases and glycoside hydrolases that are often found in the ER, Golgi, lysosomes or the extracellular spaces, *O*-GlcNAc cycling enzymes are residents of the nucleus and cytosol. In all species characterized (except zebrafish and plants), both enzymes are each encoded by a single gene in the whole genome, but present themselves with multiple splice variants. In

human, *ogt* resides on chromosome Xq13.1 [38] and *mgea5*, the gene encoding OGA, is found on chromosome 10q24.1-24.3 [39]. Elevation of OGT mRNA and protein levels in T lymphocytes due to DNA demethylation on the inactivated allele was recently found to be a predisposition for the development of lupus [40]. A single nucleotide polymorphism in the intron 10 of *mgea5*, which introduces an alternate stop codon to produce a truncated OGA isoform, was found by an epidemiology study to be correlated with the risk for type II diabetes in Mexican Americans [41].

Genetic studies focusing on the *O*-GlcNAc cycling enzyme in vertebrates have revealed that they are developmentally crucial. Deletion of *ogt* (*ogt*$^{-/-}$) in mouse is embryonic lethal [42], and mice with tissue-specific *ogt* knockouts display severe developmental and survival defects in each target tissue [32]. On the other hand, deletion of *oga* (*oga*$^{-/-}$) in mouse did not lead to any obvious anatomical abnormalities in embryonic stages, albeit the mutant embryos are smaller in size. However, all the knockout littermates die within one day after birth with a clear histological irregularity in lung suggesting a developmental problem [43]. The involvement of *O*-GlcNAc in the development process was further supported by observations from zebrafish, whereby overexpressing *O*-GlcNAc cycling enzymes or *ogt* knockdown resulted in severe deformation and an increase in apoptosis [44]. In flies, while *oga* null flies has not been reported in the literature, loss of function in the gene encoding Drosophila *ogt*, (dubbed *super sex combs*, or *scx*) showed a defect in embryonic development [45] due to a loss in the master control for transcriptional repression and epigenetic gene silencing [46, 47].

Surprisingly, *Caenorhabditis elegans* lacking either *ogt* or *oga* are viable and fertile. That being said, *ogt*$^{-/-}$ and *oga*$^{-/-}$ nematodes exhibit very distinct and opposing lifespan and stress-induced dauer formation phenotypes [27, 29, 31, 48-50], all of which match with those in mutant worms with various defects in the insulin-like signaling

pathway [51]. Implications of the *O*-GlcNAc cycling enzymes in modulating insulin action are not restricted to *C. elegans*. Transgenic flies with RNAi knockdown of the *O*-GlcNAc cycling enzymes or overexpression of OGT in their insulin-producing cells resulted in flies with altered body sizes (a phenotype associated with mutants with perturbations in the insulin signaling pathway [52]) as well as a gross reduction in the endogenous insulin signaling at the peripheral tissues [26]. Moreover, transgenic mice with muscle and fat overexpressing OGT resulted in whole-body insulin resistance [33], whereas in diabetic mouse models, the insulin resistant phenotypes were remedied by overexpressing OGA in affected tissues [28, 30]. These evidences strongly suggest the involvement of *O*-GlcNAc modification in regulating insulin actions.

OGT (CAZy family GT41) contains an N-terminal tetratricopeptide repeat (TPR)-containing domain and C-terminal glycosyltransferase catalytic domain. In human, alternative splicing leads to the formation of three OGT isoforms with varying number of TPR domains and distinct cellular localization [36]: a full length OGT (nucleocytoplasmic or ncOGT, 13.5 TPRs) is a nuclear and cytosolic protein; a short isoform OGT (sOGT, 3 TPRs) localizes in the cytosol, and a mitochondrial OGT (mOGT, 9 TPRs) as its name implies, is shuttled into the mitochondria. While the mechanisms that OGT utilizes to select or differentiate its acceptor substrates under various cellular conditions *in vivo* remains unclear, the TPR domains are believed to serve as a platform for OGT to engage in substrate binding. To date, direct evidence for the biological impacts of sOGT remain elusive; however, implications that mOGT may play a role in eliciting apoptosis [53, 54] have been made. On the contrary, the bulk of our current knowledge on the biological function of OGT has been gathered from stydying ncOGT [21]. Since many other GlcNAc transferases and OGT share the same donor nucleotide sugar, UDP-GlcNAc, it is a challenge to design a nucleotide sugar analog that selectively inhibits OGT without affecting other types of GlcNAc transferases. In the literature, there are few

reported OGT inhibitors available, but none of them are very potent or show great selectivity towards OGT over other GlcNAc transferases. Thus, none are widely used in the field [55-57].

Similarly, OGA (CAZy family GH84) also contains two major domains: a N-terminal glycoside hydrolase catalytic domain and a C-terminal putative histone acetyltransferase (HAT) domain. These two domains are separated with a stalk region that bears a non-conical caspase-3 cleavage site that is targeted by caspase-3 upon apoptosis, with the cleaved OGA remaining active [58, 59]. Alternative splicing yields two OGA isoforms [36]: full length OGA (OGA-L, the long form) that is predominantly expressed and resides in the cytosol as well as a truncated version that lacks the HAT domain (OGA-S, the short form) and localizes in the nucleus [39]. As for the case with OGT, the current understanding of OGA action is mainly derived from research using full length OGA (OGA-L). Having said that, Keembiyehetty and colleagues recently reported that, in 3T3-L1 adipocytes, OGA-S is associated with lipid droplets and regulates ubiquitinylation-dependent proteasomal degradation [60]. Additionally, whether the C-terminal domain on the OGA-L truly possesses HAT activity as reported by Toleman and colleagues remains an issue of debate in the *O*-GlcNAc field [58, 61, 62]. Unlike the lackluster performance in the *O*-GlcNAc field in hunting for OGT inhibitors, more success have been made for procuring potent OGA inhibitors as OGA utilizes a unique substrate-assisted catalytic mechanism that is strategically distinct from other hexosaminidases [37]. Since the late 90s, administration of OGA inhibitors to elevate global *O*-GlcNAc levels in cell culture models has been a routine practice in the field to gain insights into the biological functions of *O*-GlcNAc. PUGNAc was the first reported and characterized OGA inhibitor in the literature [24, 63] and has been extensively used in the short history of *O*-GlcNAc research. Notably, elevating global *O*-GlcNAc levels with PUGNAc was first implicated in the development of insulin resistance in cultured adipocytes [64],

contributing to the foundation for the *O*-GlcNAc-mediated insulin resistance research. However, upon closer examinations, studies have shown that PUGNAc also inhibits lysosomal hexosaminidases leading to an increase in GM2 gangliosides [65] and an accumulation of free oligosaccharides [66] as results of a disruption of the ganglioside metabolism and incomplete degradation of recycled complex N-glycans, respectively. Equipped with knowledge of OGA's enzymatic mechanism and structural features, tremendous efforts have been invested in for the search of inhibitors with higher selectivity toward OGA over other hexosaminidases [34]. Towards this end, van Aalten's and Vocadlo's groups have independently produced a series of potent and more selective OGA inhibitors with distinct structures (Figure 1-2, Figure A-2 [67-69]). Unexpectedly, when Vocadlo's group used the more selective OGA inhibitors to raise *O*-GlcNAc levels in cell culture and animal models, none of the models developed insulin resistance [65, 70, 71]. The dispute of the impact of *O*-GlcNAc on insulin resistance between PUGNAc and more selective OGA inhibitors has instigated further experimentation that will be further discussed in Chapter 3 of this dissertation. However, given that transgenic animal models with altered *O*-GlcNAc levels clearly demonstrated distinct effects in insulin actions, the molecular mechanisms to explain these discrepancies require further, in-depth investigation.

3. Regulation of the O-GlcNAc cycling enzymes

Collectively, *O*-GlcNAc modification and the cycling enzymes have been implicated in a vast number of signaling networks that modulate a variety of cellular processes. During the infancy of *O*-GlcNAc research, many groups reported nucleopore complexes [72, 73] and transcription factors [74, 75] along with RNA polymerase II (RNA pol II, [76, 77]) as *O*-GlcNAc proteins, suggesting the role of *O*-GlcNAc in nuclear protein translocation and transcriptional controls. In the late 90s, following the discovery of the

relationship between excessive hexosamine flux and insulin resistance [78] as well as the cloning of the *O*-GlcNAc cycling enzymes [22, 23], *O*-GlcNAc research started to branch into biomedical science, focusing on diabetes [28, 30, 33, 64], Alzheimer's diseases [79-81] and cancers [82-85]. In recent years, *O*-GlcNAc has been found to be an important regulator in epigenetic/chromatin remodeling [86-90], circadian clock [91, 92], neuronal signaling [93, 94] and embryonic stem cell pluripotency and reprogramming [95-98].

As partners in mediating protein PTM, the *O*-GlcNAc cycling enzymes are also subjected to many PTMs. When OGT was first purified from the rat liver, it was found to be capable of autoglycosylation and also to be tyrosine phosphorylated [23]. To date, one *O*-GlcNAc site (Thr1043) has been mapped on OGT [99] with an additional known but unassigned glycosylated site on the ninth TPR domain [100]. However, the biological impact of these self-glycosylation events remains unknown. There is one putative receptor tyrosine kinase site (Tyr989) on OGT sequence, but no concrete evidence shows that this site is indeed phosphorylated. Whelan *et al.* established that, in 3T3-L1 adipocytes, tyrosine phosphorylation on OGT depends on insulin stimulation, which in turn correlated with an increase in OGT enzymatic activity as well as a switch in its subcellular localization from the nucleus to the cytosol [101]. Whether the insulin-induced phosphorylation site occurs on Tyr989 and is responsible for modulating the insulin signaling network remains unclear. Interestingly, tyrosine-phosphorylation is not the only PTM reported to be associated with an increase in OGT activity; during neuronal depolarization, OGT was phosphorylated by calmodulin-dependent protein kinase IV (CaMKIV) and showed an increase in its enzymatic activity [102]. In resting macrophages, OGT is decorated with *S*-nitrosylation on cysteine residue(s), and, upon lipopolysaccharide (LPS) stimulation, OGT was denitrosylated accompanying by an increase in its enzymatic activity [103]. While these reports provided a glimpse of

functional switches in OGT, many questions remain unanswered: How does the addition or removal of a particular PTM lead to the change in the kinetic parameters of OGT? Does OGT with different PTM stage engage a different set of interacting partner, which in turn act toward a distinct group of substrates? Is the specific modification on OGT a cell- or tissue-type specific phenomenon? In contrast to aforementioned examples, additional PTMs are mapped on OGT without any hint of biological information. For instance, OGT is phosphorylated at Tyr976 in human embryonic stem cells [104]. Additionally, phosphorylation on Ser20 and Thr325 is found on OGT during mitosis [105]. Since OGT not only plays an essential role in maintaining a normal chromatin structure during the mitotic state [89], but also forms a protein complex with OGA and additional signaling proteins during mitosis [106], it would be interesting to investigate whether phospho-Ser20 and phospho-Thr325 contribute to the regulatory role of OGT during this process.

OGA is also an *O*-GlcNAc modified and a Ser/Thr phosphorylated protein. The *O*-GlcNAc site on OGA is mapped to Ser405 in the presence of its own inhibitor, PUGNAc [107]. Given that pharmacologically inhibiting OGA *in vivo* elevates not only global *O*-GlcNAc levels but also OGA protein level (Figure A-2), one can imagine a feedback mechanism utilized by the cycling enzymes on each other in attempt to maintain a balance in global *O*-GlcNAc levels. To date, three phosphorylation sites, namely Ser268, Ser364 and Thr370, have been found on OGA, but their biological significance has yet to be unveiled. Phospho-Ser268 was found in human embryonic stem cells [104] and phospho-Thr370 was mapped in lung cancer cell line [108]. Phosphorylation on Ser364 is particular intriguing, because it has been repeatedly identified in multiple phosphoproteomic studies. In addition to the aforementioned human embryonic stem cells and lung cancer studies, it was also found in phosphoproteomic studies aiming to understand mTOR-mediated nutrient sensing [109], mitosis [105], T

cell receptor signaling [110] and B-Raf signaling [111]. However, in these circumstances, phospho-Ser364 seems to be a static decoration that remains unchanged under the comparative experimentations. Interestingly, the starting material used by Gygi's group in the first report of phospho-Ser364 on OGA was a mixture of nuclear proteins isolated from HeLa cells [112]. Given that OGA is dominantly localized in the cytosol [22, 39], one can postulate that Ser364 phosphorylation on OGA might serve as a nuclear-targeting signal and might play a role for the formation of transcriptional co-repression complexes in estrogen signaling [113] or OGT/OGA signaling complex that is found during mitosis [106].

Recently, several proteomic studies also revealed that many lysine residues on both OGT and OGA are ubiquitinylated [114-116]. Moreover, several of the lysines on OGT are also subjected to SUMOylation [117]. Given that ubiquitin and SUMO are also versatile PTMs that participate in multiple cellular processes, including proteasome degradation, authophagy, subcellular localization, cell cycle and DNA damage controls [118-122], addressing how these small protein modifiers affect *O*-GlcNAc cycling enzyme functions and identifying responsible ubiquitin and SUMO ligases would undoubtedly be important in deciphering *O*-GlcNAc biology. Recently, Dey and colleagues detected the presence of OGT in a large protein complex that is consist of BAP1 (BRAC-1-associated protein 1), HCF-1 (host cell factor-1) and additional chromatin modulators from the polycomb-group (PcG) protein family [123]. BAP-1 is a tumor suppressor with a de-ubiquitinating activity [124]. In the BAP-1 knockout mouse model, a reduction in OGT protein level in conjunction with a drop in global *O*-GlcNAc levels due to destabilization of OGT and a decrease in HCF-1 protein level were observed [123]. Given that OGT was previously found to regulate the proteolytic maturation of HCF-1 and that roughly half of the OGT residing inside the nucleus was found to associate with HCF-1 [125, 126], research focusing on dissecting the interplay

within the BAP1/OGT/HCF1/PcG protein complex could accelerate the process in decoding the multifaceted roles of OGT and *O*-GlcNAc in chromatin remodeling.

4. O-GlcNAc and O-phosphate modification- beyond the "yin-yang" hypothesis

To date, more than 1000 proteins and many more *O*-GlcNAc sites have been reported in the literature (completed list of *O*-GlcNAc modified proteins and site information reported up to year 2010 can be found in dbOGAP [127], an online database. Additional information, see the following large-scale glycoproteome studies by Alfraro *et al.* [99], Trinidad *et al.* [128], and Wang *et al.* [129]). Not surprisingly, all identified glycoproteins are also phosphoproteins given that both PTMs target the same amino acid side chains and occur in the same cellular compartments. Indeed, results built on earlier studies have proposed a "yin-yang" hypothesis to depict the reciprocal relationship between *O*-GlcNAc and *O*-phosphate modifications in which the presence of one modification exclude the another on one particular target protein. One of such classical example is the C-terminal domain (CTD) of the Rpb1, the largest subunit of RNA pol II, on which glycosylation and phosphorylation are found to be in mutual existence both *in vivo* [76] and *in vitro* [130] on the heptapeptide (YSPTSPS) repeats. Indeed, a recent study by Ranuncolo *et al.* further illustrated that the reciprocity of *O*-GlcNAc and *O*-phosphate moieties is essential for RNA pol II to switch from the formation of preinitiation complex to the initiation/elongation modes. Furthermore, the discovery of a functional OGT-protein phosphatase 1 complex also favors the yin-yang model [131].

However, using mass-spectrometry (MS) based approaches to interrogate the interplay between *O*-GlcNAc modification and phosphorylation at the global scale, a more complex regulatory network mediated by both PTMs has been revealed. In the first wave of this revolution, Wang *et al.* quantified a list of *O*-GlcNAc modified proteins upon

the inhibition of glycogen synthase kinase-3 (GSK-3) using a combination of SILAC (stable isotope labeling by amino acids in cell culture)-based MS and immunoaffinity enrichment of *O*-GlcNAc modified proteins [132]. Interestingly, the reduction in GSK-3-dependent phosphorylation resulted in 10 proteins with an increase in their *O*-GlcNAc status and 19 proteins with a decrease in their *O*-GlcNAc levels [132]. While those proteins with elevated *O*-GlcNAc levels upon GSK-3 inhibition supported the notion of reciprocity between both PTMs, the concurrent decrease in both phosphorylation and *O*-GlcNAc modification indicated a deeper layer of regulation. Therefore, the "yin-yang" hypothesis is proven to be an insufficient concept to depict the extensive crosstalk between these PTMs. To further decipher the interconnecting relationships in a more macroscopic scale, Wang *et al.* performed another series of elegant experiments in which they applied iTRAQ (isobaric tags for relative and absolute quantification)-based MS coupled to phosphopeptide enrichment to monitor the site-specific alteration in phosphorylation upon a combination treatments of phosphatases and OGA inhibitors (okadaic acid for phosphatases, whereas PUGNAc and NAG-thiazoline for OGA) to modulate both PTMs globally [133]. In line with their previous observation, increase in global *O*-GlcNAc modification led to not only decreased in 280, but also increased in 148 phosphorylation sites [133], further strengthening the scenario in which both PTMs are participating in complex signaling cross-talk. With the advance of strategies for *O*-GlcNAc modified peptide enrichment and MS-based *O*-GlcNAc site identification, large scale quantitative *O*-GlcNAc- and phospho-proteomes have been performed to examine the dynamic PTM change in cellular processes such as cytokinesis [129] and synaptic signaling [128].

It is noteworthy that, prior to the era of quantitative *O*-GlcNAc- and phospho-proteomics, many studies undertook the traditional route in attempt to understand the functional role of *O*-GlcNAc modification on target proteins [82, 88, 90, 93, 98, 134].

Armed with the current breakthroughs and ongoing efforts to improve techniques for *O*-GlcNAc field, we are now able to test and address new hypotheses at a more global scale before narrowing down onto specific signaling events. For instance, we have observed that blocking the mTOR-mediated nutrient sensing pathway, via rapamycin treatment, results in a reduction of global *O*-GlcNAc levels (Figure A-3). On the other hand, perturbing global nutrient status by inducing glucose deprivation, leads to an elevation in global *O*-GlcNAc levels [135-139]. By incorporating quantitative glycoproteomics and phosphoproteomics into an experiment workflow, it is possible to examine the changes in both *O*-GlcNAc modification and phosphorylation under various conditions in order to shed lights on the signaling events that are relevant in sensing different nutrient status. In short, it is foreseeable to observe a surge in research from the global MS studies in unveiling the functional role of *O*-GlcNAc at molecular levels.

5. Conclusive remarks

At the first glance, *O*-GlcNAc appears to be the simplest glycosylation in biological systems with its non-extended nature and minimal regulatory machinery with only two processing enzymes. Yet, the underlying functionalities and regulatory mechanisms of *O*-GlcNAc form a massive labyrinth of which surface we have barely scratched. While decades of research have provided the framework for our understandings of the *O*-GlcNAc biology, major breakthroughs in the regulatory network of the *O*-GlcNAc cycling enzymes are urgently needed to further the quest. Recent advance in technologies that are designed and implemented for *O*-GlcNAc research (further discussed in Chapter 4) will undoubtedly open more doors for *O*-GlcNAc biology.

6. References

1. Hart, G.W. and R.J. Copeland, *Glycomics hits the big time.* Cell, 2010. **143**(5): p. 672-6.
2. Spiro, R.G., *Protein glycosylation: nature, distribution, enzymatic formation, and disease implications of glycopeptide bonds.* Glycobiology, 2002. **12**(4): p. 43R-56R.
3. Varki, A., *Biological roles of oligosaccharides: all of the theories are correct.* Glycobiology, 1993. **3**(2): p. 97-130.
4. Schauer, R., *Sialic acids as regulators of molecular and cellular interactions.* Curr Opin Struct Biol, 2009. **19**(5): p. 507-14.
5. Yoshida-Moriguchi, T., et al., *O-mannosyl phosphorylation of alpha-dystroglycan is required for laminin binding.* Science, 2010. **327**(5961): p. 88-92.
6. Kawashima, H. and M. Fukuda, *Sulfated glycans control lymphocyte homing.* Ann N Y Acad Sci, 2012. **1253**: p. 112-21.
7. Marth, J.D. and P.K. Grewal, *Mammalian glycosylation in immunity.* Nat Rev Immunol, 2008. **8**(11): p. 874-87.
8. Ohtsubo, K. and J.D. Marth, *Glycosylation in cellular mechanisms of health and disease.* Cell, 2006. **126**(5): p. 855-67.
9. Moran, A.P., A. Gupta, and L. Joshi, *Sweet-talk: role of host glycosylation in bacterial pathogenesis of the gastrointestinal tract.* Gut, 2011. **60**(10): p. 1412-25.
10. Mora-Montes, H.M., et al., *Protein glycosylation in Candida.* Future Microbiol, 2009. **4**(9): p. 1167-83.
11. Vigerust, D.J. and V.L. Shepherd, *Virus glycosylation: role in virulence and immune interactions.* Trends Microbiol, 2007. **15**(5): p. 211-8.
12. Anantharaman, V., et al., *Adhesion molecules and other secreted host-interaction determinants in Apicomplexa: insights from comparative genomics.* Int Rev Cytol, 2007. **262**: p. 1-74.
13. Khoo, K.H. and A. Dell, *Glycoconjugates from parasitic helminths: structure diversity and immunobiological implications.* Adv Exp Med Biol, 2001. **491**: p. 185-205.
14. Torres, C.R. and G.W. Hart, *Topography and polypeptide distribution of terminal N-acetylglucosamine residues on the surfaces of intact lymphocytes. Evidence for O-linked GlcNAc.* J Biol Chem, 1984. **259**(5): p. 3308-17.
15. Holt, G.D. and G.W. Hart, *The subcellular distribution of terminal N-acetylglucosamine moieties. Localization of a novel protein-saccharide linkage, O-linked GlcNAc.* J Biol Chem, 1986. **261**(17): p. 8049-57.
16. Kearse, K.P. and G.W. Hart, *Lymphocyte activation induces rapid changes in nuclear and cytoplasmic glycoproteins.* Proc Natl Acad Sci U S A, 1991. **88**(5): p. 1701-5.
17. Roquemore, E.P., et al., *Dynamic O-GlcNAcylation of the small heat shock protein alpha B-crystallin.* Biochemistry, 1996. **35**(11): p. 3578-86.
18. Dieckmann-Schuppert, A., E. Bause, and R.T. Schwarz, *Studies on O-glycans of Plasmodium-falciparum-infected human erythrocytes. Evidence for O-GlcNAc and O-GlcNAc-transferase in malaria parasites.* Eur J Biochem, 1993. **216**(3): p. 779-88.
19. Perez-Cervera, Y., et al., *Direct evidence of O-GlcNAcylation in the apicomplexan Toxoplasma gondii: a biochemical and bioinformatic study.* Amino Acids, 2011. **40**(3): p. 847-56.

20. Hanover, J.A., M.W. Krause, and D.C. Love, *The hexosamine signaling pathway: O-GlcNAc cycling in feast or famine.* Biochim Biophys Acta, 2010. **1800**(2): p. 80-95.
21. Hart, G.W., M.P. Housley, and C. Slawson, *Cycling of O-linked beta-N-acetylglucosamine on nucleocytoplasmic proteins.* Nature, 2007. **446**(7139): p. 1017-22.
22. Gao, Y., et al., *Dynamic O-glycosylation of nuclear and cytosolic proteins: cloning and characterization of a neutral, cytosolic beta-N-acetylglucosaminidase from human brain.* J Biol Chem, 2001. **276**(13): p. 9838-45.
23. Kreppel, L.K., M.A. Blomberg, and G.W. Hart, *Dynamic glycosylation of nuclear and cytosolic proteins. Cloning and characterization of a unique O-GlcNAc transferase with multiple tetratricopeptide repeats.* J Biol Chem, 1997. **272**(14): p. 9308-15.
24. Dong, D.L. and G.W. Hart, *Purification and characterization of an O-GlcNAc selective N-acetyl-beta-D-glucosaminidase from rat spleen cytosol.* J Biol Chem, 1994. **269**(30): p. 19321-30.
25. Haltiwanger, R.S., G.D. Holt, and G.W. Hart, *Enzymatic addition of O-GlcNAc to nuclear and cytoplasmic proteins. Identification of a uridine diphospho-N-acetylglucosamine:peptide beta-N-acetylglucosaminyltransferase.* J Biol Chem, 1990. **265**(5): p. 2563-8.
26. Sekine, O., et al., *Blocking O-linked GlcNAc cycling in Drosophila insulin-producing cells perturbs glucose-insulin homeostasis.* J Biol Chem, 2010. **285**(49): p. 38684-91.
27. Rahman, M.M., et al., *Intracellular protein glycosylation modulates insulin mediated lifespan in C.elegans.* Aging (Albany NY), 2010. **2**(10): p. 678-90.
28. Dentin, R., et al., *Hepatic glucose sensing via the CREB coactivator CRTC2.* Science, 2008. **319**(5868): p. 1402-5.
29. Forsythe, M.E., et al., *Caenorhabditis elegans ortholog of a diabetes susceptibility locus: oga-1 (O-GlcNAcase) knockout impacts O-GlcNAc cycling, metabolism, and dauer.* Proc Natl Acad Sci U S A, 2006. **103**(32): p. 11952-7.
30. Hu, Y., et al., *Adenovirus-mediated overexpression of O-GlcNAcase improves contractile function in the diabetic heart.* Circ Res, 2005. **96**(9): p. 1006-13.
31. Hanover, J.A., et al., *A Caenorhabditis elegans model of insulin resistance: altered macronutrient storage and dauer formation in an OGT-1 knockout.* Proc Natl Acad Sci U S A, 2005. **102**(32): p. 11266-71.
32. O'Donnell, N., et al., *Ogt-dependent X-chromosome-linked protein glycosylation is a requisite modification in somatic cell function and embryo viability.* Mol Cell Biol, 2004. **24**(4): p. 1680-90.
33. McClain, D.A., et al., *Altered glycan-dependent signaling induces insulin resistance and hyperleptinemia.* Proc Natl Acad Sci U S A, 2002. **99**(16): p. 10695-9.
34. Macauley, M.S. and D.J. Vocadlo, *Increasing O-GlcNAc levels: An overview of small-molecule inhibitors of O-GlcNAcase.* Biochim Biophys Acta, 2010. **1800**(2): p. 107-21.
35. Hu, P., S. Shimoji, and G.W. Hart, *Site-specific interplay between O-GlcNAcylation and phosphorylation in cellular regulation.* FEBS Lett, 2010. **584**(12): p. 2526-38.
36. Vocadlo, D.J., *O-GlcNAc processing enzymes: catalytic mechanisms, substrate specificity, and enzyme regulation.* Curr Opin Chem Biol, 2012. **16**(5-6): p. 488-97.

37. Davies, G.J. and C. Martinez-Fleites, *GlaxoSmithKline Award Lecture. The O-GlcNAc modification: three-dimensional structure, enzymology and the development of selective inhibitors to probe disease.* Biochem Soc Trans, 2010. **38**(5): p. 1179-88.
38. Nolte, D. and U. Muller, *Human O-GlcNAc transferase (OGT): genomic structure, analysis of splice variants, fine mapping in Xq13.1.* Mamm Genome, 2002. **13**(1): p. 62-4.
39. Comtesse, N., E. Maldener, and E. Meese, *Identification of a nuclear variant of MGEA5, a cytoplasmic hyaluronidase and a beta-N-acetylglucosaminidase.* Biochem Biophys Res Commun, 2001. **283**(3): p. 634-40.
40. Hewagama, A., et al., *Overexpression of X-Linked genes in T cells from women with lupus.* J Autoimmun, 2013.
41. Lehman, D.M., et al., *A single nucleotide polymorphism in MGEA5 encoding O-GlcNAc-selective N-acetyl-beta-D glucosaminidase is associated with type 2 diabetes in Mexican Americans.* Diabetes, 2005. **54**(4): p. 1214-21.
42. Shafi, R., et al., *The O-GlcNAc transferase gene resides on the X chromosome and is essential for embryonic stem cell viability and mouse ontogeny.* Proc Natl Acad Sci U S A, 2000. **97**(11): p. 5735-9.
43. Yang, Y.R., et al., *O-GlcNAcase is essential for embryonic development and maintenance of genomic stability.* Aging Cell, 2012. **11**(3): p. 439-48.
44. Webster, D.M., et al., *O-GlcNAc modifications regulate cell survival and epiboly during zebrafish development.* BMC Dev Biol, 2009. **9**: p. 28.
45. Ingham, P.W., *A gene that regulates the bithorax complex differentially in larval and adult cells of Drosophila.* Cell, 1984. **37**(3): p. 815-23.
46. Sinclair, D.A., et al., *Drosophila O-GlcNAc transferase (OGT) is encoded by the Polycomb group (PcG) gene, super sex combs (sxc).* Proc Natl Acad Sci U S A, 2009. **106**(32): p. 13427-32.
47. Gambetta, M.C., K. Oktaba, and J. Muller, *Essential role of the glycosyltransferase sxc/Ogt in polycomb repression.* Science, 2009. **325**(5936): p. 93-6.
48. Mondoux, M.A., et al., *O-linked-N-acetylglucosamine cycling and insulin signaling are required for the glucose stress response in Caenorhabditis elegans.* Genetics, 2011. **188**(2): p. 369-82.
49. Love, D.C., et al., *Dynamic O-GlcNAc cycling at promoters of Caenorhabditis elegans genes regulating longevity, stress, and immunity.* Proc Natl Acad Sci U S A, 2010. **107**(16): p. 7413-8.
50. Lee, J., K.Y. Kim, and Y.K. Paik, *Regulation of Dauer formation by O-GlcNAcylation in Caenorhabditis elegans.* J Biol Chem, 2010. **285**(5): p. 2930-9.
51. Kenyon, C., *The first long-lived mutants: discovery of the insulin/IGF-1 pathway for ageing.* Philos Trans R Soc Lond B Biol Sci, 2011. **366**(1561): p. 9-16.
52. Hyun, S., *Body size regulation and insulin-like growth factor signaling.* Cell Mol Life Sci, 2013.
53. Shin, S.H., D.C. Love, and J.A. Hanover, *Elevated O-GlcNAc-dependent signaling through inducible mOGT expression selectively triggers apoptosis.* Amino Acids, 2011. **40**(3): p. 885-93.
54. Love, D.C., et al., *Mitochondrial and nucleocytoplasmic targeting of O-linked GlcNAc transferase.* J Cell Sci, 2003. **116**(Pt 4): p. 647-54.
55. Gloster, T.M., et al., *Hijacking a biosynthetic pathway yields a glycosyltransferase inhibitor within cells.* Nat Chem Biol, 2011. **7**(3): p. 174-81.
56. Dorfmueller, H.C., et al., *Substrate and product analogues as human O-GlcNAc transferase inhibitors.* Amino Acids, 2011. **40**(3): p. 781-92.

57. Gross, B.J., B.C. Kraybill, and S. Walker, *Discovery of O-GlcNAc transferase inhibitors.* J Am Chem Soc, 2005. **127**(42): p. 14588-9.
58. Butkinaree, C., et al., *Characterization of beta-N-acetylglucosaminidase cleavage by caspase-3 during apoptosis.* J Biol Chem, 2008. **283**(35): p. 23557-66.
59. Wells, L., et al., *Dynamic O-glycosylation of nuclear and cytosolic proteins: further characterization of the nucleocytoplasmic beta-N-acetylglucosaminidase, O-GlcNAcase.* J Biol Chem, 2002. **277**(3): p. 1755-61.
60. Keembiyehetty, C.N., et al., *A lipid-droplet-targeted O-GlcNAcase isoform is a key regulator of the proteasome.* J Cell Sci, 2011. **124**(Pt 16): p. 2851-60.
61. Toleman, C.A., A.J. Paterson, and J.E. Kudlow, *The histone acetyltransferase NCOAT contains a zinc finger-like motif involved in substrate recognition.* J Biol Chem, 2006. **281**(7): p. 3918-25.
62. Toleman, C., et al., *Characterization of the histone acetyltransferase (HAT) domain of a bifunctional protein with activable O-GlcNAcase and HAT activities.* J Biol Chem, 2004. **279**(51): p. 53665-73.
63. Haltiwanger, R.S., K. Grove, and G.A. Philipsberg, *Modulation of O-linked N-acetylglucosamine levels on nuclear and cytoplasmic proteins in vivo using the peptide O-GlcNAc-beta-N-acetylglucosaminidase inhibitor O-(2-acetamido-2-deoxy-D-glucopyranosylidene)amino-N-phenylcarbamate.* J Biol Chem, 1998. **273**(6): p. 3611-7.
64. Vosseller, K., et al., *Elevated nucleocytoplasmic glycosylation by O-GlcNAc results in insulin resistance associated with defects in Akt activation in 3T3-L1 adipocytes.* Proc Natl Acad Sci U S A, 2002. **99**(8): p. 5313-8.
65. Macauley, M.S., et al., *Elevation of global O-GlcNAc levels in 3T3-L1 adipocytes by selective inhibition of O-GlcNAcase does not induce insulin resistance.* J Biol Chem, 2008. **283**(50): p. 34687-95.
66. Mehdy, A., et al., *PUGNAc treatment leads to an unusual accumulation of free oligosaccharides in CHO cells.* J Biochem, 2012. **151**(4): p. 439-46.
67. Dorfmueller, H.C., et al., *GlcNAcstatins are nanomolar inhibitors of human O-GlcNAcase inducing cellular hyper-O-GlcNAcylation.* Biochem J, 2009. **420**(2): p. 221-7.
68. Whitworth, G.E., et al., *Analysis of PUGNAc and NAG-thiazoline as transition state analogues for human O-GlcNAcase: mechanistic and structural insights into inhibitor selectivity and transition state poise.* J Am Chem Soc, 2007. **129**(3): p. 635-44.
69. Macauley, M.S., et al., *O-GlcNAcase uses substrate-assisted catalysis: kinetic analysis and development of highly selective mechanism-inspired inhibitors.* J Biol Chem, 2005. **280**(27): p. 25313-22.
70. Macauley, M.S., et al., *Elevation of Global O-GlcNAc in rodents using a selective O-GlcNAcase inhibitor does not cause insulin resistance or perturb glucohomeostasis.* Chem Biol, 2010. **17**(9): p. 949-58.
71. Macauley, M.S., et al., *Inhibition of O-GlcNAcase using a potent and cell-permeable inhibitor does not induce insulin resistance in 3T3-L1 adipocytes.* Chem Biol, 2010. **17**(9): p. 937-48.
72. Holt, G.D., et al., *Nuclear pore complex glycoproteins contain cytoplasmically disposed O-linked N-acetylglucosamine.* J Cell Biol, 1987. **104**(5): p. 1157-64.
73. Hanover, J.A., et al., *O-linked N-acetylglucosamine is attached to proteins of the nuclear pore. Evidence for cytoplasmic and nucleoplasmic glycoproteins.* J Biol Chem, 1987. **262**(20): p. 9887-94.
74. Reason, A.J., et al., *Localization of O-GlcNAc modification on the serum response transcription factor.* J Biol Chem, 1992. **267**(24): p. 16911-21.

75. Jackson, S.P. and R. Tjian, *O-glycosylation of eukaryotic transcription factors: implications for mechanisms of transcriptional regulation.* Cell, 1988. **55**(1): p. 125-33.
76. Kelly, W.G., M.E. Dahmus, and G.W. Hart, *RNA polymerase II is a glycoprotein. Modification of the COOH-terminal domain by O-GlcNAc.* J Biol Chem, 1993. **268**(14): p. 10416-24.
77. Jackson, S.P. and R. Tjian, *Purification and analysis of RNA polymerase II transcription factors by using wheat germ agglutinin affinity chromatography.* Proc Natl Acad Sci U S A, 1989. **86**(6): p. 1781-5.
78. Marshall, S., V. Bacote, and R.R. Traxinger, *Discovery of a metabolic pathway mediating glucose-induced desensitization of the glucose transport system. Role of hexosamine biosynthesis in the induction of insulin resistance.* J Biol Chem, 1991. **266**(8): p. 4706-12.
79. Yuzwa, S.A., et al., *Increasing O-GlcNAc slows neurodegeneration and stabilizes tau against aggregation.* Nat Chem Biol, 2012. **8**(4): p. 393-9.
80. Li, X., et al., *Concurrent alterations of O-GlcNAcylation and phosphorylation of tau in mouse brains during fasting.* Eur J Neurosci, 2006. **23**(8): p. 2078-86.
81. Lefebvre, T., et al., *Evidence of a balance between phosphorylation and O-GlcNAc glycosylation of Tau proteins--a role in nuclear localization.* Biochim Biophys Acta, 2003. **1619**(2): p. 167-76.
82. Yi, W., et al., *Phosphofructokinase 1 glycosylation regulates cell growth and metabolism.* Science, 2012. **337**(6097): p. 975-80.
83. Bachmaier, R., et al., *O-GlcNAcylation is involved in the transcriptional activity of EWS-FLI1 in Ewing's sarcoma.* Oncogene, 2009. **28**(9): p. 1280-4.
84. Yang, W.H., et al., *Modification of p53 with O-linked N-acetylglucosamine regulates p53 activity and stability.* Nat Cell Biol, 2006. **8**(10): p. 1074-83.
85. Chou, T.Y., G.W. Hart, and C.V. Dang, *c-Myc is glycosylated at threonine 58, a known phosphorylation site and a mutational hot spot in lymphomas.* J Biol Chem, 1995. **270**(32): p. 18961-5.
86. Howerton, C.L., et al., *O-GlcNAc transferase (OGT) as a placental biomarker of maternal stress and reprogramming of CNS gene transcription in development.* Proc Natl Acad Sci U S A, 2013.
87. Chen, Q., et al., *TET2 promotes histone O-GlcNAcylation during gene transcription.* Nature, 2013. **493**(7433): p. 561-4.
88. Sakabe, K., Z. Wang, and G.W. Hart, *Beta-N-acetylglucosamine (O-GlcNAc) is part of the histone code.* Proc Natl Acad Sci U S A, 2010. **107**(46): p. 19915-20.
89. Sakabe, K. and G.W. Hart, *O-GlcNAc transferase regulates mitotic chromatin dynamics.* J Biol Chem, 2010. **285**(45): p. 34460-8.
90. Fujiki, R., et al., *GlcNAcylation of a histone methyltransferase in retinoic-acid-induced granulopoiesis.* Nature, 2009. **459**(7245): p. 455-9.
91. Li, M.D., et al., *O-GlcNAc Signaling Entrains the Circadian Clock by Inhibiting BMAL1/CLOCK Ubiquitination.* Cell Metab, 2013. **17**(2): p. 303-10.
92. Kim, E.Y., et al., *A role for O-GlcNAcylation in setting circadian clock speed.* Genes Dev, 2012. **26**(5): p. 490-502.
93. Rexach, J.E., et al., *Dynamic O-GlcNAc modification regulates CREB-mediated gene expression and memory formation.* Nat Chem Biol, 2012. **8**(3): p. 253-61.
94. Tallent, M.K., et al., *In vivo modulation of O-GlcNAc levels regulates hippocampal synaptic plasticity through interplay with phosphorylation.* J Biol Chem, 2009. **284**(1): p. 174-81.
95. Zafir, A., et al., *Protein O-GlcNAcylation is a Novel Cytoprotective Signal in Cardiac Stem Cells.* Stem Cells, 2013.

96. Vella, P., et al., *Tet Proteins Connect the O-Linked N-acetylglucosamine Transferase Ogt to Chromatin in Embryonic Stem Cells.* Mol Cell, 2013. **49**(4): p. 645-56.
97. Myers, S.A., B. Panning, and A.L. Burlingame, *Polycomb repressive complex 2 is necessary for the normal site-specific O-GlcNAc distribution in mouse embryonic stem cells.* Proc Natl Acad Sci U S A, 2011. **108**(23): p. 9490-5.
98. Jang, H., et al., *O-GlcNAc regulates pluripotency and reprogramming by directly acting on core components of the pluripotency network.* Cell Stem Cell, 2012. **11**(1): p. 62-74.
99. Alfaro, J.F., et al., *Tandem mass spectrometry identifies many mouse brain O-GlcNAcylated proteins including EGF domain-specific O-GlcNAc transferase targets.* Proc Natl Acad Sci U S A, 2012. **109**(19): p. 7280-5.
100. Tai, H.C., et al., *Parallel identification of O-GlcNAc-modified proteins from cell lysates.* J Am Chem Soc, 2004. **126**(34): p. 10500-1.
101. Whelan, S.A., M.D. Lane, and G.W. Hart, *Regulation of the O-linked beta-N-acetylglucosamine transferase by insulin signaling.* J Biol Chem, 2008. **283**(31): p. 21411-7.
102. Song, M., et al., *o-GlcNAc transferase is activated by CaMKIV-dependent phosphorylation under potassium chloride-induced depolarization in NG-108-15 cells.* Cell Signal, 2008. **20**(1): p. 94-104.
103. Ryu, I.H. and S.I. Do, *Denitrosylation of S-nitrosylated OGT is triggered in LPS-stimulated innate immune response.* Biochem Biophys Res Commun, 2011. **408**(1): p. 52-7.
104. Rigbolt, K.T., et al., *System-wide temporal characterization of the proteome and phosphoproteome of human embryonic stem cell differentiation.* Sci Signal, 2011. **4**(164): p. rs3.
105. Olsen, J.V., et al., *Quantitative phosphoproteomics reveals widespread full phosphorylation site occupancy during mitosis.* Sci Signal, 2010. **3**(104): p. ra3.
106. Slawson, C., et al., *A mitotic GlcNAcylation/phosphorylation signaling complex alters the posttranslational state of the cytoskeletal protein vimentin.* Mol Biol Cell, 2008. **19**(10): p. 4130-40.
107. Khidekel, N., et al., *Probing the dynamics of O-GlcNAc glycosylation in the brain using quantitative proteomics.* Nat Chem Biol, 2007. **3**(6): p. 339-48.
108. Wang, Y.T., et al., *An informatics-assisted label-free quantitation strategy that depicts phosphoproteomic profiles in lung cancer cell invasion.* J Proteome Res, 2010. **9**(11): p. 5582-97.
109. Hsu, P.P., et al., *The mTOR-regulated phosphoproteome reveals a mechanism of mTORC1-mediated inhibition of growth factor signaling.* Science, 2011. **332**(6035): p. 1317-22.
110. Mayya, V., et al., *Quantitative phosphoproteomic analysis of T cell receptor signaling reveals system-wide modulation of protein-protein interactions.* Sci Signal, 2009. **2**(84): p. ra46.
111. Old, W.M., et al., *Functional proteomics identifies targets of phosphorylation by B-Raf signaling in melanoma.* Mol Cell, 2009. **34**(1): p. 115-31.
112. Beausoleil, S.A., et al., *Large-scale characterization of HeLa cell nuclear phosphoproteins.* Proc Natl Acad Sci U S A, 2004. **101**(33): p. 12130-5.
113. Whisenhunt, T.R., et al., *Disrupting the enzyme complex regulating O-GlcNAcylation blocks signaling and development.* Glycobiology, 2006. **16**(6): p. 551-63.

114. Wagner, S.A., et al., *A proteome-wide, quantitative survey of in vivo ubiquitylation sites reveals widespread regulatory roles.* Mol Cell Proteomics, 2011. **10**(10): p. M111 013284.
115. Kim, W., et al., *Systematic and quantitative assessment of the ubiquitin-modified proteome.* Mol Cell, 2011. **44**(2): p. 325-40.
116. Danielsen, J.M., et al., *Mass spectrometric analysis of lysine ubiquitylation reveals promiscuity at site level.* Mol Cell Proteomics, 2011. **10**(3): p. M110 003590.
117. Vertegaal, A.C., et al., *Distinct and overlapping sets of SUMO-1 and SUMO-2 target proteins revealed by quantitative proteomics.* Mol Cell Proteomics, 2006. **5**(12): p. 2298-310.
118. Shaid, S., et al., *Ubiquitination and selective autophagy.* Cell Death Differ, 2013. **20**(1): p. 21-30.
119. Rieser, E., S.M. Cordier, and H. Walczak, *Linear ubiquitination: a newly discovered regulator of cell signalling.* Trends Biochem Sci, 2013. **38**(2): p. 94-102.
120. Komander, D. and M. Rape, *The ubiquitin code.* Annu Rev Biochem, 2012. **81**: p. 203-29.
121. Kulathu, Y. and D. Komander, *Atypical ubiquitylation - the unexplored world of polyubiquitin beyond Lys48 and Lys63 linkages.* Nat Rev Mol Cell Biol, 2010. **13**(8): p. 508-23.
122. Wilson, V.G. and G. Rosas-Acosta, *Wrestling with SUMO in a new arena.* Sci STKE, 2005. **2005**(290): p. pe32.
123. Dey, A., et al., *Loss of the tumor suppressor BAP1 causes myeloid transformation.* Science, 2012. **337**(6101): p. 1541-6.
124. Eletr, Z.M. and K.D. Wilkinson, *An emerging model for BAP1's role in regulating cell cycle progression.* Cell Biochem Biophys, 2011. **60**(1-2): p. 3-11.
125. Daou, S., et al., *Crosstalk between O-GlcNAcylation and proteolytic cleavage regulates the host cell factor-1 maturation pathway.* Proc Natl Acad Sci U S A, 2011. **108**(7): p. 2747-52.
126. Capotosti, F., et al., *O-GlcNAc transferase catalyzes site-specific proteolysis of HCF-1.* Cell, 2011. **144**(3): p. 376-88.
127. Wang, J., et al., *dbOGAP - an integrated bioinformatics resource for protein O-GlcNAcylation.* BMC Bioinformatics, 2011. **12**: p. 91.
128. Trinidad, J.C., et al., *Global identification and characterization of both O-GlcNAcylation and phosphorylation at the murine synapse.* Mol Cell Proteomics, 2012. **11**(8): p. 215-29.
129. Wang, Z., et al., *Extensive crosstalk between O-GlcNAcylation and phosphorylation regulates cytokinesis.* Sci Signal, 2010. **3**(104): p. ra2.
130. Comer, F.I. and G.W. Hart, *Reciprocity between O-GlcNAc and O-phosphate on the carboxyl terminal domain of RNA polymerase II.* Biochemistry, 2001. **40**(26): p. 7845-52.
131. Wells, L., et al., *O-GlcNAc transferase is in a functional complex with protein phosphatase 1 catalytic subunits.* J Biol Chem, 2004. **279**(37): p. 38466-70.
132. Wang, Z., A. Pandey, and G.W. Hart, *Dynamic interplay between O-linked N-acetylglucosaminylation and glycogen synthase kinase-3-dependent phosphorylation.* Mol Cell Proteomics, 2007. **6**(8): p. 1365-79.
133. Wang, Z., M. Gucek, and G.W. Hart, *Cross-talk between GlcNAcylation and phosphorylation: site-specific phosphorylation dynamics in response to globally elevated O-GlcNAc.* Proc Natl Acad Sci U S A, 2008. **105**(37): p. 13793-8.

134. Klein, A.L., et al., *O-linked N-acetylglucosamine modification of insulin receptor substrate-1 occurs in close proximity to multiple SH2 domain binding motifs.* Mol Cell Proteomics, 2009. **8**(12): p. 2733-45.
135. Taylor, R.P., et al., *Up-regulation of O-GlcNAc transferase with glucose deprivation in HepG2 cells is mediated by decreased hexosamine pathway flux.* J Biol Chem, 2009. **284**(6): p. 3425-32.
136. Kang, J.G., et al., *O-GlcNAc protein modification in cancer cells increases in response to glucose deprivation through glycogen degradation.* J Biol Chem, 2009. **284**(50): p. 34777-84.
137. Taylor, R.P., et al., *Glucose deprivation stimulates O-GlcNAc modification of proteins through up-regulation of O-linked N-acetylglucosaminyltransferase.* J Biol Chem, 2008. **283**(10): p. 6050-7.
138. Cheung, W.D. and G.W. Hart, *AMP-activated protein kinase and p38 MAPK activate O-GlcNAcylation of neuronal proteins during glucose deprivation.* J Biol Chem, 2008. **283**(19): p. 13009-20.
139. Zou, L., et al., *Glucose deprivation-induced increase in protein O-GlcNAcylation in cardiomyocytes is calcium-dependent.* J Biol Chem, 2012. **287**(41): p. 34419-31.

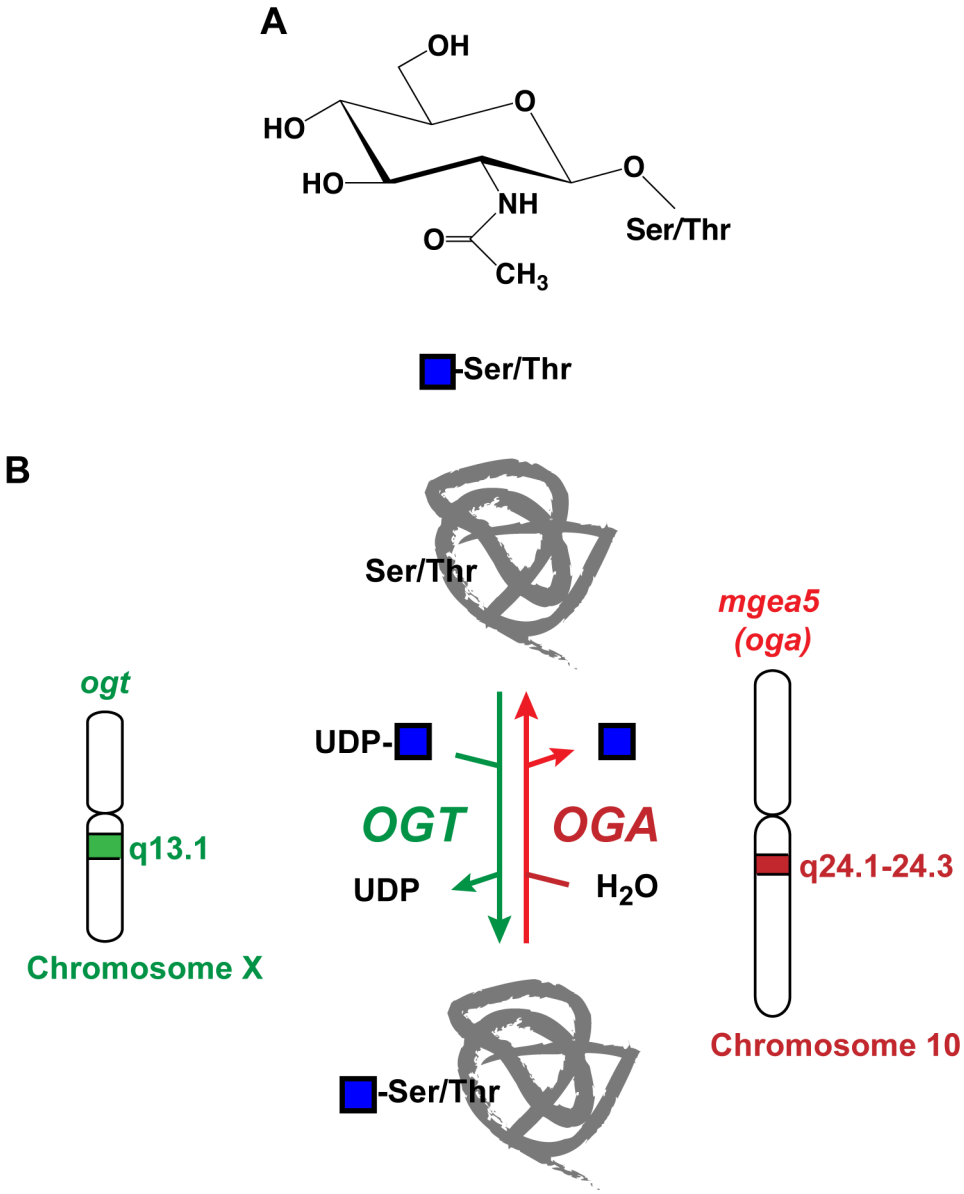

Figure 1-1. *O*-GlcNAc is a dynamic intracellular glycosylation. (A) The chemical structure and symbol nomenclature of *O*-GlcNAc: The GlcNAc moiety is added via a β-linkage to the hydroxyl side chains of either the serine or the threonine residue. No defined consensus sequence is found for the presence of *O*-GlcNAc modification. (B) The addition and removal of *O*-GlcNAc is catalyzed by a pair of *O*-GlcNAc cycling enzyme: OGT and OGA. In human, gene loci encoding *ogt* and *oga* (*mgea5*) are mapped to chromosome X (q13.1) and chromosome 10 (q24.1-24.3), respectively.

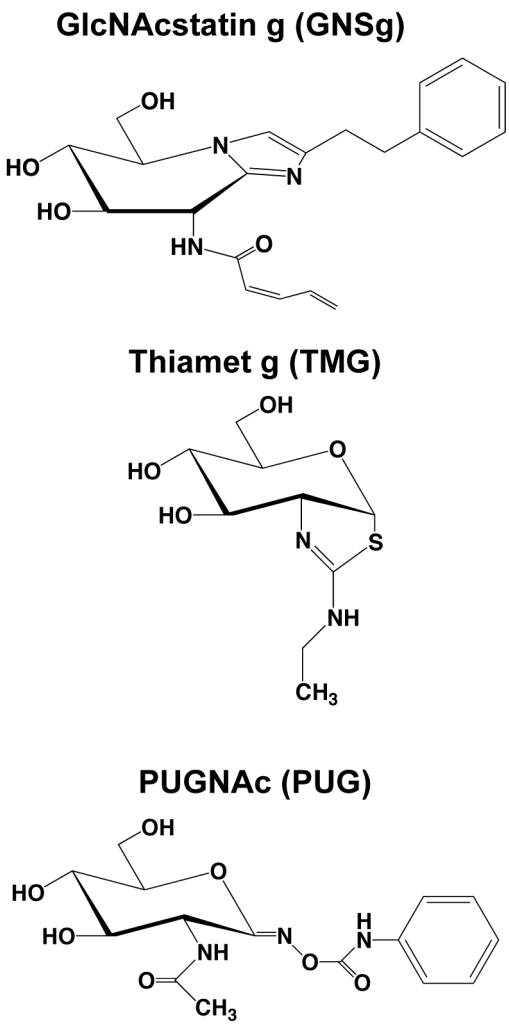

Figure 1-2. OGA inhibitors: GlcNAcstatin G, thiamet G and PUGNAc. Western blots against *O*-GlcNAc, OGT and OGA reveal that treating cells with OGA inhibitors not only lead to drastic increases in global O-GlcNAc levels and OGA protein level, but also a slight decrease in OGT protein level. Immunoblot against β-actin is also included as a loading control.

CHAPTER 2

METHODOLOGIES FOR THE DETECTION, ENRICHMENT, AND SITE-MAPPING OF THE O-GLCNAC POST-TRANSLATIONAL MODIFICATION[#]

[#]Teo C.F. and Wells L. To be submitted to *MCP.*

Abstract

The *O*-GlcNAc modification is a reversible and inducible essential post-translational modification found on a myriad of intracellular proteins in mammals. Studies have revealed the extensive cross-talk between the *O*-GlcNAc modification and phosphorylation since both PTMs can be added onto the same amino acid side chains of target proteins. Compared to the phosphorylation field, however, the *O*-GlcNAc field lags behind in terms of having a robust set of analytical tools to facilitate in-depth cell biological studies. Herein, we summarize and discuss currently available biochemical and mass spectrometry approaches for *O*-GlcNAc studies and comment on potential new additions to the toolbox.

1. Introduction

O-linked β-*N*-acetylglucosamine (*O*-GlcNAc) modification on the serine and threonine residues of nuclear and cytoplasmic proteins is a ubiquitous post-translational modification (PTM) that is modulated by a pair of *O*-GlcNAc cycling enzymes: *O*-linked GlcNAc transferase (OGT) and *O*-GlcNAc hexosaminidase (OGA). With its non-extended nature as well as dynamic temporal and spatial distributions, *O*-GlcNAc is known to act in a manner more resembling *O*-phosphorylation than complex glycosylations[1]. However, unlike the addition of phosphorylation, where a specific primary sequon is recognized by its corresponding kinase(s), no distinct primary sequon has been found for OGT though there does appear to be an enrichment for Pro, Ser, Thr, and Val residues near the site of modification similar to that seen for mucin *O*-GalNAc initiated glycosylation[2-4]. Furthermore, it has been suggested that there is a disproportionate number of *O*-GlcNAc sites in regions lacking tertiary structure[5]. So far, many studies have shown that the functional roles of phosphorylation and *O*-GlcNAc modification in numerous cellular processes, from transcription control, enzyme activity,

protein stability, to metabolic regulation, are often entwined[6]. A classical example is the mutually exclusive presence of the *O*-GlcNAc modification and phosphorylation on certain residues of the tau protein found in the brain. In Alzheimer's disease individuals, hyperphosphorylation is accompanied by a drastic reduction in *O*-GlcNAc modification[7-10]. That being said, the interplay between *O*-GlcNAc modification and phosphorylation is generally much more complicated than this simplified reciprocal model and the functional impacts of both PTMs on their target proteins are often case-dependent[5, 11-14].

The main challenge in the *O*-GlcNAc and phosphorylation research is their low substoichiometric presence in the biological systems. However, unlike phosphorylation for which a variety of tools are readily available to address outstanding biological questions, options in the *O*-GlcNAc's toolbox are relatively few. For instance, decades of trial-and-error has shaped, improved, and optimized the workflows for the generation of a very large number of phospho-site specific antibodies[15], which in turn has lead to major breakthroughs in understanding a variety of biological functions for individual sites of phosphorylation. However, the lack of *O*-GlcNAc site-specific antibodies remains a major hurdle in the *O*-GlcNAc field. Also, the negative charge of the phosphate group provides a distinct biochemical feature that can be exploited for the isolation of phospho-peptides from their unmodified counterparts. By modifying previously existing biochemical tools, strong cation exchange chromatography (SCX) and immobilized metal affinity chromatography (IMAC) have become the two main routine approaches for phosphopeptide enrichment and identification[16]. To the contrary, the attachment of small, neutral and hydrophilic GlcNAc structure does not lead to a significant change in the chemical features of glycopeptides. Furthermore, while neutral-loss or precursor-ion scanning collision-induced dissociation (CID) fragmentation strategies leave a scar at the site of phosphate removal (a dehydroamino acid, loss of 98 Da to the polypeptide

though the addition of phosphate is only 80 Da), loss of *O*-linked sugars are true neutral losses that leave the previously modified Ser or Thr residue unaffected in mass[17, 18]. Thus, innovative tools are required for improving workflows to isolate and analyze *O*-GlcNAc modified peptides.

Here, we summarize biochemical and analytical methods that are currently available for *O*-GlcNAc research, and highlight new venues that are being actively pursued in order to expand the *O*-GlcNAc toolbox.

2. Classical biochemical approaches

Enzymatic labeling− *O*-GlcNAc modification on proteins was discovered[19] based on unexpected intracellular labeling when cells were treated with bovine β1,4-galactosyltransferase (β1,4GalT) in the presence of a tritiated sugar donor (UDP-[^{3}H]galactose, or UDP-[^{3}H]Gal). In the following years, β1,4GalT-mediated radioactive incorporation became the "gold standard" for detecting *O*-GlcNAc modification. Since β1,4GalT recognizes all terminal GlcNAc residues (which are prevalently found on the complex glycan structures) as its acceptor substrates, enriched nuclear and/or cytoplasmic fractions are required as starting materials in the enzymatic reaction for global *O*-GlcNAc detection to avoid the potentially overwhelming complex glycan-derived signals. The radioactive products are visualized by autoradiography. Additionally, the disaccharide formed after β1,4GalT reaction was frequently subjected to alkali-induced β-elimination and analyzed by size exclusion chromatography[19, 20]. The main drawback of this method is that it requires extremely long exposure time (several weeks is the norm) due to the weak radioactive signal emitted from ^{3}H. Owing to the autoglycosylation capacity of β1,4GalT, a prerequisite self-labeling step with non-radioactive UDP-Gal prior to the actual radioactive labeling of target proteins is essential. Radioactive labeling of *O*-GlcNAc modified proteins has become obsolete following the

appearance of pan-*O*-GlcNAc specific antibodies[21-23], since these antibodies can be sandwiched with secondary antibodies that are coupled to other detection methods, such as chemiluminescence via conjugated horseradish peroxidase (HPR) or fluorescence via conjugated fluorochromes.

Lectin blotting− Lectins are an evolutionary heterogenous group of carbohydrate-binding proteins that have diverse and distinct glycan binding profiles. Wheat germ agglutinin (WGA) was found to bind glycans with GlcNAc and sialic acid at their reducing termini[24]. However, a succinylated form of WGA (sWGA) has higher selectivity toward GlcNAc over sialic acid[25]. sWGA conjugated to horseradish peroxidase (HRP) can be used for membrane-based *O*-GlcNAc modified protein detection (Figure 2-1A, [26]). Similar to β1,4GalT labeling, enrichment of nuclear and/or cytoplasmic fractions is necessary to eliminate signals contributed by the complex glycans. Moreover, WGA or sWGA conjugated with fluorochrome can be used to visualize *O*-GlcNAc modified protein via microscopy[27] and sWGA bound agarose can be used to pull down *O*-GlcNAc modified proteins for downstream analyses(Figure 2-2, [28]).

O-GlcNAc specific antibodies− Generating antibodies against glycopeptides is not a trivial task. This is because majority of the carbohydrate or glycopeptide epitopes are prone to trigger T cell independent innate immune response in which activated IgM-producing B cells fail to undergo isotype class switching[29]. Thus, the immunized animals do not developed IgG-producing memory B cells[30]. To date, a relatively few verified pan-*O*-GlcNAc antibodies are currently commercially available: RL-2[23, 31], HGAC85[32], CTD110.6[22], Mab3/18B10.C7, Mab10/9D10.E4 and Mab14/1F5.D6[21]. Additionally, four non-commercialized and more selective antibodies are also available: NL-6 is a *O*-GlcNAc modified neurofilament-M (NF-M) specific monoclonal antibody that binds to human and rat NF-M only when the proteins are *O*-GlcNAc modified on their tail domains[33], 3925 is a rabbit polyclonal antibody that recognizes *O*-GlcNAc modified

Tau at Ser-400[34], αH2BS112GlcNAc is an antibody against *O*-GlcNAc modified histone2B at Ser-112[35], and α-T58G is a mouse monoclonal antibody against *O*-GlcNAc modified c-Myc at Thr58[36].

RL-2 and HGAC85 are the first two reported pan-*O*-GlcNAc monoclonal antibodies and both resulted from a stroke of serendipity: RL-2 was raised against nuclear pore complexes (Figure 2-1B, [23, 31]), on which many proteins are known to be heavily glycosylated[26], whereas HGAC85 was originally generated using the capsular polysaccharides of streptococcal group A bacteria that contains β-GlcNAc side chains, as an immunogen[32]. Detailed characterization of both RL-2 and HGAC85 monoclonal IgG antibodies revealed that their binding profiles were abolished by β1,4GalT (to add an galactose decoration) or β-hexosaminidase (to remove the GlcNAc moiety) treatments, confirming their ability to specifically recognize *O*-GlcNAc modified proteins. Unlike RL-2 and HGAC85, the antigen used to generate CTD110.6 monoclonal IgM antibody (Figure 2-1C, [22]) was an *O*-GlcNAc modified peptide, YSPT***g*S**PSK (where **gS** indicates the glycosylated amino acid). Notably, this glycopeptide sequence is derived from the C-terminal domain of RNA polymerase II, on which Ser-5 is a known *O*-GlcNAc target site[37]. Although the GlcNAc is attached to a serine residue on the glycopeptides that were used for immunization, CTD110.6 was found to be a pan-*O*-GlcNAc antibody that recognized both β-*O*-GlcNAc-serine and β-*O*-GlcNAc-threonine.

In order to circumvent the lack of robust antibody production against glycopeptides, Boons' group has developed a fully synthetic three-component immunogen strategy to guide the immune system toward a proper B cell isotype switching process upon glyco-epitope containing antigen challenge[38, 39]. This innovative approach has proven to yield a powerful cancer vaccine against a glycosylated cancer biomarker[40], and potentially a useful avenue to generate *O*-GlcNAc site-specific monoclonal antibodies. Toward this end, a three-component

antigen containing an *O*-GlcNAc modified CKII peptide (GSTPV***gS***SANM) was used to immunize mice, and hybridoma lines were isolated according to standard protocols. In collaboration with Boons' group, we characterized three of the resulting monoclonal IgG antibodies (Mab3/18B10.C7, Mab10/9D10.E4 and Mab14/1F5.D6)[21]. Surprisingly, while competitive ELISA data demonstrated that all three antibodies were strongly inhibited by the original glycopeptide but not blocked by β-*O*-GlcNAc-Ser or unmodified CKII peptide, further biochemical characterization revealed that all three of the monoclonal IgG antibodies recognize a wide range of *O*-GlcNAc modified proteins[21]. Collectively, all of these pan-*O*-GlcNAc antibodies have provided the O-GlcNAc field with a useful tool for the detection of *O*-GlcNAc modification by immunoblotting, immunoaffinity chromatography, microscopy imaging and flow cytometry approaches[13, 21-23, 31, 41-43].

Potential improvements toward the goal of generating and isolating O-GlcNAc site-specific antibodies− While the availability of pan-*O*-GlcNAc antibodies have played a significant role in advancing *O*-GlcNAc research, the lack of *O*-GlcNAc site-specific antibodies remains a major problem. So far, only three *O*-GlcNAc site-specific antibodies (against c-Myc/gT-58[36], H2B/gS-112[35] and Tau/gS400[34]) are available. It is noteworthy that the immunization protocol used to generate these antibodies is a standard procedure for antibody production, in which the immunogen is composed of a glycopeptide conjugated- keyhole limpet hemocyanin (KLH), a composition that is known to be suboptimal for eliciting antibody response against glycoconjugates. In the example of obtaining 3925 polyclonal antibody reported by Yuzwa and colleagues, the key for their success laid on an affinity purification step using an *O*-GlcNAc Tau peptide as bait. Given that the three-component immunogen approach from the Boons' group [21, 38, 39] has proven to be an effective method to trigger immune response to produce higher titers of antibodies, combining both Boons' and Vocadlo's strategies to isolate an *O*-

GlcNAc site-specific polyclonal antibody from serum of immunized animals could be a promising route to pursuit. Moreover, it is worthwhile to perform a two-step affinity chromatography, first with unmodified peptide as bait to eliminate non-glycosylated target recognizing pool of antibodies, followed by an enrichment step using glycopeptides as bait. This strategy is widely used for the isolation of phospho-site-specific polyclonal antibodies and could be used to obtain *O*-GlcNAc site-specific antibodies.

Furthermore, the original screen of Boons' strategy yielded a total of 30 hybridoma lines from two animals[21]. In the competitive ELISA assays, seventeen of these hybridoma lines secreted antibodies that showed binding specificity and selectivity to the glycopeptides[21]. While none of the three lines that were selected for further characterization produced an *O*-GlcNAc CKII site-specific antibody, it is possible that upon closer examination one or more of the rest of the hybridoma clones might yield one that produces an *O*-GlcNAc CKII site-specific antibody.

3. Click-chemistry based approaches

Click reactions are thermodynamically favorable reactions that lead to the formation of desirable products with minimum work up[44]. Click chemistry based approaches for glycobiology were first implemented by Bertozzi and colleagues whereby they metabolically introduced bioorthogonal reporters (keto[45] and azido[46] functionalities) to tag sialic acid containing glycans. Since then, continuous improvements in click chemistry have tremendously benefited *O*-GlcNAc research and glycobiology generally. In principle, these strategies require two sequential steps[44]: First, the introduction of a bioorthogonal group onto the GlcNAc structure (by either chemoenzymatic or metabolic labeling), and second, baiting the bioorthogonal group by click chemistry (an azide-alkyne, an azide-phosphine, an azide-cyclooctyne or a keto-

aminooxy reaction, Figure 2-3). Through the click chemistry, one can add an extra molecular handle such as biotin or epitope tag that can be used in downstream applications, either for membrane-based detection or solid support mediated enrichment.

One of the caveats for both chemoenzymatic and metabolic labeling of *O*-GlcNAc modified proteins is the specificity issue. Chemoenzymatic approach will also tag terminal GlcNAc commonly found on the complex *N*- or *O*-glycans, as well as the recently reported extracellular *O*-GlcNAc modification. Likewise, in the case of metabolic labeling, all of the GlcNAc and GalNAc containing (not necessary terminal) glycans are labeled due to the nature of precursor sugar. That being said, using nuclear and cytosolic preparations that do not contain complex glycan-containing proteins or/and treatment with complex glycan specific hydrolase (such as PNGase F for *N*-glycans) can resolve this problem.

Chemoenzymatic labeling− First improvised in the Hsieh-Wilson's laboratory, the chemoenzymatic labeling of *O*-GlcNAc modified proteins is a modified version of the β1,4GalT-driven labeling method with some additional benefits[47-49]. This method utilizes a β1,4GalT(Y289L) mutant engineered by Ramakrishnan and Qasba that has an enlarged binding pocket for its donor substrate UDP-Gal[50]. As a result, UDP-Gal analogs with additional functional groups, such as keto or azido groups, at the C2 position are tolerated by β1,4GalT(Y289L) and transferred onto any terminal GlcNAc containing glycoconjugates, including *O*-GlcNAc modified proteins or peptides *in vitro*. Subsequently, click chemistry can be applied to introduce an additional handle, which in turn can be used to probe (with HRP conjugated streptavidin) or enrich (with solid support coupled with streptavidin or its derivatives) the modified targets[47-49]. Notably, HRP-mediated membrane-based detection of β1,4GalT(Y289L) chemoenzymatically labeled samples is much more sensitive compared to radioactive-based approach using

β1,4GalT coupling to tritated nucleotide sugar donor and the exposure time can be shortened from weeks to a seconds[49].

Metabolic labeling− In contrast to chemoenzymatic labeling, metabolic labeling introduces the bioorthogonal group directly onto the GlcNAc structure *in vivo* without the addition of an extra sugar, since OGT can efficiently utilize UDP-GlcNAz (an UDP-GlcNAc derivative with an azido moiety at the C2 position) as its donor substrate[51]. However, due to a deficit in the final biogenesis step of the GlcNAc salvage pathway, it was found that feeding cells with acetylated GlcNAz (Ac_4GlcNAz) is not the most effective way to introduce GlcNAz into glycoproteins[52]. Aiming to find a solution for *in vivo* labeling of *O*-GlcNAc modified proteins, Bertozzi's group discovered that Ac_4GalNAz can actually be used to label *O*-GlcNAc modified proteins[53]. Ac_4GalNAz was initially designed to tag mucin type α-GalNAc initiated structures via the GalNAc salvage pathway[54]. However, Boyce *et al.* recently demonstrated that the end product of GalNAc pathway, UDP-GalNAz, is readily converted into UDP-GlcNAz via an enzymatic epimerization step via the Leloir pathway[55, 56], and that UDP-GlcNAz is the predominant resulting nucleotide sugar [53]. Therefore, azido group can be added onto *O*-GlcNAc modified proteins by using Ac_4GalNAz as a metabolic labeling agent, which in turns can be further manipulated using click chemistry in downstream analyses (Figure 2-4).

Advantages for applying click chemistry to O-GlcNAc biology− Applying click chemistry to *O*-GlcNAc research provides some advantages compared to the classical biochemical approaches. One of such example is visualization and quantification of the stoichiometric distribution of *O*-GlcNAc modification on target proteins, as demonstrated elegantly by Rexach and colleagues[57]. Here, upon introducing an electrophoretically resolvable polyethylene glycol (PEG) mass tag onto *O*-GlcNAc modified proteins via click chemistry, the glycosylation status of a specific protein can be directly monitored by

immunoblotting using an antibody against the target protein. Without the accessibility of *O*-GlcNAc site-specific antibody, this method is the best way to monitor and study the *O*-GlcNAc modification of a particular protein, as demonstrated by studies of cyclic AMP-response element binding protein (CREB) in long-term memory formation[58], and phosphofructokinase 1 (PFK1) in tumorigenesis[59].

4. Mass spectrometry-based workflows for *O*-GlcNAc site identification

Given that specific functions have been assigned to numerous site-specific phosphorylations, the resemblance of phosphorylation and *O*-GlcNAc modification has led the *O*-GlcNAc field to rapidly move toward site identification on target proteins. However, progress until the late 90s has been sluggish due to the lack of effective solutions in biochemical enrichment and tandem mass spectrometry (MS^n) sequencing to overcome the following issues[60]: (1) for a particular *O*-GlcNAc modified protein, only a small fraction of the peptide bears the sugar moiety; (2) in the peptide mixture digested from a purified *O*-GlcNAc modified protein, *O*-GlcNAc modified peptides tend to co-elute with their unmodified counterparts in a C18 reverse-phase chromatography that is the most commonly used liquid chromatography (LC) modality coupled to a tandem MS analyzer; (3) *O*-GlcNAc modified peptides ionize less efficiently than their unmodified counterparts, leading to a suppression of glycopeptide signal; and (4) the glycosidic bond is the most fragile linkage in a given glycopeptides during CID, and the resulting neutral loss signal during MS/MS (MS^2) fragmentation usually leads to very few fragment ions that are useful for identifying the exact glycosylation site. Without robust strategies for isolating glycopeptides or fragmenting glycopeptides, *O*-GlcNAc site assignment is an arduous endeavor. In the last decade, however, revolutions in the MS field by introduction of different types of mass spectrometry techniques, and improvement in the

biochemical approaches for enriching *O*-GlcNAc peptides, have propelled the quest for *O*-GlcNAc site mapping forward.

Mass spectrometric approaches for O-GlcNAc site-mapping− Ion trap mass spectrometers provide a solution to overcome the lack of peptide sequence information upon neutral loss (NL) in a typical CID MS^2 experiment[61]. By using a data-dependent neutral loss (DDNL)-triggered MS^n method, it is possible to isolate the precursor ion with the loss of GlcNAc (loss of 204.09) in a MS^2 scan and subject it to MS^3 fragmentation. Since the precursor ion in the MS^2 no longer carries a glycosidic bond, subsequent MS^3 scan will reveal a typical *b*- and *y*- ions (since fragmentation occurs at a peptide bond) as observed in the MS^2 scan of an unmodified peptide. This DDNL-CID-MS^n method was first introduced by Greis and colleagues using a standard glycopeptides[18] and implemented to a complex mixture by Khidekel and colleagues to map *O*-GlcNAc sites after glycopeptides enrichment through their chemoenzymatic approach[48]. Since the enriched glycopeptides bear a disaccharide with an additional biotin group, the glycopeptides are susceptible to two sequential neutral loss events (first neutral loss ends with the cleavage of the glycosidic bond between two sugars, and the second neutral loss leads to the loss of GlcNAc from the amino acid side chain). MS^4 fragmentation is needed to reveal any useful sequence information. Importantly, if more than one serine or threonine is present on the glycopeptide, it is hard to unambiguously define the glycosylation site.

In 2005, Hunt's lab first presented a triumph in applying electron-transfer dissociation (ETD) method to pinpoint an *O*-GlcNAc site on purified paxillin, an adaptor protein involved in focal adhesion[62]. The main advantage of ETD is that the fragmentation mechanism ignores the glycosidic bond on a glycopeptide and creates a series of *c*- and *z*-type ions in the MS^2 scan[63]. As a result, the *O*-GlcNAc site can be accurately assigned based on the information from *c*- and *z*-ions. To date, ETD is the

most reliable method to identify *O*-GlcNAc sites and has been applied in many studies[64-66]. Since this method only works well with (glyco)peptides with high charge states (z > +3), standard trypsin digestion in proteomic research that mostly produces +2 and +3 charge state ions is not an ideal method to prepare samples for ETD analysis. That being said, a combined workflow with alternate CID-NL-triggered MS^3 and ETD fragmentation (CID-NL/ETD) can increase the chance of mapping *O*-GlcNAc site.

Higher-energy C-trap dissociation (HCD, [67]), first introduced by Mann and colleagues, is the newest addition to the cavalcade of mass spectrometry methods for *O*-GlcNAc site mapping. Unlike CID and ETD, both of which are available in a linear ion trap (LTQ) mass spectrometer, HCD is only available for LTQ-Orbitrap hybrid instruments[67]. During a HCD scan event, ions are first fragmented in a collision cell and sent through the C-trap for Orbitrap analysis, and the resulting fragmentation yields *b*- and *y*-ions that are similar to CID fragmentation but are not limited by the 1/3 rule of an ion-trap. However, a typical HCD MS^2 spectrum not only contains stronger signals for *b*- and *y*-ions, but also shows unique HexNAc specific oxonium ion peaks at the low m/z range (m/z at 186, 168, 144, 138 and 126) that are often undetectable in CID. Since the oxonium ions derived from the GlcNAc structure have a very distinct signature, it is possible to implement a MS workflow in which an ETD scan is triggered by the detection of GlcNAc oxonium product ions from a HCD scan. Indeed, the combined HCD/ETD workflow has been successfully employed to identify *O*-GlcNAc sites using a LTQ-Orbitrap Velos instrument[68]. Notably, when the same sample was analyzed with CID-NL/ETD on a LTQ-XL instrument, no *O*-GlcNAc sites were confidently assigned[21], demonstrating the strength of *O*-GlcNAc site mapping using the HCD/ETD alternate scanning approach.

Although proven to be a robust method for *O*-GlcNAc site identification, the need for both a HCD and ETD scan makes the HCD/ETD method only suitable for more

advanced hybrid instruments such as the LTQ-Orbitrap Velos or LTQ-Orbitrap Elite. That being said, it is still possible to implement HCD method for *O*-GlcNAc site mapping on a basic LTQ-Orbitrap XL instrument via a two-stage tandem MS strategy. The approach, as demonstrated by Hahne and Kuster[69], involves a total of three sequential steps: (1) a HCD discovery run to detect *O*-GlcNAc modified peptides, (2) a computational data processing step using Oscore software to identify precursor ions containing glycopeptides based on the signature GlcNAc oxonium ions, and (3) a parent mass list-driven precursor scanning for ETD fragmentation. This two-stage tandem MS strategy can be also applied to an LTQ-ETD XL instrument without Orbitrap, in which case, pulsed Q collision induced dissociation (PQD) fragmentation can replace HCD in the first MS run. However, as demonstrated by Hahne and Kuster, HCD instead of PQD in the first discovery run yields more meaningful information, as GlcNAc oxonium ions are more prominent in HCD than those in PQD. Additionally, by using Oscore algorithm to re-analyze existing data sets from large-scale proteomic studies, Kuster's group found hundreds of *O*-GlcNAc peptides that were not previously identified in the original reports[70]. Collectively, this shows that Oscore can be used as a complementary computational tool for *O*-GlcNAc site determination, and demonstrates the general need for improvement in the bioinformatic front of PTM sites by MS-based analyses.

Experimental strategies prior to breakthroughs in the MS techniques− Prior to improvements in MS techniques, Hart's group and others tried diligently to enrich GlcNAc-containing peptides to resolve the signal suppression issues arising from unmodified peptides, and develop strategies to overcome the neutral loss problem. The first glycopeptides enrichment method utilized immobilized *Ricinus communis* agglutinin I (RCA I, a lectin that binds Galβ1,4GlcNAc disaccharide) to isolate *O*-GlcNAc modified peptides that were previously extended with a galactose via β1,4-GalT[71]. Although RCA I lectin enrichment could effective remove unmodified peptides, it did not address

the neutral loss issue and has not been widely used in the *O*-GlcNAc field[61, 71]. Since the neutral loss-sensitive glycosidic linkage on the serine or threonine residue is also prone to under go β-elimination under alkaline conditions, leaving a “scar” on the original modified amino acid (due to the formation of an α,β-unsaturated carbonyl group), Greis and colleagues tried to detect the presence of scarred residue by MS/MS sequencing, to pinpoint the glycosylation site[18], however, this method has not been applied to any glycoproteomic study due to the lack of enrichment step.

The needed breakthrough arrived when Wells *et al.* introduced β-elimination followed by Michael addition (BEMAD) to replace the GlcNAc with dithiothreitol (DTT)[43]. The newly introduced DTT not only marks the glycosylation site with a stable linkage that is not susceptible to neutral loss during LC-MS^n analysis, but also serves as an affinity tag for enrichment using thio-group containing solid support[43]. By using BEMAD, it was possible for the first time to isolate *O*-GlcNAc modified peptides for site-mapping[43], and perform relative quantification of *O*-GlcNAc site occupancy using normal or deuterated DTT as illustrated by Vosseller and colleagues[72]. However, BEMAD has two caveats: First, phosphorylation on the serine and threonine groups is also susceptible to β-elimination reaction, necessitating parallel alkaline phosphatase treatment control, to confidently assign the glycosylation site. Second, the formation of the disulfide bonds in both affinity enrichment and the subsequent release steps are thermodynamically unfavorable, necessitating an excess of non-volatile reagents and extensive clean-up procedures following enrichment. Even if enrichment is not performed, there is still a requirement for cleanup given that excess reductant (DTT) will suppress ionization. That being said, BEMAD is still an asset to the field; It has been used to determine *O*-GlcNAc sites on proteins such as IRS-1[73], p53[74], and NDUFA9[75], as well as other types of *O*-linked post-translational modification[72, 76].

Additionally, BEMAD has been also applied in conjunction with click chemistry for MS analysis that will be discussed further in the next section.

Enrichment of native O-GlcNAc modified peptides following breakthroughs in the MS techniques− In 2006, Burlingame's group presented a method, termed lectin weak affinity chromatography (LWAC), to directly retard the elution of *O*-GlcNAc modified peptides by from complex mixture using WGA agarose resin [3]. Since the binding affinity of WGA to *O*-GlcNAc peptides is not very strong, a 39 feet long column run under isocratic conditons was required to achieve the separation of *O*-GlcNAc modified peptides from the unmodified peptides. By coupling LWAC with BEMAD, and implementing improved MS techniques, DDNL-CID-MS^3 and ETD, Vosseller *et al.* obtained what was at the time the largest number of identified *O*-GlcNAc sites using postsynaptic density preparation from mouse brain[3]. Since then, Burlingame's group has continued the coupling of the LWAC glycopeptide enrichment strategy with ever advancing tandem MS strategies (especially ETD and HCD fragmentation methods). Their efforts have resulted in the most extensive collection of *O*-GlcNAc sites on proteins that are involved in postsynaptic signaling and transcriptional control in several of their large-scale glycoproteomic studies[2, 5, 77, 78].

Enrichment of O-GlcNAc modified peptides via click chemistry− As briefly mentioned earlier, Hsieh-Wilson's group has spearheaded the chemoenzymatic labeling approach for *O*-GlcNAc peptide enrichment[14, 47-49]. By using either DDNL-CID-MS^n or ETD method, several *O*-GlcNAc sites have been determined. Furthermore, they also implemented a quantitative method (called quantitative isotopic and chemoenzymatic tagging, QUIC-tag) in attempt to monitor *O*-GlcNAc turnover during neuronal activity[14].

While proven to be a very effective approach to isolate *O*-GlcNAc modified peptides from a complex mixture, the structural extension (a galactose and a biotin) on the GlcNAc moiety lowers the ionization efficiency of the glycopeptides. In order to

improve the ionization efficiency of chemoenzymatically enriched GlcNAc peptides, Wang *et al.*, ingeniously incorporated BEMAD as the elution step in the chemoenzymatic enrichment workflow and have successfully identified *O*-GlcNAc sites in several studies[79-82]. A variant of Wang's click chemistry-BEMAD approach, in which metabolic, instead of chemoenzymatic, labeling was used to introduce a bioorthogonal group onto the GlcNAc moiety, has been recently reported[83]. It is noteworthy that since phospho-serine/threonine is also susceptible to BEMAD, the click chemistry-BEMAD method can definitive assign the glycosylation site only when there is only one serine/threonine or DTT on the peptide.

Encouraged by the success in applying chemoenzymatic approach to enrich O-GlcNAc modified peptides, Wang and colleagues further improved their workflow by introducing a photo-cleavable biotin handle in the azido-alkyne click reaction. This strategy was named chemical/enzymatic photochemical cleavage (CEPC) approach[84]. In this scheme, after biotin-avidin enrichment, the photo-cleavable group can release part of the bulky biotin group upon UV treatment and create a positively charged aminomethyltriazo (AMT) group on the resulting Gal-GlcNAc disaccharide on the peptide. As a result, the glycopeptides can be fragmented more efficiently with ETD. Furthermore, the AMT-Gal-GlcNAc group also provides a unique oxonium ion signature in HCD. CEPC has been applied in several large-scale glycoproteomic studies[11, 85].

5. A proposed novel workflow

Combining click chemistry and β-elimination for O-GlcNAc site mapping− A decade has passed since the reporting of BEMAD that brought *O*-GlcNAc research into the proteomics era. Currently, LWAC and CEPC are the two of the most powerful methods for *O*-GlcNAc site mapping (Table 1). However, both methods have their own challenges and neither is widely used in the *O*-GlcNAc field outside the original and

related laboratories where the methods were pioneered. In the case of LWAC, it is not a trivial task to pack and run a 39 feet column. Whereas for CEPC, it demands meticulous and experienced hands since laborious clean-up steps are required to remove excess reagents that otherwise would lead to signal suppression in the LC-MS^2 analysis. Additionally, inefficient ionization remains an issue for glycopeptides, even when enriched by LWAC or CEPC. Especially in the case of CEPC, the addition of AMT-Gal onto the GlcNAc moiety renders the glycopeptides even harder to ionize than the GlcNAc residue alone.

In order to devise a more user friendlier method for *O*-GlcNAc site-mapping, we propose a novel workflow that combines click-chemistry for glycopeptide capture, ammonia-based β-elimination (ABBE, [86]) for glycopeptide release, and MS analysis (Figure 2-5). As discussed in the later section, this novel workflow is not entirely flawless. Having said that, it does bear several advantages and can be used as a straightforward first approach to identify potential O-GlcNAc sites that can be further confirmed using parent mass list-driven HCD/ETD tandem MS and site-direct mutagenesis approaches.

In this workflow, an azido group is first introduced to the *O*-GlcNAc moiety either by metabolic (*in vivo,* at the protein level) or chemoenzymatic (*in vitro*, at either the protein or the peptide levels) labeling, to attain azido containing GlcNAc or Gal-GlcNAc peptides. Next, solid support bearing cyclooctyne functional group, such as difluorinated cyclooctyne (DIFO, [87]) or DIBO (difluorobenzocyclooctyne, [88]) is used to covalently capture azido-containing glycopeptides via copper-free click chemistry. Upon the formation of glycopeptide-solid support conjugates, the samples can be washed extensively with water and compatible organic solvent (for instance, methanol, or acetonitrile) to remove unmodified peptides and any non-glycopeptide components. Finally, ABBE is used to elute the captured peptide from the solid support. ABBE is a

method reported by Rademaker and colleagues in 1998 in which they tried to identify complex *O*-glycan site on glycopeptides derived from mucin, a glycoprotein that is heavily decorated with α-GalNAc-initiated structures[86]. However, without any effective glycopeptide enrichment, this method has not been applied beyond standard glycopeptides. Unlike BEMAD that requires non-volatile reagents including sodium hydroxide (acting as a base to initiate β-elimination) and DTT (a nucleophile for Michael addition), the only reagent in ABBE is ammonium hydroxide (NH_4OH). While the alkalinity of NH_4OH solution is sufficient to trigger β-elimination, ammonia (NH_3) also serves as a nucleophile and replaces the glycan on the amino acid side chains (Figure 2-6). As a result, all the ABBE modified serine and threonine residues (now with $–NH_2$ functional group) show a 0.984 Da reduction in mass compared to their unmodified counterparts (with –OH functional group), which are easily discernible in a high-resolution mass spectrometer such as LTQ-Orbitrap XL. Further advantage of the formed primary amine is that it can introduce an extra charge on the peptide.

When analyzing a standard *O*-GlcNAc modified peptides (gBPP) and its ABBE-treated derivative (aBPP), we observed an increase in charge state of the aBPP compared to both the gBPP and unmodified BPP peptide that results from the neutral loss of GlcNAc (Figure 2-7A). This feature can be used as an additional signature to validate the identity of the original glycopeptides. Importantly, the “scar” on aBPP can be useful for GlcNAc site determination, given that it results in a signature loss of 0.984 Da on *b*-and *y*-ions that carry the amino-Ser (Figure 2-7B). The major advantage of using ABBE over the more popular BEMAD is that, since the whole reaction is performed using volatile reagent, no extra clean-up step is needed. Given that the present of any non-volatile reagent will interfere with LC-MS^2 analysis and suppress the ionization of the peptides, the workflow that we proposed has the advantage of lessening potential interference from the sample preparation steps. Moreover, since ABBE has replaced the

sugar structure with a primary amine group, an ABBE-peptide is no longer susceptible for neutral loss and can be ionized as efficiently as an unmodified peptide. As a result, it is sufficient to analyze the sample with a regular CID fragmentation without the need for specialized fragmentation such as HCD for site identification. However, since an extra charge is potentially added to the ABBE-peptide as demonstrated with our standard *O*-GlcNAc modified peptide, using a decision-tree driven tandem MS to selectively trigger either CID or ETD fragmentation based on the precursor m/z and charge is recommended to obtain optimal result. Lastly, it is imperative to include alkaline phosphatase treatment to the peptide mixture prior to the ABBE reaction to minimize the mapping of phosphorylation sites. Otherwise, all the phospho-containing peptides can be removed via IMAC method before the click reaction to achieve the same purpose. The application of such an approach is described in an accompanying manuscript in this issue (ref). This approach allowed for the identification of 100's of O-GlcNAc modified proteins and sites of modification. It also demonstrated that both the chemoenzymatic and metabolic labeling approaches assign virtually the same set of proteins. This result greatly increases confidence in the identifications given the orthogonal nature of the two labeling approaches.

Furthermore, it is also possible to adapt well-established quantitative proteomic approaches into the click chemistry/ABBE workflow. The most convenient step for incorporating quantitative handlers is at the peptide level. For instance, trypsin-catalyzed oxygen-18/16 ($^{18}O/^{16}O$) labeling can be used for comparing 2 different conditions. Also, if wish to compare more than two conditions, iTRAQ (isobaric tags for relative and absolute quantification)-based technique allows comparison of up to 16 different conditions in parallel[89].

6. Conclusive Remarks

O-GlcNAc modification on the serine and threonine side chains of intracellular proteins is an indispensable dynamic modification with a regulator role that is akin to phosphorylation. However, unlike the techniques that are currently available to investigate the functional role of phosphorylation, options in the *O*-GlcNAc toolbox are less. With recent breakthroughs in methodology for generating *O*-GlcNAc specific antibodies, *O*-GlcNAc modified peptide enrichment protocols and MS-based *O*-GlcNAc site identification strategies, it should be possible for analytical biochemical approaches to drive the field forward and begin to expand on functions for *O*-GlcNAc being assigned to specific residues on defined proteins.

7. Acknowledgement

We thank Sami T. Tuomivaara for discussion and critical reading of this manuscript. This work was supported by a grant from NIH/NIDDK (1RO1DK075069 to LW). CFT is an American Heart Association predoctoral fellow (Southeast affiliate, 0715377B) and a Cousins Foundation fellow (Complex Carbohydrate Research Center, University of Georgia).

8. References

1. Hart, G.W., M.P. Housley, and C. Slawson, *Cycling of O-linked beta-N-acetylglucosamine on nucleocytoplasmic proteins.* Nature, 2007. **446**(7139): p. 1017-22.
2. Chalkley, R.J., et al., *Identification of protein O-GlcNAcylation sites using electron transfer dissociation mass spectrometry on native peptides.* Proc Natl Acad Sci U S A, 2009. **106**(22): p. 8894-9.
3. Vosseller, K., et al., *O-linked N-acetylglucosamine proteomics of postsynaptic density preparations using lectin weak affinity chromatography and mass spectrometry.* Mol Cell Proteomics, 2006. **5**(5): p. 923-34.
4. Hanisch, F.G., *O-glycosylation of the mucin type.* Biol Chem, 2001. **382**(2): p. 143-9.

5. Trinidad, J.C., et al., *Global identification and characterization of both O-GlcNAcylation and phosphorylation at the murine synapse.* Mol Cell Proteomics, 2012. **11**(8): p. 215-29.
6. Hart, G.W., et al., *Cross talk between O-GlcNAcylation and phosphorylation: roles in signaling, transcription, and chronic disease.* Annu Rev Biochem, 2011. **80**: p. 825-58.
7. Yuzwa, S.A., et al., *A potent mechanism-inspired O-GlcNAcase inhibitor that blocks phosphorylation of tau in vivo.* Nat Chem Biol, 2008. **4**(8): p. 483-90.
8. Deng, Y., et al., *Regulation between O-GlcNAcylation and phosphorylation of neurofilament-M and their dysregulation in Alzheimer disease.* FASEB J, 2008. **22**(1): p. 138-45.
9. Li, X., et al., *Concurrent alterations of O-GlcNAcylation and phosphorylation of tau in mouse brains during fasting.* Eur J Neurosci, 2006. **23**(8): p. 2078-86.
10. Lefebvre, T., et al., *Evidence of a balance between phosphorylation and O-GlcNAc glycosylation of Tau proteins--a role in nuclear localization.* Biochim Biophys Acta, 2003. **1619**(2): p. 167-76.
11. Wang, Z., et al., *Extensive crosstalk between O-GlcNAcylation and phosphorylation regulates cytokinesis.* Sci Signal, 2010. **3**(104): p. ra2.
12. Wang, Z., M. Gucek, and G.W. Hart, *Cross-talk between GlcNAcylation and phosphorylation: site-specific phosphorylation dynamics in response to globally elevated O-GlcNAc.* Proc Natl Acad Sci U S A, 2008. **105**(37): p. 13793-8.
13. Wang, Z., A. Pandey, and G.W. Hart, *Dynamic interplay between O-linked N-acetylglucosaminylation and glycogen synthase kinase-3-dependent phosphorylation.* Mol Cell Proteomics, 2007. **6**(8): p. 1365-79.
14. Khidekel, N., et al., *Probing the dynamics of O-GlcNAc glycosylation in the brain using quantitative proteomics.* Nat Chem Biol, 2007. **3**(6): p. 339-48.
15. Goto, H. and M. Inagaki, *Production of a site- and phosphorylation state-specific antibody.* Nat Protoc, 2007. **2**(10): p. 2574-81.
16. Macek, B., M. Mann, and J.V. Olsen, *Global and site-specific quantitative phosphoproteomics: principles and applications.* Annu Rev Pharmacol Toxicol, 2009. **49**: p. 199-221.
17. Beausoleil, S.A., et al., *Large-scale characterization of HeLa cell nuclear phosphoproteins.* Proc Natl Acad Sci U S A, 2004. **101**(33): p. 12130-5.
18. Greis, K.D., et al., *Selective detection and site-analysis of O-GlcNAc-modified glycopeptides by beta-elimination and tandem electrospray mass spectrometry.* Anal Biochem, 1996. **234**(1): p. 38-49.
19. Torres, C.R. and G.W. Hart, *Topography and polypeptide distribution of terminal N-acetylglucosamine residues on the surfaces of intact lymphocytes. Evidence for O-linked GlcNAc.* J Biol Chem, 1984. **259**(5): p. 3308-17.
20. Holt, G.D. and G.W. Hart, *The subcellular distribution of terminal N-acetylglucosamine moieties. Localization of a novel protein-saccharide linkage, O-linked GlcNAc.* J Biol Chem, 1986. **261**(17): p. 8049-57.
21. Teo, C.F., et al., *Glycopeptide-specific monoclonal antibodies suggest new roles for O-GlcNAc.* Nat Chem Biol, 2010. **6**(5): p. 338-43.
22. Comer, F.I., et al., *Characterization of a mouse monoclonal antibody specific for O-linked N-acetylglucosamine.* Anal Biochem, 2001. **293**(2): p. 169-77.
23. Snow, C.M., A. Senior, and L. Gerace, *Monoclonal antibodies identify a group of nuclear pore complex glycoproteins.* J Cell Biol, 1987. **104**(5): p. 1143-56.
24. Gilfix, B.M. and B.D. Sanwal, *Relationship between cell surface asparagine-linked glycoproteins and myoblast differentiation. Analysis of wheat germ agglutinin-resistant mutants.* Can J Biochem Cell Biol, 1984. **62**(1): p. 60-71.

25. Moullier, P., et al., *Comparative binding of wheat germ agglutinin and its succinylated form on lymphocytes.* Eur J Biochem, 1986. **161**(1): p. 197-204.
26. Hanover, J.A., et al., *O-linked N-acetylglucosamine is attached to proteins of the nuclear pore. Evidence for cytoplasmic and nucleoplasmic glycoproteins.* J Biol Chem, 1987. **262**(20): p. 9887-94.
27. Kelly, W.G. and G.W. Hart, *Glycosylation of chromosomal proteins: localization of O-linked N-acetylglucosamine in Drosophila chromatin.* Cell, 1989. **57**(2): p. 243-51.
28. Jackson, S.P. and R. Tjian, *Purification and analysis of RNA polymerase II transcription factors by using wheat germ agglutinin affinity chromatography.* Proc Natl Acad Sci U S A, 1989. **86**(6): p. 1781-5.
29. Isakson, P.C., et al., *T cell-derived B cell differentiation factor(s). Effect on the isotype switch of murine B cells.* J Exp Med, 1982. **155**(3): p. 734-48.
30. Buskas, T., P. Thompson, and G.J. Boons, *Immunotherapy for cancer: synthetic carbohydrate-based vaccines.* Chem Commun (Camb), 2009(36): p. 5335-49.
31. Holt, G.D., et al., *Nuclear pore complex glycoproteins contain cytoplasmically disposed O-linked N-acetylglucosamine.* J Cell Biol, 1987. **104**(5): p. 1157-64.
32. Turner, J.R., A.M. Tartakoff, and N.S. Greenspan, *Cytologic assessment of nuclear and cytoplasmic O-linked N-acetylglucosamine distribution by using anti-streptococcal monoclonal antibodies.* Proc Natl Acad Sci U S A, 1990. **87**(15): p. 5608-12.
33. Ludemann, N., et al., *O-glycosylation of the tail domain of neurofilament protein M in human neurons and in spinal cord tissue of a rat model of amyotrophic lateral sclerosis (ALS).* J Biol Chem, 2005. **280**(36): p. 31648-58.
34. Yuzwa, S.A., et al., *Mapping O-GlcNAc modification sites on tau and generation of a site-specific O-GlcNAc tau antibody.* Amino Acids, 2011. **40**(3): p. 857-68.
35. Fujiki, R., et al., *GlcNAcylation of histone H2B facilitates its monoubiquitination.* Nature, 2011. **480**(7378): p. 557-60.
36. Kamemura, K., et al., *Dynamic interplay between O-glycosylation and O-phosphorylation of nucleocytoplasmic proteins: alternative glycosylation/phosphorylation of THR-58, a known mutational hot spot of c-Myc in lymphomas, is regulated by mitogens.* J Biol Chem, 2002. **277**(21): p. 19229-35.
37. Kelly, W.G., M.E. Dahmus, and G.W. Hart, *RNA polymerase II is a glycoprotein. Modification of the COOH-terminal domain by O-GlcNAc.* J Biol Chem, 1993. **268**(14): p. 10416-24.
38. Ingale, S., et al., *Increasing the antigenicity of synthetic tumor-associated carbohydrate antigens by targeting Toll-like receptors.* Chembiochem, 2009. **10**(3): p. 455-63.
39. Ingale, S., et al., *Robust immune responses elicited by a fully synthetic three-component vaccine.* Nat Chem Biol, 2007. **3**(10): p. 663-7.
40. Lakshminarayanan, V., et al., *Immune recognition of tumor-associated mucin MUC1 is achieved by a fully synthetic aberrantly glycosylated MUC1 tripartite vaccine.* Proc Natl Acad Sci U S A, 2012. **109**(1): p. 261-6.
41. Springhorn, C., et al., *Exploring leukocyte O-GlcNAcylation as a novel diagnostic tool for the earlier detection of type 2 diabetes mellitus.* J Clin Endocrinol Metab, 2012. **97**(12): p. 4640-9.
42. Madsen-Bouterse, S.A., et al., *Quantification of O-GlcNAc protein modification in neutrophils by flow cytometry.* Cytometry A, 2008. **73**(7): p. 667-72.

43. Wells, L., et al., *Mapping sites of O-GlcNAc modification using affinity tags for serine and threonine post-translational modifications.* Mol Cell Proteomics, 2002. **1**(10): p. 791-804.
44. Boyce, M. and C.R. Bertozzi, *Bringing chemistry to life.* Nat Methods, 2011. **8**(8): p. 638-42.
45. Mahal, L.K., K.J. Yarema, and C.R. Bertozzi, *Engineering chemical reactivity on cell surfaces through oligosaccharide biosynthesis.* Science, 1997. **276**(5315): p. 1125-8.
46. Saxon, E. and C.R. Bertozzi, *Cell surface engineering by a modified Staudinger reaction.* Science, 2000. **287**(5460): p. 2007-10.
47. Tai, H.C., et al., *Parallel identification of O-GlcNAc-modified proteins from cell lysates.* J Am Chem Soc, 2004. **126**(34): p. 10500-1.
48. Khidekel, N., et al., *Exploring the O-GlcNAc proteome: direct identification of O-GlcNAc-modified proteins from the brain.* Proc Natl Acad Sci U S A, 2004. **101**(36): p. 13132-7.
49. Khidekel, N., et al., *A chemoenzymatic approach toward the rapid and sensitive detection of O-GlcNAc posttranslational modifications.* J Am Chem Soc, 2003. **125**(52): p. 16162-3.
50. Ramakrishnan, B. and P.K. Qasba, *Structure-based design of beta 1,4-galactosyltransferase I (beta 4Gal-T1) with equally efficient N-acetylgalactosaminyltransferase activity: point mutation broadens beta 4Gal-T1 donor specificity.* J Biol Chem, 2002. **277**(23): p. 20833-9.
51. Vocadlo, D.J., et al., *A chemical approach for identifying O-GlcNAc-modified proteins in cells.* Proc Natl Acad Sci U S A, 2003. **100**(16): p. 9116-21.
52. Laughlin, S.T. and C.R. Bertozzi, *Metabolic labeling of glycans with azido sugars and subsequent glycan-profiling and visualization via Staudinger ligation.* Nat Protoc, 2007. **2**(11): p. 2930-44.
53. Boyce, M., et al., *Metabolic cross-talk allows labeling of O-linked beta-N-acetylglucosamine-modified proteins via the N-acetylgalactosamine salvage pathway.* Proc Natl Acad Sci U S A, 2011. **108**(8): p. 3141-6.
54. Hang, H.C., et al., *A metabolic labeling approach toward proteomic analysis of mucin-type O-linked glycosylation.* Proc Natl Acad Sci U S A, 2003. **100**(25): p. 14846-51.
55. Holden, H.M., I. Rayment, and J.B. Thoden, *Structure and function of enzymes of the Leloir pathway for galactose metabolism.* J Biol Chem, 2003. **278**(45): p. 43885-8.
56. Frey, P.A., *The Leloir pathway: a mechanistic imperative for three enzymes to change the stereochemical configuration of a single carbon in galactose.* FASEB J, 1996. **10**(4): p. 461-70.
57. Rexach, J.E., et al., *Quantification of O-glycosylation stoichiometry and dynamics using resolvable mass tags.* Nat Chem Biol, 2010. **6**(9): p. 645-51.
58. Rexach, J.E., et al., *Dynamic O-GlcNAc modification regulates CREB-mediated gene expression and memory formation.* Nat Chem Biol, 2012. **8**(3): p. 253-61.
59. Yi, W., et al., *Phosphofructokinase 1 glycosylation regulates cell growth and metabolism.* Science, 2012. **337**(6097): p. 975-80.
60. Wang, Z. and G. Hart, *Glycomic Approaches to Study GlcNAcylation: Protein Identification, Site-mapping, and Site-specific O-GlcNAc Quantitation.* Clinical Proteomics, 2008. **4**(1-2): p. 5-13.
61. Haynes, P.A. and R. Aebersold, *Simultaneous detection and identification of O-GlcNAc-modified glycoproteins using liquid chromatography-tandem mass spectrometry.* Anal Chem, 2000. **72**(21): p. 5402-10.

62. Schroeder, M.J., et al., *Methods for the detection of paxillin post-translational modifications and interacting proteins by mass spectrometry.* J Proteome Res, 2005. **4**(5): p. 1832-41.
63. Syka, J.E., et al., *Peptide and protein sequence analysis by electron transfer dissociation mass spectrometry.* Proc Natl Acad Sci U S A, 2004. **101**(26): p. 9528-33.
64. Fong, J.J., et al., *beta-N-Acetylglucosamine (O-GlcNAc) is a novel regulator of mitosis-specific phosphorylations on histone H3.* J Biol Chem, 2012. **287**(15): p. 12195-203.
65. Klein, A.L., et al., *O-linked N-acetylglucosamine modification of insulin receptor substrate-1 occurs in close proximity to multiple SH2 domain binding motifs.* Mol Cell Proteomics, 2009. **8**(12): p. 2733-45.
66. Housley, M.P., et al., *A PGC-1alpha-O-GlcNAc transferase complex regulates FoxO transcription factor activity in response to glucose.* J Biol Chem, 2009. **284**(8): p. 5148-57.
67. Olsen, J.V., et al., *Higher-energy C-trap dissociation for peptide modification analysis.* Nat Methods, 2007. **4**(9): p. 709-12.
68. Zhao, P., et al., *Combining high-energy C-trap dissociation and electron transfer dissociation for protein O-GlcNAc modification site assignment.* J Proteome Res, 2011. **10**(9): p. 4088-104.
69. Hahne, H. and B. Kuster, *A novel two-stage tandem mass spectrometry approach and scoring scheme for the identification of O-GlcNAc modified peptides.* J Am Soc Mass Spectrom, 2011. **22**(5): p. 931-42.
70. Hahne, H., A. Moghaddas Gholami, and B. Kuster, *Discovery of O-GlcNAc-modified proteins in published large-scale proteome data.* Mol Cell Proteomics, 2012. **11**(10): p. 843-50.
71. Hayes, B.K., K.D. Greis, and G.W. Hart, *Specific isolation of O-linked N-acetylglucosamine glycopeptides from complex mixtures.* Anal Biochem, 1995. **228**(1): p. 115-22.
72. Vosseller, K., et al., *Quantitative analysis of both protein expression and serine / threonine post-translational modifications through stable isotope labeling with dithiothreitol.* Proteomics, 2005. **5**(2): p. 388-98.
73. Ball, L.E., M.N. Berkaw, and M.G. Buse, *Identification of the major site of O-linked beta-N-acetylglucosamine modification in the C terminus of insulin receptor substrate-1.* Mol Cell Proteomics, 2006. **5**(2): p. 313-23.
74. Yang, W.H., et al., *Modification of p53 with O-linked N-acetylglucosamine regulates p53 activity and stability.* Nat Cell Biol, 2006. **8**(10): p. 1074-83.
75. Hu, Y., et al., *Increased enzymatic O-GlcNAcylation of mitochondrial proteins impairs mitochondrial function in cardiac myocytes exposed to high glucose.* J Biol Chem, 2009. **284**(1): p. 547-55.
76. Olson, S.K., et al., *Identification of novel chondroitin proteoglycans in Caenorhabditis elegans: embryonic cell division depends on CPG-1 and CPG-2.* J Cell Biol, 2006. **173**(6): p. 985-94.
77. Myers, S.A., B. Panning, and A.L. Burlingame, *Polycomb repressive complex 2 is necessary for the normal site-specific O-GlcNAc distribution in mouse embryonic stem cells.* Proc Natl Acad Sci U S A, 2011. **108**(23): p. 9490-5.
78. Myers, S.A., et al., *Electron transfer dissociation (ETD): The mass spectrometric breakthrough essential for O-GlcNAc protein site assignments-a study of the O-GlcNAcylated protein Host Cell Factor C1.* Proteomics, 2013. **13**(6): p. 982-91.

79. Zeidan, Q., et al., *O-GlcNAc cycling enzymes associate with the translational machinery and modify core ribosomal proteins.* Mol Biol Cell, 2010. **21**(12): p. 1922-36.
80. Sakabe, K., Z. Wang, and G.W. Hart, *Beta-N-acetylglucosamine (O-GlcNAc) is part of the histone code.* Proc Natl Acad Sci U S A, 2010. **107**(46): p. 19915-20.
81. Wang, Z., et al., *Site-specific GlcNAcylation of human erythrocyte proteins: potential biomarker(s) for diabetes.* Diabetes, 2009. **58**(2): p. 309-17.
82. Dias, W.B., et al., *Regulation of calcium/calmodulin-dependent kinase IV by O-GlcNAc modification.* J Biol Chem, 2009. **284**(32): p. 21327-37.
83. Hahne, H., et al., *Proteome wide purification and identification of O-GlcNAc-modified proteins using click chemistry and mass spectrometry.* J Proteome Res, 2013. **12**(2): p. 927-36.
84. Wang, Z., et al., *Enrichment and site mapping of O-linked N-acetylglucosamine by a combination of chemical/enzymatic tagging, photochemical cleavage, and electron transfer dissociation mass spectrometry.* Mol Cell Proteomics, 2010. **9**(1): p. 153-60.
85. Alfaro, J.F., et al., *Tandem mass spectrometry identifies many mouse brain O-GlcNAcylated proteins including EGF domain-specific O-GlcNAc transferase targets.* Proc Natl Acad Sci U S A, 2012. **109**(19): p. 7280-5.
86. Rademaker, G.J., et al., *Mass spectrometric determination of the sites of O-glycan attachment with low picomolar sensitivity.* Anal Biochem, 1998. **257**(2): p. 149-60.
87. Sletten, E.M., et al., *Difluorobenzocyclooctyne: synthesis, reactivity, and stabilization by beta-cyclodextrin.* J Am Chem Soc, 2010. **132**(33): p. 11799-805.
88. Mbua, N.E., et al., *Strain-promoted alkyne-azide cycloadditions (SPAAC) reveal new features of glycoconjugate biosynthesis.* Chembiochem, 2011. **12**(12): p. 1912-21.
89. Evans, C., et al., *An insight into iTRAQ: where do we stand now?* Anal Bioanal Chem, 2012. **404**(4): p. 1011-27.

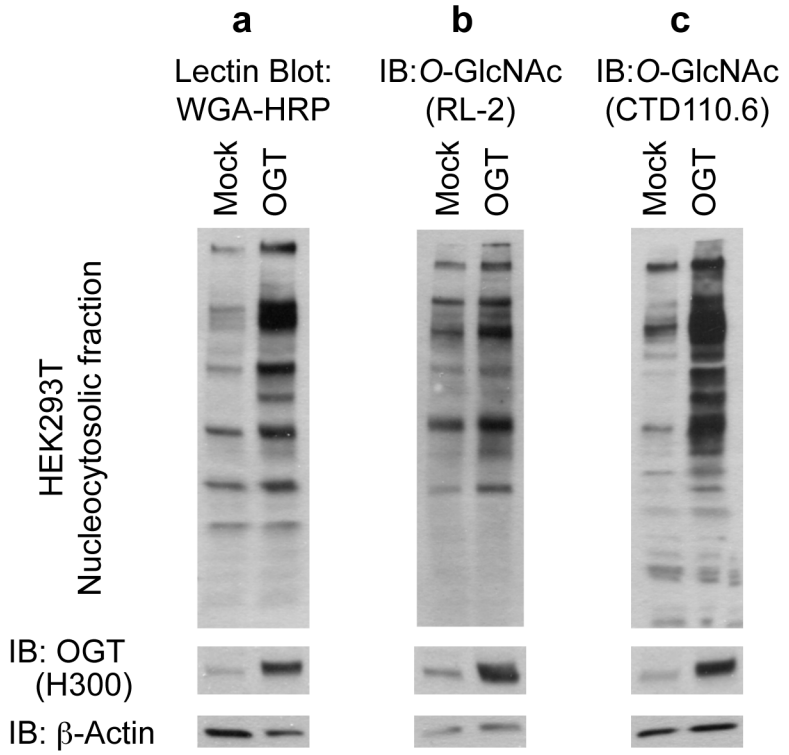

Figure 2-1. Detection of global *O*-GlcNAc levels. (a) WGA-HRP, (b) RL-2 and (c) CTD110.6 were used to probe for *O*-GlcNAc modified proteins. Compared to mock treatment, HEK293T cells overexpressing OGT show an increase in global *O*-GlcNAc levels. Western blots against OGT and β-actin are included for transfection and loading controls, respectively.

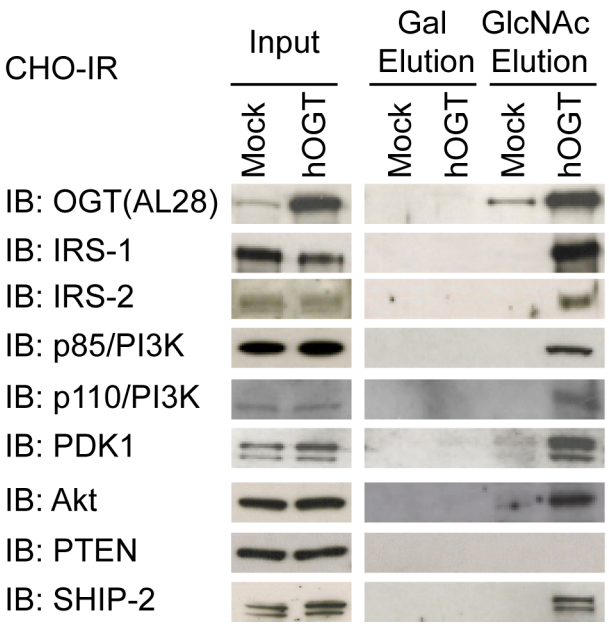

Figure 2-2. sWGA agarose affinity pull-down examination of the *O*-GlcNAc status of insulin signaling proteins. Nucleocytoplasmic extracts prepared from mock and OGT transfected CHO-IR cells were used for sWGA affinity pull-down. After sequential elutions with galactose (non-specific) and GlcNAc (specific), both input and eluates were subjected to immunoblotting using antibodies recognizing IRS-1, IRS-2, p85 (the regulatory subunit of PI3 kinase), p110 (the catalytic subunit of PI3 kinase), PDK1, Akt, PTEN and SHIP-2. OGT western blot is also included as a positive control since OGT is known to be autoglycosylated. The data reveal that, except for PTEN, proteins participating in the IRS/PI3K/Akt cascade are either *O*-GlcNAc modified or interact with *O*-GlcNAc modified proteins.

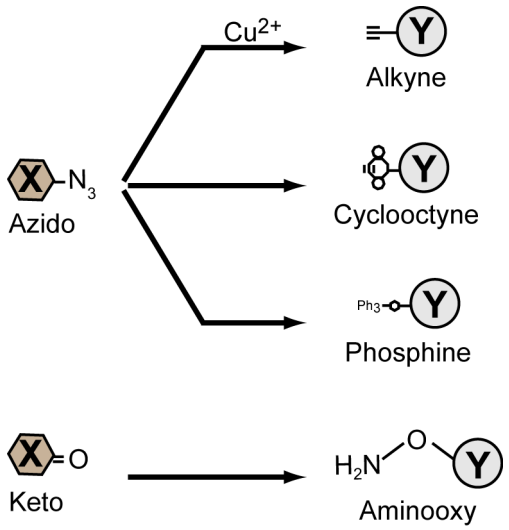

Figure 2-3. Bioorthogonal pairs for click chemistry. An azido group on a biomolecule of interest (X) can undergo either copper(II)-dependent (via alkyne) or copper(II)-independent (via cyclooctyne or phosphine) conjugation to a specific chemical handle (Y). Likewise, a keto group on X can react with an aminooxy group to form a covalent conjugate to Y.

Figure 2-4. Detection of *O*-GlcNAc modified proteins via metabolic labeling. Biotin-phosphine was reacted with nucleocytoplasmic proteins extracted from + Ac_4GalNAz treated or control HEK293FT cells. The presence of biotinylated *O*-GlcNAc modified proteins is probed with streptavidin conjugated to HPR. Western blot against β-actin is shown as a loading control.

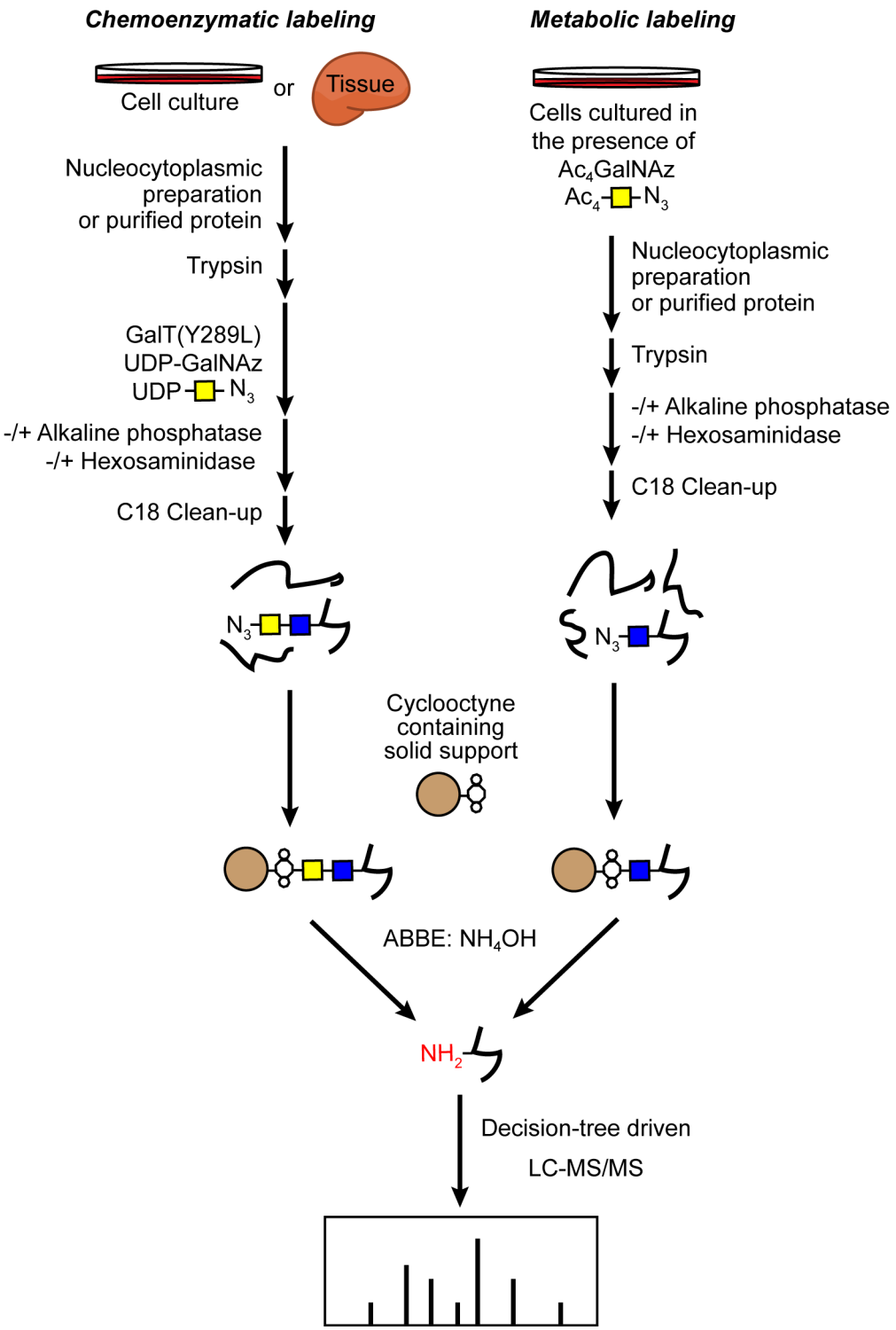
Chemoenzymatic labeling
Metabolic labeling
Cell culture
or
Tissue
Nucleocytoplasmic preparation or purified protein
Trypsin
GalT(Y289L)
UDP-GalNAz
UDP-N3
-/+ Alkaline phosphatase
-/+ Hexosaminidase
C18 Clean-up
Cells cultured in the presence of Ac4GalNAz
Ac4-N3
Nucleocytoplasmic preparation or purified protein
Trypsin
-/+ Alkaline phosphatase
-/+ Hexosaminidase
C18 Clean-up
N3
N3
Cyclooctyne containing solid support
ABBE: NH4OH
NH2
Decision-tree driven
LC-MS/MS

Figure 2-5. A proposed novel workflow that combines click-chemistry, ammonia-based β-elimination (ABBE) and tandem MS analysis. The incorporation of an azido group onto the *O*-GlcNAc moiety can be done either at the peptide or protein level by chemoenzymatic or metabolic labeling, respectively. Upon further processing as outlined in the figure, azido-containing *O*-GlcNAc modified peptides are captured via click chemistry onto a solid support. After extensive washing, conjugated peptides are eluted with ABBE to obtain peptides with "scars" on the original glycosylation sites. These peptides can be identified with LC-MS/MS analysis since they are chemically distinct from both unmodified and *O*-GlcNAc modified peptides.

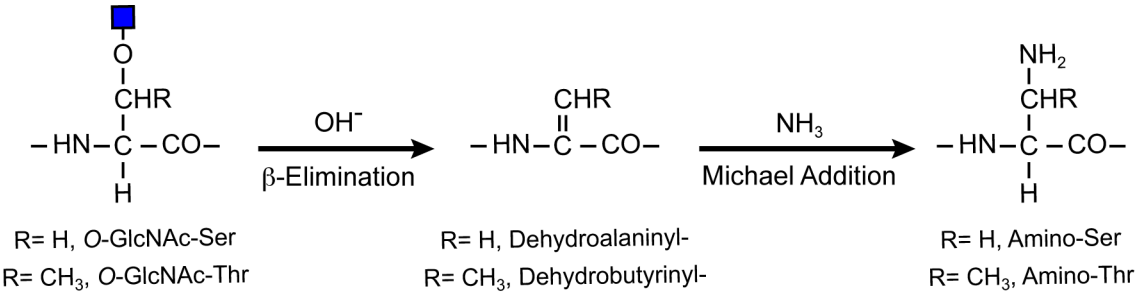

Figure 2-6. Ammonium hydroxide-based β-elimination (ABBE). The alkalinity of NH_4OH is sufficient to trigger β-elimination of the glycosidic linkage on the serine or threonine side chain leading to the formation of dehydroalanyl or dehydrobutyrinyl group, respectively. The α,β-unsaturated carbonyl group resulting from β-elimination is prone to Michael addition with ammonia (NH_3) as the nucleophile. As a consequence, the GlcNAc moiety is replaced with an amino group, which leaves a "scar" on the peptide backbone that is discernable in MS/MS fragmentation.

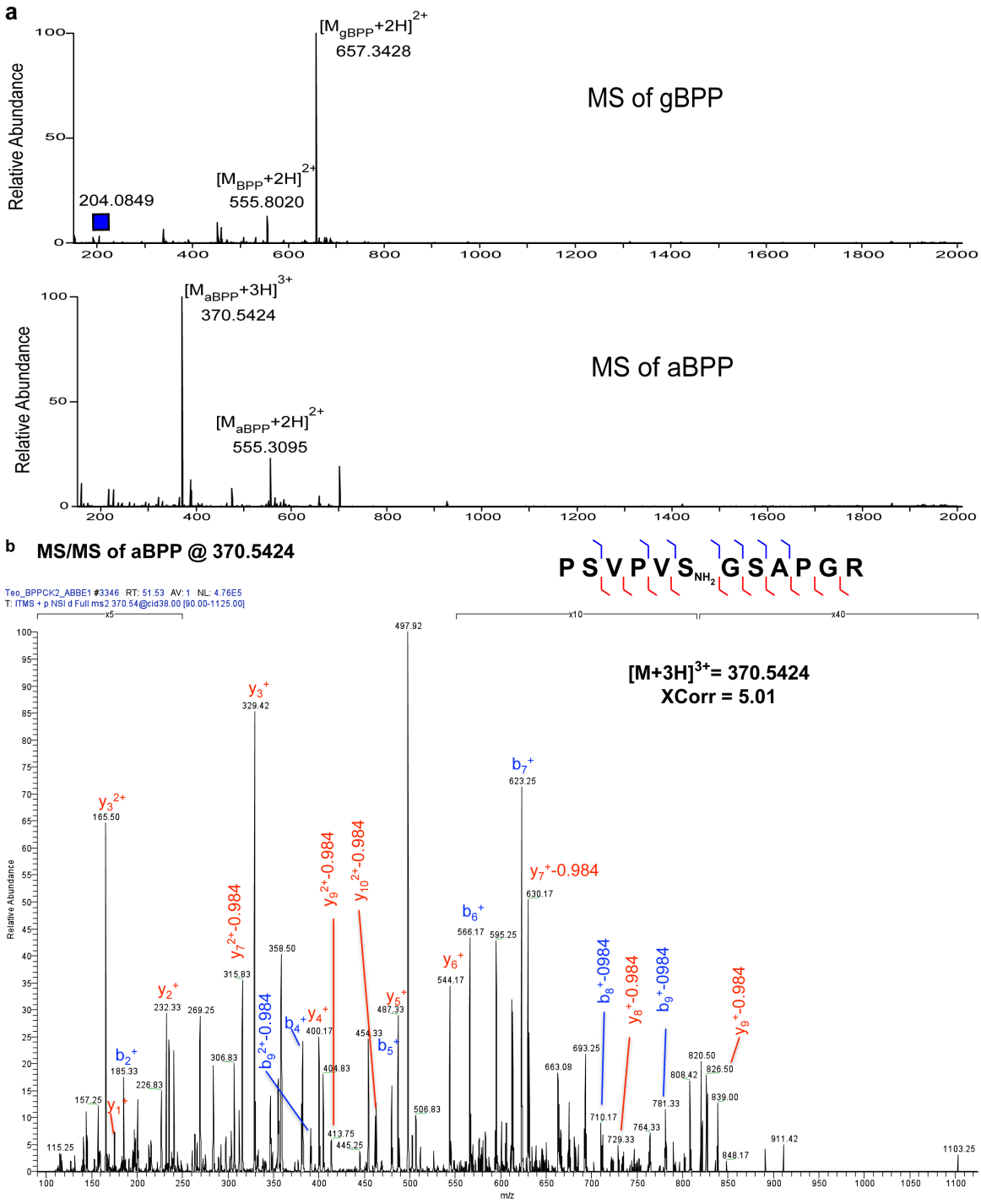
a
Relative Abundance
[MgBPP+2H]2+
657.3428
MS of gBPP
[MBPP+2H]2+
555.8020
204.0849
[MaBPP+3H]3+
370.5424
MS of aBPP
[MaBPP+2H]2+
555.3095
b
MS/MS of aBPP @ 370.5424
P S V P V S NH2 G S A P G R
[M+3H]3+= 370.5424
XCorr = 5.01
m/z

Figure 2-7. MS analysis on a standard *O*-GlcNAc modified peptide (gBPP) and its ABBE-derivative (aBPP). (a) Full MS analysis of gBPP (upper panel) reveals a doubly charged species (m/z= 657.3428) and its pseudo-neutral loss product ions (m/z= 555.8020, double charged peptide, and m/z= 204.0849, a protonated HexNAc ion). Upon ABBE treatment, full MS analysis of aBPP (lower panel) shows a predominant triply charge peak (m/z= 370.5424) and a minor doubly charge species (m/z = 555.3095). (b) CID fragmentation of aBPP. Since ABBE treatment leaves a scar (loss of 0.984 Da) on Ser-5, it is possible to pinpoint this site as the *O*-GlcNAc site based on fragment ions *b*-5 to *b*-11 and *y*-7 to *y*-11.

Table 2-1. Comparison of different approaches to determine *O*-GlcNAc site.

Method	Structural feature on the Ser/Thr side chain	Enrichment efficiency	Ease of clean-up	Ionization efficiency	Pseudo-neutral loss	LC-tandem MS technique
BEMAD	-DTT	+	+	++	No	Decision-tree MS^2
LWAC	-*O*-GlcNAc	+*	+++	++	Yes	DDNL-MS^3, ETD, HCD
Click chemistry/Biotin	-*O*-GlcNAc-Galz-PEG-Biotin or -*O*-GlcNAz-PEG-Biotin	+++	+	+	Yes	DDNL-MS^n, ETD, HCD
Click chemistry/BEMAD	-DTT	+++	+	++	No	Decision-tree MS^2
Click chemistry/Photo-cleavable biotin tag	-*O*-GlcNAc-Galz-AMT or -*O*-GlcNAz-AMT	+++	++	++	Yes	DDNL-MS^n, ETD, HCD
Click chemistry/ABBE[#]	$-NH_2$	+++	++++	+++	No	Decision-tree MS^2

* Required a 39 feet column.

[#] Proposed workflow. Have not been widely implemented compared to other approaches.

CHAPTER 3

GLYCOPEPTIDE-SPECIFIC MONOCLONAL ANTIBODIES SUGGEST NEW ROLES FOR *O*-GLCNAC[#]

[#]Teo CF*, Ingale S*, Wolfert MA*, Elsayed GA, Nöt LG, Chathem JC, Wells L & Boons GJ. 2010. *Nat. Chem. Biol.*, **6**: 338-343. (*Equal contribution)

Abstract

Studies of post-translational modification by β-*N*-acetyl-D-glucosamine (*O*-GlcNAc) are hampered by a lack of efficient tools such as *O*-GlcNAc–specific antibodies that can be used for detection, isolation and site localization. We have obtained a large panel of *O*-GlcNAc–specific IgG monoclonal antibodies having a broad spectrum of binding partners by combining three-component immunogen methodology with hybridoma technology. Immunoprecipitation followed by large-scale shotgun proteomics led to the identification of more than 200 mammalian *O*-GlcNAc–modified proteins, including a large number of new glycoproteins. A substantial number of the glycoproteins were enriched by only one of the antibodies. This observation, combined with the results of inhibition ELISAs, suggests that the antibodies, in addition to their *O*-GlcNAc dependence, also appear to have different but overlapping local peptide determinants. The monoclonal antibodies made it possible to delineate differentially modified proteins of liver in response to trauma-hemorrhage and resuscitation in a rat model.

1. Introduction

O-glycosylation of serine and threonine of nuclear and cytoplasmic proteins by a single *O*-GlcNAc moiety is a ubiquitous post-translational modification that is highly dynamic and that fluctuates in response to cellular stimuli through the action of the cycling enzymes *O*-linked GlcNAc transferase (OGT) and *O*-GlcNAcase (OGA)[1]. This type of glycosylation has been implicated in many cellular processes, frequently via interplay with phosphorylation[2, 3]. Alteration of *O*-GlcNAc levels has been linked to the etiology of prevalent human diseases including type II diabetes and Alzheimer's disease[4-7]. Furthermore, a number of recent studies have shown that acute increases in *O*-GlcNAc levels attenuate cellular injury arising from a variety of stress stimuli including hypoxia and ischemia/reperfusion[8-10].

Unlike phosphorylation, for which a wide range of pan- and site-specific phospho-antibodies are available, studies of *O*-GlcNAc modification are hampered by a lack of effective tools for its detection, quantification and site localization. Though metabolic, lectin based and chemo-enzymatic approaches have been fruitful[11, 12], only two pan-specific *O*-GlcNAc antibodies have been described: an IgM pan-*O*-GlcNAc antibody (CTD 110.6; Ref.[13]) and an IgG antibody raised against *O*-GlcNAc–modified components of the nuclear pore (RL-2; Ref.[14]) that shows restricted cross-reactivity with *O*-GlcNAc–modified proteins. Both antibodies suffer from relatively low binding affinities, and thus in many cases can only be used for the detection of multiple modified, higher molecular weight or highly abundant proteins[11]. Furthermore, IgM antibodies cannot easily be used for immunoprecipitation because they do not bind to protein A/G–agarose, and immobilization by chemical crosslinking often leads to loss of binding activity. We reasoned that *O*-GlcNAc–specific antibodies can be elicited by using a three-component immunogen (compound 1, Figure 3-1) composed of an *O*-GlcNAc–containing peptide (which in this study is derived from casein kinase II (CKII) α-subunit[15]), a well-documented mouse major histocompatibility complex (MHC) class II restricted helper T-cell epitope, and a Toll-like receptor-2 (TLR2) agonist as an in-built adjuvant. Such a compound was expected to circumvent immune suppression caused by a carrier protein or linker region of a classical conjugate vaccine; yet it contains all mediators required for eliciting a strong and relevant IgG immune response[16]. We found that immunization with 1 followed by standard hydridoma technology gives a large panel of IgG monoclonal antibodies that in addition to *O*-GlcNAc dependence also appear to have different but overlapping local peptide determinants. The power of the new monoclonal antibodies has been demonstrated by large-scale enrichment of *O*-GlcNAc–modified proteins followed by shotgun proteomics, which led to the identification of more than 200 mammalian *O*-GlcNAc–modified proteins, including a large number of

new glycoproteins. The new methodology has been applied to the identification of specific proteins that exhibit changes in *O*-GlcNAc status in response to trauma-hemorrhage and resuscitation in a rat model. We postulate that several of these proteins have the potential to modulate the response of the liver to stress.

2. Results

We obtained compound 1 by liposome-mediated native chemical ligation[16] (Figure 3-1 and Figure 3-S1) and incorporated it into phospholipid-based small unilamellar vesicles, which we then used for immunization of female BALB/c mice at biweekly intervals four times (Supplementary Methods). ELISA demonstrated that compound 1 had elicited excellent titers of IgG antibodies against CGSTPVS(β-*O*-GlcNAc)SANM (3) linked to bovine serum albumin (BSA) (Table 3-S1). Notably, immunizations with compound 2, which has an artificial thio-linked GlcNAc moiety, did not elicit substantially higher titers of glycopeptide-selective antibodies, indicating that compound 1 is sufficiently metabolically stable to induce such antibodies. Furthermore, a conjugate composed of glycopeptide 3 linked to the carrier protein KLH did not elicit relevant antibodies, and the immune response was directed to the carrier protein and linker.

We harvested the spleens of two mice immunized with 1, and standard hybridoma culture technology gave 7 IgG1-, 7 IgG2a-, 2 IgG2b- and 14 IgG3-producing hybridoma cell lines (Figure 3-S2 and Table 3-S2). All monoclonal antibodies recognized 3 linked to BSA, whereas only a small number bound to the peptide CGSTPVSSANM (4) conjugated to BSA. Furthermore, the interaction of 20 monoclonal antibodies could be inhibited with the glycopeptide GSTPVS(β-*O*-GlcNAc) SANM (5) but not with peptide GSTPVSSANM (6) and not with β-*O*-GlcNAc-Ser (7), which demonstrates that the antibodies have glycopeptide specificity.

We cultured three hybridomas (18B10.C7(3), 9D1.E4(10) and 1F5.D6(14)) at a 1-liter scale and purified the resulting IgG antibodies by saturated ammonium sulfate precipitation followed by protein G chromatography. Inhibition ELISA confirmed that the monoclonal antibodies require carbohydrate and peptide (glycopeptide) and demonstrated that they bind subtly different epitopes. 1F5.D6(14) could be inhibited by a glycosylated tripeptide (9), whereas 18B10.C7(3) required a glycosylated pentapeptide (8) and 9D1.E3(10) was inhibited only by the full-length B-epitope 5 (Supplementary Figure 3-3).

To establish the usefulness of the monoclonal antibodies for immunodetection, we immunoprecipitated the CKII α-subunit from human embryonic kidney (HEK) 293T lysates with and without exogenous overexpression of OGT, and we subjected the eluates to standard immunoblotting procedures. Whereas equal amounts of the CKII α-subunit were pulled down, the monoclonal antibodies showed cross-reactivity toward a band corresponding to the CKII α-subunit with an increased signal for the OGT overexpressed sample, which supports the notion that recognition is dependent on the presence of GlcNAc (Figure 3-2a). The specificity of the monoclonal antibodies was further evaluated in mammalian cell crude extracts by genetically manipulating OGA or OGT levels. Importantly, three distinct global *O*-GlcNAc levels were observed, in which lysates with OGA, mock and OGT transfection yielded the lowest, median and highest modification status, respectively, which is in agreement with the expression levels of the cycling enzymes (Figure 3-2b). The results imply that although the epitope was derived from a single protein, the monoclonal antibodies have a broad spectrum of binding targets. We also demonstrated that a substantial number of the glycoproteins enriched by the new monoclonal antibodies crossreact with the anti-*O*-GlcNAc IgM CTD110.6 (Figure 3-2c).

We used the new monoclonal antibodies and CTD110.6 for large scale

enrichment of *O*-GlcNAc–modified proteins for shotgun proteomics. We mixed monoclonal antibodies covalently conjugated to agarose with nucleocytoplasmic proteins extracted from HEK293T cells cultured in the presence of the OGA inhibitor PUGNAc (Ref.[17]). The released proteins were digested by Lys-C, and the recovered peptides were detected by LC-MS/MS on an LTQ-XL spectrometer and analyzed by TurboSequest and ProteoIQ. Using the three new monoclonal antibodies, we identified 215 *O*-GlcNAc–modified proteins, 140 of which are new (Tables 3-S3). We found a large number of previously characterized *O*-GlcNAc–modified proteins[18], such as SP1, OGT and nuclear pore protein p62, which adds confidence to proper assignment and further supports the selectivity of the antibodies for the *O*-GlcNAc modification. However, the possibility that some proteins may have been co-purified owing to tight association to *O*-GlcNAc–modified proteins cannot be excluded. Immunoprecipitation with the IgM antibody CTD110.6 led to the identification of a limited number of proteins, highlighting the favorable properties of the new antibodies.

The extensive list of *O*-GlcNAc–modified proteins made it possible to assign biological functions using the Human Protein Reference Database (http://www.hprd.org/) (Figure 3-2d). A large number of identified proteins are involved in transcriptional/translational regulation and signal transduction (Table 3-1; Tables 3-S4 and 3-S5), which is consistent with recent reports that functionally implicate *O*-GlcNAc modification in insulin signaling and transcriptional control[19-21]. Notably, several of the glycoproteins are involved in the ubiquitin pathway. A role for *O*-GlcNAc has already been established for regulation of the proteasome[22], but our data indicate that *O*-GlcNAc may also be actively involved in earlier steps of the degradation cascade. SEC23 components and interacting proteins were also captured by multiple antibodies, suggesting a possible role for *O*-GlcNAc modification in anterograde trafficking of intracellular vesicles. Finally, several ribosomal proteins were observed, which is in

agreement with the recent finding that *O*-GlcNAc modification of ribosomal proteins plays a role in stress granule and processing body assembly[23].

Several newly identified *O*-GlcNAc proteins were observed via only one of the new antibodies (Tables 3-S4 and 3-S5), and 1F5.D6(14) recognized the most proteins, which is consistent with the fact that it has the broadest inhibition profile (Figure 3-S3). Many of the new proteins participate in other types of posttranslational modifications, such as WNK2 and WNK3 for phosphorylation and RanBP2 and SUMO4 for SUMOylation. Also, a range of proteins that modulate gene expression at the chromatin levels, such as SMARCC1 and CARM1, were isolated by only a subset of the new antibodies.

Next, the methodology was used for characterization of *O*-GlcNAc–modified proteins in liver samples from rats subjected to trauma-hemorrhage followed by resuscitation (TH-R) and sham controls. Recent studies[4, 8-10, 24] have demonstrated that loss of *O*-GlcNAcylation following TH-R leads to organ dysfunction, increased injury and decreased survival; however, no *O*-GlcNAc proteins have been identified as potential candidates for mediating this response. As expected, evaluation of crude tissue samples by western blots showed substantially lower overall hepatic *O*-GlcNAc levels 24 h after TH-R compared to sham controls by all three monoclonal antibodies generated in this study, as well as CTD110.6 (Figure 3-3 and Figure 3-S4). To provide insight into proteins whose *O*-GlcNAc status is modified by TH-R, we enriched sham proteins from liver extracts and proteins from liver extracts treated with TH-R using the monoclonal antibody 1F5.D6(14), and we analyzed the proteins by shotgun proteomics in triplicate. Following stringent filtering, we assigned 68 proteins in the sham group and 30 proteins from the TH-R liver samples as putatively *O*-GlcNAc modified, which resulted in 46 new *O*-GlcNAc–modified proteins (Figure 3-3 and Tables 3-S6 and 3-S7). Though global *O*-GlcNAc levels were reduced in the TH-R samples compared to sham, 10 of the 30

identified proteins in the TH-R samples were not detected in samples from the sham, although there appeared to be no significant changes in selected protein abundances in crude extracts from the two groups (Figure 3-S5).

3. Discussion

High-affinity pan-specific antibodies are expected to offer convenient and robust tools for exploring the *O*-GlcNAc proteome. However, such antibodies have been difficult to generate, probably due to the fact that *O*-GlcNAc–modified epitopes are self-antigens that are tolerated by the immune system, and because carbohydrateprotein interactions are relatively weak, which complicates antibody maturation[11]. Indeed, we found that a conjugate composed of a glycopeptides derived from CKII linked to the carrier protein KLH was unable to elicit relevant antibodies, and in this case the immune response was almost entirely directed to the carrier protein and linker. However, we have been able to obtain a large panel of *O*-GlcNAc– specific IgG monoclonal antibodies having a broad spectrum of binding partners by combining three-component immunogen methodology with hybridoma technology[16]. The power of the new monoclonal antibodies has been demonstrated by identifying more than 200 mammalian *O*-GlcNAc–modified proteins, including a large number of new glycoproteins. Notably, while there was some overlap in the assigned proteins for each antibody enrichment, a substantial number of proteins were only enriched by one of the antibodies. This observation, combined with the results of inhibition ELISAs using glycopeptides of increasing complexity, suggests that the antibodies, in addition to their *O*-GlcNAc dependence, also have different but overlapping local peptide determinants.

It is to be expected that mapping of glycosylation sites of proteins immunoprecipitated with the antibodies will provide additional information about the epitope requirements of the antibodies. Although we used electron transferred

dissociation (ETD), which is a mass spectrometric approach suitable for detecting glycopeptides[25], we did not find such structures. This difficulty is probably due to the fact that glycopeptides are difficult to ionize in the presence of peptides. Enrichment of *O*-GlcNAc proteins using the new antibodies combined with chemo-enzymatic approaches for glycopeptides isolation[26, 27] and cutting-edge mass spectrometry approaches[28] should facilitate the site mapping of *O*-GlcNAc–modified proteins. It is to be expected that mapping of glycosylation sites of proteins immunoprecipitated with the antibodies will provide additional information about the epitope requirements of the antibodies. Although we used electron transferred dissociation (ETD), which is a mass spectrometric approach suitable for detecting glycopeptides[25], we did not find such structures. This difficulty is probably due to the fact that glycopeptides are difficult to ionize in the presence of peptides. Enrichment of *O*-GlcNAc proteins using the new antibodies combined with chemo-enzymatic approaches for glycopeptides isolation[27] and cutting-edge mass spectrometry approaches[28] should facilitate the site mapping of *O*-GlcNAc–modified proteins.

A number of recent studies have demonstrated that acute augmentation of *O*-GlcNAc levels is associated with increased tolerance of cells to stress, and conversely, inhibition of *O*-GlcNAc formation decreases cell survival[23, 24, 29-32]. In a rat model of trauma-hemorrhage, increasing *O*-GlcNAc synthesis with glucosamine or inhibiting *O*-GlcNAc degradation with PUGNAc during resuscitation leads to improved organ function, decreased tissue injury, reduced inflammatory responses and lower mortality[24]. Surprisingly, however, we found that resuscitation results in marked loss of overall *O*-GlcNAc levels in multiple tissues, which is sustained for up to 24 h, and that treatment with either glucosamine or PUGNAc [10] prevents this loss. Moreover, there was a strong correlation between the level of O-GlcNAcylation in the liver and markers of liver injury 24 h after TH and resuscitation. However, so far, identification of specific

proteins that exhibit changes in *O*-GlcNAc modification in response to trauma-hemorrhage and resuscitation has been difficult. Here we have used the new antibodies to identify a number of new *O*-GlcNAc protein targets, which potentially can modulate the response of the liver to stress.

A relatively large number of identified proteins are involved in metabolism, which is in agreement with the fact that the liver is a metabolically active organ. The metabolic proteins include those related to lipogenesis (including glycerol-3-phosphate dehydrogenase, ATP citrate lyase and malic enzymes), gluconeogenesis (such as fructose-1,6-biphosphatase) and lipid oxidation (such as acyl-CoA dehydrogenase and acetyl-CoA acyltransferase). Fructose-1,6-biphosphatase is particularly noteworthy because it provides an alternative to glucose-6-phosphate isomerase for the generation of fructose-6-phosphate, which is the primary substrate for the hexosamine biosynthetic pathway and the synthesis of UDP-GlcNAc, the donor sugar nucleotide for *O*-GlcNAc modification. Furthermore, recent evidence suggests that transcription of gluconeogenic enzymes is regulated by *O*-GlcNAc modification[20, 33]. The possibility of *O*-GlcNAc regulating gluconeogenic enzymes directly in addition to regulating their transcription awaits future studies. Following TH-R, there was a marked decrease in the total number of *O*-GlcNAc–modified proteins identified compared to the sham group, which is consistent with the fact that the overall *O*-GlcNAc levels are reduced upon TH-R. However, several proteins identified in the TH-R samples were not detected in the sham, which is in agreement with the recent finding that changes in *O*-GlcNAc modification can occur on a subset of modified proteins in response to a stimulus without altering *O*-GlcNAc levels on other proteins[27].

We identified a number of proteins related to oxidative stress (including superoxide dismutase, thioredoxin and glutathione S-transferase), which provides a possible rationale for the fact that increased overall *O*-GlcNAc levels protect against

oxidative stress. Identification of these glycoproteins also lends support for a potential crosstalk between redox and *O*-GlcNAc signaling pathways[4].

A subset of ten proteins was O-GlcNAcylated only in the TH-R group. One of these proteins, Death-associated protein (DAP) kinase 3, is a Ca2+/calmodulin (CaM)-regulated serine/threonine kinase that is a positive mediator of programmed cell death34. Autophosphorylation of DAP kinase is believed to restrain its proapoptotic activity, whereas dephosphorylation and subsequent binding to CaM stimulates its apoptotic functions. We are unaware of any studies demonstrating a role for DAP kinases in mediating the response of liver injury following trauma-hemorrhage and resuscitation, or indicating that they are subjected to *O*-GlcNAc modification. However, it is clear that modulation of DAP kinase activity is critical to the regulation of apoptosis and cellular homeostasis[34]. Thus, the new tools have opened up new avenues of exploration for modulation of protein function by *O*-GlcNAc and should facilitate this future research.

5. Methods

Synthetic methods. Procedures for the synthesis of (glyco)peptides, analytical data for compounds **1**–**9**, conjugation to BSA-MI and the preparation of liposomes are described in the **Supplementary Methods**.

TH-R shock model. Liver samples were obtained from rats 24 h after traumahemorrhage and resuscitation as described in detail elsewhere[35]. Briefly, under isoflurane anesthesia, soft-tissue trauma was induced by a midline laparotomy followed by hemorrhage induced by withdrawal of 55% of the calculated total blood volume. Subsequently, mean arterial pressure was maintained at 35–40 mm Hg for 45 min by intravenous administration of small volumes of NaCl (0.9%). This was followed by resuscitation with four times of total withdrawn blood volume of intravenous NaCl (0.9%),

administered over 60 min. The animals were allowed recover and observed for up to 24 h after resuscitation, at which point surviving animals were killed by intravenous injection of concentrated KCl solution and livers were collected for subsequent analysis. Sham surgery animals underwent only general anesthesia and vessel cannulation. All animals received buprenorphine (0.3 mg per kg body weight) subcutaneously immediately following and 12 h after resuscitation. All animal experiments were approved by the University of Alabama Institutional Animal Care and Use Committee.

Mass spectrometry. The dried peptide samples were resuspended in 20 µl aqueous 0.1% (v/v) formic acid in 2% (v/v) acetonitrile and filtered (0.2 µm, Nanosep, Pall Corporation). The samples were loaded off-line onto a nanospray tapered capillary column with emitter (360 Å~ 75 Å~ 15 µm, PicoFrit, New Objective) self-packed with C18 reverse-phase resin (8.5 cm, Waters) in a nitrogen pressure bomb for 10 min at 1,000 psi (5 µl load) and then separated via a 160-min linear gradient of increasing mobile at a flow rate of 200 nl min−1 directly into a linear ion trap mass spectrometer (LTQ-XL with ETD; ThermoFisher) as described previously[36]. The samples derived from HEK293T were subjected to triplicate analysis using three different modes of MS/MS analysis. The first mode was ETD mode, where a full MS spectrum was collected followed by 6 MS/MS spectra using ETD (enabled supplemental activation) of the most intense peaks. The dynamic exclusion was set at 1 for 30 s of duration. The second mode was collision-induced dissociation–pseudo neutral loss (CID-NL) mode, where a full MS spectrum was collected followed by 8 MS/MS spectra using CID of the most intense peaks. Upon encountering a pseudo neutral loss event (a loss of GlcNAc, 203.08), an MS3 spectrum was generated from the resulting ion that had undergone a neutral loss. The dynamic exclusion was the same in all methods. The third mode was DDNL-ETD (datadependent neutral loss MS^3 using CID followed by an ETD MS/MS spectra for any parent ion that generated a neutral loss), where MS/MS spectra from the top 5 peaks of each full MS

scan were collected with CID (35% normalized collision energy) and monitored for a neutral loss of 203.08. For tryptic peptides prepared from the *O*-GlcNAc–modified protein isolated from sham or TH-R–treated rat liver samples, analysis was carried out via CID-NL as described above in triplicate.

Mass spectrometry data analysis and validation. MS spectra were searched against the human or rat forward and reverse databases extracted from the appropriate species-specific Swiss-Prot proteome database using the TurboSequest algorithm (Bioworks 3.3, Thermo Finnigan). The resulting data files were generated for spectra with a threshold of 15 ions and a total ion current of 1 Å~ 103. Dynamic mass increases of 15.99, 57.02 and 203.08 Da were considered for oxidized methionine, alkylated cysteine and *O*-GlcNAc–modified serine/threonine, respectivity. The resulting OUT files obtained from a search of the forward and reverse databases obtained from the different runs were combined and parsed with ProtoeIQ (Bioinquire, Inc.) and filtered to <1% false-discovery rate (metric used: *F*-value) at the protein level using a minimum for each peptide of <3% false-discovery rate. For both the human and rat data, for each individual antibody, all results were combined using ProteoIQ. Proteins that appear in the filtered lists of both negative control and experimental groups were considered as contaminants and manually removed from the compiled lists. Statistical analysis. Statistical significance between groups was determined by a two-tailed, unpaired Student's *t*-test. Differences were considered significant when $P < 0.05$.

Other methods. See **Supplementary Methods** for preparation of liposomes, immunization schedule, hybridoma culture and antibody production, reagents, serologic assays, plasmid construction, cell culture and transfection, immunoprecipitation, preparation of liver lysates, western blotting, sample preparation for LC-MS/MS analysis and statistical analysis.

6. Acknowledgments

We thank R. Davis (University of Georgia) for monoclonal antibody production, J.-M. Lim and L. Zhao for expert assistance with mass spectrometry, E.G. El-Karim for assistance with molecular biology and T. Buskas for assistance with glycopeptide synthesis and protein conjugation. We also thank BioInquire, Inc. for access to the beta version of ProteoIQ that was used in the evaluation of the mass spectrometry data. We thank G.W. Hart (Johns Hopkins School of Medicine) for CTD110.6 and AL28 (anti-OGT antibodies) and S.W. Whiteheart (University of Kentucky) for the anti-OGA antibody. This research was supported by a grant from the US National Institute of Diabetes and Digestive and Kidney disorders (NIH RO1 DK075069 to L.W.), the Research Resource for Integrated Glycotechnology (NIH/NCRR P41R005351 to G.-J.B.) and the National Cancer Institute of the US National Institutes of Health (NIH/NCI R01CA088986 to G.-J.B.). C.F.T. was supported by a predoctoral fellowship from the American Heart Association (Southeast Affiliation). This work was further supported by grants NIH HL067464 and HL079364 (to J.C.C.).

7. Author Contributions

S.I. and G.A.E. performed the chemical synthesis. M.A.W. performed, analyzed and directed the immunological experiments. C.F.T. performed and analyzed the western blots and MS experiments. L.G.N. and J.C.C. were responsible for the rat model. L.W. and G.-J.B. were responsible for the overall experimental design and wrote the paper. G.-J.B. was responsible for compound design.

8. References

1. Hart, G.W., M.P. Housley, and C. Slawson, *Cycling of O-linked beta-N-acetylglucosamine on nucleocytoplasmic proteins.* Nature, 2007. **446**(7139): p. 1017-22.

2. Golks, A. and D. Guerini, *The O-linked N-acetylglucosamine modification in cellular signalling and the immune system. 'Protein modifications: beyond the usual suspects' review series.* EMBO Rep, 2008. **9**(8): p. 748-53.
3. Wells, L., K. Vosseller, and G.W. Hart, *Glycosylation of nucleocytoplasmic proteins: signal transduction and O-GlcNAc.* Science, 2001. **291**(5512): p. 2376-8.
4. Laczy, B., et al., *Protein O-GlcNAcylation: a new signaling paradigm for the cardiovascular system.* Am J Physiol Heart Circ Physiol, 2009. **296**(1): p. H13-28.
5. Copeland, R.J., J.W. Bullen, and G.W. Hart, *Cross-talk between GlcNAcylation and phosphorylation: roles in insulin resistance and glucose toxicity.* Am J Physiol Endocrinol Metab, 2008. **295**(1): p. E17-28.
6. Dias, W.B. and G.W. Hart, *O-GlcNAc modification in diabetes and Alzheimer's disease.* Mol Biosyst, 2007. **3**(11): p. 766-72.
7. Lefebvre, T., et al., *Does O-GlcNAc play a role in neurodegenerative diseases?* Expert Rev Proteomics, 2005. **2**(2): p. 265-75.
8. Champattanachai, V., R.B. Marchase, and J.C. Chatham, *Glucosamine protects neonatal cardiomyocytes from ischemia-reperfusion injury via increased protein O-GlcNAc and increased mitochondrial Bcl-2.* Am J Physiol Cell Physiol, 2008. **294**(6): p. C1509-20.
9. Liu, J., R.B. Marchase, and J.C. Chatham, *Increased O-GlcNAc levels during reperfusion lead to improved functional recovery and reduced calpain proteolysis.* Am J Physiol Heart Circ Physiol, 2007. **293**(3): p. H1391-9.
10. Fulop, N., et al., *Glucosamine cardioprotection in perfused rat hearts associated with increased O-linked N-acetylglucosamine protein modification and altered p38 activation.* Am J Physiol Heart Circ Physiol, 2007. **292**(5): p. H2227-36.
11. Wang, Z. and G. Hart, *Glycomic Approaches to Study GlcNAcylation: Protein Identification, Site-mapping, and Site-specific O-GlcNAc Quantitation.* Clinical Proteomics, 2008. **4**(1-2): p. 5-13.
12. Rexach, J.E., P.M. Clark, and L.C. Hsieh-Wilson, *Chemical approaches to understanding O-GlcNAc glycosylation in the brain.* Nat Chem Biol, 2008. **4**(2): p. 97-106.
13. Comer, F.I., et al., *Characterization of a mouse monoclonal antibody specific for O-linked N-acetylglucosamine.* Anal Biochem, 2001. **293**(2): p. 169-77.
14. Snow, C.M., A. Senior, and L. Gerace, *Monoclonal antibodies identify a group of nuclear pore complex glycoproteins.* J Cell Biol, 1987. **104**(5): p. 1143-56.
15. Kreppel, L.K. and G.W. Hart, *Regulation of a cytosolic and nuclear O-GlcNAc transferase. Role of the tetratricopeptide repeats.* J Biol Chem, 1999. **274**(45): p. 32015-22.
16. Ingale, S., et al., *Robust immune responses elicited by a fully synthetic three-component vaccine.* Nat Chem Biol, 2007. **3**(10): p. 663-7.
17. Haltiwanger, R.S., K. Grove, and G.A. Philipsberg, *Modulation of O-linked N-acetylglucosamine levels on nuclear and cytoplasmic proteins in vivo using the peptide O-GlcNAc-beta-N-acetylglucosaminidase inhibitor O-(2-acetamido-2-deoxy-D-glucopyranosylidene)amino-N-phenylcarbamate.* J Biol Chem, 1998. **273**(6): p. 3611-7.
18. Wells, L., S.A. Whelan, and G.W. Hart, *O-GlcNAc: a regulatory post-translational modification.* Biochem Biophys Res Commun, 2003. **302**(3): p. 435-41.
19. Yang, X., et al., *Phosphoinositide signalling links O-GlcNAc transferase to insulin resistance.* Nature, 2008. **451**(7181): p. 964-9.
20. Dentin, R., et al., *Hepatic glucose sensing via the CREB coactivator CRTC2.* Science, 2008. **319**(5868): p. 1402-5.

21. Vosseller, K., et al., *Elevated nucleocytoplasmic glycosylation by O-GlcNAc results in insulin resistance associated with defects in Akt activation in 3T3-L1 adipocytes.* Proc Natl Acad Sci U S A, 2002. **99**(8): p. 5313-8.
22. Zhang, F., et al., *O-GlcNAc modification is an endogenous inhibitor of the proteasome.* Cell, 2003. **115**(6): p. 715-25.
23. Ohn, T., et al., *A functional RNAi screen links O-GlcNAc modification of ribosomal proteins to stress granule and processing body assembly.* Nat Cell Biol, 2008. **10**(10): p. 1224-31.
24. Chatham, J.C., et al., *Hexosamine biosynthesis and protein O-glycosylation: the first line of defense against stress, ischemia, and trauma.* Shock, 2008. **29**(4): p. 431-40.
25. Viner, R.I., et al., *Quantification of post-translationally modified peptides of bovine alpha-crystallin using tandem mass tags and electron transfer dissociation.* J Proteomics, 2009. **72**(5): p. 874-85.
26. Clark, P.M., et al., *Direct in-gel fluorescence detection and cellular imaging of O-GlcNAc-modified proteins.* J Am Chem Soc, 2008. **130**(35): p. 11576-7.
27. Khidekel, N., et al., *Probing the dynamics of O-GlcNAc glycosylation in the brain using quantitative proteomics.* Nat Chem Biol, 2007. **3**(6): p. 339-48.
28. Chalkley, R.J., et al., *Identification of protein O-GlcNAcylation sites using electron transfer dissociation mass spectrometry on native peptides.* Proc Natl Acad Sci U S A, 2009. **106**(22): p. 8894-9.
29. Hu, Y., et al., *Increased enzymatic O-GlcNAcylation of mitochondrial proteins impairs mitochondrial function in cardiac myocytes exposed to high glucose.* J Biol Chem, 2009. **284**(1): p. 547-55.
30. Ramirez-Correa, G.A., et al., *O-linked GlcNAc modification of cardiac myofilament proteins: a novel regulator of myocardial contractile function.* Circ Res, 2008. **103**(12): p. 1354-8.
31. Guinez, C., et al., *Hsp70-GlcNAc-binding activity is released by stress, proteasome inhibition, and protein misfolding.* Biochem Biophys Res Commun, 2007. **361**(2): p. 414-20.
32. Zachara, N.E., et al., *Dynamic O-GlcNAc modification of nucleocytoplasmic proteins in response to stress. A survival response of mammalian cells.* J Biol Chem, 2004. **279**(29): p. 30133-42.
33. Wang, Y., et al., *The CREB coactivator CRTC2 links hepatic ER stress and fasting gluconeogenesis.* Nature, 2009. **460**(7254): p. 534-7.
34. Bialik, S. and A. Kimchi, *The death-associated protein kinases: structure, function, and beyond.* Annu Rev Biochem, 2006. **75**: p. 189-210.
35. Not, L.G., et al., *Glucosamine administration improves survival rate after severe hemorrhagic shock combined with trauma in rats.* Shock, 2007. **28**(3): p. 345-52.
36. Lim, J.M., et al., *Defining the regulated secreted proteome of rodent adipocytes upon the induction of insulin resistance.* J Proteome Res, 2008. **7**(3): p. 1251-63.

9. Supplementary Methods

Reagents and general procedures for synthesis. Fmoc-*L*-Amino acid derivatives and resins were purchased from NovaBioChem and Applied Biosystems, peptide synthesis grade *N, N*dimethylformamide (DMF) from EM Science and *N*-methylpyrrolidone (NMP) from Applied Biosystems. Egg phosphatidylcholine (PC), egg phosphatidylglycerol (PG), cholesterol, monophosphoryl lipid A (MPL-A) and dodecyl phosphocholine (DPC) were obtained from Avanti Polar Lipids. All other chemical reagents were purchased from Aldrich, Acros, Alfa Aesar and Fischer and used without further purification. All solvents employed were reagent grade. Reversed phase high performance liquid chromatography (RP-HPLC) was performed on an Agilent 1100 series system equipped with an auto-injector, fraction-collector and UV-detector (detecting at 214 nm) using an Agilent Zorbax Eclipse^{TM} C18 analytical column (5 µm, 4.6 x 150 mm) at a flow rate of 1 ml min^{-1}, an Agilent Zorbax Eclipse^{TM} C18 semi preparative column (5 µm, 10 x 250 mm) at a flow rate of 3 ml min^{-1}, an Agilent Zorbax Eclipse^{TM} C8 analytical column (5 µm, 4.6 x 150 mm) at a flow rate of 1 ml min^{-1}, an Agilent Zorbax Eclipse^{TM} C8 semi preparative column (5 µm, 10 x 250 mm) at a flow rate of 3 ml min^{-1} or a Phenomenex JupiterTM C4 semi preparative column (5 µm, 10 x 250 mm) at a flow rate of 2 ml min^{-1}. All runs used linear gradients of 0 to 100% of solvent B (5% water, 0.1% trifluoroacetic acid (TFA) in acetonitrile) in solvent A (5% acetonitrile, 0.1% TFA in water) over a 40 min period unless otherwise specified. Matrix assisted laser desorption ionization time of flight mass spectrometry (MALDI-ToF) mass spectra were recorded on an ABI 4700 proteomics analyzer.

General methods for solid-phase peptide synthesis (SPPS). Peptides were synthesized by established protocols on an ABI 433A peptide synthesizer (Applied Biosystems) equipped with UV-detector using *N*α-Fmoc-protected amino acids and 2-(1H-bezotriazole-1-yl)-oxy-1,1,3,3- tetramethyl hexafluorophosphate (HBTU)/1-

hydroxybenzotriazole (HOBt)[S1] as the activating reagents. Single coupling steps were performed with conditional capping. The following protected amino acids (Novabiochem) were used: *N*α-Fmoc-Arg(Pbf)-OH, *N*α-Fmoc-Asp(*Ot*Bu)- OH, *N*α-Fmoc-Asp-Thr(ΨMe,Mepro)-OH, *N*α-Fmoc-Ile-Thr(ΨMe,Mepro)-OH, *N*α-Fmoc-Lys(Boc)- OH, *N*α-Fmoc-Ser(*t*Bu)-OH, *N*α-Fmoc-Thr(*t*Bu)-OH, *N*α-Fmoc-Tyr(*t*Bu)-OH. The coupling of the glycosylated amino acids *N*α-Fmoc-Ser-(AcO_3-β-D-*O*-GlcNAc)OH[S2] and *N*α-Fmoc-Cys-(AcO_3-β-D-*S*-GlcNAc)OH[S3] was carried out manually using *O*-(7-azabenzotriazol-1-yl)-*N*,*N*,*N',N'*-tetramethyl-uronium hexafluorophosphate (HATU)/1-hydroxy-7-azabenzotriazole (HOAt) as a coupling agent. The coupling of *N*α-Fmoc-*S*-(2,3-bis(palmitoyloxy)-(2*R*-propyl)-(*R*)-cysteine[S4,S5], which was prepared from *(R)*-glycidol were carried out using benzotriazole-1-yl-oxy-trispyrrolidino-phosphonium hexafluorophosphate (PyBOP)/HOBt as coupling agent. Progress of the manual couplings was monitored by standard Kaiser test[S6].

Synthesis of lipopeptide 11. The synthesis of **11** was carried out on a H-Gly-sulfamylbutyryl Novasyn TG resin as described in the general method section for peptide synthesis. After coupling of the first five amino acids, the remaining steps were performed manually. *N*-α-Fmoc-*S*-(2,3-bis (palmitoyloxy)-(2*R*-propyl)-(*R*)-cysteine (267 mg, 0.3 mmol) was dissolved in DMF (5 ml) and PyBOP (156.12 mg, 0.3 mmol), HOBt (40 mg, 0.3 mmol) and DIPEA (67 µl, 0.4 mmol) were premixed for 2 min, and was added to the resin. The coupling reaction was monitored by the Kaiser test and was complete after standing for 12 h. Upon completion of the coupling, the *N*-Fmoc group was cleaved using 20% piperidine in DMF (6 ml) and palmitic acid (77 mg, 0.3 mmol) was coupled to the free amine as described above using PyBOP (156.12 mg, 0.3 mmol), HOBt (40 mg, 0.3 mmol) and DIPEA (67 µl, 0.4 mmol) in DMF. The resin was thoroughly washed with DMF (10 ml), DCM (10 ml) and MeOH (10 ml) and then dried in *vacuo*. The resin was swelled in DCM (5 ml) for 1 h and treated with DIPEA (0.5 ml, 3 mmol),

iodoacetonitrile (0.36 ml, 5 mmol) in NMP (6 ml). It is important to note that the iodoacetonitrile was filtered through a plug of basic alumina before addition to the resin. The resin was agitated under the exclusion of light for 24 h, filtered and washed with NMP (5 ml Å~ 4), DCM (5 ml Å~ 4) and THF (5 ml Å~ 4). The activated *N*-acyl sulfonamide resin was swollen in DCM (5 ml) for 1 h, drained and transferred to a 50 ml round bottom flask. To the resin-containing flask was added THF (4 ml), benzyl mercaptan (0.64 ml, 5 mmol) and sodium thiophenate (27 mg, 0.2 mmol).

After agitation for 24 h, the resin was filtered and washed with hexane (5 ml Å~ 2). The combined filtrate and washings were collected and concentrated in *vacuo* to approximately 1/3 of its original volume. The crude product was then precipitated by the addition of *tert*-butyl methyl ether (0 °C; 60 ml) and recovered by centrifugation at 3000 rpm for 15 min, and after the decanting of the ether the peptide precipitate was dissolved in mixture DCM and MeOH (1.5 ml/1.5 ml). The thiol impurity present in the peptide precipitate was removed by passing it through a LH-20 size exclusion column. The fractions containing product were collected and solvents removed to give the fully protected peptide thioester. The protected peptide was treated with a reagent B (TFA 88%, phenol 5%, H_2O 5%, TIS 2%; 5 ml) for 4 h at room temperature. The TFA solution was then added dropwise to a screw cap centrifuge tube containing ice cold *tert*-butyl methyl ether (40 ml) and the resulting suspension was left overnight at 4 °C, after which the precipitate was collected by centrifugation at 3000 rpm (20 min), and after the decanting of the ether the peptide precipitate was re-suspended in ice cold *tert*-butyl methyl ether (40 ml) and the process of washing was repeated twice. The crude peptide was purified by HPLC on a semi preparative C-4 reversed phase column using a linear gradient of 0 to 100% solvent B in A over a 40 min, and the appropriate fractions were lyophilized to afford **11** (110 mg, 65%). $C_{90}H_{165}N_{11}O_{13}S_2$, MALDI-ToF MS: observed, $[M+Na]^+$ 1695.2335 Da; calculated, $[M+Na]^+$ 1695.1927 Da.

Synthesis of glycopeptide 12. SPPS was performed on Rink amide resin (0.1 mmol) as described in the general procedures. The first four amino acids, Ser-Ala-Asn-Met, were coupled on the peptide synthesizer using a standard protocol. After the completion of the synthesis, a manual coupling was carried out using *N*α-FmocSer-(AcO_3-α-D-*O*-GlcNAc)OH (0.2 mmol, 131 mg), with *O*-(7-azabenzotriazol-1-yl)-*N*,*N*,*N',N'*-tetramethyl-uronium hexafluorophosphate (HATU; 0.2 mmol, 76 mg), 1-hydroxy-7-azabenzotriazole (HOAt; 0.2 mmol, 27 mg) and diisopropylethylamine (DIPEA; 0.4 mmol, 70 µl) in NMP (5 ml) for 12 h. The coupling reaction was monitored by standard Kaiser test. The resin was then washed with NMP (6 ml) and methylene chloride (DCM; 6 ml), and resubjected to the same coupling conditions to ensure completion of the coupling. The glycopeptide was then elongated on the peptide synthesizer after which the resin was thoroughly washed with NMP (6 ml), DCM (6 ml) and MeOH (6 ml) and dried in *vacuo*. The resin was swelled in DCM (5 ml) for 1 h and then treated with hydrazine (60%) in MeOH (10 ml) for 2 h and washed thoroughly with NMP (5 ml Å~ 2), DCM (5 ml Å~ 2) and MeOH (5 ml Å~ 2) and dried in *vacuo*. The resin was swelled in DCM (5 ml) for 1 h, after which it was treated with reagent K (TFA (81.5%), phenol (5%), thioanisole (5%), water (5%), EDT (2.5%), TIS (1%)) (30 ml) for 2 h at room temperature. The resin was filtered and washed with neat TFA (2 ml). The filtrate was then concentrated *in vacuo* to approximately 1/3 of its original volume. The peptide was precipitated using diethyl ether (0 °C; 30 ml) and recovered by centrifugation at 3000 rpm for 15 min. The crude peptide was purified by RP-HPLC on a semi preparative C-8 column using a linear gradient of 0 to 100% solvent B in solvent A over a 40 min period and the appropriate fractions were lyophilized to afford **12** (118 mg, 40%). $C_{129}H_{204}N_{32}O_{40}S_2$, MALDI-ToF MS: observed $[M+2H]^+$, 2907.5916 Da; calculated $[M+2H]^+$, 2907.4511 Da.

Synthesis of glycopeptide 13. SPPS was performed on Rink amide resin (0.1

mmol) as described in the general procedures. The first four amino acids, Ser-Ala-Asn-Met, were coupled on the peptide synthesizer using a standard protocol. After the completion of the synthesis, a manual coupling was carried out using *N*α-Fmoc-Cys-(AcO_3-β-D-*S*-GlcNAc)OH (0.2 mmol, 134 mg), with *O*-(7-azabenzotriazol-1-yl)-*N*,*N*,*N',N'*-tetramethyl-uronium hexafluorophosphate (HATU; 0.2 mmol, 76 mg), 1-hydroxy-7-azabenzotriazole (HOAt; 0.2 mmol, 27 mg) and diisopropylethylamine (DIPEA; 0.4 mmol, 70 µl) in NMP (5 ml) for 12 h. The coupling reaction was monitored by standard Kaiser test. The resin was then washed with NMP (6 ml) and methylene chloride (DCM; 6 ml), and resubjected to the same coupling conditions to ensure complete coupling. The resulting glycopeptide was then elongated on the peptide synthesizer. After the completion of the synthesis, the resin was thoroughly washed with NMP (6 ml), DCM (6 ml) and MeOH (6 ml) and dried in *vacuo*. The resin was swelled in DCM (5 ml) for 1 h and then treated with hydrazine (60%) in MeOH (10 ml) for 2 h and washed thoroughly with NMP (5 ml Å~ 2), DCM (5 ml Å~ 2) and MeOH (5 ml Å~ 2) and dried in *vacuo*. The resin was swelled in DCM (5 ml) for 1 h, after which it was treated with TFA (81.5%), phenol (5%), thioanisole (5%), water (5%), EDT (2.5%), TIS (1%) (30 ml) for 2 h at room temperature. The resin was filtered and washed with neat TFA (2 ml). The filtrate was then concentrated *in vacuo* to approximately 1/3 of its original volume. The peptide was precipitated using diethyl ether (30 ml, 0 °C) and recovered by centrifugation at 3000 rpm for 15 min. The crude peptide was purified by RP-HPLC on a semi preparative C-8 column using a linear gradient of 0 to 100% solvent B in solvent A over a 40 min period and the appropriate fractions were lyophilized to afford **13** (95 mg, 34%). $C_{129}H_{204}N_{32}O_{39}S_3$, MALDI-ToF MS: observed $[M+2H]^+$, 2923.6716 Da; calculated $[M+2H]^+$, 2923.4282 Da.

Synthesis of glycolipopeptide 1. The lipopeptide thioester **11** (4.3 mg, 2.5 µmol), glycopeptides **12** (5.0 mg, 1.7 µmol) and dodecyl phosphocholine (6.0 mg, 17.0 µmol)

were dissolved in a mixture of trifluoroethanol and CHCl3 (2.5 ml/2.5 ml). The solvents were removed under reduced pressure to give a lipid/peptide film, which was hydrated for 4 h at 37 °C using 200 mM phosphate buffer (pH 7.5, 3 ml) in the presence of tris(carboxyethyl)phosphine (2% w/v, 40.0 µg) and EDTA (0.1% w/v, 20.0 µg). The mixture was ultrasonicated for 1 min. To the vesicle suspension was added sodium 2-mercaptoethane sulfonate (2% w/v, 40.0 µg) to initiate the ligation reaction. The reaction was carried out in an incubator at 37 °C and the progress of the reaction was periodically monitored by MALDI-ToF, which showed disappearance of glycopeptide **12** within 2 h. The reaction was then diluted with 2-mercaptoethanol (20%) in ligation buffer (2 ml) and the crude peptide was purified by semi preparative C-4 reversed phase column using a linear gradient of 0 to 100% solvent B in A over a 40 min, and lyophilization of the appropriate fractions afforded **1** (4.3 mg, 57%). $C_{212}H_{361}N_{43}O_{53}S_3$, MALDI-ToF MS: observed $[M]^+$, 4461.9177 Da; calculated $[M]^+$, 4455.5781 Da.

Synthesis of glycolipopeptide 2. Lipopeptide thioester **11** (2.5 mg, 1.5 µmol), glycopeptide **13** (3.0 mg, 1.0 µmol) and dodecyl phosphocholine (3.5 mg, 10 µmol) were dissolved in a mixture of trifluoroethanol and $CHCl_3$ (2.5 ml/2.5 ml). The solvents were removed under reduced pressure to give a lipid/peptide film, which was hydrated for 4 h at 37 °C using 200 mM phosphate buffer (pH 7.5, 2 ml) in the presence of tris(carboxyethyl)phosphine (2% w/v, 40.0 µg) and EDTA (0.1% w/v, 20.0 µg). The mixture was ultrasonicated for 1 min. To initiate the ligation reaction, sodium 2-mercaptoethane sulfonate (2% w/v, 40.0 µg) was added to the vesicle suspension. The reaction was carried out in an incubator at 37 °C and the progress of the reaction was periodically monitored by MALDI-ToF, which showed disappearance of glycopeptides within 2 h. The reaction was then diluted with 2-mercaptoethanol (20%) in ligation buffer (2 ml). The crude peptide was purified by semi preparative C-4 reversed phase column using a linear gradient of 0 to 100% solvent B in A over a 40 min, and lyophilization of

the appropriate fractions afforded **2** (2.8 mg, 64%). $C_{212}H_{361}N_{43}O_{52}S_4$, MALDI-ToF MS: observed $[M]^+$, 4469.9112 Da; calculated, $[M]^+$4469.5809 Da.

Compounds **3**-**9** were prepared as described in the standard procedures section on Rink amide resin (0.1 mmol). Glycopeptide **3** (78 mg, 61 %); $C_{48}H_{82}N_{14}O_{21}S_2$, MALDI-ToF MS: observed $[M+Na]^+$, 1277.4746 Da; calculated $[M+Na]^+$, 1277.5118 Da. Peptide **4** (89 mg, 83%); $C_{40}H_{69}N_{13}O_{16}S_2$, MALDI-ToF MS: observed $[M+Na]^+$, 1074.4789 Da; calculated $[M+Na]^+$, 1074.4324 Da. Glycopeptide **5** (57 mg, 48%); $C_{45}H_{77}N_{13}O_{20}S$, MALDI-ToF MS: observed $[M+Na]^+$, 1174.4740 Da; calculated $[M+Na]^+$, 1174.5026 Da. Peptide **6** (76 mg, 78%); C37H64N12O15S, MALDI-ToF MS: observed $[M+Na]^+$, 971.2204 Da; calculated [M+Na]+, 971.4232 Da. Glycosylated amino acid **7** (12 mg, 33%); C14H25N3O8, MALDI-ToF MS: observed $[M+Na]^+$, 386.2749 Da; calculated $[M+Na]^+$, 386.1539 Da. Glycopentapeptide **8**; C27H47N7O12, MALDI-ToF MS: observed $[M+Na]^+$, 684.0485 Da; calculated $[M+Na]^+$, 684.3180 Da. Glycotripeptide **9**; C19H35N5O10, MALDI-ToF MS: observed $[M+Na]^+$, 516.1772 Da; calculated $[M+Na]^+$, 516.2282 Da.

General procedure for the conjugation to BSA-MI. The conjugations were performed as instructed by Pierce Endogen Inc. In short, the purified (glyco)peptide **3** or **4** (2.5 equiv. excess to available MI-groups on BSA) was dissolved in the conjugation buffer (sodium phosphate, pH 7.2 containing EDTA and sodium azide; 100 µl) and added to a solution of maleimide activated BSA (2.4 mg) in the conjugation buffer (200 µl). The mixture was incubated at room temperature for 2 h and then purified by a D-Salt™ dextran de-salting column (Pierce Endogen, Inc.), equilibrated and eluted with sodium phosphate buffer, pH 7.4 containing 0.15 M sodium chloride. Fractions containing the conjugate were identified using the BCA protein assay. Carbohydrate content was determined by quantitative monosaccharide analysis by high-pH anion exchange chromatography using a pulsed ampherometric detector (HPAEC/PAD,

Methrome), an analytical Carbopac PA-20 column (3x150 mm, Dionex) and a linear gradient of 8 to 100% B (200 mM NaOH) in A (H_2O) over a period of 37 min at a flow rate of 1 ml/min.

General procedure for the preparation of liposomes. Egg PC, egg PG, cholesterol, MPL-A and compound **1** or **2** (15 μmol, molar ratios 60:25:50:5:10) were dissolved in a mixture of trifluoroethanol and MeOH (1:1, v/v, 5 ml). The solvents were removed in *vacuo* to produce a thin lipid film, which was hydrated by suspending in HEPES buffer (10 mM, pH 6.5) containing NaCl (145 mM; 1 ml) under argon atmosphere at 41 °C for 3 h. The vesicle suspension was sonicated for 1 min and then extruded successively through 1.0, 0.6, 0.4, 0.2 and 0.1 μm polycarbonate membranes (Whatman, Nucleopore Track-Etch Membrane) at 50 °C to obtain SUVs. The sugar content of liposomes was determined by heating a mixture of SUVs (50 μl) and aqueous TFA (2 M, 200 μl) in a sealed tube for 4 h at 100 °C. The solution was then concentrated in *vacuo* and analyzed by high-pH anion exchange chromatography using a pulsed ampherometric detector (HPAEC/PAD, Methrome), an analytical Carbopac PA-20 column (3x150 mm, Dionex) and a linear gradient of 8 to 100% B (200 mM NaOH) in A (H_2O) over a period of 37 min at a flow rate of 1 ml/min.

Dose and immunization schedule. Groups of five mice (female BALB/c, age 8–10 weeks, from Jackson Laboratories) were immunized four times at two-week intervals. Each boost included 3 μg of saccharide in the liposome formulation. Serum samples were obtained before immunization (pre-bleed) and 1 week after the final immunization. The final bleeding was done by cardiac bleed.

Hybridoma culture and antibody production. Spleens of two mice immunized with **1** were harvested and standard hybridoma culture technology gave 30 IgG producing hybridoma cell lines. Three hybridomas (18B10.C7(3), 9D1.E4(10) and 1F5.D6(14)) were cultured at a one-liter scale and the resulting antibodies were purified by saturated

ammonium sulfate precipitation followed by Protein G column chromatography to yield, in each case, approximately 10 mg of IgG.

Reagents for biological experiments. Protease inhibitor cocktail was obtained from Roche. PUGNAc O-(2-acetamido-2-deoxy-D-glucopyranosylidene)amino N-phenyl carbamate was ordered from Toronto Research Chemicals, Inc. Mouse IgM anti-O-GlcNAc (CTD110.6,[S7]) and rabbit polyclonal anti-OGT (AL28) antibodies were previously generated in Dr. Gerald W. Hart's laboratory (Johns Hopkins University School of Medicine). Rabbit polyclonal anti-OGA antibody was a kind gift from Dr. Sidney W. Whiteheart (University of Kentucky College of Medicine). Rabbit polyclonal anti-CKII alpha antibodies (NB100-377 for immunoblotting and NB100-378 for immunoprecipitation) were purchased from Novus Biologicals. Mouse monoclonal antibody against α-tubulin and anti-mouse IgM (μ chain)-agarose was obtained from Sigma. Normal rabbit IgG agarose, normal rabbit IgG agarose and Protein A/G PLUS agarose were ordered from Santa Cruz Biotechnology, Inc.

Serologic assays. Anti-GSTPVS(β-*O*-GlcNAc)SANM (**5**) IgG, IgG1, IgG2a, IgG2b, IgG3 and IgM antibody titers were determined by enzyme-linked immunosorbent assay (ELISA), as described previouslyS8, S9. Briefly, Immulon II-HB flat bottom 96-well microtiter plates (Thermo Electron Corp.) were coated overnight at 4 °C with 100 μl per well of a conjugate of the glycopeptide conjugated to BSA through a maleimide linker (BSA-MI-GSTPVS(β-*O*GlcNAc) SANM; BSA-MI-**3**) at a concentration of 2.5 μg ml^{-1} in coating buffer (0.2 M borate buffer, pH 8.5 containing 75 mM sodium chloride). Serial dilutions of the sera or MAb containing cell supernatants were allowed to bind to immobilized GSTPVS(β-*O*-GlcNAc)SANM for 2 h at room temperature. Detection was accomplished by the addition of alkaline phosphatase-conjugated anti-mouse IgG (Jackson ImmunoResearch Laboratories Inc.), IgG1 (Zymed), IgG2a (Zymed), IgG2b (Zymed), IgG3 (BD Biosciences Pharmingen) or IgM (Jacksons ImmunoResearch

Laboratories) antibodies. After addition of *p*-nitrophenyl phosphate (Sigma), the absorbance was measured at 405 nm with wavelength correction set at 490 nm using a microplate reader (BMG Labtech). The antibody titer was defined as the highest dilution yielding an optical density of 0.1 or greater over that of background. To explore competitive inhibition of the binding of MAbs to GSTPVS(β-*O*-GlcNAc)SANM (**5**) by the corresponding glycopeptide, peptide and sugar, MAbs were diluted in diluent buffer in such a way that, without inhibitor, expected final optical density values were approximately 1. For each well 60 µl of the diluted MAbs were mixed in an uncoated microtiter plate with 60 µl diluent buffer, glycopeptide **5** (GSTPVS(β-*O*-GlcNAc)SANM), glycopentapeptide **8** (PVS(β-*O*GlcNAc) SA), glycotripeptide **9** (VS(β-*O*-GlcNAc)S), peptide **6** (GSTPVSSANM) or sugar **7** (β-*O*-GlcNAc-Ser) in diluent buffer with a final concentration of 0-500 µM. After incubation at room temperature for 30 min, 100 µl of the mixtures were transferred to a plate coated with BSA-MI CGSTPVS(β-*O*-GlcNAc)SANM (BSA-MI-**3**). The microtiter plates were incubated and developed as described above using the appropriate alkaline phosphatase-conjugated detection antibody. Optical density values were normalized for the optical density values obtained with monoclonal antibody alone (0 µM inhibitor, 100%).

Plasmids construction. The human OGT and OGA cDNA were PCR amplified in a two-step manner to introduce an attB1 site and a HA epitope at the 5' end as well as an attB2 site at the 3' end to facilitate Gateway cloning strategy (Invitrogen). The primers include (1) Sense primer for first PCR to incorporate HA epitope into ogt after the start codon: 5'-CCCCATGTATCCATATGACGTCCCAGACTATGCCGCGTCTTCCGTGGGCAACGT-3'; (2) Sense primer containing an attB1 site for using HA-ogt PCR product as the template: 5'GGGGACAAGTTTGTACAAAAAAGCAGGCTGGATGATGTATCCATATGACGTCCCAGACTATGCCGCGTCTTCCG-3'; (3) Antisense primer with 3' attB2 site for both ogt

PCR: 5'-GGGGACCACTTTGTACAAGAAAGCTGGGTTCTATGCTGACTCAGTGACTTCAACGGGCTTAATCATGTGG-3'; (4) Sense primer for first PCR to incorporate HA epitope into oga after the start codon: 5'-CCCCATGTATCCATATGACGTCCCAGACTATGCCGTGCAGAAGGA GAGTCAAGC-3'; (5) Sense primer containing an attB1 site for using HA-oga PCR product as the template: 5' GGGGACAAGTTTGTACAAAAAAGCAGGCTGGATGATGTATCCATATG ACGTCCCAGACTATGCCGTGCAGAAGG-3'; (6) Antisense primer with 3' attB2 site for both oga PCR: 5'-GGGGACCACTTTGTACAAGAAAGCTGGGTTCACAGGCTCCGACCAAGTAT-3'. The purified DNA fragments were then subjected to Gateway cloning according to manufacturer's instruction yielding final expression constructs, pDEST26/HA-OGT and pDEST26/HA-OGA.

Cell culture, transfection and treatment. HEK 293T cells were obtained from ATCC and maintained in Dulbecco's modified Eagle's medium (4.5 g l^{-1} glucose; Cellgro/Mediatech, Inc.) supplemented with 10% fetal bovine serum (GIBCO/Invitrogen) in 37 °C incubator humidified with 5% CO2. Transfection was performed with 8 μg of DNA and Lipofectamine 2000 reagent (Invitrogen) per 10 cm plate of cells according to the manufacturer's instruction. Mock transfection was performed in the absence of DNA. Cells were harvested 48 h post-transfection.

For immunoprecipitation experiments, cells were washed of the plates with ice-cold PBS and stored as a pellet at -80 °C until used. For immunoblotting experiments, cells were washed twice with ice-cold PBS and scraped in lysis buffer (10 mM Tris-HCl, pH 7.5, 150 mM NaCl, 1% Igepal CA-630, 0.1% SDS, 4 mM EDTA, 1 mM DTT, 0.1 mM PUGNAc, Protease inhibitor cocktail) and the lysates were clarified in a microfuge with

16,000 g for 25 min at 4 °C. The protein concentration was quantified with Bradford protein assay using standard procedure (Bio-Rad, Hercules, CA) and boiled in sample buffer for 5 min. For mass spectrometry experiment, two 15 cm plates of 293T cells were treated with 50 μM of PUGNAc for 24 h, cells were pelleted and stored as above.

Immunoprecipitation. To prepare the nucleocytosolic fraction for CKII immunoprecipitation, HEK293T cell pellets of mock or OGT transfection were resuspended in 4 volumes of hypotonic buffer (5 mM Tris-HCl, pH 7.5, Protease inhibitor cocktail) and transferred into a 2 ml homogenizer. After incubating on ice for 10 min, the cell suspension was subjected to dounce homogenization followed by another 5 min incubation on ice. One volume of hypertonic buffer (0.1 M Tris-HCl, pH 7.5, 2 M NaCl, 5 mM EDTA, 5 mM DTT, Protease inihibitor cocktail) was then added to the lysate. The lysate was incubated on ice for 5 min followed by another round of dounce homogenization. The resulting lysates were transferred to microfuge tubes containing PUGNAc (final concentration 10 μM) and centrifuged at 18,000 g for 25 min at 4 °C. Protein concentration was determined using Bradford protein assay (Bio-Rad, Hercules, CA). Prior to IP, the lysates were supplemented with Igepal CA-630 (1%) and SDS (0.1%), and precleared with a mixture of normal rabbit or mouse IgG AC and protein A/G PLUS agarose at 4 °C for 30 min. The precleared supernatant was incubated at 4 °C in the presence of antibodies of interest for 4 h at 4 °C. After adding protein A/G PLUS agarose, the samples were incubated for another 2 h at 4 °C and extensively washed with IP wash buffer (10 mM Tris-HCl, pH 7.5, 150 mM NaCl, 1% Igepal CA-630, 0.1% SDS). Finally, SDS-PAGE sample buffer was added to the IP complex and boiled for 3 min. After centrifugation, supernatant was transferred to a fresh tubes and stored at - 20 °C.

Preparation of liver lysates. Liver protein powder (1 g) isolated from rat with Sham or TH-R treatments were resuspended in lysis buffer (PBS containing 0.5% Igepal

CA-630, protease inhibitor cocktail, phosphatase inhibitor cocktail, 0.5 mM EDTA, 0.1 mM DTT, 5 μM PUGNAc) and homogenized with Polytron. The lysate was left on ice for 10 min prior to centrifugation (35,000g for 30 min at 4 °C). Clarified supernatant was filtered through a 1 μm glass filter disc, quantified by Bradford protein assay according standard procedure (Bio-Rad) and stored in aliquots at -80 °C.

Western blotting. Immunoprecipitated samples or crude lysates were resolved by a 7.5%, 10%, 4-15% or 4-20% Tris-HCl precast minigel (Bio-Rad), and semi-dry transferred to Immobilon-P transfer membrane (Millipore). The membranes were blocked with either BSA (3%; *O*-GlcNAc blots) or milk (5%; protein blots) in TBST (TBS with 0.1% Tween 20), and probed with each antibody at 4 °C overnight as follows: 1:1,000 dilution for *O*-GlcNAc blots, 1:8,000 dilution for CKII (Novus Biologicals, Inc.), OGT and OGA blots, 1:10,000 dilution for α-tubulin (Sigma-Aldrich). After the addition of secondary antibodies conjugated to HRP at room temperature for 2 h, the final detection of HRP activity was performed using SuperSignal chemiluminescent substrates (Thermo Scientific) as follows: MAbs 18B10.C7(3), 9D1.E4(10) and 1F5.D6(14) used Femto; CKII, OGT, OGA and tubulin used PICO. The films were exposed to CL-XPosure film (Thermo Scientific). After developing the image on the film, the blot was then stripped with 0.1 M glycine (pH 2.5) at room temperature for 1 h, washed with ddH_2O and reprobed for loading control (CKII or α-tubulin) as described above. Similar protocols were used to confirm the presence of proteins of interest in crude lysates from the liver samples using commercially available antibodies as follow: mouse monoclonal anti-Hsp60 (LK1, 1:10,000 dilution; Novus Biologicals, Inc.), chicken anti-HmgCS2 (1:15,000 dilution; Sigma-Aldrich), Aifm1 polyclonal antibody (PAB0324, 1:2,000 dilution; Abnova), anti-Glud1 (1:10,000 dilution; Rockland, Inc.), anti-DAPK3/ZIPK (1:2,000 dilution; Biomol International), rabbit polyclonal to CPS1-Liver mitochondrial marker (ab3682, 1:40,000 dilution; Abcam), mouse monoclonal to Atp5a1 (15H4, ab14748, 1:25,000 dilution;

Abcam), rabbit polyclonal to Sod1 (ab13499, 1:20,000 dilution; Abcam). To examine global protein levels on the membrane after transfer, the membrane was soaked in 100% methanol for 30 sec, and incubated in Coomassie G250 (0.1% w/v in 30% methanol and 10% acetic acid) for 1 min. The membrane was then destained in 50% methanol (3 washes, 3 min each). Normalized area densities were determined using ImageJ (National Institutes of Health).

Conjugation of MAbs to agarose and sample preparation for LC-MS/MS analysis. MAbs 18B10.C7(3), 9D1.E4(10) and 1F5.D6(14) or CTD110.6 were covalently conjugated to protein A/G PULS agarose or anti-mouse IgM agarose via disuccinimidyl suberate (DSS, Thermo Scientific) according to manufacturer's instruction. PUGNAc treated HEK293T nucleocytosolic fraction was prepared as above on larger scale, incubated with antibody-conjugated agarose, and washed as described above. A mixture of normal mouse IgG-conjugated agarose and anti-mouse IgM agarose was subjected to the identical procedure in parallel for the negative control. To elute proteins from the agarose, glycine (0.1 M, pH 2.5) was added and the eluates were immediately neutralized with Tris-HCl (1 M, pH 8.0). The samples were then reduced and alkylated as described previously[10] and subjected to LysC (Roche) digestion at 37 °C for 24 h. After digestion, the samples were processed as previously described10. For Sham or TH-R treated liver lysates, only IF5.D6(14)-conjugated agarose was used for *O*-GlcNAc modified protein enrichment, in which normal mouse IgG-conjugated agarose was included as a negative control. The eluates were treated in a similar procedure except trypsin (Promega, Madison, WI) was used for the digestion.

S1. Knorr, R., Trzeciak, A., Bannwarth, W. & Gillessen, D. New coupling reagents in peptide chemistry. *Tetrahedron Lett.* 30, 1927-1930 (1989).
S2. Salvador, L.S., Elofsson, M. & Kihlberg, J. Preparation of building blocks for glycopeptide synthesis by glycosylation of Fmoc amino acids having unprotected carboxyl groups. *Tetrahedron* 51, 5643-5656 (1995).

S3. Zhu, X. & Schmidt, R.R. Efficient synthesis of *S*-linked glycopeptides in aqueous solution by a convergent strategy. *Chem. Eur. J.* 10, 875-887 (2004).
S4. Metzger, J.W., Wiesmuller, K.H. & Jung, G. Synthesis of *N*-alpha-Fmoc protected derivatives of *S*-(2,3-dihydroxypropyl)-cysteine and their application in peptide synthesis. *Int. J. Pept. Protein Res.* 38, 545-554 (1991).
S5. Roth, A., Espuelas, S., Thumann, C., Frisch, B. & Schuber, F. Synthesis of thiol-reactive lipopeptide adjuvants. Incorporation into liposomes and study of their mitogenic effect on mouse splenocytes. *Bioconjugate Chem.* 15, 541-553 (2004).
S6. Kaiser, E., Colescot.Rl, Bossinge.Cd & Cook, P.I. Color test for detection of free terminal amino groups in solid-phase synthesis of peptides. *Anal. Biochem.* 34, 595 (1970).
S7. Comer, F.I., Vosseller, K., Wells, L., Accavitti, M.A. & Hart, G.W. Characterization of a mouse monoclonal antibody specific for *O*-linked *N*-acetylglucosamine. *Anal. Biochem.* 293, 169-177 (2001).
S8. Buskas, T., Li, Y.H. & Boons, G.J. The immunogenicity of the tumor-associated antigen Lewis(y) may be suppressed by a bifunctional cross-linker required for coupling to a carrier protein. *Chem. Eur. J.* 10, 3517-3524 (2004).
S9. Ingale, S., Wolfert, M.A., Gaekwad, J., Buskas, T. & Boons, G.J. Robust immune responses elicited by a fully synthetic three-component vaccine. *Nat. Chem. Biol.* 3, 663-667 (2007).
S10. Lim, J.M. *et al.* Defining the regulated secreted proteome of rodent adipocytes upon the induction of insulin resistance. *J. Proteome Res.* 7, 1251-1263 (2008).

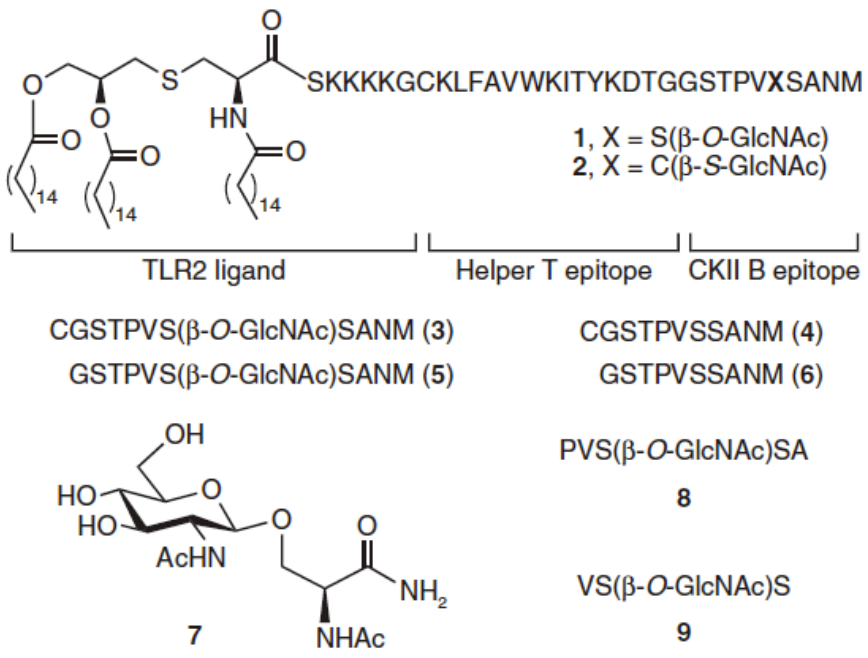

Figure 3-1. Structures of fully synthetic three-component immunogens 1 and 2. Compounds 3–9 were used for ELISA and inhibition ELISA to determine epitope selectivities of the antibodies.

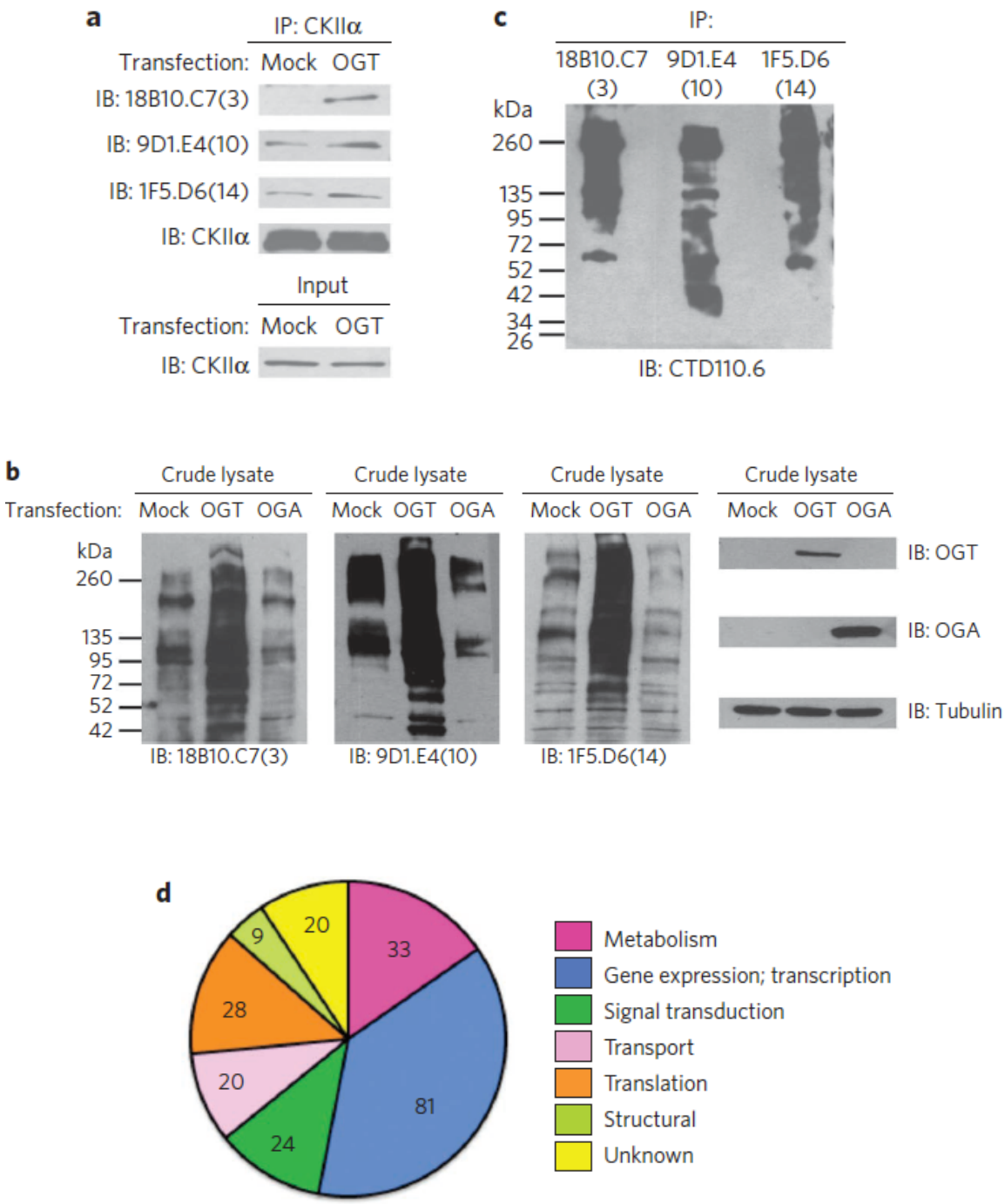

Figure 3-2. Immunoblots of three monoclonal antibodies. **(a)** The CKII α-subunit was immunoprecipitated from HEK293T cells with or without OGT overexpression. Eluates were resolved by SDS-PAGE and immunoblotted with monoclonal antibodies 18B10.C7(3), 9D1.E4(10) and 1F5.D6(14). A band corresponding to the CKII α-subunit

was detected with signal intensity correlated with *O*-GlcNAc status. All blots were stripped and reprobed with antibody against the CKII α-subunit (only one representative blot is shown here). Also, an equal amount of the CKII α-subunit was present in the input regardless of the status of *O*-GlcNAc levels. (**b**) HEK293T lysates with low (OGA overexpression), median (mock transfection) and high (OGT overexpression) levels of *O*-GlcNAc modification were exposed to monoclonal antibodies 18B10.C7(3), 9D1.E4(10) and 1F5.D6(14), respectively. The signals obtained mirror the corresponding *O*-GlcNAc status in each sample. Immunoblots against OGT, OGA and tubulin are also shown. While equal loading of tubulin was detected in all samples, higher OGA and OGT protein levels were detected with lysates from OGA and OGT transfections, respectively. Note that endogenous OGT and OGA levels do appear after longer exposure. (**c**) *O*-GlcNAc proteins were immunoprecipitated from HEK293T cells treated with PUGNAc (an OGA inhibitor), resolved by SDS-PAGE and subjected to CTD 110.6 (an IgM isotype *O*-GlcNAc–specific antibody) blotting. Cross-reactivity of monoclonal antibodies 18B10.C7(3), 9D1.E4(10) and 1F5.D6(14) with CTD 110.6, albeit distinct in pattern, was detected. See **Figure 3-S6** for uncut gel images. (**d**) Application of monoclonal antibodies for *O*-GlcNAc-omics in cell culture. Distribution of *O*-GlcNAc– modified proteins based on their biological process categorized in HPRD (the number of individual proteins assigned to each category is displayed).

Table 3-1. Novel proteins enriched from HEK293T cells by more than one of the antibodies.

UniProt Accsion Number	Gene Name	Sequence Name	Total Peptides				Biological Process	Primary Localization	Alternate Localization
			18B4AC7 (3)	9D1JE4 (10)	3F5J06 (14)	CTD11B.5			
P49790	NUP153	Nuclear pore complex protein Nup153	3	6	30	22	Tp	N	
Q2KH83	QSER1	Glutamine and serine-rich protein 1 (FLJ21924)	1	3	11	3	U	U	
Q02543	RPL18A	60S ribosomal protein L18a	4	3	3	3	Tl	C	No,M
P35658	NUP214	Nuclear pore complex protein Nup214	6	7	27	0	Tp	N	
Q17RM7	C11orf30	Chromosome 11 open reading frame 30 (Protein EMSY)	0	1	11	0	Gn	N	C,PM
Q8WWM7	ATXN2L	Ataxin-2-like protein	3	0	10	4	U	N	C
P63173	RPS6	40S ribosomal protein S6	3	0	7	0	Tl	C	No,C
P52948	NUP98	Nuclear pore complex protein Nup98-Nup96 precursor [Contains: Nuclear pore complex protein Nup98]	0	7	6	6	Tp	N	
Q9P2N5	RBM27 (KIAA1311)	RNA-binding protein 27	0	5	6	3	U	C,N	
P78406	RAE1 (MRNP41)	mRNA export factor (mRNA-associated protein mrnp 41; Rae1 protein homolog)	0	1	6	2	Tp	N	C,M
Q12771	--	P37 AUF1	5	4	5	0	U	U	
Q8NC51	PAIRB (SERBP1)	Plasminogen activator inhibitor 1 RNA-binding protein (SERPINE1 mRNA-binding protein 1)	3	0	4	3	Gn	C	N
P36373	RPL13	60S ribosomal protein L13	3	0	4	3	Tl	C	No,N, M
P09211	GSTP1 (GST1)	Glutathione S-transferase P	5	6	4	0	Mb	C	N,M
Q15436	SEC23A	Protein transport protein Sec23A (Sec23 related protein A)	2	3	4	0	Tp	C	ER
Q99567	NUP88	Nuclear pore complex protein Nup88	0	2	4	0	Tp	N	
P11940	PABPC1 (PABP1)	Polyadenylate-binding protein 1 (Poly(A)-binding protein 1; Polyadenylate binding protein, cytoplasmic, 1)	3	1	4	0	Gn	C	N
Q14684N	RRP1B (KIAA0179)	RRP1-like protein B (Ribosomal RNA processing protein 1 homolog B)	1	0	4	0	Tl	Na	N
P83731	RPL24	60S ribosomal protein L24	2	0	3	3	Tl	C	
P16402	H1ST1H1D	Histone H1.3	1	0	3	1	Gn	N	No,M
P14866	HNRNPL	Heterogeneous nuclear ribonucleoprotein L	4	0	2	2	Gn	N	No,C, M
Q15437	SEC23B	Protein transport protein Sec23B (Sec23 related protein B)	1	4	2	0	Tp	ER	G,C
Q9C221	NAT13	N-acetyltransferase 13 (MAK3)	3	2	2	0	U	C	
P46779	RPL28	60S ribosomal protein L28	2	0	2	0	Tl	C	Na
P05387	RPLP2	60S acidic ribosomal protein P2	2	0	2	0	Tl	C	Na
Q12906	ILF3 (NFAR)	Interleukin enhancer-binding factor 3 (Nuclear factor associated with dsRNA)	4	3	1	0	Gn	N	C,Na, M
Q13200	PSMD2	26S proteasome non-ATPase regulatory subunit 2	0	1	1	0	Mb	C	
P31689	DNAJA1 (HSPF4)	Dna) homolog subfamily A member 1 (Heat shock 40 kDa protein 4)	1	0	1	0	Mb	C	N,No, G
P16403	H1ST1H1C	Histone H1.2	1	0	1	0	Gn	N	Na,M
Q9Y3F4	STRAP	Serine-threonine kinase receptor-associated protein	6	5	0	0	Sg	C	N
Q14011	CIRBP (A18HNRNP)	Cold-inducible RNA-binding protein (Glycine-rich RNA-binding protein; hnRNPA18)	3	3	0	0	Sg	N	
P10599	TXN	Thioredoxin	2	2	0	0	Mb	C	N,Ex
Q13151	HNRNPA0	Heterogeneous nuclear ribonucleoprotein A0	3	1	0	0	Gn	N	C,No, M
P07195	LDHB	L-lactate dehydrogenase B chain	2	1	0	0	Mb	C	
Q09028	RBBP4	Histone-binding protein RBBP4 (Retinoblastoma binding protein 4)	1	1	0	0	Gn	N	Na,M

Abbreviations:
Gn, Gene expression / Transcription; Mb, Metabolism; Sg, Signal transduction; St, Structural; Tl, Translation; Tp, Transport; U, Unknown; C, Cytoplasm; N, Nucleus;M, Mitochondrial; No, Nucleolus; ER, Endoplasmic reticulum; G, Golgi apparatus; Ex, Extracellular; PM, Plasma membrane.a

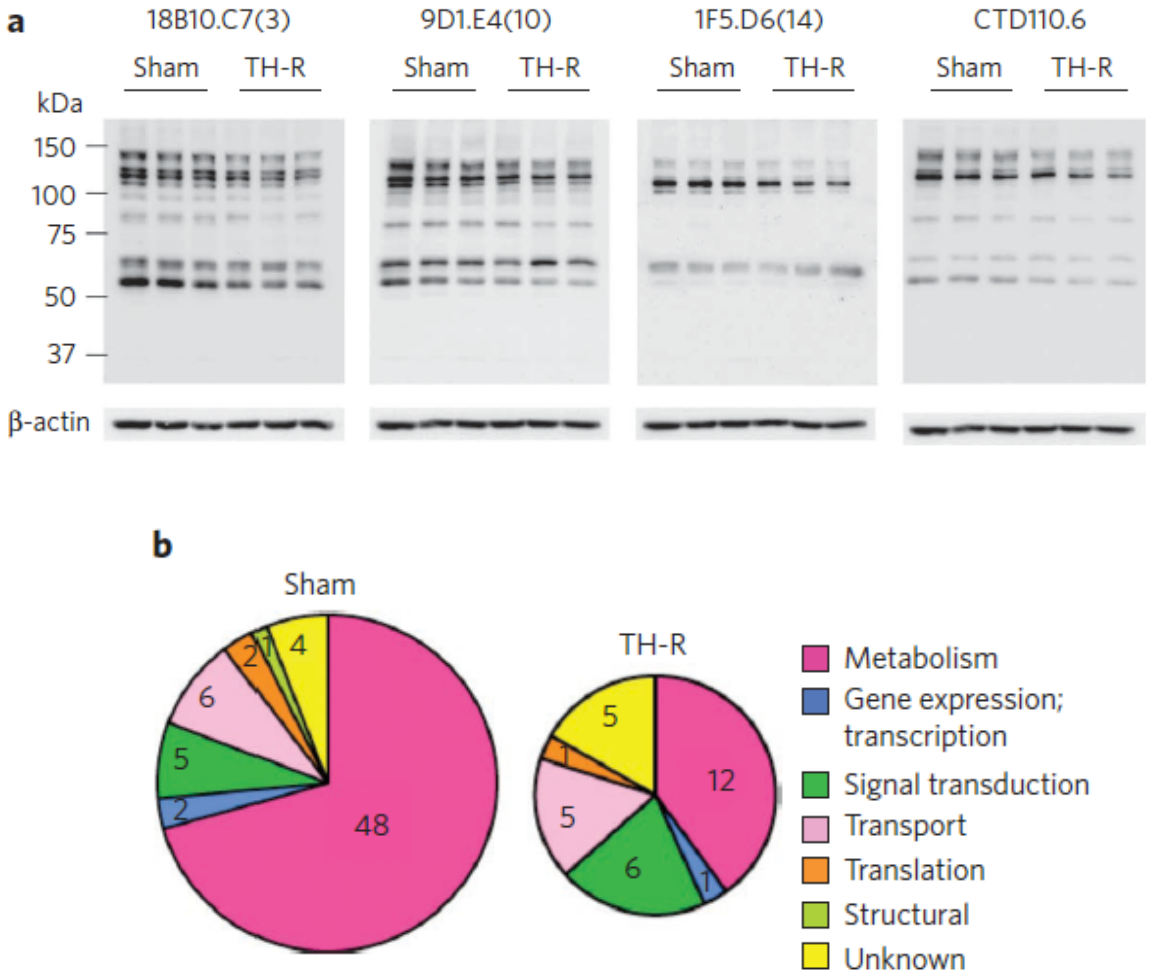

Figure 3-3. Application of monoclonal antibodies for *O*-GlcNAc-omics in mammalian tissue. (**a**) Western blot analysis using the *O*-GlcNAc antibodies of rat liver extracts following sham or TH-R treatment. See **Figure 3-S6** for uncut gel images. (**b**) Distribution of *O*-GlcNAc–modified proteins in rat liver based on their biological process following sham or THR treatment (the number of individual proteins assigned to each category is displayed).

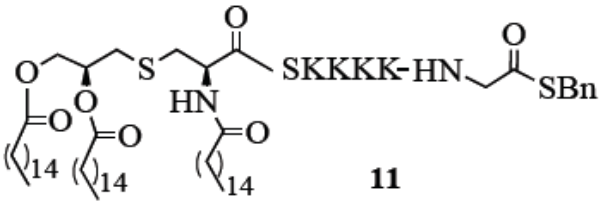

11

CKLFAVWKITYKDTGGSTPVXSANM

12. X = S(β-*O*-GlcNAc)
13. X = C(β-*S*-GlcNAc)

Figure 3-S1. Reagents **11**-**13** used for the preparation of immunogens **1** and **2**.

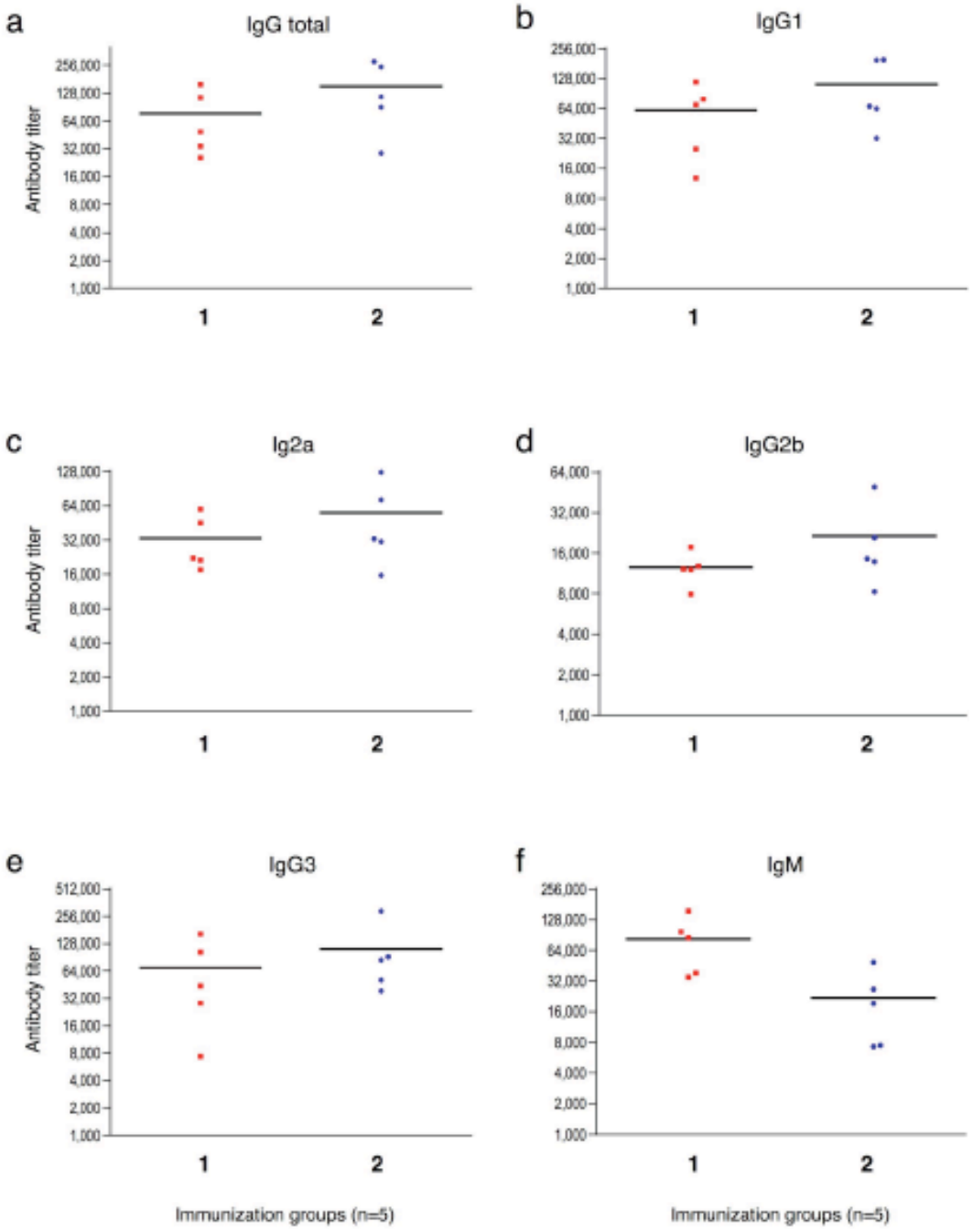

Figure 3-S2. ELISA anti-GSTPVS(β-*O*-GlcNAc)SANM (**5**) antibody titers after 4 immunizations with **1** and **2**. ELISA plates were coated with BSA-MI-GSTPVS(β-*O*-GlcNAc)SANM (BSA-MI-**3**) conjugate and (**a**) IgG total, (**b**) IgG1, (**c**) IgG2a, (**d**) IgG2b, (**e**) IgG3 and (**f**) IgM titers were determined by linear regression analysis, plotting dilution vs. absorbance. Titers were defined as the highest dilution yielding an optical density of

0.1 or greater over that of normal control mouse sera. Each data point represents the titer for an individual mouse after 4 immunizations and the horizontal lines indicate the mean for the group of five mice.

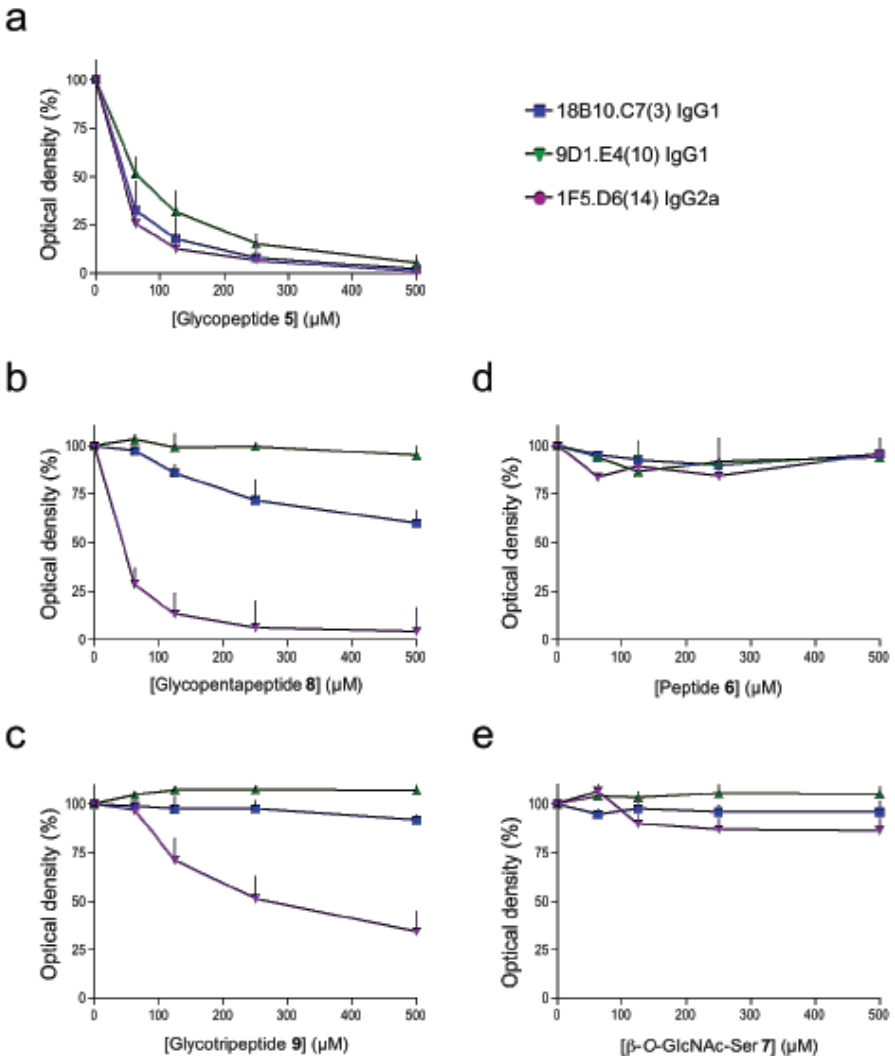

Figure 3-S3. Competitive inhibition of monoclonal antibody binding to GSTPVS(β-*O*-GlcNAc)SANM (**5**) by the corresponding glycopeptides, peptide and sugar. ELISA plates were coated with BSA-MI-CGSTPVS(β-*O*-GlcNAc)SANM (BSA-MI-**3**) conjugate. MAbs, diluted to obtain in the absence of an inhibitor an OD of approximately 1 in the ELISA,

were first mixed with (**a**) glycopeptide **5** (GSTPVS(β-*O*-GlcNAc)SANM), (**b**) glycopentapeptide **8** (PVS(β-*O*-GlcNAc)SA), (**c**) glycotripeptide **9** (VS(β-*O*-GlcNAc)S), (**d**) peptide **6** (GSTPVSSANM) or (**e**) sugar **7** (β-*O*-GlcNAc-Ser) (0-500 μM final concentration) and then applied to the coated microtiter plate. Optical density values were normalized for the optical density values obtained with monoclonal antibody alone (0 μM inhibitor, 100%). The data are reported as the means ± s.d. of three independent experiments.

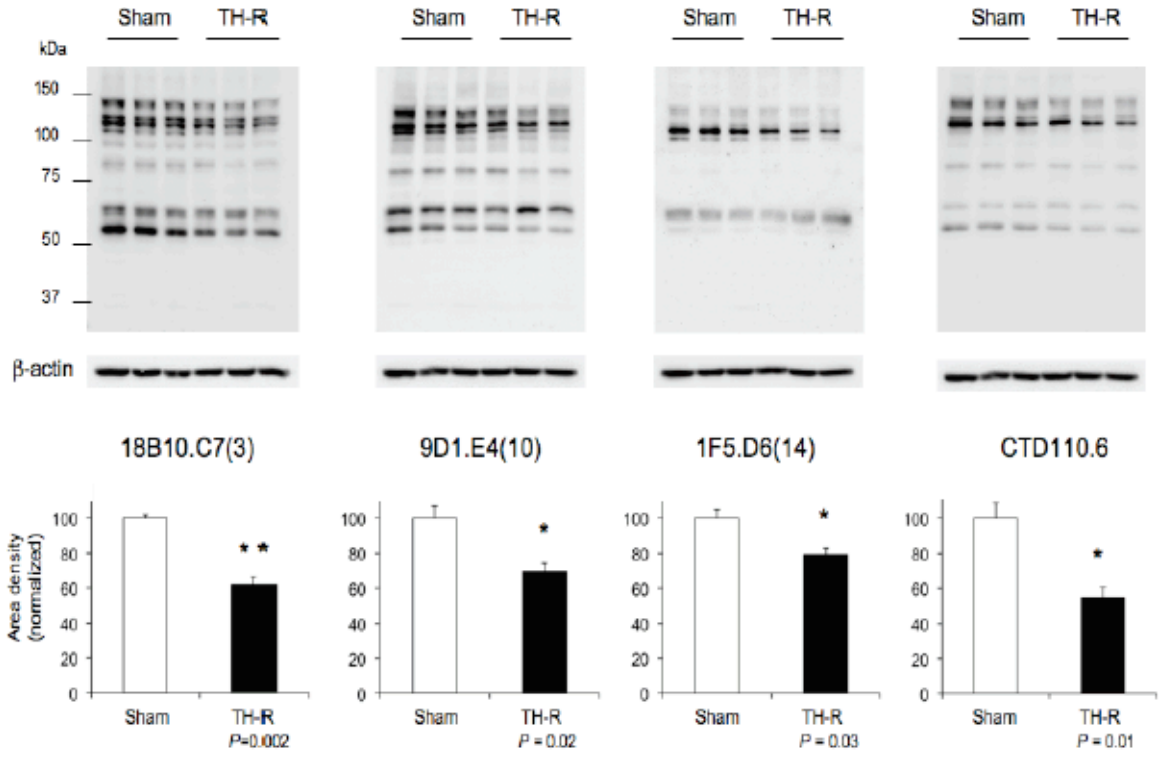

Figure 3-S4. Application of MAbs for *O*-GlcNAc-omics in mammalian tissue. Western blot analysis and densitometry using the *O*-GlcNAc antibodies of rat liver extracts following Sham or TH-R treatment. A statistically significant difference ($P<0.05$) was observed between Sham versus TH-R treatment for all four antibodies. The bars represent mean values ± s.e.m. ($n=3$).

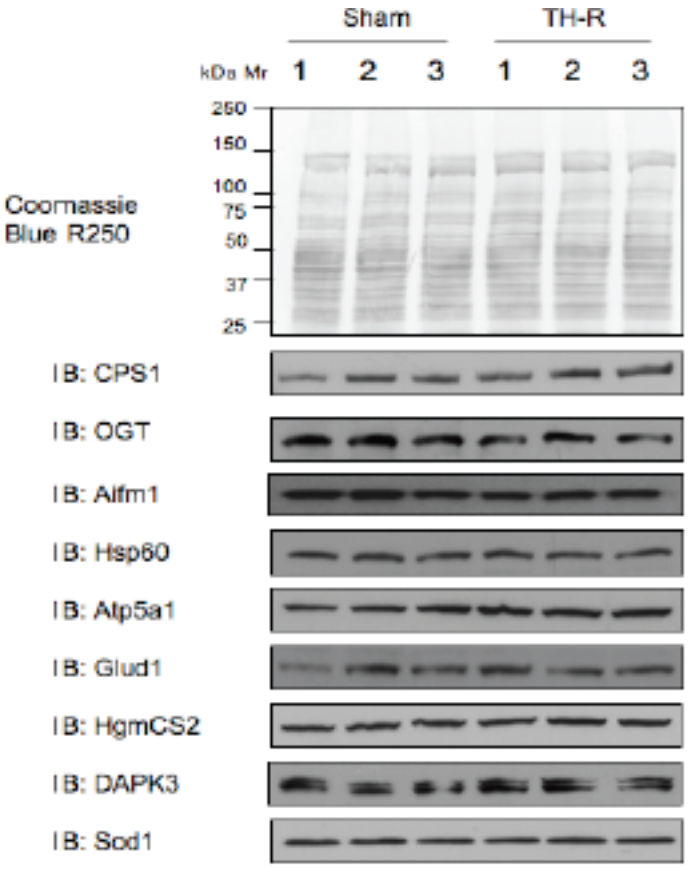

Figure 3-S5. Abundance of *O*-GlcNAc modified proteins in crude extracts. SDSPAGE followed by protein staining or western blotting for proteins of interest of crude liver extracts from 3 rats each of Sham or TH-R treatment, demonstrating that the proteins levels are not significantly altered in crude extracts though several of these proteins were only detected in the Sham or TH-R animals by mass spectrometry following enrichment with a pan anti-*O*-GlcNAc MAb.

a

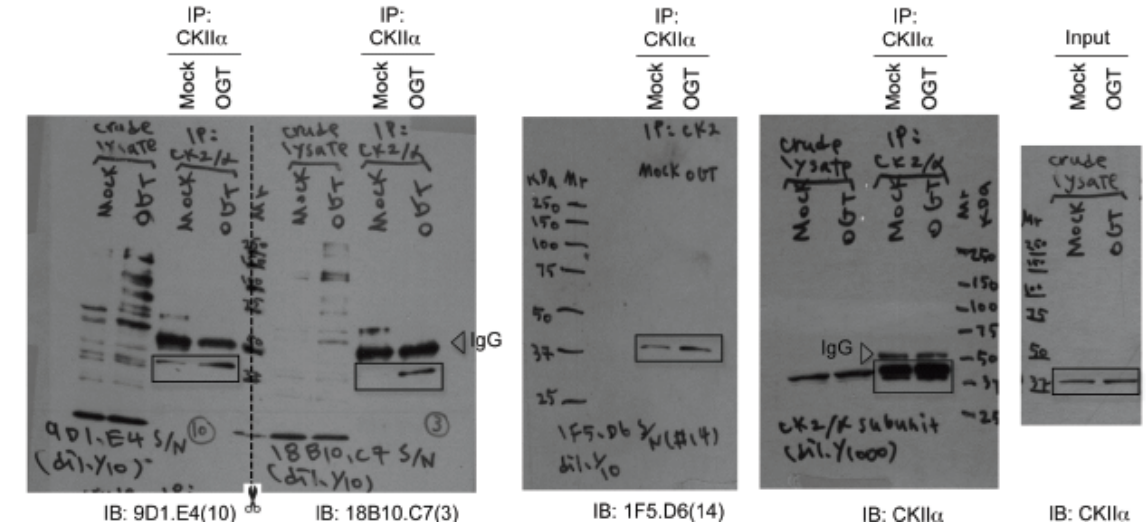
IP: CKIIα
Mock
OGT
IgG
IB: 9D1.E4(10)
IB: 18B10.C7(3)
IB: 1F5.D6(14)
IB: CKIIα
Input
IB: CKIIα

b

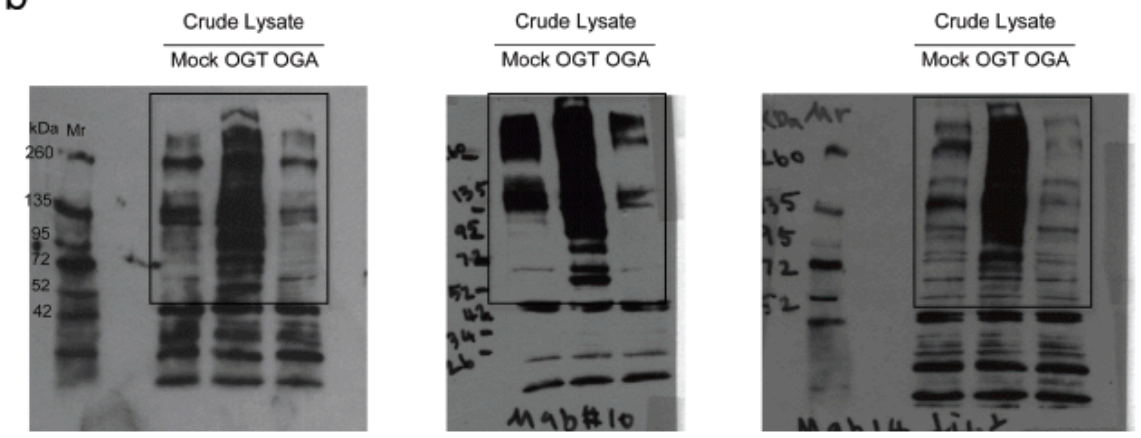
Crude Lysate
Mock OGT OGA
kDa Mr
260
135
95
72
52
42
IB: 18B10.C7(3)
IB: 9D1.E4(10)
IB: 1F5.D6(14)

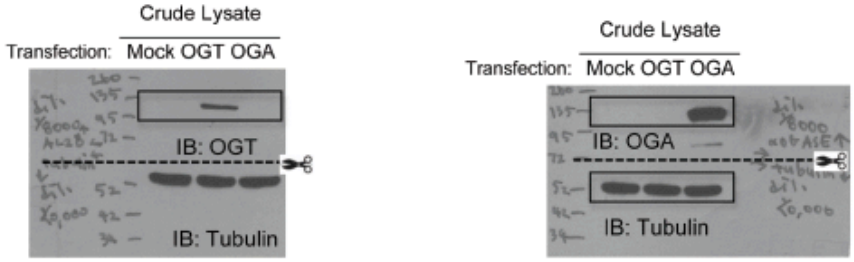
Crude Lysate
Transfection:
Mock OGT OGA
IB: OGT
IB: Tubulin
IB: OGA
IB: Tubulin

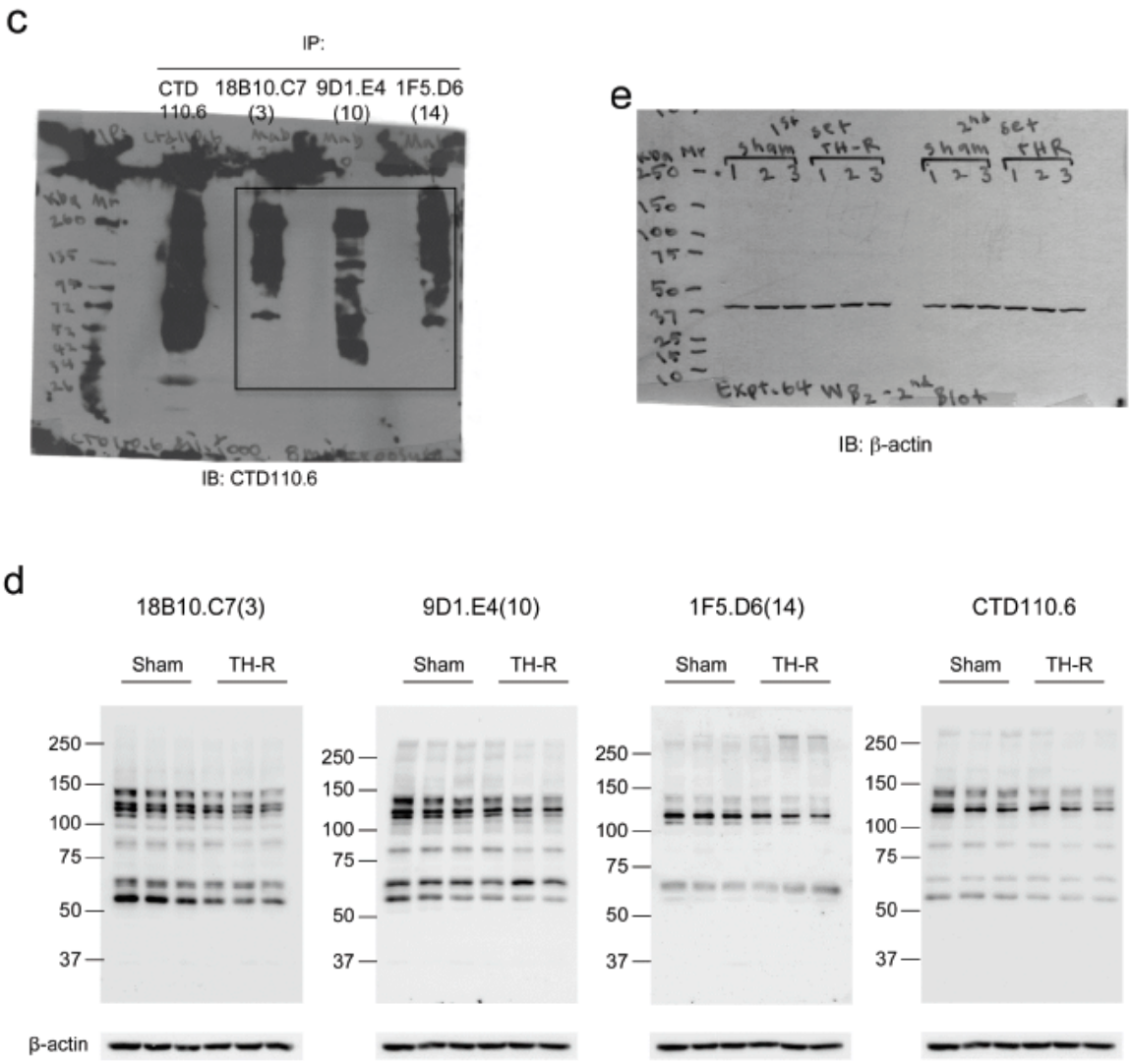

Figure 3-S6. Uncut gel images of gels shown in **Figures 3-2** and **3-3**. Gels shown: (**a**) from **Figure 3-2a**, (**b**) from **Figure 3-2b**, (**c**) from **Figure 3-2c**, (**d**) from **Figure 3-3a** and (**e**) β-actin images of identical samples as shown in **Figure 3-3a**.

Table 3-S1. ELISA anti-GSTPVS(β-*O*-GlcNAc)SANM (**5**) antibody titersa after 4 immunizations with two different preparations.

Immunization[b]	IgG total	IgG1	IgG2a	IgG2b	IgG3	IgM
O-GlcNAc **1**[c]	76,500	61,400	33,200	12,500	69,400	81,900
S-GlcNAc **2**[d]	151,600	111,800	55,600	21,300	111,700	21,900

[a] Anti-GSTPVS(β-*O*-GlcNAc)SANM (**5**) antibody titers are presented as the mean of groups of five mice. ELISA plates were coated with BSA-MI-GSTPVS(β-*O*-GlcNAc)SANM (BSA-MI-**6**) conjugate and titers were determined by linear regression analysis, plotting dilution vs. absorbance. Titers are defined as the highest dilution yielding an optical density of 0.1 or greater over that of normal control mouse sera.
[b] Liposomal preparations were employed.
[c] *O*-GlcNAc **1**; Pam_3CysSK_4G-C-KLFAVWKITYKDT-G-GSTPVS(β-*O*-GlcNAc)SANM.
[d] *S*-GlcNAc **2**; Pam_3CysSK_4G-C-KLFAVWKITYKDT-G-GSTPVC(β-*S*-GlcNAc)SANM.
A statistically significant difference was observed between **1** versus **2** for IgM titers ($P = 0.0327$).
Individual titers for IgG total, IgG1, IgG2a, IgG2b, IgG3 and IgM are reported in **Supplementary Figure 1** online.

Table 3-S2. Monoclonal antibodies against GSTPVS(β-*O*-GlcNAc)SANM (**5**).

Fusion	Cell Line	ELISA coating: glycopeptide[a]	Isotype	Titer Isotype[b]	Inhibition with *O*-GlcNAc glycopeptide[c]	ELISA coating: peptide[d]
Mouse #1	1D3.D6(1)	+	IgG1	38,000	-	-
	3C1.E8(2)	+		38,000	++	-
	18B10.C7(3)	+		19,000	+++	-
	5H11.H6(4)	+		6,000	+++	+
	6G3.A5(5)	+	IgG2a	17,000	+++	-
	7A3.G8.F7(6)	+		9,000	-	-
	13F10.G6(7)	+	IgG2b	NA[e]	-	+
	11D6.C1(8)	+	IgG3	29,000	+++	-
	1H2.F2(27)	+		NA	+++	+
Mouse #4	7B8.F5(9)	+	IgG1	38,000	+	-
	9D1.E4(10)	+		38,000	+++	-
	16B9.F1(11)	+		38,000	++	-
	1D5.C1(12)	+	IgG2a	3,000	+++	-
	1E5.H3(13)	+		< 500		-
	1F5.D6(14)	+		4,000	+++	-
	8G11.D6(22)	+		2,000	+++	-
	14D9.D4(23)	+		17,000	+	-
	3G5.A2(15)	+	IgG2b	15,000	+	-
	1E9.E3(16)	+	IgG3	14,000	+++	-
	2A8.F3(17)	+		7,000	+	-
	2D5.E6(18)	+		7,000	-	-
	5F6.G4(19)	+		14,000	+++	-
	7B3.A3(20)	+		14,000	+++	-
	8C3.H2(24)	+		7,000	-	-
	11C6.E5(25)	+		14,000	+	-
	16E2.A3(26)	+		14,000	-	-
	6B5.A8(21)	+		< 500		+
	1D7.B4(28)	+		< 500		+
	6A5.H1.C6(29)	+		< 500		+
	8F12.A6.C5(30)	+		14,000	+++	+

[a] ELISA plates were coated with BSA-MI-CGSTPVS(β-*O*-GlcNAc)SANM (BSA-MI-**3**) conjugate and supernatants of the different cell lines were screened undiluted.
[b] ELISA plates were coated with BSA-MI-CGSTPVS(β-*O*-GlcNAc)SANM (BSA-MI-**3**) conjugate and titers were determined by linear regress ion analysis, plotting dilution vs. absorbance. Titers are defined as the highest dilution yielding an optical density of 0.1 or greater over that of background.
[c] ELISA plates were coated with BSA-MI-CGSTPVS(β-*O*-GlcNAc)SANM (BSA-MI-**3**) conjugate and inhibition by GSTPVS(β-*O*-GlcNAc)SANM (**5**) was determined: -, +, ++ and +++ indicate no inhibition, weak inhibition, inhibition approximately 50% at 500 μM and complete inhibition at 500 μM, respectively.
[d] ELISA plates were coated with BSA-MI-CGSTPVSSANM (BSA-MI-**4**) conjugate and supernatants of the different cell lines were screened undiluted.
[e] NA indicates not analyzed.

Table 3-S3. Application of MAbs for *O*-GlcNAc-omics in cell culture: Number of *O*-GlcNAc modified proteins pulled down with different MAbs.

	Number of proteins
Total[a]	215
novel	140
known	75
18B10.C7(3)	101
novel	57
known	44
9D1.E4(10)	69
novel	35
known	34
1F5.D6(14)	132
novel	84
known	48
CTD110.6	43
novel	27
known	16

[a] A total of 215 proteins were assigned to be *O*-GlcNAc modified in the combination of all MAbs, where 140 appeared to be novel.

Table 3-S4. List of enriched novel *O*-GlcNAc proteins from HEK293T cells.

UniProt Acssion Number	Gene Name	Sequence Name	Total Peptides				Biological Process	Primary Localization	Alternate Localization
			18B10.C7 (3)	9D1.E4 (10)	1F5.D6 (14)	CTD110.6			
P35658	NUP214	Nuclear pore complex protein Nup214	6	7	27	0	Tp	N	
Q9Y3F4	STRAP	Serine-threonine kinase receptor-associated protein	6	5	0	0	Sg	C	N
P09211	GSTP1 (GST1)	Glutathione S-transferase P	5	6	4	0	Mb	C	N,M
Q12771	--	P37 AUF1	5	4	5	0	U	U	
Q02543	RPL18A	60S ribosomal protein L18a	4	3	3	3	Tl	C	No,M
Q12906	ILF3 (NFAR)	Interleukin enhancer-binding factor 3 (Nuclear factor associated with dsRNA)	4	3	1	0	Gn	N	C,No, M
P14866	HNRNPL	Heterogeneous nuclear ribonucleoprotein L	4	0	2	2	Gn	N	No,C, M
P49790	NUP153	Nuclear pore complex protein Nup153	3	6	30	22	Tp	N	
Q9GZZ1	NAT13	N-acetyltransferase 13 (MAK3)	3	2	2	0	U	C	
P11940	PABPC1 (PABP1)	Polyadenylate-binding protein 1 (Poly(A)-binding protein 1; Polyadenylate binding protein, cytoplasmic, 1)	3	1	4	0	Gn	C	N
Q8NC51	PAIRB (SERBP1)	Plasminogen activator inhibitor 1 RNA-binding protein (SERPINE1 mRNA-binding protein 1)	3	0	4	2	Gn	C	N
Q15436	SEC23A	Protein transport protein Sec23A (Sec23 related protein A)	2	3	4	0	Tp	C	ER
Q14011	CIRBP (A18HNRNP)	Cold-inducible RNA-binding protein (Glycine-rich RNA-binding protein; hnRNPA18)	2	2	0	0	Sg	N	
P10599	TXN	Thioredoxin	2	2	0	0	Mb	C	N,Ex
Q13151	HNRNPA0	Heterogeneous nuclear ribonucleoprotein A0	2	1	0	0	Gn	N	C,No, M
P07195	LDHB	L-lactate dehydrogenase B chain	2	1	0	0	Mb	C	
Q8WWM7	ATX2L	Ataxin-2-like protein	2	0	10	4	U	N	C
P62753	RPS6	40S ribosomal protein S6	2	0	7	0	Tl	C	No,C

Abbreviations:

Gn, Gene expression / Transcription; Mb, Metabolism; Sg, Signal transduction; St, Structural; Tl, Translation; Tp, Transport; U, Unknown; C, Cytoplasm; N, Nucleus;M, Mitochondrial; No, Nucleolus; ER, Endoplasmic reticulum; G, Golgi apparatus; Ex, Extracellular; PM, Plasma membrane.

Table 3-S4. List of enriched novel *O*-GlcNAc proteins from HEK293T cells.

UniProt Acssion Number	Gene Name	Sequence Name	Total Peptides				Biological Process	Primary Localization	Alternate Localization
			18B10.C7 (3)	9D1.E4 (10)	1F5.D6 (14)	CTD110.6			
P26373	RPL13	60S ribosomal protein L13	2	0	4	2	Tl	C	No,N, M
P83731	RPL24	60S ribosomal protein L24	2	0	3	3	Tl	C	
P46779	RPL28	60S ribosomal protein L28	2	0	2	0	Tl	C	No
P05387	RPLP2	60S acidic ribosomal protein P2	2	0	2	0	Tl	C	No
O75821	EIF3S4 (EIF3G)	Eukaryotic translation initiation factor 3 subunit 4(Eukaryotic translation initiation factor 3 subunit G)	2	0	0	1	Tl	C	
Q8N6N7	ACBD7	Acyl-CoA-binding domain-containing protein 7	2	0	0	0	U	U	
P48634	BAT2	Large proline-rich protein BAT2	2	0	0	0	U	C	N
P61927	RPL37	60S ribosomal protein L37	2	0	0	0	Tl	C	
P30086	PEBP1	Phosphatidylethanolamine-binding protein 1 (Raf kinase inhibitor protein)	2	0	0	0	Sg	C	PM
Q9NZI7	UBP1 (LBP1)	Upstream-binding protein 1 (Transcription factor LBP 1b)	2	0	0	0	Gn	N	
Q14192	FHL2 (SLIM3)	Four and a half LIM domains protein 2 (Skeletal muscle LIM-protein 3)	2	0	0	0	Gn	N	C,M
O75534	CSDE1 (NRU)	Cold shock domain-containing protein E1 (N-ras upstream gene protein)	2	0	0	0	Gn	C	
Q92522	H1FX	Histone H1x	2	0	0	0	Gn	N	No,M
P27694	RPA1	Replication protein A 70 kDa DNA-binding subunit (Replication factor A protein 1)	2	0	0	0	Gn	N	
Q15437	SEC23B	Protein transport protein Sec23B (Sec23 related protein B)	1	4	2	0	Tp	ER	G,C
Q2KHR3	QSER1	Glutamine and serine-rich protein 1 (FLJ21924)	1	2	11	3	U	U	
Q09028	RBBP4	Histone-binding protein RBBP4 (Retinoblastoma binding protein 4)	1	1	0	0	Gn	N	No,M

Abbreviations:

Gn, Gene expression / Transcription; Mb, Metabolism; Sg, Signal transduction; St, Structural; Tl, Translation; Tp, Transport; U, Unknown; C, Cytoplasm; N, Nucleus;M, Mitochondrial; No, Nucleolus; ER, Endoplasmic reticulum; G, Golgi apparatus; Ex, Extracellular; PM, Plasma membrane.

Table 3-S4. List of enriched novel *O*-GlcNAc proteins from HEK293T cells.

UniProt Acssion Number	Gene Name	Sequence Name	Total Peptides				Biological Process	Primary Localization	Alternate Localization
			18B10.C7 (3)	9D1.E4 (10)	1F5.D6 (14)	CTD110.6			
Q14684N	RRP1B (KIAA0179)	RRP1-like protein B (Ribosomal RNA processing protein 1 homolog B)	1	0	4	0	Tl	No	N
P16402	HIST1H1D	Histone H1.3	1	0	3	1	Gn	N	No,M
P31689	DNAJA1 (HSPF4)	DnaJ homolog subfamily A member 1 (Heat shock 40 kDa protein 4)	1	0	1	0	Mb	C	N,No, G
P16403	HIST1H1C	Histone H1.2	1	0	1	0	Gn	N	No,M
Q52LJ0	FAM98B	Protein FAM98B (Family with sequence similarity 98, member B; FLJ38426)	1	0	0	0	U	U	
Q9NY37	ACCN5	Amiloride-sensitive cation channel 5	1	0	0	0	Tp	PM	
Q14444	CAPRIN1 (GPIP137)	Caprin-1 (Cytoplasmic activation- and proliferation-associated protein 1; GPI-anchored protein p137)	1	0	0	0	Tp	C	PM
Q13347	EIF3S2 (EIF3I)	Eukaryotic translation initiation factor 3 subunit 2 (Eukaryotic translation initiation factor 3 subunit I)	1	0	0	0	Tl	C	
P39019	RPS19	40S ribosomal protein S19	1	0	0	0	Tl	No	M
P32969	RPL9	60S ribosomal protein L9	1	0	0	0	Tl	C	No,M
P43487	RANBP1	Ran-specific GTPase-activating protein (Ran binding protein 1)	1	0	0	0	Sg	C	N
P22234	PAICS	Multifunctional protein ADE2 [Includes: Phosphoribosylaminoimidazole-succinocarboxamide synthase] (Phosphorybosylaminoimidazole carboxylase)	1	0	0	0	Mb	N	
P00492	HPRT1	Hypoxanthine-guanine phosphoribosyltransferase	1	0	0	0	Mb	C	
A2A3N6	PIPSL	Novel protein similar to phosphatidylinositol-4-phosphate 5-kinase, type I, alpha (Putative PIP5K1A and PSMD4-like protein)	1	0	0	0	Mb	C	
Q9UJV9	DDX41	Probable ATP-dependent RNA helicase (DEAD box protein 41)	1	0	0	0	Gn	No	C,N

Abbreviations:

Gn, Gene expression / Transcription; Mb, Metabolism; Sg, Signal transduction; St, Structural; Tl, Translation; Tp, Transport; U, Unknown; C, Cytoplasm; N, Nucleus;M, Mitochondrial; No, Nucleolus; ER, Endoplasmic reticulum; G, Golgi apparatus; Ex, Extracellular; PM, Plasma membrane.

Table 3-S4. List of enriched novel *O*-GlcNAc proteins from HEK293T cells.

UniProt Acssion Number	Gene Name	Sequence Name	Total Peptides				Biological Process	Primary Localization	Alternate Localization
			18B10.C7 (3)	9D1.E4 (10)	1F5.D6 (14)	CTD110.6			
Q96AE4	FUBP1	Far upstream element-binding protein 1	1	0	0	0	Gn	N	C
Q5RLJ0	C14orf166	CLE (C14orf166)	1	0	0	0	Gn	N	No,C
Q13310	PABPC4 (PABP4; APP1)	Polyadenylate-binding protein 4 (Poly(A)-binding protein 4; Activated-platelet protein 1)	1	0	0	0	Gn	C	
P62633	CNBP (ZNF9)	Cellular nucleic acid-binding protein (Zinc finger protein 9)	1	0	0	0	Gn	C	ER
P09429	HMGB1 (HMG1)	High mobility group protein B1 (High mobility group box 1)	1	0	0	0	Gn	N	
O43148	RNMT	mRNA cap guanine-N7 methyltransferase	1	0	0	0	Gn	C	N
P54652	HSPA2	Heat shock-related 70 kDa protein 2 (Heat shock 70 kDa protein 2)	1	0	0	0	Mb	N	C,No
P52948	NUP98	Nuclear pore complex protein Nup98-Nup96 precursor [Contains: Nuclear pore complex protein Nup98	0	7	6	6	Tp	N	
Q9P2N5	RBM27 (KIAA1311)	RNA-binding protein 27	0	5	6	2	U	C,N	
P31151	S100A7 (PSOR1)	Protein S100-A7 (100 calcium-binding protein A7; Psoriasin)	0	4	0	0	Sg	C	ER,N, PM,Ex
P05109	S100A8 (CAGA; MRP8)	Protein S100-A8 (Calgranulin-A; Migration inhibitory factor-related protein)	0	4	0	0	Sg	C	PM,Ex
P10412	HIST1H1E	Histone H1.4	0	4	0	0	Gn	N	No
P06702	S100A9 (CAGB; MRP14)	Protein S100-A9 (Calgranulin-B; Migration inhibitory factor-related protein 14)	0	3	0	0	Sg	C	PM,Ex

Abbreviations:

Gn, Gene expression / Transcription; Mb, Metabolism; Sg, Signal transduction; St, Structural; Tl, Translation; Tp, Transport; U, Unknown; C, Cytoplasm; N, Nucleus;M, Mitochondrial; No, Nucleolus; ER, Endoplasmic reticulum; G, Golgi apparatus; Ex, Extracellular; PM, Plasma membrane.

Table 3-S4. List of enriched novel *O*-GlcNAc proteins from HEK293T cells.

UniProt Acssion Number	Gene Name	Sequence Name	Total Peptides				Biological Process	Primary Localization	Alternate Localization
			18B10.C7 (3)	9D1.E4 (10)	1F5.D6 (14)	CTD110.6			
Q99567	NUP88	Nuclear pore complex protein Nup88	0	2	4	0	Tp	N	
Q15717	ELAVL1 (HUR)	ELAV-like protein 1 (Embryonic lethal abnormal vision like 1; Hu-antigen R)	0	2	0	2	Gn	N	C,No, M
P55735	SEC13	Protein SEC13 homolog	0	2	0	0	Tp	ER	N,C
A2A3R7	RPS6	Ribosomal protein S6	0	2	0	0	Tl	C	No
Q05BK6	TFG	TFG (Trk-fuse gene) protein	0	2	0	0	Sg	C	
P48594	SERPINB4 (SCCA2)	Serpin B4 (Squamous cell carcinoma antigen 2)	0	2	0	0	Mb	C	
Q17RM7	C11orf30	Chromosome 11 open reading frame 30 (Protein EMSY)	0	1	11	0	Gn	N	C,PM
P78406	RAE1 (MRNP41)	mRNA export factor (mRNA-associated protein mrnp 41; Rae1 protein homolog)	0	1	6	2	Tp	N	C,M
Q13200	PSMD2	26S proteasome non-ATPase regulatory subunit 2	0	1	1	0	Mb	C	
O75607	NPM3	Nucleoplasmin-3	0	1	0	0	Mb	N	C,No
P19474	RO52 (TRIM21)	52 kDa Ro protein (Tripartite motif containing protein 21)	0	1	0	0	Gn	N,C	
O75840	KLF7 (UKLF)	Krueppel-like factor 7 (Ubiquitous kruppel like factor)	0	1	0	0	Gn	N	
Q5T8P6	RBM26 (C13orf10)	RNA-binding protein 26 (CTCL tumor antigen se70-2)	0	0	19	0	Gn	N	
O14776	TCERG1	Transcription elongation regulator 1 (TATA box binding protein associated factor 2S)	0	0	12	1	Gn	N	No
Q03164	MLL	Zinc finger protein HRX (Histone-lysine N-methyltransferase HRX; ALL-1)	0	0	10	0	Gn	N	
Q99700	ATX2	Ataxin-2	0	0	9	0	Gn	C	N
Q5JRC2	WNK3	WNK lysine deficient protein kinase 3	0	0	7	0	U	U	

Abbreviations:

Gn, Gene expression / Transcription; Mb, Metabolism; Sg, Signal transduction; St, Structural; Tl, Translation; Tp, Transport; U, Unknown; C, Cytoplasm; N, Nucleus;M, Mitochondrial; No, Nucleolus; ER, Endoplasmic reticulum; G, Golgi apparatus; Ex, Extracellular; PM, Plasma membrane.

Table 3-S4. List of enriched novel *O*-GlcNAc proteins from HEK293T cells.

UniProt Acssion Number	Gene Name	Sequence Name	Total Peptides				Biological Process	Primary Localization	Alternate Localization
			18B10.C7 (3)	9D1.E4 (10)	1F5.D6 (14)	CTD110.6			
Q58EY4	SMARCA5	SWI/SNF related, matrix associated, actin dependent regulator of chromatin, subfamily c, member 1	0	0	7	0	Gn	N	No
O75822	EIF3S1 (EIF3J)	Eukaryotic translation initiation factor 3 subunit 1 (Eukaryotic translation initiation factor 3 subunit J)	0	0	6	0	Tl	C	
Q9ULM3	YEATS2	YEATS domain-containing protein 2	0	0	6	0	Gn	N	
Q32M68	LIN54 (CXCDC1)	LIN54 protein (CXC domain-containing protein 1)	0	0	6	0	Gn	N	
Q8IWZ2	ORF name: hCG_2045902	Multiple ankyrin repeats single KH domain protein isoform 2	0	0	5	0	U	U	
P49750	YLPM1 (ZAP3)	YLP motif-containing protein 1 (Nuclear protein ZAP3)	0	0	5	0	U	N	
Q9NYV4	CRKRS (CRK7)	Cell division cycle 2-related protein kinase 7 (CDC2-related protein kinase 7)	0	0	5	0	Sg	N	
Q9BTC0	DIDO1 (DATF1)	Death-inducer obliterator 1 (Death-associated transcription factor 1)	0	0	5	0	Sg	C,N	
Q9Y3S1	WNK2	Serine/threonine-protein kinase WNK2	0	0	5	0	Mb	C,N	
Q7Z417	NUFIP2	Nuclear fragile X mental retardation-interacting protein 2 (82 kDa FMRP-interacting protein)	0	0	5	0	Gn	N	C
Q14978	NOLC1	Nucleolar phosphoprotein p130	0	0	5	0	Gn	No	C
Q12830	BPTF	Nucleosome-remodeling factor subunit BPTF (Bromodomain and PHD finger-containing transcription factor; Fetal Alzheimer antigen)	0	0	5	0	Gn	N	C
P61254	RPL26	60S ribosomal protein L26	0	0	4	2	Tl	C	No
Q8N6V5	NUP50	Nucleoporin 50kDa	0	0	4	0	Tp	N	C

Abbreviations:

Gn, Gene expression / Transcription; Mb, Metabolism; Sg, Signal transduction; St, Structural; Tl, Translation; Tp, Transport; U, Unknown; C, Cytoplasm; N, Nucleus;M, Mitochondrial; No, Nucleolus; ER, Endoplasmic reticulum; G, Golgi apparatus; Ex, Extracellular; PM, Plasma membrane.

Table 3-S4. List of enriched novel *O*-GlcNAc proteins from HEK293T cells.

UniProt Acssion Number	Gene Name	Sequence Name	Total Peptides				Biological Process	Primary Localization	Alternate Localization
			18B10.C7 (3)	9D1.E4 (10)	1F5.D6 (14)	CTD110.6			
Q9P2N6	KIAA1310 (SI1)	Uncharacterized protein KIAA1310 (Serum inhibited-related protein; Hypothetical protein FLJ10081)	0	0	4	0	U	U	
Q96HA1	POM121 (NUP121)	POM121 membrane glycoprotein (Nuclear envelope pore membrane protein POM 121)	0	0	4	0	Tp	N	
Q8IX12	CCAR1 (DIS)	Cell division cycle and apoptosis regulator protein 1 (Death inducer with SAP domain)	0	0	4	0	Sg	C	
O60884	DNAJA2	DnaJ homolog subfamily A member 2 (HIRA interacting protein 4)	0	0	3	2	Mb	C	N,M
Q8NEZ7	PRRC1	FLJ00410 protein (Proline-rich coiled-coil 1)	0	0	3	0	U	G	C
Q15046	KARS	Lysyl-tRNA synthetase	0	0	3	0	Tl	C	M
Q92560	BAP1	Ubiquitin carboxyl-terminal hydrolase BAP1 (BRCA1-associated protein 1)	0	0	3	0	Sg	N	
P61964	WDR5 (BIG3)	WD repeat protein 5 (BMP2-induced 3-kb gene protein)	0	0	3	0	Sg	C	N,No
P54259	ATN1	Atrophin-1	0	0	3	0	Sg	N	C
Q9UBL3	ASH2L	Set1/Ash2 histone methyltransferase complex subunit ASH2 (ASH2-like protein)	0	0	3	0	Gn	N	
Q96RK0	CIC	Protein capicua homolog	0	0	3	0	Gn	N	C
Q13547	HDAC1	Histone deacetylase 1	0	0	3	0	Gn	N	No,M
O15047	SETD1A	Histone-lysine N-methyltransferase, H3 lysine-4 specific SET1	0	0	3	0	Gn	N	
O15026	SRCAP	KIAA0309 protein (Transcriptional activator SRCAP; Snf2 related CBP activator protein; Helicase SRCAP)	0	0	3	0	Gn	N	
A0T124	JMJD1C	Jumonji domain-containing 1 C splice variant (Thyroid hormone receptor interactor 8)	0	0	3	0	Gn	N	

Abbreviations:

Gn, Gene expression / Transcription; Mb, Metabolism; Sg, Signal transduction; St, Structural; Tl, Translation; Tp, Transport; U, Unknown; C, Cytoplasm; N, Nucleus;M, Mitochondrial; No, Nucleolus; ER, Endoplasmic reticulum; G, Golgi apparatus; Ex, Extracellular; PM, Plasma membrane.

Table 3-S4. List of enriched novel *O*-GlcNAc proteins from HEK293T cells.

UniProt Acssion Number	Gene Name	Sequence Name	Total Peptides				Biological Process	Primary Localization	Alternate Localization
			18B10.C7 (3)	9D1.E4 (10)	1F5.D6 (14)	CTD110.6			
P14859	POU2F1 (OCT1)	POU domain, class 2, transcription factor 1 (Octamer-binding transcription factor 1)	0	0	3	0	Gn		
O75937	DNAJC8	DnaJ homolog subfamily C member 8	0	0	2	0	Mb	No	
Q99496	RNF2	E3 ubiquitin-protein ligase RING2 (RING finger protein 2)	0	0	2	0	Gn	C	N
Q8TB57	RAD54L2	RAD54-like 2 (Androgen receptor-interacting protein 4; Helicase ARIP4)	0	0	2	0	Gn	N	
Q8NFD5	ARID1B (OSA2)	AT-rich interactive domain-containing protein 1B (BRG1-binding protein ELD/OSA1; SWI1-like)	0	0	2	0	Gn	N	
Q06587	RING1 (RNF1)	E3 ubiquitin-protein ligase RING1 (RING finger protein 1; Polycomb complex protein RING1)	0	0	2	0	Gn	N	No,C
P15822	HIVP1 (ZNF40)	Zinc finger protein 40 (HIV type I enhancer-binding protein 1; Major histocompatibility complex binding protein 1)	0	0	2	0	Gn	N	
Q96QT6	PHF12	PHD finger protein 12 (PHD factor 1)	0	0	2	0	Gn	N	
P26599	PTBP1	Polypyrimidine tract-binding protein 1 (Heterogeneous nuclear ribonucleoprotein I; hnRNPI)	0	0	2	0	Gn	N	C,No
P49458	SRP9	Signal recognition particle 9 kDa protein	0	0	1	2	Tl	C	No
Q8NCA5	FAM98A	Protein FAM98A (DKFZP564F0522 protein)	0	0	1	0	U	U	
Q969Q0	RPL36AL	60S ribosomal protein L36a-like	0	0	1	0	Tl	C	C
P62269	RPS18	40S ribosomal protein S18	0	0	1	0	Tl	C	No
P62249	RPS16	40S ribosomal protein S16	0	0	1	0	Tl	C	No
A2A2D0	STMN1	Stathmin 1/oncoprotein 18 (Leukemia associated phoshoprotein p18)	0	0	1	0	Sg	C	
Q5T0K1	TBN	Protein Taube nuss (Transcription initiation factor TFIID subunit 8; TBP-associated factor 43 kDa)	0	0	1	0	Gn	N	C

Abbreviations:

Gn, Gene expression / Transcription; Mb, Metabolism; Sg, Signal transduction; St, Structural; Tl, Translation; Tp, Transport; U, Unknown; C, Cytoplasm; N, Nucleus;M, Mitochondrial; No, Nucleolus; ER, Endoplasmic reticulum; G, Golgi apparatus; Ex, Extracellular; PM, Plasma membrane.

Table 3-S4. List of enriched novel *O*-GlcNAc proteins from HEK293T cells.

UniProt Acssion Number	Gene Name	Sequence Name	Total Peptides				Biological Process	Primary Localization	Alternate Localization
			18B10.C7 (3)	9D1.E4 (10)	1F5.D6 (14)	CTD110.6			
O75909	CCNK	Cyclin K	0	0	1	0	Gn	N	
O60506	SYNCRIP (HNRPQ)	Heterogeneous nuclear ribonucleoprotein Q3 (Synaptotagmin-binding, cytoplasmic RNA-interacting protein; NS1 associated protein 1)	0	0	1	0	Gn	C	N,ER, No
O43670	ZNF207	Zinc finger protein 207 (DKFZp761N202)	0	0	1	0	Gn	N	No
O14497	ARID1A (OSA1; SMARCF1)	AT-rich interactive domain-containing protein 1A (SWI-SNF complex protein p270; B120; SWI-like protein; Osa homolog 1)	0	0	1	0	Gn	C	N
P16401	HIST1H1B	Histone H1.5	0	0	1	0	Gn	N	No,M
P46976	GYG1	Glycogenin-1	0	0	0	7	Mb	U	
P46776	RPL27A	60S ribosomal protein L27a	0	0	0	5	Tl	C	No,M
P46013	MKI67	Antigen KI-67 (Proliferation related Ki 67 antigen)	0	0	0	3	Sg	No	N,C
Q8WUR7	C15orf40	UPF0235 protein C15orf40 (LOC123207; MGC29937)	0	0	0	2	U	U	
Q15637	SF1 (ZNF162; ZFM1)	Splicing factor 1 (Zinc finger protein 162; Transcription factor ZFM1)	0	0	0	2	Gn	N	
Q13765	NACA	Nascent polypeptide-associated complex subunit alpha	0	0	0	1	Tl	N	C
Q8NHY0	B4GALNT2	Beta-1,4 N-acetylgalactosaminyltransferase 2	0	0	0	1	Mb	G	PM
P62318	SNRPD3	Small nuclear ribonucleoprotein Sm D3 (snRNP core protein D3)	0	0	0	1	Gn	N	No
P62316	SNRPD2	Small nuclear ribonucleoprotein Sm D2 (snRNP core protein D2)	0	0	0	1	Gn	N	
P27635	RPL10	60S ribosomal protein L10	0	0	0	0	Tl	C	ER,No

Abbreviations:

Gn, Gene expression / Transcription; Mb, Metabolism; Sg, Signal transduction; St, Structural; Tl, Translation; Tp, Transport; U, Unknown; C, Cytoplasm; N, Nucleus;M, Mitochondrial; No, Nucleolus; ER, Endoplasmic reticulum; G, Golgi apparatus; Ex, Extracellular; PM, Plasma membrane.

Table 3-S5. List of enriched previously identified *O*-GlcNAc proteins from HEK293T cells.

UniProt Accesion Number	Gene Name	Sequence Name	Total Peptides				Biological Process	Primary Localization	Alternate Localization	Previously Identified Method (Ref)
			18B10.C7 (3)	9D1.E4 (10)	1F5.D6 (14)	CTD110.6				
Q00839	HNRNPU (SAFA)	Heterogeneous nuclear ribonucleoprotein U (Scaffold attachment factor A)	10	10	13	0	Gn	N	M,C	CTD110.6 immunopurify, LC-MS/MS (1)
P51610	HCFC1	Host cell factor	7	12	16	14	Gn	N	C,M	CTD110.6 immunopurify, LC-MS/MS (2)
Q5T6F2	UBAP2	Ubiquitin-associated protein 2	6	7	10	1	U	U		Chemoenzymatic labeling, LC-MS/MS (3)
P08107	HSPA1A	Heat shock 70 kDa protein 1	5	4	10	0	Mb	C	No,N	CTD110.6 immunopurify, LC-MS/MS (2)
P19338	NCL	Nucleolin	5	4	7	0	Gn	No	N,C	CTD110.6 immunopurify, LC-MS/MS (1)
P68104	EEF1A1	Elongation factor 1-alpha 1	5	1	7	0	Sg	C,N		Metabolic labeling, LC-MS/MS (4)
P62937	PPIA	Peptidyl-prolyl cis-trans isomerase A (Cyclophilin A)	4	4	6	0	Mb	C	No,M	CTD110.6 immunopurify, LC-MS/MS (2)
P07737	PFN1	Profilin-1	4	1	0	0	St	C	Ex	Metabolic labeling, LC-MS/MS (4)
Q01844	EWSR1 (EWS)	RNA-binding protein EWS (Ewing sarcoma breakpoint region 1 protein)	3	3	7	0	Gn	N	C,No, M	CTD110.6 immunopurify, LC-MS/MS (2)
Q06830	PRDX1	Peroxiredoxin-1 (Thioredoxin peroxidase 2)	3	2	3	3	Mb	C	N,No, M	Metabolic labeling, LC-MS/MS (4)

Abbreviations:

Gn, Gene expression / Transcription; Mb, Metabolism; Sg, Signal transduction; St, Structural; Tl, Translation; Tp, Transport; U, Unknown; C, Cytoplasm; N, Nucleus;M, Mitochondrial; No, Nucleolus; ER, Endoplasmic reticulum; G, Golgi apparatus; Ex, Extracellular; PM, Plasma membrane.

Table 3-S5. List of enriched previously identified *O*-GlcNAc proteins from HEK293T cells.

UniProt Accesion Number	Gene Name	Sequence Name	Total Peptides				Biological Process	Primary Localization	Alternate Localization	Previously Identified Method (Ref)
			18B10.C7 (3)	9D1.E4 (10)	1F5.D6 (14)	CTD110.6				
P06748	NPM1	Nucleophosmin	3	0	6	0	Mb	No	C,N	CTD110.6 immunopurify, LC-MS/MS (2)
P30405	PPIF	Peptidyl-prolyl cis-trans isomerase, mitochondrial precursor (Cyclophilin F)	3	0	1	0	Mb	M	No	CTD110.6 immunopurify, LC-MS/MS (2)
P23528	CFL1	Cofilin-1	3	0	0	0	St	C	N,PM,M	CTD110.6 immunopurify, LC-MS/MS (2)
Q9Y520	BAT2D1	BAT2 domain-containing protein 1 (HBxAg transactivated protein 2)	2	11	16	3	U	C		Chemoenzymatic labeling, LC-MS/MS (3)
Q9H4A3	WNK1	Serine/threonine-protein kinase WNK1	2	4	14	6	Sg	C	N	Chemoenzymatic labeling, LC-MS/MS (5)
Q9Y6Y8	SEC23IP	SEC23-interacting protein	2	4	9	3	Tp	ER	C,N,G	Chemoenzymatic labeling, LC-MS/MS (3)
P08670	VIM	Vimentin	2	3	3	1	St	C		CTD110.6 immunopurify, LC-MS/MS (1)
P09651	HNRPA1	Heterogeneous nuclear ribonucleoprotein A1	2	2	7	0	Gn	N	C,No,M	CTD110.6 immunopurify, LC-MS/MS (1)
P22626	HNRPA2B1	Heterogeneous nuclear ribonucleoproteins A2/B1	2	2	3	0	Gn	N	C,No,M	CTD110.6 immunopurify, LC-MS/MS (1)

Abbreviations:

Gn, Gene expression / Transcription; Mb, Metabolism; Sg, Signal transduction; St, Structural; Tl, Translation; Tp, Transport; U, Unknown; C, Cytoplasm; N, Nucleus;M, Mitochondrial; No, Nucleolus; ER, Endoplasmic reticulum; G, Golgi apparatus; Ex, Extracellular; PM, Plasma membrane.

Table 3-S5. List of enriched previously identified *O*-GlcNAc proteins from HEK293T cells.

UniProt Accesion Number	Gene Name	Sequence Name	Total Peptides				Biological Process	Primary Localization	Alternate Localization	Previously Identified Method (Ref)
			18B10.C7 (3)	9D1.E4 (10)	1F5.D6 (14)	CTD110.6				
A4UCT1	GAPDH	Glyceraldehyde 3-phosphate dehydrogenase	2	1	0	0	Mb	C	N,No, M,Ex	CTD110.6 immunopurify, LC-MS/MS (2)
P08238	HSP90AB1	Heat shock protein HSP 90-beta	2	0	0	0	Sg	C	N,No, M	Metabolic labeling, LC-MS/MS (4)
P27816	MAP4	Microtubule-associated protein 4	2	0	0	0	St	C		GalT radaioactive labeling (6)
Q14157	UBAP2L	Ubiquitin-associated protein 2-like	1	7	9	4	U	U		Chemoenzymatic labeling, LC-MS/MS (3)
P37198	NUP62	Nuclear pore glycoprotein p62	1	6	5	5	Tp	N		GalT radaioactive labeling (7)
Q53H29	--	Nucleoporin 54kDa variant	1	5	5	0	Tp	N		CTD110.6 immunopurify, LC-MS/MS (2)
P51991	HNRPA3	Heterogeneous nuclear ribonucleoprotein A3	1	2	4	0	Gn	N	C	Chemoenzymatic labeling, LC-MS/MS (3)
P38159	HNRPG (RBMX)	Heterogeneous nuclear ribonucleoprotein G (RNA-binding motif protein, X chromosome)	1	1	0	0	Gn	N		WGA blotting (7)
P60709	ACTB	Actin, cytoplasmic 1	1	1	0	0	St	C		Metabolic labeling, LC-MS/MS (4)
P18621	RPL17	60S ribosomal protein L17	1	0	5	2	Tl	C	No	Metabolic labeling, LC-MS/MS (8)
Q59GV2	RBM14 (SIP)	RNA binding motif protein 14 variant (Synaptotagmin-interacting protein; Paraspeckle protein 2)	1	0	3	0	Gn	N	No,C	CTD110.6 immunopurify, LC-MS/MS (1)

Abbreviations:

Gn, Gene expression / Transcription; Mb, Metabolism; Sg, Signal transduction; St, Structural; Tl, Translation; Tp, Transport; U, Unknown; C, Cytoplasm; N, Nucleus;M, Mitochondrial; No, Nucleolus; ER, Endoplasmic reticulum; G, Golgi apparatus; Ex, Extracellular; PM, Plasma membrane.

Table 3-S5. List of enriched previously identified *O*-GlcNAc proteins from HEK293T cells.

UniProt Accesion Number	Gene Name	Sequence Name	Total Peptides				Biological Process	Primary Localization	Alternate Localization	Previously Identified Method (Ref)
			18B10.C7 (3)	9D1.E4 (10)	1F5.D6 (14)	CTD110.6				
P34932	HSPA4	Heat shock 70 kDa protein 4	1	0	3	0	Mb	G,C	N,PM ,Ex	Metabolic labeling, LC-MS/MS (4)
Q6IBH5	PPIB	Peptidyl-prolyl cis-trans isomerase B (Cyclophilin B)	1	0	0	0	Mb	ER	Ex,P M,N, G,C, No,M	CTD110.6 immunopurify, LC-MS/MS (2)
P61604	HSP10 (CPN10; HSPE1)	10 kDa heat shock protein, mitochondrial (10 kDa chaperonin)	1	0	0	0	Mb	M	No	CTD110.6 immunopurify, LC-MS/MS (1)
P32119	PRDX2	Peroxiredoxin-2 (Thioredoxin peroxidase 1)	1	0	0	0	Mb	C	PM	Metabolic labeling, LC-MS/MS (9)
P23246	SFPQ	Splicing factor, proline- and glutamine-rich	1	0	0	3	Gn	N	No,C	CTD110.6 immunopurify, LC-MS/MS (1)
P35579	MYH9	Myosin-9 (Nonmuscle myosin heavy chain-A)	1	0	0	0	St	C	N,M	Metabolic labeling, LC-MS/MS (4)
P12268	IMPDH2	Inosine-5'-monophosphate dehydrogenase 2	1	0	0	2	Mb	C		Metabolic labeling, LC-MS/MS (4)
P50990	CCT8	T-complex protein 1 subunit theta (Chaperonin containing TCP1, subunit 8)	1	0	0	0	Mb	C	M	Metabolic labeling, LC-MS/MS (4)
P23526	AHCY (SAHH)	Adenosylhomocysteinase (S-adenosyl-L-homocysteine hydrolase)	1	0	0	0	Mb	C		Metabolic labeling, LC-MS/MS (4)
P13639	EEF2	Elongation factor 2	1	0	0	0	Tl	C	N,No, M	Chemoenzymatic labeling, LC-MS/MS (3)
P35580	MYH10	Myosin-10	1	0	0	0	St	C		Chemoenzymatic labeling, LC-MS/MS (3)

Abbreviations:

Gn, Gene expression / Transcription; Mb, Metabolism; Sg, Signal transduction; St, Structural; Tl, Translation; Tp, Transport; U, Unknown; C, Cytoplasm; N, Nucleus;M, Mitochondrial; No, Nucleolus; ER, Endoplasmic reticulum; G, Golgi apparatus; Ex, Extracellular; PM, Plasma membrane.

Table 3-S5. List of enriched previously identified *O*-GlcNAc proteins from HEK293T cells.

UniProt Accesion Number	Gene Name	Sequence Name	Total Peptides				Biological Process	Primary Localization	Alternate Localization	Previously Identified Method (Ref)
			18B10.C7 (3)	9D1.E4 (10)	1F5.D6 (14)	CTD110.6				
P63244	GNB2L1	Guanine nucleotide-binding protein subunit beta 2-like 1	1	0	0	0	Sg	C	N,PM	Chemoenzymatic labeling, LC-MS/MS (3)
P04075	ALDOA	Fructose-bisphosphate aldolase A	1	0	0	2	Mb	C	N,M	WGA enrichment, LC-MS/MS (10)
Q5JRG1	NUPL1	Nucleoporin like 1 (Nucleoporin p58/p45)	0	5	4	0	Tp	N	M	CTD110.6 immunopurify, LC-MS/MS (1)
P14618	PKM2	Pyruvate kinase isozymes M1/M2	0	4	0	0	Mb	C		Chemoenzymatic labeling, LC-MS/MS (3)
P68363	TUBA1B	Tubulin alpha-1B chain	0	2	3	0	St	C,PM	M	Metabolic labeling, LC-MS/MS (8)
Q86X55	CARM1	Histone-arginine methyltransferase CARM1	0	2	3	0	Gn	N		Chemoenzymatic labeling, LC-MS/MS (3)
P53992	SEC24C	Protein transport protein Sec24C (Sec24 related protein C)	0	1	5	0	Tp	ER	C	Chemoenzymatic labeling, LC-MS/MS (3)
P67809	YBX1 (NSEP1; YB1)	Nuclease sensitive element-binding protein 1 (Y-box-binding protein 1; Y-box transcription factor)	0	1	0	0	Gn	N	C	CTD110.6 immunopurify, LC-MS/MS (1)
O14979	HNRPDL	Heterogeneous nuclear ribonucleoprotein D-like (AU-rich element RNA-binding factor)	0	1	0	0	Gn	N	M	CTD110.6 immunopurify, LC-MS/MS (1)
Q14974	KPNB1	Importin subunit beta-1 (Karyopherin subunit beta-1)	0	1	0	0	Tp	C	N,Ex, M	Metabolic labeling, LC-MS/MS (4)
P60174	TPI1	Triosephosphate isomerase	0	1	0	0	Mb	C		WGA enrichment, LC-MS/MS (10)

Abbreviations:

Gn, Gene expression / Transcription; Mb, Metabolism; Sg, Signal transduction; St, Structural; Tl, Translation; Tp, Transport; U, Unknown; C, Cytoplasm; N, Nucleus;M, Mitochondrial; No, Nucleolus; ER, Endoplasmic reticulum; G, Golgi apparatus; Ex, Extracellular; PM, Plasma membrane.

Table 3-S5. List of enriched previously identified *O*-GlcNAc proteins from HEK293T cells.

UniProt Accesion Number	Gene Name	Sequence Name	Total Peptides				Biological Process	Primary Localization	Alternate Localization	Previously Identified Method (Ref)
			18B10.C7 (3)	9D1.E4 (10)	1F5.D6 (14)	CTD110.6				
P04083	ANXA1	Annexin A1	0	1	0	0	Sg	PM	C,N, M	CTD110.6 immunopurify, LC-MS/MS (2)
O14974	PPP1R12A (MYPT1)	Protein phosphatase 1 regulatory subunit 12A (Myosin phosphatase target subunit 1)	0	0	10	0	Mb	C	PM	Chemoenzymatic labeling, LC-MS/MS (3)
Q14119	VEZF1 (ZNF161)	Vascular endothelial zinc finger 1 (Zinc finger protein 161)	0	0	8	0	Gn	N		Chemoenzymatic labeling, LC-MS/MS (3)
O94979	SEC31A	Protein transport protein Sec31A (Sec31 like1)	0	0	7	0	Tp	ER	C,N, G	Chemoenzymatic labeling, LC-MS/MS (3)
Q96KR1	ZFR	Zinc finger RNA-binding protein (M-phase phosphoprotein homolog)	0	0	6	0	Gn	N	No	Chemoenzymatic labeling, LC-MS/MS (5)
P08047	SP1	Transcription factor Sp1	0	0	5	2	Gn	N		GalT radaioactive labeling, LC-MS/MS (11)
A0AVA9	EPRS	EPRS protein (Glutamyl-prolyl-tRNA synthetase)	0	0	4	0	Tl	C	N	Metabolic labeling, LC-MS/MS (4)
Q7Z739	YTHDF3	YTH domain family protein 3 (FLJ31657)	0	0	4	0	U	U		Chemoenzymatic labeling, LC-MS/MS (5)
P46778	RPL21	60S ribosomal protein L21	0	0	4	3	Tl	C	No	Metabolic labeling, LC-MS/MS (8)
O15294	OGT	UDP-N-acetylglucosamine--peptide N-acetylglucosaminyltransferase 110 kDa subunit	0	0	4	0	Sg	N,C, M		GalT radaioactive labeling (12)
Q6P4R8	NFRKB	Nuclear factor related to kappa-B-binding protein	0	0	3	0	Gn	N		Chemoenzymatic labeling, LC-MS/MS (5)

Abbreviations:

Gn, Gene expression / Transcription; Mb, Metabolism; Sg, Signal transduction; St, Structural; Tl, Translation; Tp, Transport; U, Unknown; C, Cytoplasm; N, Nucleus;M, Mitochondrial; No, Nucleolus; ER, Endoplasmic reticulum; G, Golgi apparatus; Ex, Extracellular; PM, Plasma membrane.

Table 3-S5. List of enriched previously identified *O*-GlcNAc proteins from HEK293T cells.

UniProt Accesion Number	Gene Name	Sequence Name	Total Peptides				Biological Process	Primary Localization	Alternate Localization	Previously Identified Method (Ref)
			18B10.C7 (3)	9D1.E4 (10)	1F5.D6 (14)	CTD110.6				
Q15233	NONO (NRB54)	Non-POU domain-containing octamer-binding protein (54 kDa nuclear RNA- and DNA-binding protein)	0	0	3	0	Gn	N	No,M	CTD110.6 immunopurify, LC-MS/MS (1)
P52594	AGFG1 (HRB)	Nucleoporin-like protein RIP (Arf-GAP domain and FG repeats-containing protein 1; HIV-1 Rev-binding protein; Rev-interacting protein)	0	0	3	0	Gn	N	C,No	Chemoenzymatic labeling, LC-MS/MS (5)
Q8NDX5	PHC3	Polyhomeotic-like protein 3	0	0	3	0	Gn	N	C	LWGA enrichment, LC-MS/MS (13)
P07910	HNRPC	Heterogeneous nuclear ribonucleoproteins C1/C2	0	0	2	0	Gn	N	C,No, M	CTD110.6 immunopurify, LC-MS/MS (1)
O43390	HNRNPR	Heterogeneous nuclear ribonucleoprotein R	0	0	1	0	Gn	N	No,M	CTD110.6 immunopurify, LC-MS/MS (1)
Q13283	G3BP1	Ras GTPase-activating protein-binding protein 1	0	0	1	0	Sg	C	N,PM	LWGA enrichment, LC-MS/MS (14)
Q9BYJ9	YTHDF1	YTH domain family protein 1 (Dermatomyositis associated with cancer putative autoantigen 1 homolog; DACA-1 homolog)	0	0	1	0	U	U		Chemoenzymatic labeling, LC-MS/MS (5)
P04350	TUBB4 (TUBB5)	Tubulin beta-4 chain (Tubulin 5 beta)	0	0	1	0	St	C		Chemoenzymatic labeling, LC-MS/MS (3)
P19784	CSNK2A2	Casein kinase II subunit alpha'	0	0	1	0	Sg	N	C,No, PM	*In vitro* OGT activity assay (15)

Abbreviations:

Gn, Gene expression / Transcription; Mb, Metabolism; Sg, Signal transduction; St, Structural; Tl, Translation; Tp, Transport; U, Unknown; C, Cytoplasm; N, Nucleus;M, Mitochondrial; No, Nucleolus; ER, Endoplasmic reticulum; G, Golgi apparatus; Ex, Extracellular; PM, Plasma membrane.

Table 3-S5. List of enriched previously identified *O*-GlcNAc proteins from HEK293T cells.

UniProt Accesion Number	Gene Name	Sequence Name	Total Peptides				Biological Process	Primary Localization	Alternate Localization	Previously Identified Method (Ref)
			18B10.C7 (3)	9D1.E4 (10)	1F5.D6 (14)	CTD110.6				
P67870	CSNK2B	Casein kinase II subunit beta	0	0	1	0	Gn	C	N,No, M	*In vitro* OGT activity assay (15)
P36578	RPL4	60S ribosomal protein L4	0	0	0	1	Tl	C	No	Metabolic labeling, LC-MS/MS (4)

Abbreviations:

Gn, Gene expression / Transcription; Mb, Metabolism; Sg, Signal transduction; St, Structural; Tl, Translation; Tp, Transport; U, Unknown; C, Cytoplasm; N, Nucleus;M, Mitochondrial; No, Nucleolus; ER, Endoplasmic reticulum; G, Golgi apparatus; Ex, Extracellular; PM, Plasma membrane.

Refernces:

1. Wang Z, Pandey A, Hart GW. (2007) MCP, 6: 1365-1379.
2. Wells L, Vosseller K, Cole RN, Cronshaw JM, Matunis MJ, Hart GW. (2002) MCP, 1: 791-804.
3. Clark PM, Dweck JF, Mason DE, Hart CR, Buck SB, Peters EC, Agnew BJ, Hsieh-Wilson LC. (2008) JACS, 130: 11576-11577.
4. Nandi A, Sprung R, Barma DK, Zhao Y, Kim SC, Falck JR, Zhao Y. (2006) Anal Chem, 78: 452-458.
5. Khidekel N, Ficarro SB, Peters EC, Hsieh-Wilson LC. (2004) PNAS, 101: 13132-13137.
6. Ding M, Vandré DD. (1996) JBC, 271: 12555-12561.
7. Hanover JA, Cohen CK, Willingham MC, Park MK. (1987) JBC, 262: 9887-9894.
8. Gurcel C, Vercoutter-Edouart AS, Fonbonne C, Mortuaire M, Salvador A, Michalski JC, Lemoine J. (2008) Anal Bioanal Chem 390 : 2089-2097.
9. Sprung R, Nandi A, Chen Y, Kim SC, Barma D, Falck JR, Zhao Y. (2005) J Proteome Res, 4: 950-957.
10. Cieniewski-Bernard C, Bastide B, Lefebvre T, Lemoine J, Mounier Y, Michalski JC. (2004) MCP, 3: 577-585.
11. Roos MD, Su K, Baker JR, Kudlow JE., (1997) MCB, 17(11): 6472-6480. 1988, Cell, 55: 125-133.
12. Kreppel LK, Blomberg MA, Hart GW. (1997) JBC, 272: 9308-9315.
13. Chalkley RJ, Thalhammer A, Schoepfer R, Burlingame AL. (2009) PNAS, 106: 8894-8911.
14. Vosseller K, Trinidad JC, Chalkley RJ, Specht CG, Thalhammer A, Lynn AJ, Snedecor JO, Guan S, Medzihradszky KF, Maltby DA, Schoepfer R, Burlingame AL. (2006) MCP, 5: 923-934.
15. Lazarus BD, Love DC, Hanover JA. (2006) Glycobiology. 16: 415-421.

Note: For proteins that have been previously shown to be O-GlcNAc modified by multiple studies, only a represented reference is cited.

Table 3-S6. List of enriched novel *O*-GlcNAc proteins from Sham and TH-R treated rat livers determined by MAb1F5.D6(14).

UniProt (NCBI) Accesion Number	Gene Name	Sequence Name	Total Peptides		Biological Process	Primary Localization	Alternate Localization
			Sham	THR			
(gi:109469533)	NUP214	PREDICTED: similar to nucleoporin 214kDa	3	7	Tp	N	
Q5XFW8	SEC13	SEC13 homolog	5	4	Tp	ER	N,C
P00884	ALDOB	Aldolase B, fructose-bisphosphate	4	3	Mb	C	
O09171	BHMT	Betaine-homocysteine methyltransferase 1	3	3	Mb	C	
(gi:109502089)	SEC24C	PREDICTED: similar to SEC24 related gene family, member C isoform 5	2	3	Tp	ER	C
O08658	NUP88	Nucleoporin 88kDa	0	3	Tp	N	
Q3T1I4	PRRC1	Proline-rich coiled-coil 1	0	3	U	G	C
Q66HA5	CC2D1A	Coiled-coil and C2 domain containing 1A	0	3	Sg	C	N
P22791	HMGCS2	Hydroxymethylglutaryl-CoA synthase 2 , mitochondrial	6	2	Mb	M	
P13437	ACAA2	Acetyl-Coenzyme A acyltransferase 2	4	2	Mb	M	
P11884	ALDH2	Mitochondrial aldehyde dehydrogenase 2	3	2	Mb	M	C
Q6AYR1	TFG	Trk-fused	0	2	Sg	C	
P06757	ADH1	Alcohol dehydrogenase 1	2	1	Mb	C	
B5DF65	BLVRb	Biliverdin reductase B (NADPH-flavin reductase)	1	1	Mb	C	
O88764	DAPK3 (ZIPK)	Death-associated protein kinase 3 (ZIP-kinase)	0	1	Sg	N	C
P23785	GRN	Granulin isoform a	0	1	Sg	Ex	C
Q9WVK7	HADH (HCDH)	L-3-hydroxyacyl-Coenzyme A dehydrogenase (Hydroxyacyl-coenzyme A dehydrogenase, mitochondrial)	4	0	Mb	M	
O35077	GPD1	Glycerol-3-phosphate dehydrogenase 1 (soluble)	3	0	Mb	C	
P02692	FABP1	Fatty acid binding protein 1	3	0	Tp	C	N
P04903	GSTA2	Glutathione S-transferase alpha 2	3	0	Mb	C	
P52759	HRSP12 (PSP1)	Heat-responsive protein 12 (Ribonuclease UK114; 14.5 kDa translational inhibitor protein; Perchloric acid soluble protein)	3	0	Tl	C	N, ER, G, PM
P07824	ARG1	Arginase 1	2	0	Mb	C, PM	Ex

Abbreviations:
Gn, Gene expression / Transcription; Mb, Metabolism; Sg, Signal transduction; St, Structural; Tl, Translation; Tp, Transport; U, Unknown; C, Cytoplasm; N, Nucleus;M, Mitochondrial; No, Nucleolus; ER, Endoplasmic reticulum; G, Golgi apparatus; Ex, Extracellular; PM, Plasma membrane.

Table 3-S6. List of enriched novel *O*-GlcNAc proteins from Sham and TH-R treated rat livers determined by MAb1F5.D6(14).

UniProt (NCBI) Accesion Number	Gene Name	Sequence Name	Total Peptides		Biological Process	Primary Localization	Alternate Localization
			Sham	THR			
(gi:62078937)	-	Hypothetical protein LOC316426 (SPATS2-like protein)	2	0	U	U	
P11232	TXN	Thioredoxin	2	0	Mb	C	N, Ex
P25093	FAH	Fumarylacetoacetate hydrolase (Fumarylacetoacetase; Beta-diketonase)	2	0	Mb	C	Ex
P67779	PHB	Prohibitin	2	0	Sg	C	P, N, No,Ex
Q02974	KHK	Ketohexokinase	2	0	Mb	C,N	
Q6P6R2	DLD	Dihydrolipoamide dehydrogenase (Dihydrolipoyl dehydrogenase, mitochondrial)	2	0	Mb	M	
Q9JM53	AIFM1	Apoptosis-inducing factor, mitochondrion-associated 1	2	0	Sg	M	N, C
Q9WVK3	PECR (PX-2,4-DCR1)	Peroxisomal trans-2-enoyl-CoA reductase (Peroxisomal 2,4-dienoyl-CoA reductase)	2	0	Mb	P	
(gi:109473096)	SLC25A13	PREDICTED: similar to Calcium-binding mitochondrial carrier protein Aralar2 (Mitochondrial aspartate glutamate carrier 2) (Solute carrier family 25 member 13) (Citrin)	1	0	Tp	M	
B0BN46	GRHPR	Glyoxylate reductase/hydroxypyruvate reductase	1	0	Mb	C	
B6ID08	MT2A	Metallothionein 2A	1	0	U	U	
O70351	HSD17B10 (HADH2)	Hydroxysteroid (17-beta) dehydrogenase 10 (Hydroxyacyl-Coenzyme A dehydrogenase type II)	1	0	Mb	M	ER, PM
P05179	CYP2C7	Cytochrome P450, family 2, subfamily c, polypeptide 7	1	0	Mb	M	
P07633	PCCB	Propionyl Coenzyme A carboxylase, beta polypeptide	1	0	Mb	M	
P13803	ETFA	Electron transfer flavoprotein, alpha polypeptide	1	0	Tp	M	
P14173	DDC	Dopa decarboxylase (aromatic L-amino acid decarboxylase)	1	0	Mb	C	
P19112	FBP1	Fructose-1,6- biphosphatase 1	1	0	Mb	C	
P29147	BDH1	3-hydroxybutyrate dehydrogenase, type 1	1	0	Mb	M	

Abbreviations:
Gn, Gene expression / Transcription; Mb, Metabolism; Sg, Signal transduction; St, Structural; Tl, Translation; Tp, Transport; U, Unknown; C, Cytoplasm; N, Nucleus;M, Mitochondrial; No, Nucleolus; ER, Endoplasmic reticulum; G, Golgi apparatus; Ex, Extracellular; PM, Plasma membrane.

Table 3-S6. List of enriched novel *O*-GlcNAc proteins from Sham and TH-R treated rat livers determined by MAb1F5.D6(14).

UniProt (NCBI) Accesion Number	Gene Name	Sequence Name	Total Peptides		Biological Process	Primary Localization	Alternate Localization
			Sham	THR			
P38918	AKR7A3 (AFAR2)	Aldo-keto reductase family 7, member A3 (aflatoxin aldehyde reductase)	1	0	Mb	C	
Q02253	ALDH6A1 (MMSDH)	Aldehyde dehydrogenase family 6, subfamily A1 (Methylmalonate-semialdehyde dehydrogenase [acylating], mitochondrial)	1	0	Mb	M	
Q5I0P2	GCSH	Glycine cleavage system protein H (aminomethyl carrier)	1	0	Mb	M	Ex
Q5M9H2	ACADVL	Acyl-Coenzyme A dehydrogenase, very long chain	1	0	Mb	M	
Q5SGE0	LRPPRC (LRP157)	Leucine-rich PPR-motif containing protein (Leucine-rich protein 157)	1	0	Gn	N	C, PM
Q64057	ALDH7A1	PREDICTED: similar to aldehyde dehydrogenase family 7, member A1	1	0	Mb	U	

Abbreviations:
Gn, Gene expression / Transcription; Mb, Metabolism; Sg, Signal transduction; St, Structural; Tl, Translation; Tp, Transport; U, Unknown; C, Cytoplasm; N, Nucleus;M, Mitochondrial; No, Nucleolus; ER, Endoplasmic reticulum; G, Golgi apparatus; Ex, Extracellular; PM, Plasma membrane.

Table 3-S7. List of enriched previously identified *O*-GlcNAc proteins from Sham and TH-R treated rat livers determined by MAb 1F5.D6(14).

UniProt (NCBI) Accesion Number	Gene Name	Sequence Name	Total Peptides		Biological Process	Primary Localization	Alternate Localization	Previously Identified Method (Ref)
			Sham	THR				
Q66HA8	HSPH1	Heat shock protein 1 (Chaperonin)	7	0	Sg	M	C, ER, G, No	Chemoenzymatic labeling, LC-MS/MS (1)
P63018	Hspa8 (Hsc70; Hsc73)	Heat shock protein 8 (Heat shock cognate 71 kDa protein)	5	0	Mb	C	N, No	CTD110.6 immunopurify, LC-MS/MS (2)
P10860	GLUD1	Glutamate dehydrogenase 1	4	0	Mb	M		Chemoenzymatic labeling, LC-MS/MS (1)
P0C2X9	ALDH4A1 (P5CDH)	Aldehyde dehydrogenase 4A1 (Delta-1-pyrroline-5-carboxylate dehydrogenase)	3	0	Mb	M		CTD110.6 immunopurify, LC-MS/MS (2)
P15999	ATP5a1	ATP synthase, H+ transporting, mitochondrial F1 complex, alpha subunit 1, cardiac muscle	3	0	Tp	M		Chemoenzymatic labeling, LC-MS/MS (1)
P63259	ACTG1	Actin, gamma, cytoplasmic 1	2	0	St	C		Metabolic labeling, LC-MS/MS (3)
P16638	ACLY	ATP citrate lyase isoform 2 (ATP-citrate synthase)	2	0	Mb	C		Metabolic labeling, LC-MS/MS (3)
P14141	CA3	Carbonic anhydrase III	2	0	Mb	C	Ex	Chemoenzymatic labeling, LC-MS/MS (4)
P04642	LDHA	PREDICTED: similar to L-lactate dehydrogenase A chain (LDH-A) (LDH muscle subunit) (LDH-M)	2	0	Mb	C	N	CTD110.6 immunopurify, LC-MS/MS (2)
Q9Z2Q1	SEC31A	SEC31 homolog A	2	0	Tp	ER	C, G	Chemoenzymatic labeling, LC-MS/MS (1)
Q9WTT6	GDA (GAH)	Guanine deaminase (Guanine aminohydrolase)	1	0	Mb	C	PM	Chemoenzymatic labeling, LC-MS/MS (1)
P63245	GNB2L1	Guanine nucleotide binding protein, beta polypeptide 2-like 1 (RACK1)	1	0	Sg	C	N, PM	Chemoenzymatic labeling, LC-MS/MS (1)

Abbreviations:
Gn, Gene expression / Transcription; Mb, Metabolism; Sg, Signal transduction; St, Structural; Tl, Translation; Tp, Transport; U, Unknown; C, Cytoplasm; N, Nucleus;M, Mitochondrial; No, Nucleolus; ER, Endoplasmic reticulum; G, Golgi apparatus; Ex, Extracellular; PM, Plasma membrane.

Table 3-S7. List of enriched previously identified *O*-GlcNAc proteins from Sham and TH-R treated rat livers determined by MAb 1F5.D6(14).

UniProt (NCBI) Accesion Number	Gene Name	Sequence Name	Total Peptides		Biological Process	Primary Localization	Alternate Localization	Previously Identified Method (Ref)
			Sham	THR				
P13697	ME1	Malic enzyme 1 (Malate dehydrogenase NADP(+)-dependent soluble)	1	0	Mb	C		Metabolic labeling, LC-MS/MS (3)
Q66HF1	NDUFS1	NADH dehydrogenase (ubiquinone) Fe-S protein 1, 75kDa	1	0	Mb	M		Chemoenzymatic labeling, LC-MS/MS (1)
Q09073	SLC25A5	Solute carrier family 25, member 5 (ADP/ATP translocase 2)	1	0	Mb	M		Chemoenzymatic labeling, LC-MS/MS (1)
P07632	SOD1	Superoxide dismutase 1, soluble	1	0	Mb	C	P, N, Ex	Metabolic labeling, LC-MS/MS (5)
Q4V8I9	UGP2	UDP-glucose pyrophosphorylase 2	1	0	Mb	C		CTD110.6 immunopurify, LC-MS/MS (6)
P04785	P4HB (PDIA1)	Prolyl 4-hydroxylase, beta polypeptide (Protein disulfide-isomerase)	5	1	Mb	ER	N, No, Ex	Metabolic labeling, LC-MS/MS (5)
P04764	ENO1	Enolase 1, (alpha) isoform 1	3	1	Mb	C	N, PM, Ex	Chemoenzymatic labeling, LC-MS/MS (1)
P05197	EEF2	Eukaryotic translation elongation factor 2	3	1	Tl	C	N	Chemoenzymatic labeling, LC-MS/MS (1)
B5DFC3	SEC23A	SEC23 homolog A	4	2	Tp	C	ER	CTD110.6 immunopurify, LC-MS/MS (6)
P06761	HSPA5 (GRP78)	Heat shock protein 5 (BIP; Heat shock 70 kDa protein 5; 78 kDa glucose-regulated protein)	3	2	Mb	ER	C, No, PM	Metabolic labeling, LC-MS/MS (3)
(gi:157817500)	UBAP2	Ubiquitin-associated protein 2	0	2	U	U		Chemoenzymatic labeling, LC-MS/MS (1)
(gi:109513908)	XOC3L2	PREDICTED: similar to HBxAg transactivated protein 2	0	2	U	C		Chemoenzymatic labeling, LC-MS/MS (1)
P56558	OGT	O-linked N-acetylglucosamine transferase	0	2	Sg	N	C, M	GalT radioactive labeling (7)

Abbreviations:
Gn, Gene expression / Transcription; Mb, Metabolism; Sg, Signal transduction; St, Structural; Tl, Translation; Tp, Transport; U, Unknown; C, Cytoplasm; N, Nucleus;M, Mitochondrial; No, Nucleolus; ER, Endoplasmic reticulum; G, Golgi apparatus; Ex, Extracellular; PM, Plasma membrane.

Table 3-S7. List of enriched previously identified *O*-GlcNAc proteins from Sham and TH-R treated rat livers determined by MAb 1F5.D6(14).

UniProt (NCBI) Accesion Number	Gene Name	Sequence Name	Total Peptides		Biological Process	Primary Localization	Alternate Localization	Previously Identified Method (Ref)
			Sham	THR				
P70581	NUPL1	Nucleoporin like 1 (Nucleoporin p58/p45)	3	3	U	N		Metabolic labeling, LC-MS/MS (3)
P48500	TPI1	Triosephosphate isomerase 1	0	4	Mb	C		Chemoenzymatic labeling, LC-MS/MS (1)
(gi:109467037)	NICE4 (UBAP2L)	PREDICTED: similar to Nice-4 protein homolog isoform 1 (Ubiquitin-associated protein 2-like)	1	5	U	N		Chemoenzymatic labeling, LC-MS/MS (1)
P07756	CPS1	Carbamoyl-phosphate synthetase 1	20	7	M	M		Metabolic labeling, LC-MS/MS (3)
Q9JIH7	WNK1	WNK lysine deficient protein kinase 1	6	12	Sg	C		Chemoenzymatic labeling, LC-MS/MS (1)
(gi:213385315)	HCFC1	Host cell factor C1	8	14	Gn	N	C	Chemoenzymatic labeling, LC-MS/MS (1)

Abbreviations:
Gn, Gene expression / Transcription; Mb, Metabolism; Sg, Signal transduction; St, Structural; Tl, Translation; Tp, Transport; U, Unknown; C, Cytoplasm; N, Nucleus;M, Mitochondrial; No, Nucleolus; ER, Endoplasmic reticulum; G, Golgi apparatus; Ex, Extracellular; PM, Plasma membrane.

Refernces:
1. Clark PM, Dweck JF, Mason DE, Hart CR, Buck SB, Peters EC, Agnew BJ, Hsieh-Wilson LC. (2008) JACS, 130: 11576-11577.
2. Wang Z, Pandey A, Hart GW. (2007) MCP, 6: 1365-1379.
3. Nandi A, Sprung R, Barma DK, Zhao Y, Kim SC, Falck JR, Zhao Y. (2006) Anal Chem, 78: 452-458.
4. Wang Z, Park K, Comer F, Hsieh-Wilson LC, Saudek CD, Hart GW. (2009) Diabetes, 58: 309-317.
5. Sprung R, Nandi A, Chen Y, Kim SC, Barma D, Falck JR, Zhao Y. (2005) J Proteome Res, 4: 950-957.
6. Wells L, Vosseller K, Cole RN, Cronshaw JM, Matunis MJ, Hart GW. (2002) MCP, 1: 791-804.
7. Kreppel LK, Blomberg MA, Hart GW. (1997) JBC, 272: 9308-9315.
8.Tai HC, Khidekel N, Ficarro SB, Peters EC, Hsieh-Wilson LC. (2004) JACS, 126:10500-10501.

Note: For proteins that have been previously shown to be O-GlcNAc modified by multiple studies, only a represented reference is cited.

CHAPTER 4

HEXOSAMINE FLUX, THE *O*-GLCNAC MODIFICATION, AND THE DEVELOPMENT OF INSULIN RESISTANCE IN ADIPOCYTES[#]

[#]Teo C.F., Wollaston-Hayden E.E. and Wells L. 2010. *Mol. Cell. Endocrinol.*, **318**: 44-53. Reprinted here with permission of the publisher.

Abstract

Excess flux through the hexosamine biosynthesis pathway in adipocytes is a fundamental cause of “glucose toxicity” and the development of insulin resistance that leads to type II diabetes. Adipose tissue-specific elevation in hexosamine flux in animal models recapitulates whole-body insulin-resistant phenotypes, and increased hexosamine flux in adipocyte cell culture models impairs insulin-stimulated glucose uptake. Many studies have been devoted to unveiling the molecular mechanisms in adipocytes in response to excess hexosamine flux-mediated insulin resistance. As a major downstream event consuming and incorporating the final product of the hexosamine biosynthesis pathway, dynamic and inducible *O*-GlcNAc modification is emerging as a modulator of insulin sensitivity in adipocytes. Given that *O*-GlcNAc is implicated in both insulin-mediated signal transduction and transcriptional events essential for adipocytokine secretion, direct functional studies to pinpoint the roles of *O*-GlcNAc in the development of insulin resistance via excess flux through hexosamine biosynthesis pathway are needed.

1. Introduction

Clinically, insulin resistance is characterized by a chronic elevation in circulating glucose and insulin levels as the peripheral tissues normally executing glucose clearance, namely adipose tissue and striated muscle, become desensitized despite the elevated hormonal signal. These hyperglycemic and hyperinsulinemic conditions also progressively impair insulin secretion, and, in the later stages of diabetes mellitus, lead to pancreatic beta-cell death. The development of insulin resistance along with the subsequent chronic “glucose toxicity” is widely accepted as a prerequisite condition for the disease progression from metabolic syndrome to type II diabetes and a variety of associated micro- and macrovascular diseases[1].

In adipocytes, glucose uptake is initiated through the insulin-responsive glucose transporter-4 (GLUT4). Upon entering cells, glucose is converted by glucokinase into glucose-6-phosphate (Glc-6-P), a portion of which can be shuttled into either glycogen synthesis or the pentose phosphate pathway, depending on the metabolic needs of the cell. Glc-6-P is also a substrate for Glc-6-P isomerase to form fructose-6-phosphate (Fruc-6-P), the majority of which enters glycolysis and the tricarboxylic acid (TCA) cycle for the support of basic anabolic processes[2]. However, 2 to 5 % of the Fruc-6-P enters the hexosamine biosynthesis pathway (HBP, Figure 4-1) to generate uridine diphosph*O*-N-acetylglucosamine (UDP-GlcNAc). While the detailed metabolic reactions and feedback regulation of HBP were unveiled nearly half a century ago[3], the modulatory role of HBP in the development of insulin resistance was not established until almost 30 years later[4]. The end product of the HBP, UDP-GlcNAc, is a nucleotide sugar essential for glycan biosynthesis on a myriad of macromolecules. Of all the glycosylation types, global level of *O*-linked β-N-acetyl-glucosamine (*O*-GlcNAc), a ubiquitous intracellular single-sugar glycosylation (Figure 4-2), has been demonstrated to correlate with HBP flux[5-9]. In conjunction to the emerging roles of *O*-GlcNAc modification in multiple aspects of cellular homeostasis[10], the molecular mechanism of the HBP in insulin resistance has just begun to be elucidated[11, 12].

With its robust rate of hormonally-stimulated nutrient uptake, adipose tissue is classically viewed as a key energy deposit site. Following the discovery of the adipocyte-derived *OB* gene product, leptin, as a central player in energy homeostasis[13-16], adipose tissue is now also categorized as a major endocrine organ[17]. The cross-talk between adipocyte-secreted factors and insulin resistance has been revealed by several lines of evidence in tissue-specific GLUT4 transgenic mouse models. Briefly, mice with either adipocyte- or muscle-specific GLUT4 gene knockout develop whole-body insulin resistance[18, 19]. Furthermore, adipose tissue-specific overexpression of GLUT4 in

transgenic mice bearing muscle-specific inactivated GLUT4 gene effectively rescue the insulin-resistant phenotype in these animals[20]. These findings suggest that adipose tissue-secreted factors are key regulators in maintaining glucose homeostasis in whole animals. In an attempt to have a broader understanding of the adipocyte secretome, functional proteomics approaches using media collected from adipocyte cultures have been utilized to identify hundreds of secreted proteins, collectively termed adipocytokines (or adipokines), many of which have been established to act as autocrine, paracrine and endocrine factors[21-25].

In this review, we will first discuss the impact of adipocyte-specific excess HBP flux in animal models followed by the signaling events that are impinged on upon HBP-induced insulin resistance in adipocyte cell culture models. Also, we will include *O*-GlcNAc-induced insulin resistance in both animal and cell culture models in our discussion in an attempt to explore the potential role of *O*-GlcNAc as an executor of the HBP with regards to insulin resistance in adipocytes. Finally, we will touch on the influence of the HBP and *O*-GlcNAc modification on the endocrine function of adipocytes in mediating insulin resistance.

2. Hexosamine Biosynthesis Pathway

The first and rate-limiting enzyme in the HBP is glutamine:fructose-6-phosphate aminotransferase (GFAT) that utilizes glutamine and Fruc-6-P for the formation of glucosamine-6-P (GlcN-6-P) and glutamate (Figure 4-1). Following subsequent enzymatic reactions, the pathway eventually leads to the formation of UDP-GlcNAc, a nucleotide sugar that can be either converted into other types of nucleotide sugars or directly incorporated into a variety of glycosyl-containing macromolecules. In addition to serving as a precursor for a diverse set of glycoconjugates, UDP-GlcNAc also inhibits

GFAT activity through a negative feedback mechanism to reduce the flux through the HBP[3].

Evidence linking the correlation between the HBP and insulin resistance in adipocytes was illustrated by Marshall and colleagues two decades ago with a series of elegant experiments[4, 26-29]. By using cultured primary rat adipocytes, the authors observed that: (1) A chronic exposure to both insulin and glucose was required for the adipocytes to become insulin resistant. (2) The impairment in insulin-stimulated glucose uptake during hyperglycemic and hyperinsulinemic conditions was exclusively dependent on the presence of L-glutamine. (3) While simultaneous treatment with high glucose, insulin and glutamine led to the accumulation of UDP-GlcNAc, inhibition of GFAT activity, presumably via a negative feedback mechanism, was also observed. (4) Pharmacological inhibition of GFAT using amidotransferase inhibitors such as *O*-diazoacetyl-L-serine (azaserine) or 6-diaz*O*-5-oxonorleucine (DON) prevented the glucose-induced insulin resistance. (5) A greater reduction in insulin-mediated glucose uptake was observed when the cells were treated with glucosamine (which enters the HBP downstream of GFAT) compared to high glucose condition, although the metabolic machinery that converts both glucose and glucosamine into the HBP's intermediates is more effective in utilizing glucose. (6) The glucosamine-induced insulin resistance did not require L-glutamine, nor was the effect inhibited by azaserine. While glucose and glutamine metabolism are key inducers of HBP flux, free fatty acid (FFA) and uridine are also potent modulators of the HBP[30].

After the findings from Marshall and colleagues, many groups have proceeded to manipulate HBP flux using pharmacological or genetic approaches in order to study the biological mechanisms of insulin resistance in both cell culture and animal models. It is noteworthy that the final outcome of excess HBP flux may be manifested in a tissue-

specific manner. For the scope of this review, we focus our discussion on studies involving adipose tissue and cultured adipocytes.

3. Manipulation of HBP Flux in Animal Models

To verify that the HBP is the glucose sensing pathway for the development of insulin resistance in whole animals, a series of experiments, using animals with either glucosamine infusion or GFAT overexpression, have been conducted (Table 4-1).

3.1 Glucosamine Infusion

In vivo glucosamine infusion to rats, with or without pre-exposure to hyperglycemic condition, revealed that euglycemic rats start to develop insulin resistance, yet chronically hyperglycemic rats are insensitive to the treatment[31]. In addition, Virkamäki and colleagues showed that rats subjected to *in vivo* glucosamine infusion have a lower whole body glucose disposal rate than that in saline-infused control animals[32]. Epididymal fat pads isolated from the insulin resistant animals mirrored the reduction in insulin-stimulated glucose uptake during the *in vitro* measurement[32]. These studies provided the preliminary observations of the development of insulin resistance in whole animals resulting from excess hexosamine flux.

3.2 GLUT4-GFAT Transgenic Mice

More direct evidence that excess HBP flux modulates insulin sensitivity in adipocytes, contributed mainly by McClain's laboratory, is derived from transgenic mice overexpressing GFAT. Their first transgenic mouse model with ectopic expression of GFAT under control by the *GLUT4* promoter (GLUT4-GFAT mice, with GFAT overexpression in adipose and striated muscle tissues) led to animals with a classical

insulin-resistant phenotype with hyperinsulinemia and reduction in whole-body glucose disposal rate[33]. Elevation in serum leptin level was also observed in these transgenic animals[34]. Interestingly, muscle explants from GLUT4-GFAT mice showed normal insulin-stimulated glucose uptake[7], strongly suggesting that adipocytes play a regulatory role in the HBP-mediated whole-body insulin resistance. However, it has not been ruled out that the degree of insulin resistance exhibited by explanted muscle strips from GLUT4-GFAT mice eluded the detection threshold.

3.3 aP2-GFAT Transgenic Mice

A second strain of transgenic mice utilizing an *aP2* (adipocyte lipid binding protein) gene promoter driven GFAT construct was created, which allowed an adipocyte site-specific overexpression of GFAT. In this transgenic mouse model, an adipose tissue-restricted elevation in UDP-HexNAc and *O*-GlcNAc levels was detected, which is associated with the increase of GFAT in the target tissue[7]. These transgenic animals also developed whole-body insulin resistance characterized by a reduction in both glucose disposal rate and skeletal muscle glucose uptake. An increase in serum leptin and a decrease in serum adiponectin levels were detected in agreement with their transcript levels in adipose tissue. Furthermore, *ex vivo* skeletal muscle cultures from aP2-GFAT mice displayed normal insulin response[7]. Intriguingly, regardless the similarity in their body weight, the both adipocytes and epididymal fat pads derived from aP2-GFAT animals are larger in size compared to that from their wild type littermates[35]. Higher GLUT4 mRNA and protein levels were also detected in the fat pads derived from the transgenic animals. These characteristics reflect a slight increase in the basal and maximal glucose uptake in conjunction to the overall reduction in the insulin sensitivity from the aP2-GFAT adipocytes. However, whether hepatic gluconeogenesis participates in the reduction of whole body insulin sensitivity in aP2-

GFAT mice remains unclear. An increase in total fatty acid synthesis and oxidation rates accompanied by activated AMP-activated protein kinase (AMPK) activity was also observed in the fat pad of aP2-GFAT animals[35, 36]. While AMPK is well known for its sensitivity toward intracellular nucleotide levels (*i.e.* AMP/ATP ratio), its major function in adipose tissue is to regulate lipid metabolism by reducing the availability of FFA[37]. Future investigation into the cause of elevated AMPK activity and reduced FFA levels in aP2-GFAT animals should provide insight into the control[35].

4. Impact of HBP Flux on Insulin Action

From a signaling perspective, HBP-mediated glucose desensitization can occur at multiple stages, including insulin-mediated signal transduction, predominantly via the insulin receptor substrate (IRS)/phosphatidylinositol-3 kinase (PI3K) cascade, leading to Akt phosphorylation and/or signaling control of cargo/cytoskeletal protein-mediated GLUT4 translocation (Figure 4-3). To understand the signaling processes that are affected by HBP-induced insulin resistance, researchers have induced insulin resistance in differentiated 3T3-L1 adipocytes (an immortal murine cell line) by chronic administration of either high glucose (25 mM) in the presence of physiological concentration of insulin (0.6 nM), or glucosamine (2 mM) in low glucose (5 mM) containing medium (Table 4-1).

4.1 The Metabolic Branch of Insulin Signaling in Cell Culture Models

While cumulative data indicate that both glucose- and glucosamine-induced insulin resistance consistently impede insulin-mediated glucose uptake via a deficiency in GLUT4 translocation[38, 39], a slight discrepancy was observed in the action of insulin-mediated PI3K action. Under high glucose-induced insulin resistance, there is a reduction in insulin-stimulated phospho-Akt levels, especially in the subset of plasma-

membrane-associated phospho-Akt[39]. This was not observed when cells were pre-exposed to glucosamine[39]. However, no change in IRS-associated PI3K activity was detected in either model[40]. The distinct outcomes in Akt phosphorylation in 3T3-L1 adipocytes are unexpected, because both high glucose and glucosamine treatments are equally effective in causing a defect in the insulin-stimulated Akt phosphorylation in rat retinal neurons where insulin acts as a pro-survival factor[41].

Having ruled out the impact of HBP flux on the cross-talk between IRS and PI3K, Buse's laboratory sought to pinpoint the molecular effector involved in insulin signaling that is responsible for reducing Akt phosphorylation. In a recent publication, they reported a reduction in phosphatidylinositol 3,4,5-triphosphate (PIP_3, a PI3K product) levels correlating with an increase in PTEN (phosphatase and tensin homolog deleted on chromosome 10) protein levels when the cells were exposed to chronic high glucose and insulin[42]. Since rapamycin treatment inhibits the alteration of PIP_3 and PTEN levels under insulin-resistant condition, it is believed that mammalian target of rapamycin complex 1 (mTORC1) is involved in negatively regulating the IRS/PI3K/Akt signaling cascade downstream of the insulin receptor. Also, an increase in IRS-1 phosphorylation on Ser 636/639 residues (sites known to be substrates of mTORC1) was detected[42], further suggesting the potential role of mTORC1 in modulating the development of insulin resistance in adipocytes. Notably, mTORC1 is a primary amin*O*-acid sensor and a direct downstream effector of AMPK (Figure 4-3). As AMPK is activated in the fat pads of aP2-GFAT mice, it will be informative to see whether AMPK is involved in modulating HBP-mediated downregulation of insulin signaling via mTORC1 in 3T3-L1 adipocytes.

4.2 Insulin-stimulated GLUT4 Translocation

The regulation of insulin-stimulated GLUT4 translocation is a field of active research. We now know that GLUT4 is stored inside intracellular vesicles and readily

distributed to the plasma membrane via fusion between a pair of t-(target membrane) and GLUT4-containing v-(vesicle membrane) SNARE (soluble-N-ethylmaleimide-sensitive factor attachment protein receptor) complexes upon insulin stimulation[43-45]. This step is mediated by AS160 (Akt substrate of 160 kDa) in a PI3K-dependent manner[45, 46]. Cumulative evidence also convincingly points to the phosphatidylinositol 4,5-biphosphate (PIP_2)-assisted remodeling of filamentous actin at the inner leaflet of the plasma membrane (cortical F-actin) as another crucial step for insulin-stimulated GLUT4 translocation[45, 47, 48].

In both glucose- and glucosamine-induced insulin-resistant cell culture models, a reduction in the acute insulin-stimulated GLUT4 translocation was detected accompanied by a significant alteration in membrane redistribution of Munc18-c, a negative regulator of t- and v-SNAREs[49, 50]. A reduction in insulin-stimulated interaction between two Munc-18c targets, syntaxin 4 and VAMP 2 (key components in t-SNARE and insulin-responsive v-SNARE complexes, respectively) was detected upon glucosamine treatment[50]. However, it is not clear whether the change in HBP-associated Munc18-c membrane distribution is responsible for the inhibition of syntaxin 4 and VAMP4. Collectively, these data suggest a direct involvement of excess HBP flux in desensitizing the fusion between GLUT4-containing intracellular vesicles and the plasma membrane (Figure 4-3).

Recently, Elmendorf's group has added another possible explanation for the defect in GLUT4 translocation under HBP-induced insulin resistance[51]. By exposing 3T3-L1 adipocytes to excess HBP flux, the authors detected a reduction in plasma membrane PIP_2 content with a concomitant loss in cortical F-actin. Interestingly, experimental replenishment of PIP_2 protects cells from the development of insulin resistance, whereas administration of DON reverses the PIP_2 and F-actin levels. While these preliminary observations give an alternative model for HBP-induced insulin

resistance-associated glucose uptake in adipocytes, the mechanistic details bridging GLUT4 translocation and PIP_2 and F-actin levels require further exploration.

4.3 Glycogen Synthesis

In addition to GLUT4 translocation, insulin-mediated PI3K/Akt activation also stimulates glycogen synthesis to balance the intracellular glucose metabolism in response to excess glucose influx. Insulin-dependent glycogen synthesis is triggered by activation of glycogen synthase (GS) through (1) Akt-mediated inhibition of glycogen synthase kinase-3 b (GSK3b, a negative modulator of GS), and (2) dephosphorylation by protein phosphatase 1 (PP1, more details, see accompanying chapter). Presumably, upon insulin stimulation, elevated glycogen synthesis decreases Glc-6-P and subsequently Fruc-6-P levels, and hence restricts HBP flux due to a decrease in GFAT's substrate.

Given that excess HBP flux blunts the insulin-stimulated GLUT4 action, Parker and colleagues also examined the status of insulin-stimulated glycogen synthesis in 3T3-L1 adipocytes. Exposing cells to either high glucose or glucosamine led to a lower insulin-stimulated GS activity. While involvement of GSK3b was excluded, it was demonstrated that GS becomes more resistant to PP1 activity under excess HBP flux[52]. However, further investigation is needed to complete the interaction network between these events.

4.4 Lipid Metabolism

Unlike insulin-mediated signal transduction, relatively little is known of the role of HBP flux in lipid metabolism in 3T3-L1 adipocytes. In agreement with the observation in aP2-GFAT mice-derived fat pads, McClain's group showed that glucosamine-treated 3T3-L1 adipocytes also have higher levels of fatty acid oxidation and AMPK activity[36].

No significant change in the nucleotide ratio was detected under glucosamine treatment, strongly suggesting that the increase in AMPK activity is a direct action of excess HBP flux. Controversially, Ceddia's group showed that activation of AMPK by using an AMPK-specific activator, 5-aminoimidazole-4-carboxamide ribonucleoside (AICAR), inhibits insulin-stimulated glucose uptake as well as total fatty acid synthesis and fatty acid oxidation rates in primary rat adipocytes[53]. In addition, the exact action of AICAR in insulin-induced glucose uptake remains a topic of debate[53-55]. Further experiments to examine glucosamine-induced AMPK activity in response to acute insulin stimulation are needed to resolve this discrepancy.

5. O-GlcNAc Modification

The end product of the HBP, UDP-GlcNAc, can be either converted into other types of nucleotide sugars or directly incorporated into a variety of glycosyl-containing biomolecules, including N- and *O*-linked glycoproteins, glycolipids, GPI-anchored proteins, proteoglycans and glycosaminoglycans. Among them, nucleocytosolic *O*-GlcNAc modification (Figure 4-2) is a particularly appealing candidate for the HBP sensor for the following reasons: (1) the enzyme responsible for *O*-GlcNAc modification consumes UDP-GlcNAc with a relatively high K_M that is close to the physiological level of the nucleotide sugar available[56]. (2) Global *O*-GlcNAc levels have been shown to correlate with HBP flux in many cell culture and animal models[6-9]. (3) Using EMeg32 knockout mouse embryonic fibroblasts (MEFs) lacking Glc-6-P acetyltransferase (the second enzyme in the HBP), it was observed that perturbation in HBP flux is directly associated with a significant reduction in global *O*-GlcNAc levels, yet no significant alteration in other glycosylation products was detected[5].

O-GlcNAc is an abundant monosaccharide modification found on the serine and threonine residues of nucleocytoplasmic proteins (Figure 4-2, [57, 58]). Since it was first

reported in 1984 by Hart's laboratory[59], *O*-GlcNAc modification has been found on more than 500 proteins and shown to regulate a variety of cellular processes[10]. With a distinct spatial localization compared to complex glycosylations, and its inducible and dynamic nature, *O*-GlcNAc modification is conceptually more related to phosphorylation than other glycosylations[57, 60-64]. Due to the technological improvements for post-translational modification studies, we now know that the dynamic interplay of *O*-GlcNAc and *O*-phosphate modifications is more sophisticated than the original 'Ying-yang hypothesis'[63-67]. One such example is the reciprocal action of *O*-GlcNAc and *O*-phosphate modifications on CCAAT enhancer binding protein (C/EBP) b [68]. It is clearly demonstrated that the interplay of phosphorylation and *O*-GlcNAc modification on (C/EBP) b is crucial for determining *in vitro* differentiation of 3T3-L1 adipocytes[68].

The cycling of *O*-GlcNAc is achieved by a pair of cycling enzymes: *O*-GlcNAc transferase (OGT) and *O*-GlcNAcase (OGA) that control the addition and removal of a β-GlcNAc moiety, respectively (Figure 4-2, [69-74]). In mammals, there is only a single gene encoding OGT and likewise a single gene encoding OGA[75, 76]. In contrast to phosphorylation, where numerous kinases and phosphatases are required to achieve its target diversity, accumulative evidence suggest that the occurrence of *O*-GlcNAc modification is largely regulated at the levels of *O*-GlcNAc cycling enzymes via differential transcription, post-translational modification and transient complex conformation[77]. Importantly, two independent epidemiological studies have revealed that nucleotide polymorphisms in *mgea5* (the gene encoding OGA) are associated with the onset of type II diabetes in different populations[78, 79]. These studies further imply that *O*-GlcNAc modification of intracellular proteins participates in the development of insulin resistance and disease progression in type II diabetes.

5.1 O-GlcNAc Modification and Insulin Resistance in Animals

Complementary to the transgenic mouse models of GFAT overexpression, a transgenic mouse model with OGT driven under *GLUT4* gene promoter was reported from a collaboration between McClain's and Hanover's groups (Table 4-1). Not surprisingly, the animals, with elevated OGT expression in adipose and striated muscle tissues, developed a classical insulin-resistant phenotype characterized by a reduction in whole-body glucose disposal rate, as well as elevated plasma insulin and leptin levels[80]. However, no detailed follow-up characterization of the GLUT4-OGT transgenic mice is available. It would be informative to examine whether the insulin-resistant status of different tissues and muscle explants derived from GLUT4-OGT transgenic mice can recapitulate the observation in transgenic mice overexpressing GFAT. Studies using transgenic mice bearing adipocyte-specific OGT overexpression would also give insight into the role of the *O*-GlcNAc modification in adipocyte differentiation and the development of insulin resistance.

While no published report on the OGA transgenic animals is currently available, Got*O*-Kakizaki (GK) rats provide a glimpse of information regarding the role of OGA in the development of insulin resistance (Table 4-1). GK rats are an inbred strain of Wistar rats with spontaneous development of type II diabetes[81, 82]. Unlike many of the diabetic animal models, GK rats are not obese, yet they exhibit phenotypic resemblance to type II diabetes in humans. The adipocytes isolated from GK rats have a reduction in insulin sensitivity in conjunction with a defect in IRS-1 phosphorylation and GLUT4 translocation[83]. Genetic studies have identified the major diabetes-associated locus in GK rats to be *Niddm1*[84]. Interesting, the rat OGA gene is assigned to the Niddm1 locus in proximity to the gene encoding the insulin-degrading enzyme[85]. Also, a short variant of OGA was isolated from GK rats by Kudlow's laboratory, which acts in a dominant-negative manner *in vitro* to elevate *O*-GlcNAc levels[86, 87]. While increased

global *O*-GlcNAc levels have been found in the cornea and pancreas isolated from GK rats[88, 89], it will be intriguing to see the *O*-GlcNAc status in the adipose tissue of GK rats in order to establish the connection between *O*-GlcNAc levels and the insulin-resistant phenotype in these animals.

5.2. O-GlcNAc Modification and Insulin Resistance in Culture Adipoctyes

Direct evidence showing that *O*-GlcNAc modification is the interconnecting factor between the HBP and insulin resistance comes from the study Hart's group did using a potent OGA inhibitor (PUGNAc, *O*-(2-acetamid*O*-2-deoxy-D-glucopyranosylidene)-amin*O*-N-phenylcarbamate, [90]) to increase global *O*-GlcNAc level in 3T3-L1 adipocytes[6]. It was shown that PUGNAc treatment suppresses insulin-mediated glucose uptake in the absence of chronic insulin exposure. A concomitant defect in Akt phosphorylation and activation was also observed while no significant inhibition at signaling events proximal to the insulin receptor was detected[6]. The same conclusions were drawn from another study by ectopically overexpressing OGT in 3T3-L1 adipocytes in parallel to the PUGNAc treatment[9]. Moreover, an increase in phosphorylation on both Ser307 and Ser636/639 of IRS-1 was observed[9] (Table 4-1). These data partially agree with the phenomena obtained from high glucose-induced insulin resistance. However, since none of the experiments from either of the studies were dedicated to examine the status of GLUT4 translocation, it is premature to pinpoint the exact role of *O*-GlcNAc on this event.

The effect of *O*-GlcNAc-mediated insulin resistance was examined also in primary rat adipocytes[8]. In addition to the similar defects in insulin-stimulated glucose uptake and Akt phosphorylation as mentioned earlier, a reduction in IRS-1 tyrosine phosphorylation and GLUT4 translocation were also detected in agreement with the findings in the adipocytes extracted from GK rats[8, 83]. While a discrepancy in insulin

signaling events in response to external stimuli, such as an exposure to branched-chain amino acids, has previously been observed between differentiated immortal adipocytes and freshly isolated primary adipocytes[91], the distinctive impact of *O*-GlcNAc in IRS-1 phosphorylation between 3T3-L1 adipocytes and primary rat adipocytes may be explained by the specific physiological conditions of these cell culture models.

While increased global *O*-GlcNAc levels are implicated in the development of insulin resistance, OGT is also regulated by insulin in 3T3-L1 adipocytes. It was found that OGT is tyrosine-phosphorylated by the insulin receptor upon acute insulin stimulation, which subsequently enhances OGT activity. Moreover, a localization shift from nucleus to cytosol is also observed under these conditions[92]. Since these experiments were monitored with acute insulin treatment under insulin-responsive condition, it is not clear whether insulin receptor-mediated OGT tyrosine phosphorylation is involved in the course of insulin resistance. Furthermore, a PIP_3 binding motif was found on OGT using an *in vitro* binding assay[9]. Although it remains unknown in the case of 3T3-L1 adipocytes, studies from COS-7 and 3T3-A14 cells showed that OGT is translocated to the plasma membrane in a PI3K-dependent manner in response to acute insulin stimulation[9]. In contrast to animals ectopically overexpressing wild type OGT, introducing an OGT mutant lacking the PIP_3 binding ability in mouse liver does not impair hepatic insulin action[9]. Future studies are needed to determine whether the insulin sensitivity of transgenic mice with adipose-specific overexpression of PIP_3-binding-deficient OGT are altered.

5.3 O-GlcNAc Modification on Specific Proteins

While dissecting the signaling steps affected by the HBP or *O*-GlcNAc-induced insulin resistance, many studies have also investigated whether the proteins participating in such an event are *O*-GlcNAc modified. Indeed, almost all of the proteins

discussed in the earlier sections are known to be *in vivo* substrates of OGT. However, due to a lack of robust site-mapping methods and site-specific *O*-GlcNAc antibodies, the exact functional targets of *O*-GlcNAc remain elusive. Below, we summarize a series of observations of insulin resistance-associated signaling events that may be modulated by *O*-GlcNAc modification (Figure 4-3).

(1) *O*-GlcNAc modification has been found on proteins involved in insulin-mediated signal transduction, including insulin receptor, IRS-1/2, p85 and p110 of PI3K, PDK1 and Akt. To date, only four sites on IRS-1 (Ser914, Ser1009, Ser1036 and Ser1041) and another on Ser473 of Akt-1 have been confirmed to be *O*-GlcNAc modified in non-adipocyte cell cultures[93-95]. It is not known whether these sites impact function and if they are preferential substrates for OGT in adipocytes.

(2) Munc18-c was found to be *O*-GlcNAc modified under glucosamine-induced insulin resistance[50]. Whether the glycosylated form of Munc18c serves as a direct factor causing a reduction in membrane association with syntaxin 4 and VAMP2 requires further exploration.

(3) It was found that chronic HBP flux effectively induces *O*-GlcNAc modification on AMPK a subunit in both immortal and primary murine adipocytes. Importantly, the *O*-GlcNAc modified AMPK has a higher activity compared to the non-glycosylated form of AMPK[36]. However, since the site on AMPK has not been mapped, one cannot rule out the possibility of *O*-GlcNAc modification interfering with the protein-protein interaction between AMPK and its binding partners, and subsequently leading to an increase in its activity.

(4) Overall *O*-GlcNAc levels on glycogen synthase fluctuate in a HBP flux-dependent manner. It is believed that glycosylated glycogen synthase is more resistant to PP1-mediated activation[52]. A previous study has shown that the catalytic subunits of PP1 form a ‘ying-yang’ complex with OGT in rat brain extracts[96]. While the formation

of a PP1-OGT complex has not been established in adipocytes, it is possible that glycogen synthase is not the only target of *O*-GlcNAc in modulating glycogen synthesis under insulin-resistant conditions.

5.4 Paradoxes in O-GlcNAc-Induced Insulin Resistance in Culture Adipoctyes

Given that pharmacologically and genetically elevated *O*-GlcNAc levels in cultured adipocytes and mouse models are associated with insulin-resistant phenotypes, one might expect that reducing *O*-GlcNAc levels in adipocytes should reverse the HBP-induced insulin resistance. However, a study reported by Robinson and colleagues contradicted this conventional thought[97]. They showed that when 3T3-L1 adipocytes are exposed to high glucose and insulin containing medium, genetically overexpressing OGA or knocking down OGT does not protect cells from developing insulin resistance as the reduction in insulin-stimulated glucose uptake and Akt phosphorylation persist[42] (Table 4-1). However, in an insulin-resistant *db/db* mouse model (a diabetic mouse model with mutated leptin receptor), the overexpression of OGA via adenovirus significantly improved whole-body glucose tolerance and insulin sensitivity[98], suggesting that lowering of *O*-GlcNAc levels *in vivo* is beneficial. Knowing that many proteins involved in modulating insulin sensitivity are potential substrates for OGT, and that *O*-GlcNAc modification can either positively or negatively regulate protein functions, further experiments establishing the functional role of *O*-GlcNAc on each protein are needed to explain the phenomena observed by Robinson and colleagues.

Another disputable input complicating the model of *O*-GlcNAc-induced insulin resistance comes from a report from Vocadlo's laboratory using 1,2-dideoxy-2'-propyl-a-D-glucopyranos *O*-[2,1,D]-Δ2'-thiazoline (NButGT) to elevate global *O*-GlcNAc levels[99] (Table 4-1). NButGT is an OGA inhibitor that was designed based on the structural information attained from a bacterial homolog of human OGA[99, 100]. Kinetic studies

showed that NButGT has a better selectivity toward OGA over lysosomal β-hexosaminidases. When 3T3-L1 adipocytes were treated with NButGT, the cells remained insulin-sensitive and no defect in glucose uptake or Akt phosphorylation was detected[99]. These observations are puzzling, as *O*-GlcNAc-induced insulin resistance has been previously demonstrated by both pharmacological and genetic approaches (Table 4-1). Future investigation for the potential biological difference between PUGNAc and NButGT treated cells is essential to explain these results.

6. Adipocytokines

Several adipocytokines have been implicated in obesity-mediated insulin-resistant models. However, relatively little information is available on the HBP-induced adipocytokines. Rossetti's group first showed that manipulating HBP flux in rats, via glucose, glucosamine or FFA infusions, leads to an increased plasma leptin level, which correlates with an upregulation of leptin mRNA levels in adipose tissue[30]. This is further supported by a series of findings: (1) Both GLUT4-GFAT and aP2-GFAT transgenic mice are hyperleptinemic[7, 34]. (2) Exposing isolated human subcutaneous adipocytes to glucosamine released more leptin into the medium, whereas treating the cells with DON to block GFAT successfully reduced leptin reproduction at both the mRNA and protein levels[101]. (3) Increased HBP flux, by either high glucose or glucosamine, induces leptin production in a dose- and time-dependent manner in primary human adipocytes[101, 102]. (4) Hyperleptinemia is also detected in GLUT4-OGT transgenic mice[80].

In addition to leptin, several other diabetes-related adipocytokines have been examined in aP2-GFAT transgenic mice. Whereas insignificant changes in the transcript levels of TNFa and resistin were measured, a slight reduction in the mRNA level of adiponectin correlated with a marked decreased in serum adiponectin was observed[7].

Further study on HBP-induced leptin secretion by Considine's group showed that Sp1, a housekeeping transcription factor, participates in such events[102]. Notably, Sp1 is a heavily *O*-GlcNAc modified protein (at least 9 sites, of which only Ser491 has been confirmed[103, 104]). *O*-GlcNAc modification on Sp1 has been demonstrated to influence its stability, subcellular localization, transcription activity, accessibility to phosphorylation and ability to engage protein-protein interactions[104-108]. Future experiments to mutate *O*-GlcNAc sites on Sp1 to address functional impact of *O*-GlcNAc modified-Sp1-associated adipocytokine production under insulin-resistant condition are needed.

In order to obtain a more comprehensive picture of adipocytokine secretion that is modulated by HBP- or *O*-GlcNAc-mediated insulin resistance, our laboratory performed a quantitative functional proteomic study to identify regulated adipocytokines under different conditions[25]. After inducing insulin resistance with high glucose/insulin or PUGNAc treatments in immortal or primary rodent adipocytes, adipocyte-spent media was harvested and subjected to non-isotope-based quantitative mass-spectrometry analysis. Altogether, more than 200 adipocytokines were identified, with 8 and 20 regulated adipocytokines (including quiescin Q6, angiotensin and slit homologue 3) in 3T3 and primary rat adipocytes, respectively. Follow-up experiments to examine whether these proteins are also regulated at the transcriptional level in a manner similar to leptin are in progress.

7. Conclusions

Increased flux through the HBP under excess glucose availability is a direct cause of insulin resistance in adipocytes, though a variety of mechanisms likely regulate this process[109]. *O*-GlcNAc modification, in response to hexosamine flux, appears to be one of the main mechanisms directly downstream of the HBP to modulate metabolic

changes by dynamically modifying intracellular proteins, thus affecting protein functions and cellular processes. Indeed, many proteins established in mediating insulin resistance at the molecular level are known to be *O*-GlcNAc modified. With recent improvements in technologies for detecting and site-mapping *O*-GlcNAc modified proteins, experiments can now be designed to provide insights into the functional role of *O*-GlcNAc modification at specific sites on individual proteins in the development of insulin resistance in adipocytes.

8. Acknowledgements

This work was supported by a grant from NIH/NIDDK (1RO1DK075069 to LW). CFT is an American Heart Association predoctoral fellow (Southeast affiliate, 0715377B).

9. References

1. Matveyenko, A.V. and P.C. Butler, *Relationship between beta-cell mass and diabetes onset.* Diabetes Obes Metab, 2008. **10 Suppl 4**: p. 23-31.
2. Bouche, C., et al., *The cellular fate of glucose and its relevance in type 2 diabetes.* Endocr Rev, 2004. **25**(5): p. 807-30.
3. Kornfeld, S., et al., *The Feedback Control of Sugar Nucleotide Biosynthesis in Liver.* Proc Natl Acad Sci U S A, 1964. **52**: p. 371-9.
4. Marshall, S., V. Bacote, and R.R. Traxinger, *Discovery of a metabolic pathway mediating glucose-induced desensitization of the glucose transport system. Role of hexosamine biosynthesis in the induction of insulin resistance.* J Biol Chem, 1991. **266**(8): p. 4706-12.
5. Boehmelt, G., et al., *Decreased UDP-GlcNAc levels abrogate proliferation control in EMeg32-deficient cells.* EMBO J, 2000. **19**(19): p. 5092-104.
6. Vosseller, K., et al., *Elevated nucleocytoplasmic glycosylation by O-GlcNAc results in insulin resistance associated with defects in Akt activation in 3T3-L1 adipocytes.* Proc Natl Acad Sci U S A, 2002. **99**(8): p. 5313-8.
7. Hazel, M., et al., *Activation of the hexosamine signaling pathway in adipose tissue results in decreased serum adiponectin and skeletal muscle insulin resistance.* Endocrinology, 2004. **145**(5): p. 2118-28.
8. Park, S.Y., J. Ryu, and W. Lee, *O-GlcNAc modification on IRS-1 and Akt2 by PUGNAc inhibits their phosphorylation and induces insulin resistance in rat primary adipocytes.* Exp Mol Med, 2005. **37**(3): p. 220-9.
9. Yang, X., et al., *Phosphoinositide signalling links O-GlcNAc transferase to insulin resistance.* Nature, 2008. **451**(7181): p. 964-9.

10. Hart, G.W., M.P. Housley, and C. Slawson, *Cycling of O-linked beta-N-acetylglucosamine on nucleocytoplasmic proteins.* Nature, 2007. **446**(7139): p. 1017-22.
11. Buse, M.G., *Hexosamines, insulin resistance, and the complications of diabetes: current status.* Am J Physiol Endocrinol Metab, 2006. **290**(1): p. E1-E8.
12. Copeland, R.J., J.W. Bullen, and G.W. Hart, *Cross-talk between GlcNAcylation and phosphorylation: roles in insulin resistance and glucose toxicity.* Am J Physiol Endocrinol Metab, 2008. **295**(1): p. E17-28.
13. Campfield, L.A., et al., *Recombinant mouse OB protein: evidence for a peripheral signal linking adiposity and central neural networks.* Science, 1995. **269**(5223): p. 546-9.
14. Halaas, J.L., et al., *Weight-reducing effects of the plasma protein encoded by the obese gene.* Science, 1995. **269**(5223): p. 543-6.
15. Maffei, M., et al., *Increased expression in adipocytes of ob RNA in mice with lesions of the hypothalamus and with mutations at the db locus.* Proc Natl Acad Sci U S A, 1995. **92**(15): p. 6957-60.
16. Pelleymounter, M.A., et al., *Effects of the obese gene product on body weight regulation in ob/ob mice.* Science, 1995. **269**(5223): p. 540-3.
17. Halberg, N., I. Wernstedt-Asterholm, and P.E. Scherer, *The adipocyte as an endocrine cell.* Endocrinol Metab Clin North Am, 2008. **37**(3): p. 753-68, x-xi.
18. Abel, E.D., et al., *Adipose-selective targeting of the GLUT4 gene impairs insulin action in muscle and liver.* Nature, 2001. **409**(6821): p. 729-33.
19. Kim, J.K., et al., *Glucose toxicity and the development of diabetes in mice with muscle-specific inactivation of GLUT4.* J Clin Invest, 2001. **108**(1): p. 153-60.
20. Carvalho, E., et al., *Adipose-specific overexpression of GLUT4 reverses insulin resistance and diabetes in mice lacking GLUT4 selectively in muscle.* Am J Physiol Endocrinol Metab, 2005. **289**(4): p. E551-61.
21. Kratchmarova, I., et al., *A proteomic approach for identification of secreted proteins during the differentiation of 3T3-L1 preadipocytes to adipocytes.* Mol Cell Proteomics, 2002. **1**(3): p. 213-22.
22. Wang, P., et al., *Profiling of the secreted proteins during 3T3-L1 adipocyte differentiation leads to the identification of novel adipokines.* Cell Mol Life Sci, 2004. **61**(18): p. 2405-17.
23. Chen, X., et al., *Quantitative proteomic analysis of the secretory proteins from rat adipose cells using a 2D liquid chromatography-MS/MS approach.* J Proteome Res, 2005. **4**(2): p. 570-7.
24. Alvarez-Llamas, G., et al., *Characterization of the human visceral adipose tissue secretome.* Mol Cell Proteomics, 2007. **6**(4): p. 589-600.
25. Lim, J.M., et al., *Defining the regulated secreted proteome of rodent adipocytes upon the induction of insulin resistance.* J Proteome Res, 2008. **7**(3): p. 1251-63.
26. Marshall, S. and R. Monzon, *Amino acid regulation of insulin action in isolated adipocytes. Selective ability of amino acids to enhance both insulin sensitivity and maximal insulin responsiveness of the protein synthesis system.* J Biol Chem, 1989. **264**(4): p. 2037-42.
27. Traxinger, R.R. and S. Marshall, *Role of amino acids in modulating glucose-induced desensitization of the glucose transport system.* J Biol Chem, 1989. **264**(35): p. 20910-6.
28. Marshall, S., W.T. Garvey, and R.R. Traxinger, *New insights into the metabolic regulation of insulin action and insulin resistance: role of glucose and amino acids.* FASEB J, 1991. **5**(15): p. 3031-6.

29. Traxinger, R.R. and S. Marshall, *Coordinated regulation of glutamine:fructose-6-phosphate amidotransferase activity by insulin, glucose, and glutamine. Role of hexosamine biosynthesis in enzyme regulation.* J Biol Chem, 1991. **266**(16): p. 10148-54.
30. Wang, J., et al., *A nutrient-sensing pathway regulates leptin gene expression in muscle and fat.* Nature, 1998. **393**(6686): p. 684-8.
31. Rossetti, L., et al., *In vivo glucosamine infusion induces insulin resistance in normoglycemic but not in hyperglycemic conscious rats.* J Clin Invest, 1995. **96**(1): p. 132-40.
32. Virkamaki, A., et al., *Activation of the hexosamine pathway by glucosamine in vivo induces insulin resistance in multiple insulin sensitive tissues.* Endocrinology, 1997. **138**(6): p. 2501-7.
33. Hebert, L.F., Jr., et al., *Overexpression of glutamine:fructose-6-phosphate amidotransferase in transgenic mice leads to insulin resistance.* J Clin Invest, 1996. **98**(4): p. 930-6.
34. McClain, D.A., et al., *Hexosamines stimulate leptin production in transgenic mice.* Endocrinology, 2000. **141**(6): p. 1999-2002.
35. McClain, D.A., et al., *Adipocytes with increased hexosamine flux exhibit insulin resistance, increased glucose uptake, and increased synthesis and storage of lipid.* Am J Physiol Endocrinol Metab, 2005. **288**(5): p. E973-9.
36. Luo, B., et al., *Chronic hexosamine flux stimulates fatty acid oxidation by activating AMP-activated protein kinase in adipocytes.* J Biol Chem, 2007. **282**(10): p. 7172-80.
37. Daval, M., F. Foufelle, and P. Ferre, *Functions of AMP-activated protein kinase in adipose tissue.* J Physiol, 2006. **574**(Pt 1): p. 55-62.
38. Ross, S.A., et al., *Development and comparison of two 3T3-L1 adipocyte models of insulin resistance: increased glucose flux vs glucosamine treatment.* Biochem Biophys Res Commun, 2000. **273**(3): p. 1033-41.
39. Nelson, B.A., K.A. Robinson, and M.G. Buse, *Defective Akt activation is associated with glucose- but not glucosamine-induced insulin resistance.* Am J Physiol Endocrinol Metab, 2002. **282**(3): p. E497-506.
40. Nelson, B.A., K.A. Robinson, and M.G. Buse, *High glucose and glucosamine induce insulin resistance via different mechanisms in 3T3-L1 adipocytes.* Diabetes, 2000. **49**(6): p. 981-91.
41. Nakamura, M., et al., *Excessive hexosamines block the neuroprotective effect of insulin and induce apoptosis in retinal neurons.* J Biol Chem, 2001. **276**(47): p. 43748-55.
42. Robinson, K.A. and M.G. Buse, *Mechanisms of high-glucose/insulin-mediated desensitization of acute insulin-stimulated glucose transport and Akt activation.* Am J Physiol Endocrinol Metab, 2008. **294**(5): p. E870-81.
43. Cheatham, B., et al., *Insulin-stimulated translocation of GLUT4 glucose transporters requires SNARE-complex proteins.* Proc Natl Acad Sci U S A, 1996. **93**(26): p. 15169-73.
44. Volchuk, A., et al., *Syntaxin 4 in 3T3-L1 adipocytes: regulation by insulin and participation in insulin-dependent glucose transport.* Mol Biol Cell, 1996. **7**(7): p. 1075-82.
45. Brozinick, J.T., Jr., B.A. Berkemeier, and J.S. Elmendorf, *"Actin"g on GLUT4: membrane & cytoskeletal components of insulin action.* Curr Diabetes Rev, 2007. **3**(2): p. 111-22.

46. Zeigerer, A., M.K. McBrayer, and T.E. McGraw, *Insulin stimulation of GLUT4 exocytosis, but not its inhibition of endocytosis, is dependent on RabGAP AS160.* Mol Biol Cell, 2004. **15**(10): p. 4406-15.
47. Kanzaki, M. and J.E. Pessin, *Insulin-stimulated GLUT4 translocation in adipocytes is dependent upon cortical actin remodeling.* J Biol Chem, 2001. **276**(45): p. 42436-44.
48. Kanzaki, M., et al., *Phosphatidylinositol 4,5-bisphosphate regulates adipocyte actin dynamics and GLUT4 vesicle recycling.* J Biol Chem, 2004. **279**(29): p. 30622-33.
49. Nelson, B.A., K.A. Robinson, and M.G. Buse, *Insulin acutely regulates Munc18-c subcellular trafficking: altered response in insulin-resistant 3T3-L1 adipocytes.* J Biol Chem, 2002. **277**(6): p. 3809-12.
50. Chen, G., et al., *Glucosamine-induced insulin resistance is coupled to O-linked glycosylation of Munc18c.* FEBS Lett, 2003. **534**(1-3): p. 54-60.
51. Bhonagiri, P., et al., *Hexosamine biosynthesis pathway flux contributes to insulin resistance via altering membrane phosphatidylinositol 4,5-bisphosphate and cortical filamentous actin.* Endocrinology, 2009. **150**(4): p. 1636-45.
52. Parker, G.J., et al., *Insulin resistance of glycogen synthase mediated by O-linked N-acetylglucosamine.* J Biol Chem, 2003. **278**(12): p. 10022-7.
53. Gaidhu, M.P., S. Fediuc, and R.B. Ceddia, *5-Aminoimidazole-4-carboxamide-1-beta-D-ribofuranoside-induced AMP-activated protein kinase phosphorylation inhibits basal and insulin-stimulated glucose uptake, lipid synthesis, and fatty acid oxidation in isolated rat adipocytes.* J Biol Chem, 2006. **281**(36): p. 25956-64.
54. Salt, I.P., J.M. Connell, and G.W. Gould, *5-aminoimidazole-4-carboxamide ribonucleoside (AICAR) inhibits insulin-stimulated glucose transport in 3T3-L1 adipocytes.* Diabetes, 2000. **49**(10): p. 1649-56.
55. Yamaguchi, S., et al., *Activators of AMP-activated protein kinase enhance GLUT4 translocation and its glucose transport activity in 3T3-L1 adipocytes.* Am J Physiol Endocrinol Metab, 2005. **289**(4): p. E643-9.
56. Kreppel, L.K. and G.W. Hart, *Regulation of a cytosolic and nuclear O-GlcNAc transferase. Role of the tetratricopeptide repeats.* J Biol Chem, 1999. **274**(45): p. 32015-22.
57. Holt, G.D. and G.W. Hart, *The subcellular distribution of terminal N-acetylglucosamine moieties. Localization of a novel protein-saccharide linkage, O-linked GlcNAc.* J Biol Chem, 1986. **261**(17): p. 8049-57.
58. Kearse, K.P. and G.W. Hart, *Topology of O-linked N-acetylglucosamine in murine lymphocytes.* Arch Biochem Biophys, 1991. **290**(2): p. 543-8.
59. Torres, C.R. and G.W. Hart, *Topography and polypeptide distribution of terminal N-acetylglucosamine residues on the surfaces of intact lymphocytes. Evidence for O-linked GlcNAc.* J Biol Chem, 1984. **259**(5): p. 3308-17.
60. Kearse, K.P. and G.W. Hart, *Lymphocyte activation induces rapid changes in nuclear and cytoplasmic glycoproteins.* Proc Natl Acad Sci U S A, 1991. **88**(5): p. 1701-5.
61. Wells, L., K. Vosseller, and G.W. Hart, *Glycosylation of nucleocytoplasmic proteins: signal transduction and O-GlcNAc.* Science, 2001. **291**(5512): p. 2376-8.
62. Kneass, Z.T. and R.B. Marchase, *Neutrophils exhibit rapid agonist-induced increases in protein-associated O-GlcNAc.* J Biol Chem, 2004. **279**(44): p. 45759-65.

63. Khidekel, N., et al., *Probing the dynamics of O-GlcNAc glycosylation in the brain using quantitative proteomics.* Nat Chem Biol, 2007. **3**(6): p. 339-48.
64. Wang, Z., A. Pandey, and G.W. Hart, *Dynamic interplay between O-linked N-acetylglucosaminylation and glycogen synthase kinase-3-dependent phosphorylation.* Mol Cell Proteomics, 2007. **6**(8): p. 1365-79.
65. Hart, G.W., et al., *O-linked N-acetylglucosamine: the "yin-yang" of Ser/Thr phosphorylation? Nuclear and cytoplasmic glycosylation.* Adv Exp Med Biol, 1995. **376**: p. 115-23.
66. Wells, L., et al., *Mapping sites of O-GlcNAc modification using affinity tags for serine and threonine post-translational modifications.* Mol Cell Proteomics, 2002. **1**(10): p. 791-804.
67. Wang, Z., M. Gucek, and G.W. Hart, *Cross-talk between GlcNAcylation and phosphorylation: site-specific phosphorylation dynamics in response to globally elevated O-GlcNAc.* Proc Natl Acad Sci U S A, 2008. **105**(37): p. 13793-8.
68. Li, X., et al., *O-linked N-acetylglucosamine modification on C/EBPbeta: Role during adipocyte differentiation.* J Biol Chem, 2009.
69. Haltiwanger, R.S., G.D. Holt, and G.W. Hart, *Enzymatic addition of O-GlcNAc to nuclear and cytoplasmic proteins. Identification of a uridine diphosphO-N-acetylglucosamine:peptide beta-N-acetylglucosaminyltransferase.* J Biol Chem, 1990. **265**(5): p. 2563-8.
70. Haltiwanger, R.S., M.A. Blomberg, and G.W. Hart, *Glycosylation of nuclear and cytoplasmic proteins. Purification and characterization of a uridine diphosphO-N-acetylglucosamine:polypeptide beta-N-acetylglucosaminyltransferase.* J Biol Chem, 1992. **267**(13): p. 9005-13.
71. Dong, D.L. and G.W. Hart, *Purification and characterization of an O-GlcNAc selective N-acetyl-beta-D-glucosaminidase from rat spleen cytosol.* J Biol Chem, 1994. **269**(30): p. 19321-30.
72. Kreppel, L.K., M.A. Blomberg, and G.W. Hart, *Dynamic glycosylation of nuclear and cytosolic proteins. Cloning and characterization of a unique O-GlcNAc transferase with multiple tetratricopeptide repeats.* J Biol Chem, 1997. **272**(14): p. 9308-15.
73. Gao, Y., et al., *Dynamic O-glycosylation of nuclear and cytosolic proteins: cloning and characterization of a neutral, cytosolic beta-N-acetylglucosaminidase from human brain.* J Biol Chem, 2001. **276**(13): p. 9838-45.
74. Wells, L., et al., *Dynamic O-glycosylation of nuclear and cytosolic proteins: further characterization of the nucleocytoplasmic beta-N-acetylglucosaminidase, O-GlcNAcase.* J Biol Chem, 2002. **277**(3): p. 1755-61.
75. Comtesse, N., E. Maldener, and E. Meese, *Identification of a nuclear variant of MGEA5, a cytoplasmic hyaluronidase and a beta-N-acetylglucosaminidase.* Biochem Biophys Res Commun, 2001. **283**(3): p. 634-40.
76. Nolte, D. and U. Muller, *Human O-GlcNAc transferase (OGT): genomic structure, analysis of splice variants, fine mapping in Xq13.1.* Mamm Genome, 2002. **13**(1): p. 62-4.
77. Butkinaree, C., K. Park, and G.W. Hart, *O-linked beta-N-acetylglucosamine (O-GlcNAc): Extensive crosstalk with phosphorylation to regulate signaling and transcription in response to nutrients and stress.* Biochim Biophys Acta, 2009.
78. Farook, V.S., C. Bogardus, and M. Prochazka, *Analysis of MGEA5 on 10q24.1-q24.3 encoding the beta-O-linked N-acetylglucosaminidase as a candidate gene for type 2 diabetes mellitus in Pima Indians.* Mol Genet Metab, 2002. **77**(1-2): p. 189-93.

79. Lehman, D.M., et al., *A single nucleotide polymorphism in MGEA5 encoding O-GlcNAc-selective N-acetyl-beta-D glucosaminidase is associated with type 2 diabetes in Mexican Americans.* Diabetes, 2005. **54**(4): p. 1214-21.
80. McClain, D.A., et al., *Altered glycan-dependent signaling induces insulin resistance and hyperleptinemia.* Proc Natl Acad Sci U S A, 2002. **99**(16): p. 10695-9.
81. Goto, Y., M. Kakizaki, and N. Masaki, *Production of spontaneous diabetic rats by repetition of selective breeding.* Tohoku J Exp Med, 1976. **119**(1): p. 85-90.
82. Kimura, K., et al., *Impaired insulin secretion in the spontaneous diabetes rats.* Tohoku J Exp Med, 1982. **137**(4): p. 453-9.
83. Begum, N. and L. Ragolia, *Altered regulation of insulin signaling components in adipocytes of insulin-resistant type II diabetic GotO-Kakizaki rats.* Metabolism, 1998. **47**(1): p. 54-62.
84. Galli, J., et al., *Pathophysiological and genetic characterization of the major diabetes locus in GK rats.* Diabetes, 1999. **48**(12): p. 2463-70.
85. Van Tine, B.A., A.J. Patterson, and J.E. Kudlow, *Assignment of N-acetyl-D-glucosaminidase (Mgea5) to rat chromosome 1q5 by tyramide fluorescence in situ hybridization (T-FISH): synteny between rat, mouse and human with Insulin Degradation Enzyme (IDE).* Cytogenet Genome Res, 2003. **103**(1-2): p. 202B.
86. Toleman, C., et al., *Characterization of the histone acetyltransferase (HAT) domain of a bifunctional protein with activable O-GlcNAcase and HAT activities.* J Biol Chem, 2004. **279**(51): p. 53665-73.
87. Bowe, D.B., et al., *O-GlcNAc integrates the proteasome and transcriptome to regulate nuclear hormone receptors.* Mol Cell Biol, 2006. **26**(22): p. 8539-50.
88. Akimoto, Y., et al., *Elevated expression of O-GlcNAc-modified proteins and O-GlcNAc transferase in corneas of diabetic GotO-Kakizaki rats.* Invest Ophthalmol Vis Sci, 2003. **44**(9): p. 3802-9.
89. Akimoto, Y., et al., *Elevation of the post-translational modification of proteins by O-linked N-acetylglucosamine leads to deterioration of the glucose-stimulated insulin secretion in the pancreas of diabetic GotO-Kakizaki rats.* Glycobiology, 2007. **17**(2): p. 127-40.
90. Haltiwanger, R.S., K. Grove, and G.A. Philipsberg, *Modulation of O-linked N-acetylglucosamine levels on nuclear and cytoplasmic proteins in vivo using the peptide O-GlcNAc-beta-N-acetylglucosaminidase inhibitor O-(2-acetamidO-2-deoxy-D-glucopyranosylidene)aminO-N-phenylcarbamate.* J Biol Chem, 1998. **273**(6): p. 3611-7.
91. Hinault, C., E. Van Obberghen, and I. Mothe-Satney, *Role of amino acids in insulin signaling in adipocytes and their potential to decrease insulin resistance of adipose tissue.* J Nutr Biochem, 2006. **17**(6): p. 374-8.
92. Whelan, S.A., M.D. Lane, and G.W. Hart, *Regulation of the O-linked beta-N-acetylglucosamine transferase by insulin signaling.* J Biol Chem, 2008. **283**(31): p. 21411-7.
93. Ball, L.E., M.N. Berkaw, and M.G. Buse, *Identification of the major site of O-linked beta-N-acetylglucosamine modification in the C terminus of insulin receptor substrate-1.* Mol Cell Proteomics, 2006. **5**(2): p. 313-23.
94. Kang, E.S., et al., *O-GlcNAc modulation at Akt1 Ser473 correlates with apoptosis of murine pancreatic beta cells.* Exp Cell Res, 2008. **314**(11-12): p. 2238-48.
95. Klein, A.L., et al., *O-GlcNAc modification of insulin receptor substrate-1 (IRS-1) occurs in close proximity to multiple SH2 domain binding motifs.* Mol Cell Proteomics, 2009.

96. Wells, L., et al., *O-GlcNAc transferase is in a functional complex with protein phosphatase 1 catalytic subunits.* J Biol Chem, 2004. **279**(37): p. 38466-70.
97. Robinson, K.A., L.E. Ball, and M.G. Buse, *Reduction of O-GlcNAc protein modification does not prevent insulin resistance in 3T3-L1 adipocytes.* Am J Physiol Endocrinol Metab, 2007. **292**(3): p. E884-90.
98. Dentin, R., et al., *Hepatic glucose sensing via the CREB coactivator CRTC2.* Science, 2008. **319**(5868): p. 1402-5.
99. Macauley, M.S., et al., *Elevation of global O-GlcNAc levels in 3T3-L1 adipocytes by selective inhibition of O-GlcNAcase does not induce insulin resistance.* J Biol Chem, 2008. **283**(50): p. 34687-95.
100. Macauley, M.S., et al., *O-GlcNAcase uses substrate-assisted catalysis: kinetic analysis and development of highly selective mechanism-inspired inhibitors.* J Biol Chem, 2005. **280**(27): p. 25313-22.
101. Considine, R.V., et al., *Hexosamines regulate leptin production in human subcutaneous adipocytes.* J Clin Endocrinol Metab, 2000. **85**(10): p. 3551-6.
102. Zhang, P., et al., *Hexosamines regulate leptin production in 3T3-L1 adipocytes through transcriptional mechanisms.* Endocrinology, 2002. **143**(1): p. 99-106.
103. Jackson, S.P. and R. Tjian, *O-glycosylation of eukaryotic transcription factors: implications for mechanisms of transcriptional regulation.* Cell, 1988. **55**(1): p. 125-33.
104. Roos, M.D., et al., *O glycosylation of an Sp1-derived peptide blocks known Sp1 protein interactions.* Mol Cell Biol, 1997. **17**(11): p. 6472-80.
105. Han, I. and J.E. Kudlow, *Reduced O glycosylation of Sp1 is associated with increased proteasome susceptibility*. Mol Cell Biol, 1997. **17**(5): p. 2550-8.
106. Yang, X., et al., *O-linkage of N-acetylglucosamine to Sp1 activation domain inhibits its transcriptional capability.* Proc Natl Acad Sci U S A, 2001. **98**(12): p. 6611-6.
107. Majumdar, G., et al., *O-glycosylation of Sp1 and transcriptional regulation of the calmodulin gene by insulin and glucagon.* Am J Physiol Endocrinol Metab, 2003. **285**(3): p. E584-91.
108. Solomon, S.S., et al., *A critical role of Sp1 transcription factor in regulating gene expression in response to insulin and other hormones.* Life Sci, 2008. **83**(9-10): p. 305-12.
109. Brownlee, M., *Biochemistry and molecular cell biology of diabetic complications.* Nature, 2001. **414**(6865): p. 813-20.

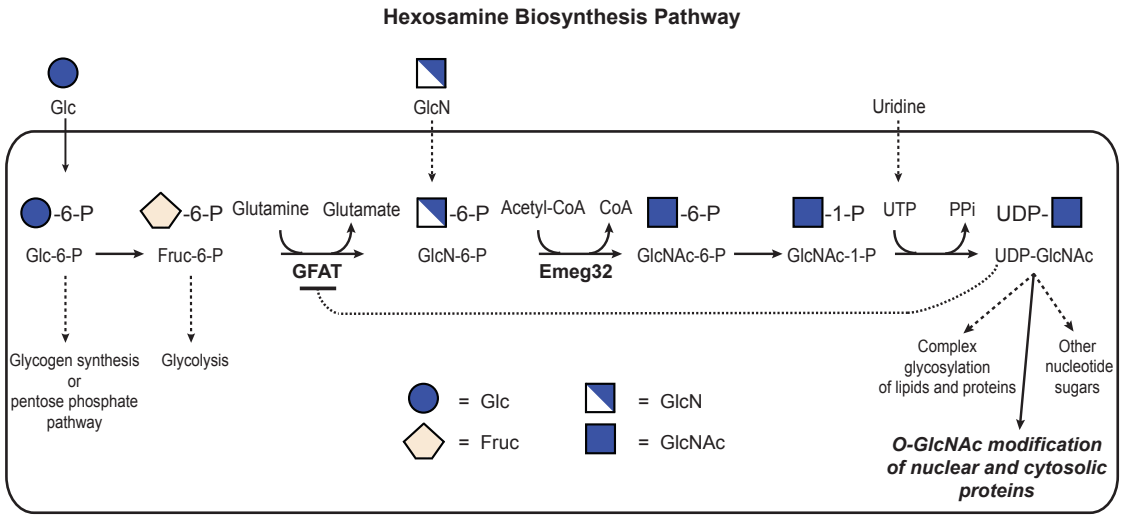

Figure 4-1. The hexosamine biosynthesis pathway (HBP). The HBP is posed to act as a "glucose sensor" since the synthesis of UDP-GlcNAc relies on the incorporation of products from glucose, amino acid (glutamine), fatty acid (acetyl-CoA), and nucleotide (uridine) metabolism. While the majority of the glucose entering the cell is committed to glycogen synthesis, the pentose phosphate pathway and glycolysis, 2 to 5 % of it enters the HBP for the formation of UDP-GlcNAc, a precursor for a variety of glycosylations, including *O*-GlcNAc modification. As is typical to metabolic pathways, the first and rate-limiting enzyme, GFAT, is negatively regulated by the end product, UDP-GlcNAc. Although the HBP requires several enzymatic steps, the two most well-studied enzymes (depicted in bold) in terms of insulin resistance are GFAT, the rate-limiting enzyme, and Emeg32.

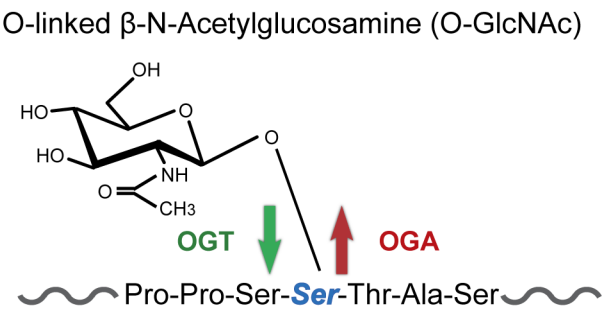

Figure 4-2. *O*-GlcNAc modification. This dynamic and inducible post-translational modification on nucleocytoplasmic proteins is catalyzed by OGT (in green) and OGA (in red) for the addition to, and removal from the serine and threonine residues, respectively. While no single consensus sequence for *O*-GlcNAc addition has been identified, the sequence shown here is derived from IRS-1 that contains a known *O*-GlcNAc residue on Ser1046 (shown in blue).

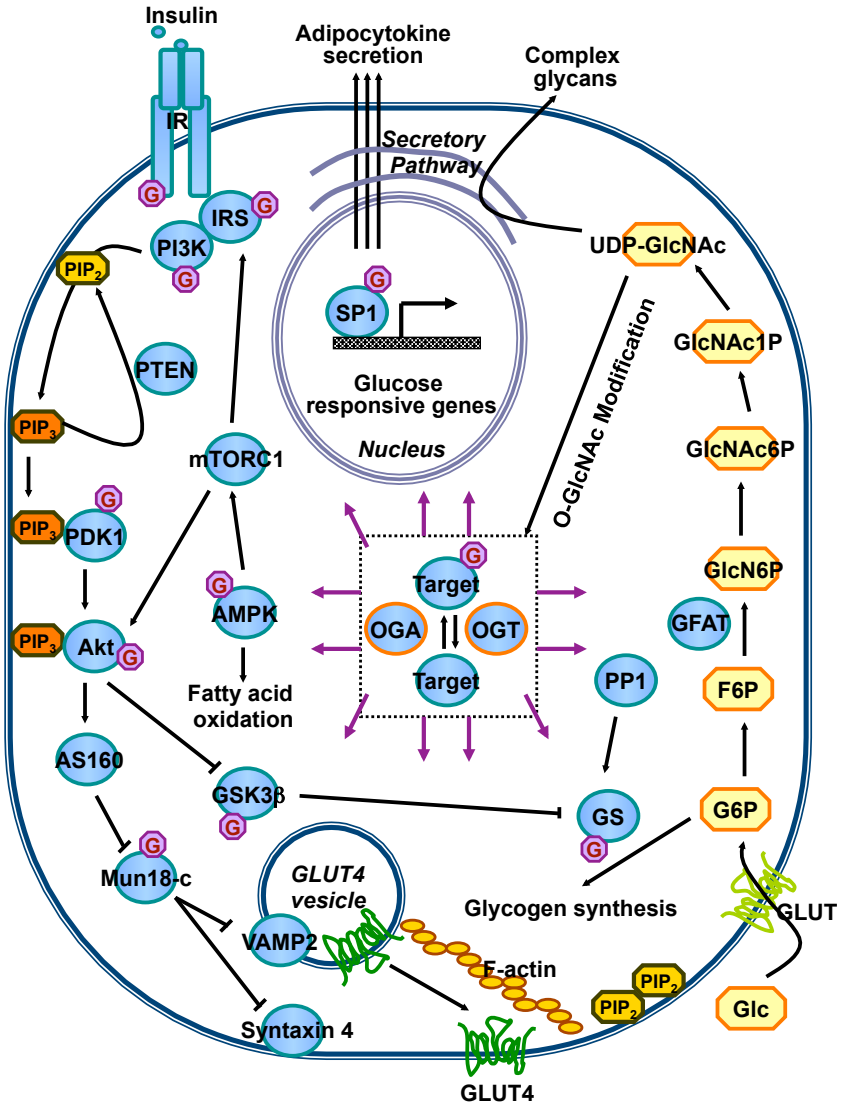

Figure 4-3. Cross-talk between the hexosamine biosynthesis pathway, *O*-GlcNAc modification of proteins, signaling events downstream of insulin action, and glucose-induced adipocytokine secretion. Many of the proteins involved in this signaling network are known to be *O*-GlcNAc modified, but the functional roles of this modification in each case remain to be established.

Model System	UDP-GlcNAc Level	O-GlcNAc Level	Insulin Resistance?	References
Animal models				
Glucosamine Infusion	+	+	Yes	Rossetti *et al.*, 1995; Virkamäki *et al.*, 1997
GFAT Transgenic Mice	+	+	Yes	Hebert *et al.*, 1996; Hazel *et al.*, 2004
OGT Transgenic Mice	∅	+	Yes	McClain *et al.*, 2002
GK Rats	∅	+*	Yes	Goto *et al.*, 1976; Akimoto *et al.*, 2003; Akimoto *et al.*, 2007
Cultured Adipocytes				
High Glucose/Insulin	+	+	Yes	Nelson *et al.*, 2000; Ross *et al.*, 2000
Glucosamine	+	+	Yes	Nelson *et al.*, 2000; Ross *et al.*, 2000
PUGNAc	⊗	+	Yes	Vosseller *et al.*, 2002; Park *et al.*, 2005; Yang *et al.*, 2008
NButGT	∅	+	No	Macauley *et al.*, 2008
OGT Overexpression	∅	+	Yes	Yang *et al.*, 2008
OGA Overexpression	∅	-	Yes	Robinson *et al.*, 2008
OGT Knockdown	∅	-	Yes	Robinson *et al.*, 2008

+: Increased; -: Decreased; ⊗: No change; ∅: No information available.
* Observed in non-adipose tissues, has yet to examine in adipose tissue.

Table 4-1. A summary of animal and cultured adipocyte models used in studying insulin resistance, HBP flux or global *O*-GlcNAc levels.

CHAPTER 5

DISSECTING THE IMPACT OF *O*-GLCNAC MODIFICATION ON INSULIN ACTION USING DIFFERENT OGA INHIBITORS[#]

[#]Teo C.F. and Wells L. To be submitted to *JBC.*

Abstract

O-GlcNAc modification is a ubiquitous and reversible glycosylation found on intracellular proteins. The spatial and temporal presence of *O*-GlcNAc is orchestrated by a pair of cycling enzymes, *O*-GlcNAc transferase (OGT) and β-*N*-acetylglucosaminidase (OGA), in response to a variety of cellular and environmental stimuli. Given that UDP-GlcNAc, the end product of the hexosamine biosynthetic pathway (HBP), is an obligatory donor substrate of OGT, *O*-GlcNAc is considered as an effector of excessive glucose flux through the HBP which in turn can lead to the development of insulin resistance, a hallmark of type 2 diabetes. Previous studies have utilized PUGNAc, the first reported OGA inhibitor that inhibits lysosomal hexosaminidases as well, to increase global *O*-GlcNAc levels and observed a correlation of elevated *O*-GlcNAc with the development of insulin resistance. This notion was challenged by results from Vocadlo's group, in which elevated global *O*-GlcNAc levels using a more selective OGA inhibitor, NButGT, did not lead to insulin resistance in cell culture or *in vivo*. In this study, we evaluated the impact of the *O*-GlcNAc modification on the pro-survival action of insulin under serum-deprivation induced apoptosis using three different OGA inhibitors, GlcNAcstatin-g (another OGA selective inhibitor), Thiamet-G (a derivative of NButGT), and PUGNAc. We found that only PUGNAc inhibits the protective action of insulin. To address whether inhibition of the lysosomal hexosaminidase activity via PUGNAc, which would elevate global GM2 ganglioside levels, leads to its unique characteristic in blocking insulin action, we also examined the pro-survival role of insulin in the presence of a selective lysosomal hexosaminidase inhibitor, INJ2. We established that neither INJ2 alone nor the combination of OGA selective inhibitors with INJ2 mimic the inhibitory effect of PUGNAc. These results strongly suggest that the defect in insulin action upon PUGNAc treatment does not derive from its inhibition of OGA or lysososomal hexosaminidases,

and that there is a third, yet unknown, target of PUGNAc that is the likely culprit in inhibiting the protective effect of insulin from apoptosis.

1. Introduction

Insulin resistance is a condition whereby insulin responsive organs of affected individuals are desensitized to insulin action subsequent to a prolonged elevation in systemic glucose and insulin levels. Uncontrolled and chronic insulin resistance eventually leads to the deterioration of various physiological conditions, collectively termed the metabolic syndrome, that increase the risk for type II diabetes, various micro- and macro-vascular diseases such as diabetes associated kidney failure, blindness, arterial diseases, and several types of cancer. In the 1990s, seminal findings from Marshall and coworkers revealed a potential mechanism[1] for the development of insulin resistance in which hyperglycemia- and hyperinsulinemia-induced insulin resistance in primary rat adipocytes can be reversed by pharmacologically inhibiting glutamine:fructose-6-phosphate aminotransferase (GFAT), the rate-limiting enzyme of the hexosamine biosynthetic pathway (HBP). Given that the HBP is one of the immediate metabolic routes for glucose, many studies have further explored and confirmed the direct impact of excessive glucose and HBP fluxes on the development of insulin resistance by dampening insulin mediated glucose uptake in cultured adipocytes and skeletal muscle, or reduction in glucose disposal rate in the peripheral tissues of animals[2, 3]. In addition to its anabolic function, insulin also plays a significant pro-survival role in a group of non-canonical insulin-sensitive tissues, namely the retina, brain and peripheral nerves[4, 5]. Study from Gardner's group has provided evidence that excess HBP flux in a retinal neuron cell model (differentiated R28 cells) impedes the anti-apoptotic action of insulin upon serum deprivation, which places HBP-induced

insulin resistant as one of the causative factors for the development of diabetic retinopathy[6].

The end product of the HBP, UDP-GlcNAc, can be either directly utilized as an activated glycan donor in numerous types of glycan and glycoconjugate biosyntheses, or converted into other nucleotide sugars for the same purpose[7]. Of all types of glycosylations, *O*-linked β-*N*-acetylglucosamine (*O*-GlcNAc) modification emerged as a key candidate for modulating the development of insulin resistance upon excess glucose influx. With the exception of yeast, *O*-GlcNAc modification has been reported in most eukaryotic model organisms and is ubiquitously found on the side chains of serine and threonine residues of many intracellular proteins[8]. Similar to protein phosphorylation, the occurrence of *O*-GlcNAc on target proteins is dynamic and inducible[9]. Due to these features, both phosphorylation and *O*-GlcNAc modification are common regulatory switches for numerous cellular processes, including signaling and metabolic pathways. However, unlike the regulation of phosphorylation by large sets of kinases and phosphatases, *O*-GlcNAc modification is modulated by a duo of cycling enzymes comprised of *O*-GlcNAc transferase (OGT) and β-*N*-acetylglucosaminidase (OGA), for the addition and removal of the GlcNAc moiety, respectively.

The impact of *O*-GlcNAc on the development of insulin resistance has been extensively explored in the context of dysregulation in insulin-mediated glucose homeostasis[2, 3]. For instance, pharmacologically elevated *O*-GlcNAc levels in rodent adipocytes using PUGNAc, a previously established OGA inhibitor, has been repeatedly shown to result in a reduction in acute insulin stimulated glucose uptake and signal transmission through the IRS/PI3K/Akt cascade[10-12]. These findings mirror the observations in the same cell models exposed to HBP-induced insulin resistance[13, 14]. Complementary to PUGNAc administration, transgenic mice overexpressing OGT in adipose and other peripheral tissues displayed insulin resistant phenotype despite

normal blood glucose level, a condition that closely resembles transgenic mice overexpressing GFAT[15]. Moreover, in a genetically diabetic *db/db* mouse model, overexpressing OGA was reported to alleviate whole-body insulin resistant condition in experimental animals[16]. In addition to mammalian models, the implication of *O*-GlcNAc in the insulin signaling pathway has been further strengthened with studies using two other model organisms, *Drosophila melanogaster*[17] and *Caenorhabditis elegans*[18-23], in which genetic perturbation of *O*-GlcNAc cycling enzymes results in distinct phenotypes that recapitulate their corresponding insulin signaling mutant phenotypes: body size in fruit flies and life span/dauer regulation in nematodes.

While PUGNAc has been widely used as an OGA inhibitor to manipulate *O*-GlcNAc levels *in vivo* since the 90s[24, 25], recently available structural information and catalytic mechanism of OGA revealed the possibility for obtaining more selective OGA inhibitors than PUGNAc[26]. Several groups have undertaken this rational inhibitor design challenge and generated a series of more selective and potent OGA inhibitors[27-33]. Unexpectedly, when Vocadlo's laboratory treated cultured adipocytes with NButGT (one of the more selective OGA specific inhibitors) to increase global *O*-GlcNAc levels, they did not observe any negative effect in insulin-stimulated glucose uptake or Akt phosphorylation as established in PUGNAc treated adipocytes[31]. Additionally, animals subjected to NButGT regime remain insulin sensitive with a normal whole-body glucose homeostasis profile[27]. In order to rule out the potential side effect derived from NButGT treatment, Vocadlo's group also synthesized a structurally unrelated and less selective OGA inhibitor, termed 6-Ac-Cas, and examined its effect on insulin action in adipocytes. In line with their findings on NButGT, global elevation in *O*-GlcNAc levels upon 6-Ac-Cas treatment does not lead to insulin resistance[34]. Collectively, these studies initiated a debate for the role of *O*-GlcNAc in the development of insulin resistance.

In this study, we aimed to dissect the impact of different OGA inhibitors on insulin action. Specifically, we wanted to examine the anti-apoptotic function of insulin upon serum-deprivation induced apoptosis. We used Chinese hamster ovary cells ectopically overexpressing human insulin receptor (CHO-IR, [35]) that have been extensively used to study insulin-mediated signal transduction [36-38], as our cell model. Importantly, a unique feature of insulin action in CHO-IR cells is its pro-survival function upon serum deprivation induced apoptosis[39, 40], a phenomenon observed in retinal neuron cell model as well. However, in contrast to the retinal neuron model, CHO-IR cells do not required laborious differentiation steps that are imperative for culturing retinal neurons, hence allowing us to streamline the experimental workflow. To raise the global *O*-GlcNAc level, we used PUGNAc and two more selective OGA inhibitors, GlcNAcstatin-G (developed by van Aalten's group[28]) and Thiamet-G (a more stable version of NButGT synthesized by Vocadlo's group[30]). To investigate the potential involvement of PUGNAc's secondary target in affecting insulin action, we compared PUGNAc treatment with a selective hexosaminidase A/B (HexA/B) inhibitor, INJ2, generated in Lin's laboratory[41]. We report that while GlcNAcstatin G, Thiamet-G and PUGNAc all effectively elevate global *O*-GlcNAc levels in CHO-IR cells, only PUGNAc abolishes the insulin protection under serum deprivation induced apoptosis. Moreover, since neither INJ2 treatment alone nor in combination with GlcNAcstatin G or Thiamet-G affects the anti-apoptotic action of insulin action, we concluded that there is a third, yet unknown, target of PUGNAc that is the likely culprit in inhibiting the protective effect of insulin from apoptosis.

2. Results

2.1 Elevation of global O-GlcNAc levels does not necessary affect the pro-survival action of insulin

To investigate the impact of different OGA inhibitors on the pro-survival role of insulin, we implemented two parallel experiments to evaluate the anti-apoptotic action of insulin upon serum-withdrawal induced apoptosis in CHO-IR cells. The first approach monitors the formation of internucleosomal DNA fragments, a well-established signature for cells undergoing programmed cell death, using propidium iodione (PI) to stain and the quantify the subG1 distribution of the intracellular DNA content. The second approach employs immunoblot detection of activated/cleaved caspase-3 (an executioner of apoptosis) and the cleavage product of its downstream substrate, poly-ADP ribose polymerase-1 (cl-PARP-1), both processes precede the formation of DNA fragments during the course of apoptosis.

As demonstrated in Figure 5-1, when CHO-IR cells were cultured in the absence of serum for 24 hours, approximately 6% of cells were committed to programmed cell death as represented by the appearance of apoptotic DNA fragments, a population of cells that are absence when cells were grown in the presence of serum. Likewise, cleavage products from caspase-3 and PARP-1 were also detected in cell lysate prepared from cells that were serum-deprived but not from those that were cultured in the presence of serum. To establish the lowest concentration of insulin that is sufficient for its anti-apoptotic function, we cultured CHO-IR in the serum free medium supplemented with 0.01, 0.1, 1 or 10 nM of insulin. We did not detect any of the apoptosis markers (fragmented DNA, cleaged caspase-3, or cleaved PARP-1) with 1 or 10 nM insulin treatment, indicating that 1 nM of insulin is sufficient to effectively rescue CHO-IR cells from undergoing serum-withdrawal induced apoptosis. All three of the apoptosis markers were detected with 0.1 nM insulin treatment, whereas almost no

protection was observed with 0.01 nM insulin treatment. As, these results were in good agreement with the previous observation by Bertrand *et al.*, we selected 1 and 10 nM insulin concentrations for the rest of our studies.

Notably, unlike Bertrand *et al.*[40] who reported that 30% of CHO-IR undergoes apoptosis after 24 h of serumwithdrawal, we detected only approximately 6% apoptotic cells with identical treatment. The discrepancy may derive from the difference in methods used for quantifying apoptosis: We used a Nexcelom automatic cell counter to measure the distribution of PI-DNA fluorescence intensities from cells in different stages of cell cycle, including cells undergoing apoptosis (shown as the subG1 peak in the histogram). While this automated method can characterize a large number of cells in an unbiased and consistent manner across several experiments, it potentially underestimates the true apoptotic population since apoptotic cells arising from S, M or G2 phase cells might be not have accumulated enough DNA fragments that can be accounted for in the subG1 population. Nevertheless, since the G1 phase cells are the single most abundant population, this method can provide a good approximation of the total apoptotic cells. The method reported by Bertrand and colleagues[40], on the other hand, relies on manually counting of apoptotic nuclei after Hoechest 33258 staining, which is prone to human bias. Since the results from the immunoblot detection of cleaved caspase-3 and PARP-1 correlate well with the fluorescence assay, we were confident that regardless the seemingly low percentage of apoptotic cells in subG1 stage, we were indeed able to induce apoptosis and monitor the protective effect of insulin. However, we chose the cleaved caspase-3 and PARP-1 as our primary apoptotic markers in the following experiments.

To increase the global *O*-GlcNAc levels, we cultured CHO-IR cells in the presence of GlcNAcstatin G (0.5 μM), Thiamet-G (2.5 μM) as well as PUGNAc (50 μM) for 24 h (Figure 5-2A). Since GlcNAcstatin G and Thiamet-G were rationally designed

based on the structural and catalytic information of OGA and its bacterial homologs, both inhibitors are more potent and showed greater selectivity against OGA over lysosomal hexosaminidases in comparison to PUG. As a result, instead of treating cells with the same concentration for all three inhibitors, we selected concentrations for each inhibitor that gave us consistent and comparable global *O*-GlcNAc levels as detected on one-dimensional immunoblot against a pan-*O*-GlcNAc specific antibody, CTD110.6 (Figure 5-2).

When CHO-IR cells were treated with either GlcNAcstatin G or Thiamet-G in the presence of insulin (Figure 5-2), we did not observe any cleavage products of caspase-3 and PARP-1. On the other hand, both of the apoptotic markers were readily detectable when cells were cultured in the presence of both insulin and PUGNAc. Collectively, these results indicated that, unlike PUGNAc, GlcNAcstatin G and Thiamet-G do not lead to any detrimental effect on the anti-apoptotic action of insulin. Since both GlcNAcstatin G and Thiamet-G are more potent and selective OGA inhibitor than PUGNAc, our observation suggests that elevated global *O*-GlcNAc level alone is not responsible for dampening the protective action of insulin. In agreement with Macauley *et al.* whose reports primarily focused on the glucose homeostasis aspect of insulin function, our data also indicates that PUGNAc impinges on insulin actions via a secondary target rather than inhibition of OGA.

2.2 PUG-mediated accumulation of GM2 level does not explain the defect in insulin action

After ruling out the involvement of elevated global *O*-GlcNAc levels in blocking the protective action of insulin, we were curious to understand the inhibitory effect of PUGNAc on insulin action. In mammals, there are two additional enzymes that recognize and hydrolyse terminal GlcNAc structure, namely lysosomal hexosaminidases

A and B (HexA and HexB, or HexA/B). Although OGA and HexA/B belong to different CAZy families and reside in distinct cellular compartments, all of them utilize the same substrate-assisted catalytic mechanism. Not surprisingly, PUGNAc was found to inhibit HexA/B leading to an accumulation of GM2 ganglioside level[41, 42]. Dysregulation in ganglioside metabolism has been proposed to be one of the causative factors in the development of insulin resistance because transgenic animals that lack GM3, a biosynthetic precursor of GM2, show improved insulin sensitivity[43]. Additionally, it was recently reported that obese type II diabetic individuals have increased GM2 levels compared to non-diabetic individuals[44]. Given that PUGNAc targets HexA/B as well, one possible scenario is that PUGNAc-mediated elevation in the GM2, but not the *O*-GlcNAc levels, contributes to insulin resistant condition. We reasoned that if we could use a more selective lysosomal hexosaminidase inhibitor to modulate GM2 level without affecting OGA (Figure 5-3), it could assist us to understand whether PUGNAc-mediated increase in GM2 level is responsible for the ablation of insulin action. We chose a highly selective HexA/B inhibitor, INJ2, which is a GlcNAc-type iminocyclitiol derivative developed by Lin's group[41], to specifically increase global GM2 levels without altering intracellular *O*-GlcNAc profile.

As demonstrated in Figure 5-4, we did not detect the formation of any apoptotic markers (cleaved caspase-3 and cleaved PARP-1) when CHO-IR cells were cultured in the presence of INJ2. Thus, our observation indicates that elevation of GM2 level did not explain the inhibitory effect of PUG on the protection of insulin upon serum-withdrawal induced apoptosis.

2.3 An unknown target of PUGNAc is causing the inhibitory effect on insulin

Having excluded the scenarios in which global increase in either *O*-GlcNAc or GM2 levels alone impinge on insulin's anti-apoptotic function, we wanted to explore the

possibility that a simultaneous increase in both *O*-GlcNAc and GM2 levels resulting from PUGNAc treatment is essential for the inhibitory outcome. To address this question, we compared the protective action of insulin with PUGNAc alone and the combination of OGA and HexA/B selective inhibitors. We hypothesized that if the concurrent increases in both *O*-GlcNAc and GM2 levels are required to impinge on insulin action, the presence of GNSg or TMG in conjunction to INJ2 would mimic PUG treatment.

Surprisingly, when CHO-IR cells were treated with either GlcNAcstatin G/INJ2 or Thiamet-G/INJ2 combinations in conjunction with insulin, we were not able to detect the cleavage products of caspase-3 and PARP-1 (Figure 5-5). Since, none of the treatments recapitulated the negative effect of PUGNAc on the pro-survival role of insulin, we concluded that the inhibition of OGA and HexA/B by PUGNAc are irrelevant in PUGNAc-induced insulin resistance. Thus, this strongly suggests that PUGNAc has a third unknown target, which is responsible for its role in negating insulin action.

3. Discussion

Controversy surrounding the role of *O*-GlcNAc in regulating insulin signaling using PUGNAc and two other OGA inhibitors (NButGT and 6-Ac-Cas) inspired us to compare the effect of PUGNAc to GlcNAcstatin G and Thiamet-G (which is structurally similar to NButGT), both of which are more selective and potent OGA inhibitors, on insulin action. Unlike Vocadlo and colleagues who studied NButGT[27, 31] and 6-Ac-Cas[34] and focused on the impact of *O*-GlcNAc on insulin-mediated glucose uptake in adipocytes, our primary goal was to investigate the effect of *O*-GlcNAc on the anti-apoptotic action of insulin. This is because insulin not only serves as a regulator for glucose homeostasis but also acts as a survival factor in some target tissues and cell types[4, 5]. In accordance with findings from Vocadlo's group using NButGT and 6-Ac-Cas, we observed that elevation of global *O*-GlcNAc levels with GlcNAcstatin G and

Thiamet-G does not affect the biological function of insulin.

In their report, Macauley *et al.* [31] concluded that, in 3T3-L1 adipocytes, 10 μM PUGNAc treatment was sufficient to increase global *O*-GlcNAc levels as efficiently as 100 μM PUGNAc, a concentration used by Vosseller *et al.* to first establish the link between *O*-GlcNAc and insulin resistance[12]. However, in CHO-IR cells, we established that 10 μM PUGNAc was a suboptimal concentration for elevating *O*-GlcNAc levels, as lysate from cells treated with this concentration frequently showed significantly less *O*-GlcNAc compared to GlcNAcstatin G and Thiamet-G treatments. That being said, we also observed DNA fragmentation when cells were treated with insulin and 10 μM PUGNAc (data not shown), suggesting the ablation of insulin action is not due to dosage toxicity from PUGNAc.

While Macauley *et al.*[31] did not observed an inhibitory effect of insulin-mediated glucose uptake when 3T3-L1 adipocytes were treated with 10 μM PUGNAc, they were able to induce insulin resistance with 100 μM PUGNAc treatment as reported by Vosseller *et al.*[12]. Therefore, they postulated that excessive dosage of PUGNAc might trigger its selectivity against lysosomal HexA/B which in turns lead to an accumulation in GM2 ganglioside level and insulin resistance. Results from our INJ2 studies excluded this possibility, since neither INJ2 alone nor INJ2 in conjunction with OGA selective inhibitors (GlcNAcstatin G and Thiamet-G) blocked insulin from rescuing CHO-IR cells from serum-deprivation induced apoptosis. Collectively, we have rule out two possible PUGNAc targets, namely OGA and HexA/B, as the culprit in dampening insulin action. Given that PUGNAc has been extensively used in cell biology research to modulate global *O*-GlcNAc levels, it is prudent to scrutinize those conclusions that were made solely based on PUGNAc treatment.

Having eliminated OGA and lysosomal HexA/B as PUGNAc's targets in down-regulating insulin action, there are several less obvious culprits that might be responsible

for this perplexing outcome and warrant further investigations. Given that the structure of PUGNAc is based on an *N*-acetylglucosamine (GlcNAc) scaffold, one can speculate that PUGNAc may affect the functions of proteins or enzymes that interact with GlcNAc-containing molecules. These potential PUGNAc targets include (1) sugar and nucleot0de sugar transporters; (2) metabolic enzymes; (3) GlcNAc transferases for complex glycosylations; and (4) lectins that binds GlcNAc containing structures. In order to discover the identity of additional PUGNAc targeting proteins in addition to OGA and lysosomal HexA/B, one possibility is to prepare a PUGNAc-conjugated solid support followed by affinity isolation and by shotgun proteomics experiments. Alternative approaches would be to perform mass spectrometry based quantitative metabolomics and glycomics analyses in order to pinpoint the cellular process(es) affected by PUGNAc.

4. Methods

Reagents and Antibodies. Reagents and their sources are as follows: PUGNAc [*O*-(2-acetamido-2-deoxy-D-glucopyranosylidene)amino *N*-phenyl carbamate] was purchased from Toronto Research Chemicals, Inc. (Ontario, Canada). Thiamet-G, propidium iodine (PI) and RNAse A were purchased from Sigma-Aldrich (St. Louis, MO). GlcNAcstatin G was a kind gift from Dr. Daan van Aalten (University of Dundee, United Kingdom). INJ2 was a kind gift from Dr. Chun-Hung Lin (Academia Sinica, Taiwan). Protease inhibitor and phosphatase inhibitor cocktails were purchased from Calbiochem (Gibbstown, NJ). Human insulin was purchased from Roche (Indianapolis, IN).

Cell culture and treatments. CHO-IR cells (Chinese hamster ovary cells overexpressing human insulin receptor, a gift from Dr. Richard Roth) were maintained in Ham's F-12 medium (Corning/Mediatech, Manassas, VA) supplemented with 10% fetal bovine serum (Life Technologies/Invitrogen, Carlsbad, CA) as previously described (ref).

Cells were seeded in 12-well plates (5 X 10^4 cells per well, for PI staining) or 35 mm dishes (1.5 x10^5 cells per dish, for western blotting) and cultured for 48 hour before treatments. For each treatment, the cells were first twice with PBS, and re-fed for an additional 24 hours with Ham's F-12 medium with or without supplemented 10%FBS, insulin (1 or 10 nM) or inhibitors (0.5 μM GlcNAcstatin G, 2.5 μM Thiamet-G, 50 μM PUGNAc, or 0.5 μM INJ2) as indicated in figure legends.

PI staining for apoptotic DNA fragments. At the end of the incubation period, treated cells were washed twice with PBS and incubated with 60 mM EDTA/PBS for 5 min at room temperature. Dislodged cells were transferred into 15 ml centrifuge tubes and centrifuged at 800 g for 8 min at 4 °C. Cell pellets were resuspended with 200 μl of 60 mM EDTA/PBS, mixed with 1.8 ml of 70% pre-chilled ethanol and incubated at 4°C for 15 min or -20°C for overnight. The cells were centrifuged (800 g for 15 min at 4 °C), resuspended in staining buffer (PI, RNAse A, TritonX-100). After incubating at 37°C for 1 hour, the cells were pelleted, resuspended in 20 μl of PBS and analyzed on a Nexcelom automatic cell counter using the default setting for cell cycle analysis.

Whole cell lysate preparation. At the end of the incubation period, treated cells were washed twice with PBS and incubated with 60 mM EDTA/PBS for 5 min at room temperature. Dislodged cells were transferred into 15 ml centrifuge tubes and centrifuged at 800 g for 8 min at 4 °C. Cell pellets were resuspended in TNS lysis buffer (10 mM Tris, pH 7.5, 150 mM NaCl, 1% Igepal CA-630, 0.1% SDS, 4 mM EDTA, 1 mM DTT, 10 mM PUGNAc, protease inhibitor cocktail and phosphatase inhibitor cocktail) and incubated on ice for 15 min. Cell lysates were then transferred into microtubes and centrifuged at 12,000 g for 15 min at 4 °C. Clarified supernatants were transferred into fresh tubes and protein concentration from each sample was quantified using Bradford protein assay according to manufacturer's instructions (Bio-Rad, Hercules, CA) using bovine serum albumin (BSA, from Thermo Fisher Scientific, Pittsburgh, PA) as a

standard. Equal amount of protein from each lysate was mixed with 5x Laemmli sample buffer, heated at 80°C for 15 min, and stored at -20°C until further immunoblot analyses.

Immunoblotting. Equal amount of total protein (typically 5 to 10 µg per lane) was subjected to SDS-PAGE analysis using Mini-PROTEAN TGX precast gels (7,5%? 7.5%, 4-15% or 4-20% gels, Bio-Rad, electrophoresis settings: 200 V, 30 to 35 min). The gels were subsequently electrotransferred (Trans-Blot SD semi-dry apparatus, Bio-Rad, electrotransfer settings: 20 V, 30 min) onto Immobilon-P membranes (0.45 µm, EMD Millipore) and the membranes were subjected to immunoblotting per standard procedure. The membranes were blocked with either 3% BSA (CTD110.6, AL28 and PY99 blots) or 5% non-fat milk (the rest of the blots) in TBST (TBS supplemented with 0.1% Tween 20). The primary antibodies used included (source and dilution factor as indicated): Anti-caspase-3 (Cell Signaling Technology, Beverly, MA, 1:1,000), anti-cleaved caspase-3 (Cell Signaling Technology, 1:2,500), PARP-1/2 (Santa Cruz Biotechnology, Santa Cruz, CA, 1:4,000) and cleaved PARP-1/p25 (EMD Millipore Corporation, Bedford, MA, 1:20,000). Membranes were incubated with primary antibodies for overnight at 4. All the primary antibodies were incubated for overnight at 4 °C. The secondary antibody-HRP conjugates were used in accordance to the species in which the primary antibodies were generated [sheep anti-mouse IgG-HRP (GE Healthcare, Piscataway, NJ, 1:20,000), goat anti-rabbit IgG-HRP (GE Healthcare, 1:20,000)] and the final detection of HRP activity was performed using Pierce ECL western blotting substrate (Thermo Fisher Scientific/Pierce, Rockford, IL). The only exception was cleaved caspase-3 blot, in which stabilized goat anti-rabbit IgG (H+L)-HRP (Thermo/Pierce, 1:5,000) and SuperSignal west Femto (Thermo/Pierce) were used instead of the secondary antibody and ECL substrate, respectively. Finally, the membranes were exposed to HyBlotCL films (Denville Scientific, Metuchen, NJ). Upon the completion of the aforementioned procedure, each of the blot was subsequently

stripped (either with 0.1 M glycine, pH 2.5 or 30% H_2O_2) and reprobed with β-actin (Sigma-Aldrich, 1:50,000) antibody as loading control.

5. References

1. Marshall, S., V. Bacote, and R.R. Traxinger, *Discovery of a metabolic pathway mediating glucose-induced desensitization of the glucose transport system. Role of hexosamine biosynthesis in the induction of insulin resistance.* J Biol Chem, 1991. **266**(8): p. 4706-12.
2. Teo, C.F., E.E. Wollaston-Hayden, and L. Wells, *Hexosamine flux, the O-GlcNAc modification, and the development of insulin resistance in adipocytes.* Mol Cell Endocrinol, 2010. **318**(1-2): p. 44-53.
3. Buse, M.G., *Hexosamines, insulin resistance, and the complications of diabetes: current status.* Am J Physiol Endocrinol Metab, 2006. **290**(1): p. E1-E8.
4. Barber, A.J., T.W. Gardner, and S.F. Abcouwer, *The significance of vascular and neural apoptosis to the pathology of diabetic retinopathy.* Invest Ophthalmol Vis Sci, 2011. **52**(2): p. 1156-63.
5. Reiter, C.E. and T.W. Gardner, *Functions of insulin and insulin receptor signaling in retina: possible implications for diabetic retinopathy.* Prog Retin Eye Res, 2003. **22**(4): p. 545-62.
6. Nakamura, M., et al., *Excessive hexosamines block the neuroprotective effect of insulin and induce apoptosis in retinal neurons.* J Biol Chem, 2001. **276**(47): p. 43748-55.
7. Boehmelt, G., et al., *Decreased UDP-GlcNAc levels abrogate proliferation control in EMeg32-deficient cells.* EMBO J, 2000. **19**(19): p. 5092-104.
8. Hart, G.W., M.P. Housley, and C. Slawson, *Cycling of O-linked beta-N-acetylglucosamine on nucleocytoplasmic proteins.* Nature, 2007. **446**(7139): p. 1017-22.
9. Hart, G.W., et al., *Cross talk between O-GlcNAcylation and phosphorylation: roles in signaling, transcription, and chronic disease.* Annu Rev Biochem, 2011. **80**: p. 825-58.
10. Whelan, S.A., et al., *Regulation of insulin receptor substrate 1 (IRS-1)/AKT kinase-mediated insulin signaling by O-Linked beta-N-acetylglucosamine in 3T3-L1 adipocytes.* J Biol Chem, 2010. **285**(8): p. 5204-11.
11. Yang, X., et al., *Phosphoinositide signalling links O-GlcNAc transferase to insulin resistance.* Nature, 2008. **451**(7181): p. 964-9.
12. Vosseller, K., et al., *Elevated nucleocytoplasmic glycosylation by O-GlcNAc results in insulin resistance associated with defects in Akt activation in 3T3-L1 adipocytes.* Proc Natl Acad Sci U S A, 2002. **99**(8): p. 5313-8.
13. Nelson, B.A., K.A. Robinson, and M.G. Buse, *Defective Akt activation is associated with glucose- but not glucosamine-induced insulin resistance.* Am J Physiol Endocrinol Metab, 2002. **282**(3): p. E497-506.
14. Nelson, B.A., K.A. Robinson, and M.G. Buse, *High glucose and glucosamine induce insulin resistance via different mechanisms in 3T3-L1 adipocytes.* Diabetes, 2000. **49**(6): p. 981-91.
15. McClain, D.A., et al., *Altered glycan-dependent signaling induces insulin resistance and hyperleptinemia.* Proc Natl Acad Sci U S A, 2002. **99**(16): p. 10695-9.

16. Dentin, R., et al., *Hepatic glucose sensing via the CREB coactivator CRTC2.* Science, 2008. **319**(5868): p. 1402-5.
17. Sekine, O., et al., *Blocking O-linked GlcNAc cycling in Drosophila insulin-producing cells perturbs glucose-insulin homeostasis.* J Biol Chem, 2010. **285**(49): p. 38684-91.
18. Forsythe, M.E., et al., *Caenorhabditis elegans ortholog of a diabetes susceptibility locus: oga-1 (O-GlcNAcase) knockout impacts O-GlcNAc cycling, metabolism, and dauer.* Proc Natl Acad Sci U S A, 2006. **103**(32): p. 11952-7.
19. Hanover, J.A., et al., *A Caenorhabditis elegans model of insulin resistance: altered macronutrient storage and dauer formation in an OGT-1 knockout.* Proc Natl Acad Sci U S A, 2005. **102**(32): p. 11266-71.
20. Rahman, M.M., et al., *Intracellular protein glycosylation modulates insulin mediated lifespan in C.elegans.* Aging (Albany NY), 2010. **2**(10): p. 678-90.
21. Mondoux, M.A., et al., *O-linked-N-acetylglucosamine cycling and insulin signaling are required for the glucose stress response in Caenorhabditis elegans.* Genetics, 2011. **188**(2): p. 369-82.
22. Love, D.C., et al., *Dynamic O-GlcNAc cycling at promoters of Caenorhabditis elegans genes regulating longevity, stress, and immunity.* Proc Natl Acad Sci U S A, 2010. **107**(16): p. 7413-8.
23. Lee, J., K.Y. Kim, and Y.K. Paik, *Regulation of Dauer formation by O-GlcNAcylation in Caenorhabditis elegans.* J Biol Chem, 2010. **285**(5): p. 2930-9.
24. Haltiwanger, R.S., K. Grove, and G.A. Philipsberg, *Modulation of O-linked N-acetylglucosamine levels on nuclear and cytoplasmic proteins in vivo using the peptide O-GlcNAc-beta-N-acetylglucosaminidase inhibitor O-(2-acetamido-2-deoxy-D-glucopyranosylidene)amino-N-phenylcarbamate.* J Biol Chem, 1998. **273**(6): p. 3611-7.
25. Dong, D.L. and G.W. Hart, *Purification and characterization of an O-GlcNAc selective N-acetyl-beta-D-glucosaminidase from rat spleen cytosol.* J Biol Chem, 1994. **269**(30): p. 19321-30.
26. Macauley, M.S. and D.J. Vocadlo, *Increasing O-GlcNAc levels: An overview of small-molecule inhibitors of O-GlcNAcase.* Biochim Biophys Acta, 2010. **1800**(2): p. 107-21.
27. Macauley, M.S., et al., *Elevation of Global O-GlcNAc in rodents using a selective O-GlcNAcase inhibitor does not cause insulin resistance or perturb glucohomeostasis.* Chem Biol, 2010. **17**(9): p. 949-58.
28. Dorfmueller, H.C., et al., *Cell-penetrant, nanomolar O-GlcNAcase inhibitors selective against lysosomal hexosaminidases.* Chem Biol, 2010. **17**(11): p. 1250-5.
29. Dorfmueller, H.C., et al., *GlcNAcstatins are nanomolar inhibitors of human O-GlcNAcase inducing cellular hyper-O-GlcNAcylation.* Biochem J, 2009. **420**(2): p. 221-7.
30. Yuzwa, S.A., et al., *A potent mechanism-inspired O-GlcNAcase inhibitor that blocks phosphorylation of tau in vivo.* Nat Chem Biol, 2008. **4**(8): p. 483-90.
31. Macauley, M.S., et al., *Elevation of global O-GlcNAc levels in 3T3-L1 adipocytes by selective inhibition of O-GlcNAcase does not induce insulin resistance.* J Biol Chem, 2008. **283**(50): p. 34687-95.
32. Whitworth, G.E., et al., *Analysis of PUGNAc and NAG-thiazoline as transition state analogues for human O-GlcNAcase: mechanistic and structural insights into inhibitor selectivity and transition state poise.* J Am Chem Soc, 2007. **129**(3): p. 635-44.

33. Dorfmueller, H.C., et al., *GlcNAcstatin: a picomolar, selective O-GlcNAcase inhibitor that modulates intracellular O-glcNAcylation levels.* J Am Chem Soc, 2006. **128**(51): p. 16484-5.
34. Macauley, M.S., et al., *Inhibition of O-GlcNAcase using a potent and cell-permeable inhibitor does not induce insulin resistance in 3T3-L1 adipocytes.* Chem Biol, 2010. **17**(9): p. 937-48.
35. Ebina, Y., et al., *Expression of a functional human insulin receptor from a cloned cDNA in Chinese hamster ovary cells.* Proc Natl Acad Sci U S A, 1985. **82**(23): p. 8014-8.
36. Myers, M.G., Jr., et al., *IRS-1 is a common element in insulin and insulin-like growth factor-I signaling to the phosphatidylinositol 3'-kinase.* Endocrinology, 1993. **132**(4): p. 1421-30.
37. Wilden, P.A., et al., *The role of insulin receptor kinase domain autophosphorylation in receptor-mediated activities. Analysis with insulin and anti-receptor antibodies.* J Biol Chem, 1992. **267**(19): p. 13719-27.
38. Sun, X.J., et al., *Expression and function of IRS-1 in insulin signal transmission.* J Biol Chem, 1992. **267**(31): p. 22662-72.
39. Lee-Kwon, W., et al., *Antiapoptotic signaling by the insulin receptor in Chinese hamster ovary cells.* Biochemistry, 1998. **37**(45): p. 15747-57.
40. Bertrand, F., et al., *A role for nuclear factor kappaB in the antiapoptotic function of insulin.* J Biol Chem, 1998. **273**(5): p. 2931-8.
41. Ho, C.W., et al., *Development of GlcNAc-inspired iminocyclitiols as potent and selective N-acetyl-beta-hexosaminidase inhibitors.* ACS Chem Biol, 2010. **5**(5): p. 489-97.
42. Stubbs, K.A., M.S. Macauley, and D.J. Vocadlo, *A selective inhibitor Gal-PUGNAc of human lysosomal beta-hexosaminidases modulates levels of the ganglioside GM2 in neuroblastoma cells.* Angew Chem Int Ed Engl, 2009. **48**(7): p. 1300-3.
43. Yamashita, T., et al., *Enhanced insulin sensitivity in mice lacking ganglioside GM3.* Proc Natl Acad Sci U S A, 2003. **100**(6): p. 3445-9.
44. Tanabe, A., et al., *Obesity causes a shift in metabolic flow of gangliosides in adipose tissues.* Biochem Biophys Res Commun, 2009. **379**(2): p. 547-52.

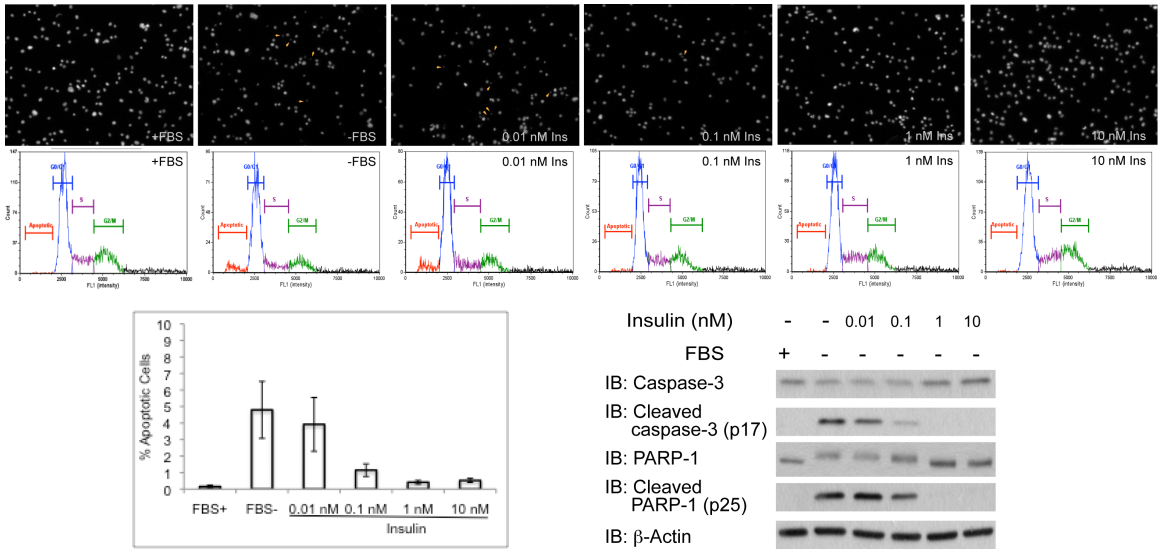

Figure 5-1. Insulin rescues CHO-IR cells from undergoing serumwithdrawal induced programmed cell death. (a) Representative fields, and (b) distribution of fluorescence intensity of propidium iodine stained CHO-IR cells (yellow arrows indicate apoptotic cells?) that were cultured in the presence or absence of serum and 0.01 nM, 0.1 nM, 1 nM and 10 nM insulin for 24 hours. (c) Histogram represents the percentage of apoptotic cells from each condition. Each bar contains the average percentage from six independent experiments. (d) Western blots of apoptotic markers, cleaved caspase-3 and cleaved PARP-1. Antibodies against full-length caspase-3 and PARP-1, as well as β-actin are included as controls.

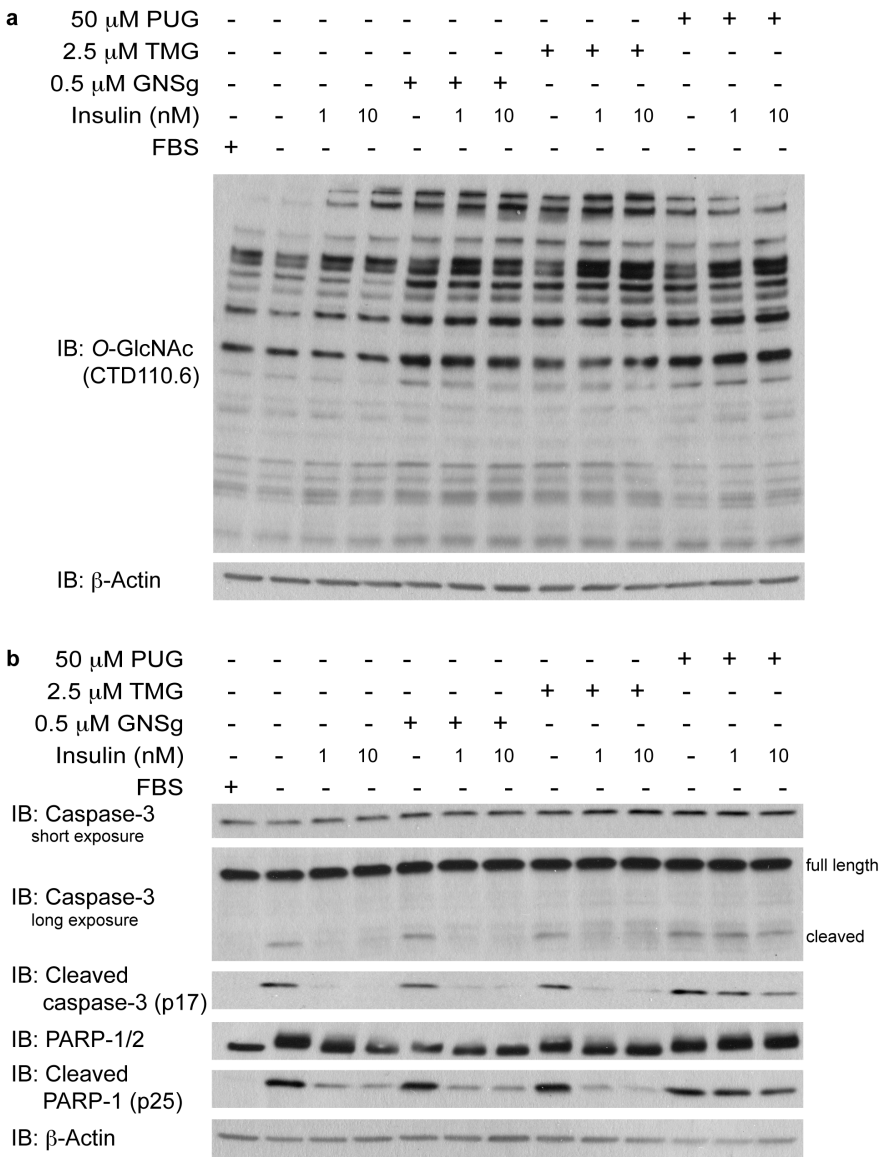

Figure 5-2. PUGNAc, but not GlcNAcstatin g or Thiamet g, blocks the pro-survival role of insulin. (a) O-GlcNAc western blots of cell lysate from CHO-IR cells treated with various OGA inhibitors (0.5 μM GlcNAcstatin g, 2.5 μM thiamet G or 50 μM PUGNAc) in the absence or presence of insulin (1 nM or 10 nM). (b) Western blots of apoptotic markers, cleaved caspase-3 and cleaved PARP-1, and their full-length counterparts as well as β-actin on cell lysates treated with various OGA inhibitors in the absence or presence of insulin (1 nM or 10 nM).

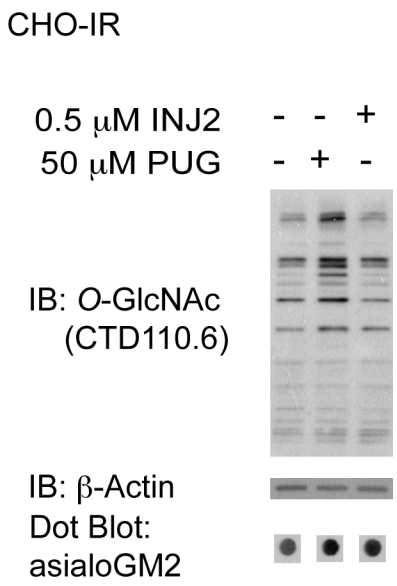

Figure 5-3. PUG and INJ2 treatments lead to an increase in the GM2 level. Cell lysates from CHO-IR cells treated with 50 μM PUGNAc or 0.5 μM INJ2 along with vehicle (DMSO) were subjected to dot blot analysis using asialo-GM2 specific antibody. *O*-GlcNAc and β-actin western blots were also shown.

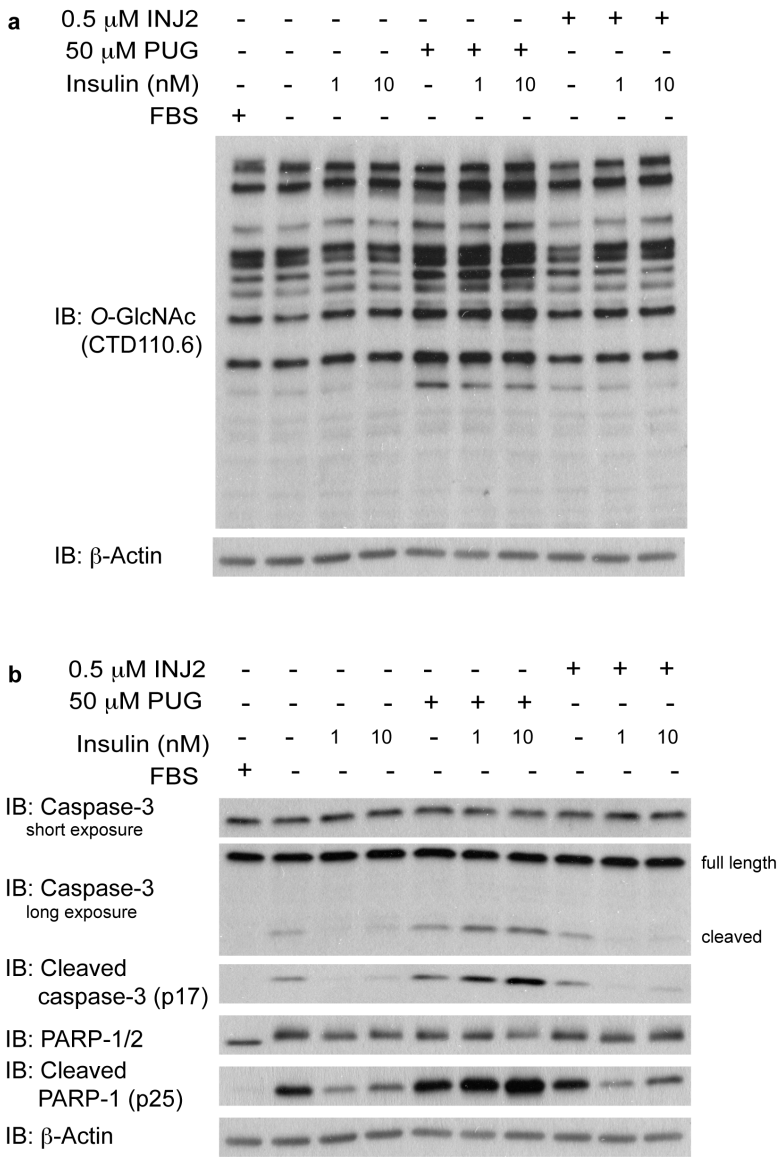

Figure 5-4. INJ2 does not inhibit the protective action of insulin. (a) *O*-GlcNAc western blots of cell lysates from CHO-IR cells treated with 50 μM PUGNAc or 0.5 μM INJ2 (a selective HexA/B inhibitor) in the absence or presence of insulin (1 nM or 10 nM). (b) Western blots of apoptotic markers, cleaved caspase-3 and cleaved PARP-1, and their full-length counterparts as well as β-actin on cell lysates treated with 50 μM PUGNAc or 0.5 μM INJ2 in the absence or presence of insulin (1 nM or 10 nM).

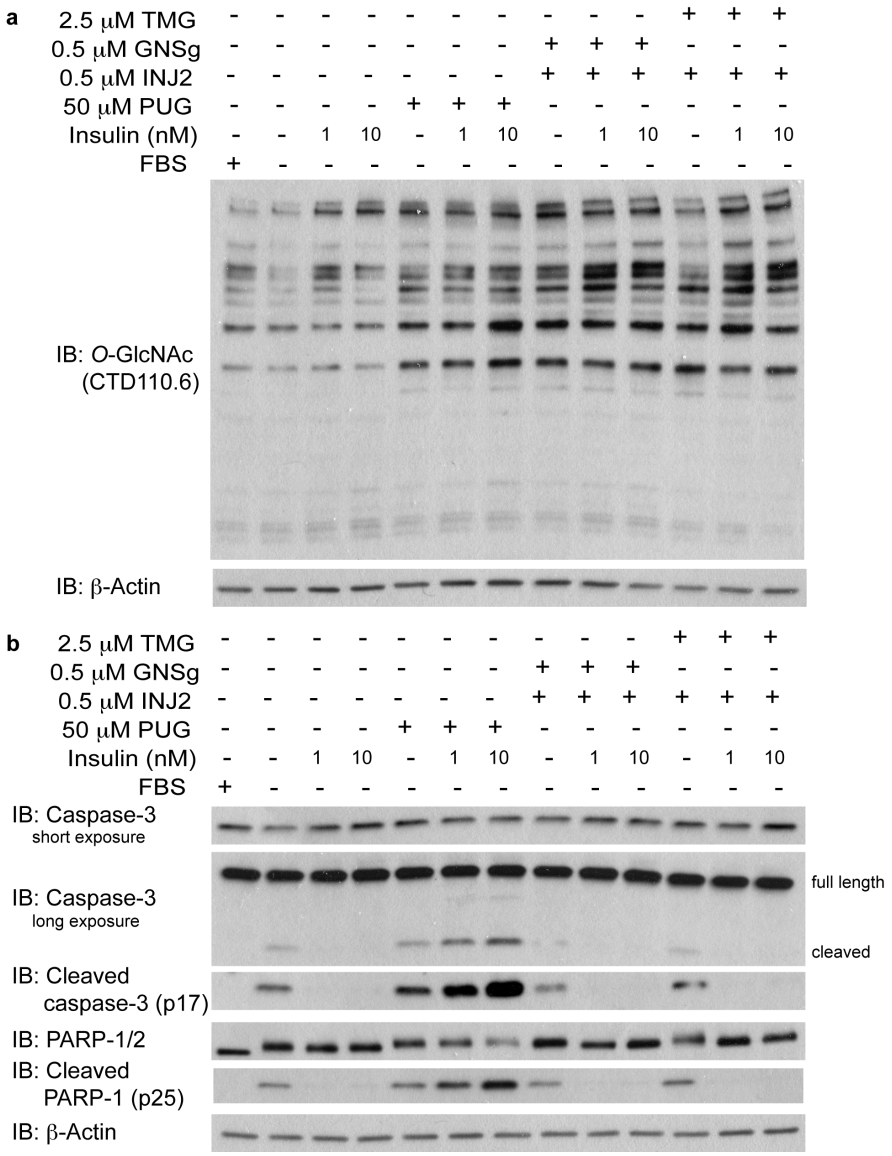

Figure 5-5. A combination of selective OGA and HexA/B inhibitors do not recapitulate PUGNAc action. (a) *O*-GlcNAc western blot of CHO-IR cells treated with 50 μM PUGNAc or the combination of INJ2 (0.5 μM) with GlcNAcstatin G (0.5 μM) or Thiamet-G (2.5 μM) in the absence or presence of insulin (1 nM or 10 nM). (b) Western blots of apoptotic markers, cleaved caspase-3 and cleaved PARP-1, and their full-length counterparts as well as β-actin on cell lysates treated with the same conditions as in (a).

CHAPTER 6

CONCLUSIONS

This dissertation summarizes various aspects of the *O*-GlcNAc research I experimented with, in which I aimed to expand the available tools for *O*-GlcNAc detection and dissect the impact of elevated global *O*-GlcNAc levels on the pro-survival role of insulin.

Chapter 1 of this dissertation provides a general view of the *O*-GlcNAc biology, including the serendipitous discovery of the intracellular *O*-GlcNAc in 1983 and further discussion of ongoing studies that unearth biological processes in which *O*-GlcNAc is found to play an indispensable role in fine-tuning the functionality of modified proteins.

Chapter 2 of this dissertation reviews extensively presently available tools for *O*-GlcNAc research, including a reference to some of the results presented in Chapter 3. Furthermore, I also provide insights for additional solutions and improvements to currently existing tools, including a novel *O*-GlcNAc site-mapping strategy that combines click chemistry and ammonia-based β-elimination (ABBE) for *O*-GlcNAc peptide enrichment and labeling.

Chapter 3 of this dissertation is a published manuscript that resulted from a collaborative project with Dr. Geert-Jan Boons's laboratory to characterize three pan-*O*-GlcNAc specific monoclonal IgG antibodies. I am one of the three co-first authors on this paper. To achieve the goal of this project, I established all the cell culture models and used these models for downstream immunoblotting, immunoprecipitation as well as

mass-spectrometry experiments. In addition, I contributed to the writing of the initial draft of this manuscript.

Chapter 4 of this dissertation is an invited review that I wrote for a special issue published in Molecular and Cellular Endocrinology, entitled “Molecular and Cellular Aspects of Adipocyte Development and Function”. In the article, I summarize findings from a series of studies focusing on the relationship between excessive flux through the hexosamine biosynthesis pathway, *O*-GlcNAc modification and insulin resistance in adipocytes. While the bulk of my research has nothing to do with adipocytes, the main project of my dissertation centers around *O*-GlcNAc modification and the insulin signaling pathway, specifically the pro-survival action of insulin. Insulin is an anabolic hormone secreted by pancreatic β cells to coordinate whole-body glucose homeostasis with three canonical insulin-responsive organs, liver, skeletal muscle, and adipose tissue. In non-canonical insulin responsive cells, such as central and peripheral neurons, insulin plays a major role in supporting cell survival by serving as an anti-apoptotic factor. Under insulin resistant conditions, the insulin-mediated signal transduction, regardless of the origin of the cells, is negatively affected.

Chapter 5 of this dissertation describes the impact of different OGA inhibitors on the pro-survival role of insulin. For many years, I had been working on dissecting the role of *O*-GlcNAc modification on the pro-survival role of insulin and pin-pointing the defect in insulin-mediated signal transduction using PUGNAc to elevate global *O*-GlcNAc levels. PUGNAc is the first established OGA inhibitor and has been widely used in the field since the late 90s. However, with the structural information available for human OGA homologs, several more selective and potent OGA inhibitors than PUGNAc have been synthesized. Starting from 2008, Vocadlo’s group initiated the debate of the role of elevation in global *O*-GlcNAc levels in negating insulin action. According to their findings, the PUGNAc-mediated inhibitory effect of insulin action might result from a

secondary target and that increased global *O*-GlcNAc levels are irrelevant in this process. Their conclusions are based on a series of *in vivo* and *in vitro* studies using two structurally distinct OGA specific inhibitors. Having spent many years treating cells with PUGNAc, I decided to compare PUGNAc and two other selective OGA inhibitors, GlcNAcstatin G and Thiamet-G. To my surprise, I discovered that some of my previous results were caused by the secondary effect of PUGNAc. Hence, this chapter covers my short journey in an attempt to determine the effect of PUGNAc in hampering insulin action. While the exact mechanism of how PUGNAc treatment leads to insulin resistance remain elusive, I have eliminated OGA and lysosomal HexA/B, the two most obvious PUGNAc targets, as the culprit. Further experiments are needed to fully explain this outcome of PUGNAc treatment.

In the past three decades, the status of *O*-GlcNAc modification in the glycobiology field has transformed from being “the simplest carbohydrate found in an unorthodox location” to “the most abundant glycan found on mammalian cells”. In 2008, Matsuura and colleagues presented the first evidence of extracellular *O*-GlcNAc modification on Drosophila Notch [1] and expanded the horizon of the *O*-GlcNAc biology. Although this extracellular *O*-GlcNAc modification is chemically identical and also cross-reacts with pan-*O*-GlcNAc specific antibodies that are used to detect intracellular *O*-GlcNAc modification, its transferase, Eogt, is localized in the lumen of endoplasmic reticulum and Eogt substrates are committed to the secretory pathway [2,3]. Furthermore, homozygous mutation in *eogt* has recently been reported to cause autosomal-recessive Adams-Oliver syndrome in affected individuals [4,5]. Given that both intracellular and extracellular O-GlcNAc modifications are posited directly downstream of the HBP, it would be interesting to further investigate whether there is any cross-talk between both type of O-GlcNAc modifications in response to the HBP flux.

References

1. Matsuura, A., et al., *O-linked N-acetylglucosamine is present on the extracellular domain of notch receptors.* J Biol Chem, 2008. **283**(51): p. 35486-95.
2. Sakaidani, Y., et al., *O-linked N-acetylglucosamine on extracellular protein domains mediates epithelial cell-matrix interactions.* Nat Commun, 2011. **2**: p. 583.
3. Sakaidani, Y., et al., *O-linked N-acetylglucosamine modification of mammalian Notch receptors by an atypical O-GlcNAc transferase Eogt1.* Biochem Biophys Res Commun, 2012. **419**(1): p. 14-9.
4. Shaheen, R., et al., *Mutations in EGOT confirm the genetic heterogeneity of autosomal-recessive Adams-Oliver syndrome.* Am J Hum Genet, 2013. **92**(4): p. 598-604.
5. Cohen, I., et al., *Autosomal recessive Adams-Oliver syndrome caused by homozygous mutation in EOGT, encoding an EGF domain-specific O-GlcNAc transferase.* Eur J Hum Genet, 2013. **in press**.

APPENDIX A

MANIPULATING GLOBAL *O*-GLCNAC LEVELS IN MAMMALIAN CELLS

This section demonstrates various ways to manipulate global *O*-GlcNAc levels in mammalian cells. After each treatment, global *O*-GlcNAc levels were detected using an anti-pan-*O*-GlcNAc specific antibody, CTD110.6, which is discussed in Chapter 2.

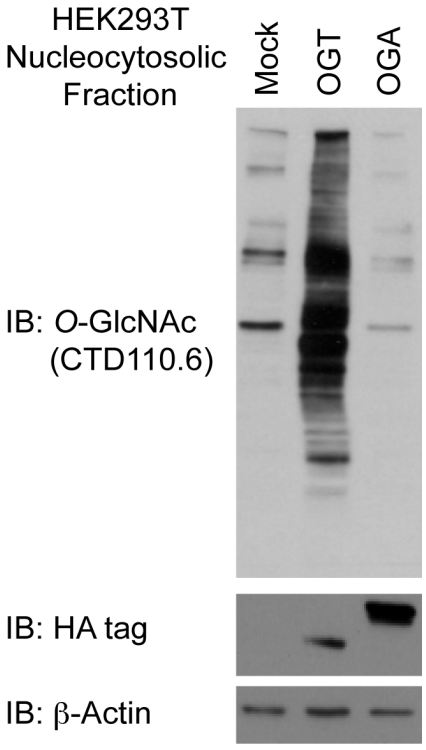

Figure A-1. Genetic manipulation of *O*-GlcNAc cycling enzymes. Detection of global *O*-GlcNAc levels from HEK293T cell lysates with mock, OGT or OGA overexpression using with a pan-*O*-GlcNAc specific monoclonal antibody, CTD110.6, reveals the change in glycosylation status in agreement the ectopically expression of the cycling enzymes. Western blot against HA-tag that is fused to the N-terminal of the cycling enzymes is shown to confirm their overexpression. Western blot against β-actin is also included as a loading control.

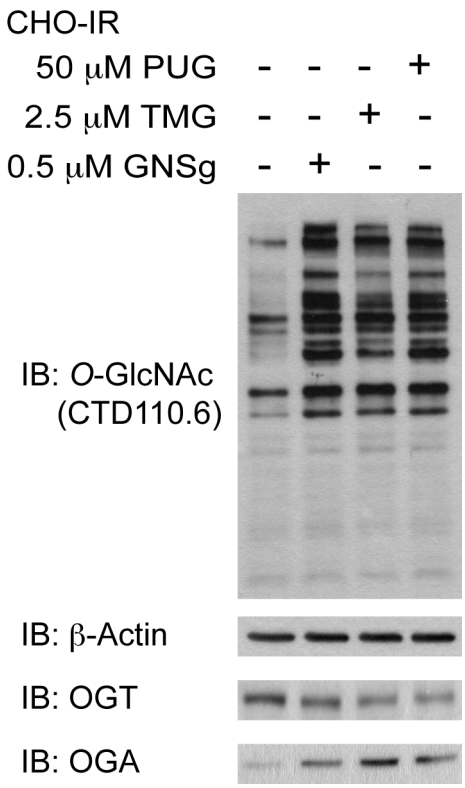

Figure A-2. Inhibiting OGA activity leads to an elevation in global *O*-GlcNAc levels. CHO-IR cells were treated with three OGA inhibitors GlcNAcstatin G, thiamet G and PUGNAc. Western blots against *O*-GlcNAc, OGT and OGA reveal that treating cells with OGA inhibitors not only lead to drastic increases in global O-GlcNAc levels and OGA protein level, but also a slight decrease in OGT protein level. Immunoblot against β-actin is also included as a loading control.

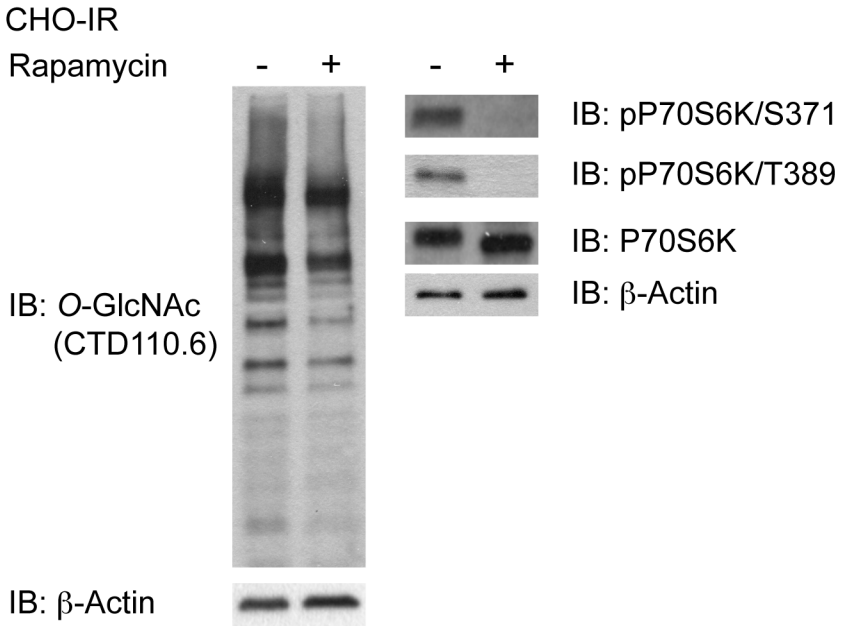

Figure A-3. Inhibition of mTOR leads to a reduction in global *O*-GlcNAc levels. CHO-IR lysates without or with rapamycin (a mTOR inhibitor) analyzing with CTD110.6 show a decrease in global *O*-GlcNAc proteins. Moreover, phosphorylation status on Ser371 and Thr389 of P70S6 kinase (P70S6K), two well-characterized mTOR substrates, was included to demonstrate the inhibitory effect of rapamycin on mTOR. Antibodies against β-actin and total P70S6K were included as loading controls.

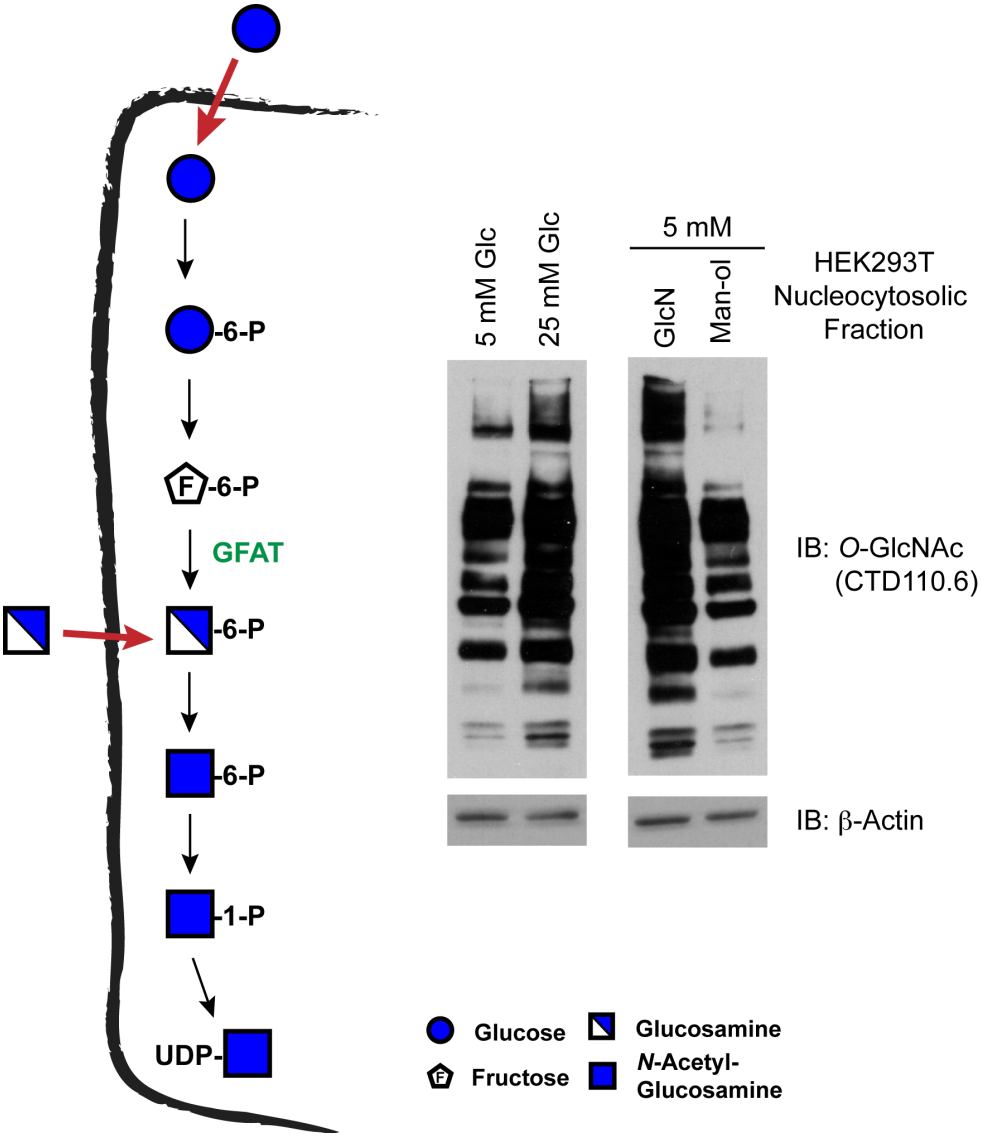

Figure A-4. Increasing the HBP flux leads to an elevation in global *O*-GlcNAc levels. HEK293T cells were treated with 5 mM (loq) or 20 mM (high) glucose (Glc) and (Right) 5 mM glucosamine (GlcN) or Mannitol (Man-ol, osmotic control). Glc and GlcN enter the HBP at different step. Western blots against *O*-GlcNAc reveal drastic increases in global *O*-GlcNAc levels upon high glucose and glucosamine treatments. Immunoblot against β-actin is also included as a loading control.

Experimental procedures

Cell cultures, transfection and cell treatments. CHO-IR cells (Chinese hamster ovary cells overexpressing human insulin receptor, a kind gift from Dr. Richard Roth, Standford University) were cultured in Ham's F-12 medium (Corning/Mediatech, Manassas, VA) supplemented with 10% of fetal bovine serum (Life Technologies/Invitrogen, Carlsbad, CA). HEK293T cells (human embryonic kidney 293 cells expressing SV40 T antigen, ATCC, Manassas, VA) were grown in DMEM/high glucose medfium (Mediatech) in the presence of 10% of fetal bovine serum (Invitrogen). Both cell lines were incubated in a 37°C incubator with 5% CO_2 under humidified atmosphere. To overexpress *O*-GlcNAc cycling enzymes, previously described constructs encoding either OGT or OGA from human (both carry N-terminal HA tag), pDEST26/HA-OGT and pDEST26/HA-OGA, were used. JetPRIME reagent (VWR International/Polyplus transfection, Radnor, PA) was used for transfection. Briefly, 4 µg of DNA was mixed with 500 µl of jetPRIME buffer followed by adding 10 µl of jetPRIME reagent. The DNA-jetPRIME mixture was incubated for 10 min at room temperature and added onto 100 mm plate of subconfluent cells (~80%) containing 6 ml of fresh culture medium. Culture medium was changed the next day and the cells were ready for harvesting 48 hours post-transfection. For OGA inhibitors treatment, GlcNAcstatin G (a kind gift from Dr. Daan van Aalten, University of Dundee), Thiamet G (Sigma-Aldrich, St. Louis MO) and PUGNAc (Toronto Research Chemicals, Ontario, Canada) were diluted in Hams' F-12/10% FBS to final concentrations of 0.5, 2.5 and 50 µM, respectively, and added onto CHO-IR cultures (in 35 mm dishes) for 20 h before harvesting. For mTOR inhibitor treatment, rapamycin (Sigma-Aldrich) was diluted in Hams' F-12/10% FBS to a final concentration of 100 nM, and added onto CHO-IR cultures (in 35 mm dishes) for 12 h prior to harvest.

Nuclear and cytosolic subcellular fractionation. After two PBS washes, CHO-IR cells were dislodged from the cell culture dishes using cell dissociation buffer (60 mM EDTA in PBS). Suspended cells were collected in a 50 ml centrifuge tube and pelleted by centrifugation (800 g for 8 min at 4°C). Cell pellets were resuspended in buffer A [10 mM HEPES, pH7.9, 10 mM KCl, 1.5 mM $MgCl_2$, protease inhibitor cocktail (set V, EDTA-free, from EMD Millipore/Calbiochem, Billerica, MA) and 1 μM PUGNAc]. Cell suspensions were transferred into a Potter-Elvehjem homogenizer, incubated on ice for 5 min and subjected to dounce homogenization for 20 times. The lysate was transferred into a microfuge tube and centrifuged at 300 g for 8 min at 4°C to separate crude nuclei (1° pellet) from cytoplasmic and additional organelles (1° supernatant). To obtain cytoplasmic fraction, 1° supernatant was further centrifuged at 18,000 g for 15 min at 4°C to remove insoluble organelles. To obtain pure nuclear fraction, 1° pellet containing crude nuclei was resuspended in buffer B (250 mM sucrose, 10 mM $MgCl_2$), layered over equal volume of buffer C (880 mM sucrose, 0.5 mM $MgCl_2$) and centrifuged at 2,800 g for 10 min at 4°C. To attain nuclear extract, 2° pellet was vortexed vigorously in the presence of buffer D (20 mM HEPES, pH7.9, 400 mM NaCl, 1% Triton X-100, protease inhibitor cocktail and 1 μM PUGNAc) and incubated on ice for 15 min, and subjected to centrifugation (18,000 g for 15 min at 4°C). For experiments where "nucleocytoplasmic fraction" is labeled, nuclear and cytoplasmic fractions were pooled into the same tubes after each fraction was obtained. Protein quantification was performed using Bradford-dye binding method according to Bio-Rad protein assay (Bio-Rad, Hercules, CA) with bovine serum albumin (BSA, from Thermo Fisher Scientific, Pittsburgh, PA) as a standard. Each sample was normalized to equal concentration, mixed with 5x Laemmli sample buffer (0.25 M Tris-HCl, pH6.8, 10% SDS, 50% glycerol, 0.5 M DTT and 1 mg/ml of bromophenol blue), heated at 80°C for 15 min, and stored at -20°C until further immunoblot analysis.

Whole cell lysate preparation. After treatments, cells were washed twice with ice-cold PBS, incubated on ice in the presence of TNS lysis buffer [10 mM Tris, pH 7.5, 150 mM NaCl, 1% Igepal CA-630, 0.1% SDS, 2 mM EDTA, 1 mM DTT, 10 μM PUGNAc, protease inhibitor cocktail and phosphatase inhibitor cocktail (set II, from Calbiochem)] for 15 min and scraped off the plates (100 μl per 35 mm dish). Cell lysates were collected in microfuge tubes and centrifuged at 18,000 g for 15 min at 4°C. Clarified supernatants were transferred into fresh tubes, protein concentration was quantified using Bio-Rad protein assay, protein samples were diluted in 5x Laemmli sample buffer as described in the earlier section.

Immunoblotting. Equal amount of total protein was resolved on Mini-PROTEAN TGX precast gels (7.5%, 4-15% or 4-20% gels, Bio-Rad, electrophoresis settings: 200 V, 30 to 35 min). The gels were subsequently electrotransferred (Trans-Blot SD semi-dry apparatus from Bio-Rad, electrotransfer settings: 20 V, 30 min) onto Immobilon-P membranes (0.45 μm, EMD Millipore) and the membranes were subjected to immunoblotting per standard procedure. For blocking, either 3% BSA or 5% milk prepared in TBST (25 mM Tris, pH 7.5, 150 mM NaCl and 0.1% Tween 20) was used. Primary antibodies and secondary antibodies conjugated to horseradish peroxidase (HRP) were used as the following dilutions: anti-OGT/H300 (Santa Cruz Biotechnology, Santa Cruz, CA, 1:1,000), anti-OGA/MGEA5 (Proteintech Group, Chicago, IL, 1:2,000), anti-*O*-GlcNAc/CTD110.6 (in-house ascites, 1:1,000), anti-HA tag (Abcam, Cambridge, MA, 1:10,000), β-actin (Sigma-Aldrich, 1:50,000), P70S6K (Santa Cruz Biotechnology, 1:1,000), pP70S6K/Ser371 (Cell Signaling Technology, Beverly, MA, 1:1,000), pP70S6K/Thr389 (Cell Signaling Technology, 1:1,000), sheep anti-mouse IgG-HRP (GE Healthcare, Piscataway, NJ, 1:20,000), goat anti-rabbit IgG-HRP (GE Healthcare, 1:20,000) and goat anti-mouse IgM (μ chain specific)-HRP (Sigma-Aldrich, 1:10,000). All primary antibodies were incubated at 4°C for overnight and secondary antibodies were

incubated at room temperature for 1 to 2 h. Membrane-bound HRP activities were detected using Pierce ECL western blotting substrate (Thermo Fisher Scientific/Pierce, Rockford, IL) and the chemiluminescence signal was captured on HyBlotCL films (Denville Scientific, Metuchen, NJ) for final visualizations. The antibody complexes from each membrane was either stripped off (0.2 M glycine, pH 2.5, room temperature for 1 h; when the primary antibody was generated in mouse) or inactivated (30% H_2O_2, 37°C for 15 min; when the primary antibody was originated from species other than mouse) and subjected to second round of blotting against β-actin as a loading control.

APPENDIX B

COLLABORATIONS

In addition to my dissertation project as described in the main chapters, I have made significant contributions leading to several publications during the course of my graduation study at the Complex Carbohydrate Research Center, the University of Georgia, Athens. Below, I include the title, my personal contribution and the abstract, respectively, for each of these publications. Complete versions of each publication are provided accompanying Appendix A.

DEFINING THE REGULATED SECRETED PROTEOME OF RODENT ADIPOCYTES UPON THE INDUCTION OF INSULIN RESISTANCE[1]

In response to Dr. Jae-Min Lim's request, I performed immunoblot analyses to demonstrate changes in global *O*-GlcNAc levels in different adipocyte models that Jae-Min used in his dissertation research focusing on secreted proteome and extracellular glycome.

Abstract

Insulin resistance defines the metabolic syndrome and precedes, as well is the hallmark of, type II diabetes. Adipocytes, besides being a major site for energy storage, are endocrine in nature and secrete a variety of proteins, adipocytokines (adipokines), that can modulate insulin sensitivity, inflammation, obesity, hypertension, food intake

[1] Lim, J.M., Sherling, D., Teo, C.F., Hausman, D.B., Lin, D., and Wells, L. 2008, *J. Proteome. Res.*, **7**, 1251-63.

(anorexigenic and orexigenic), and general energy homeostasis. Recent data demonstrates that increased intracellular glycosylation of proteins via *O*-GlcNAc can induce insulin resistance and that a rodent model with genetically elevated *O*-GlcNAc levels in muscle and fat displays hyperleptinemia. The link between *O*-GlcNAc levels, insulin resistance, and adipocytokine secretion is further explored here. First, with the use of immortalized and primary rodent adipocytes, the secreted proteome of differentiated adipocytes is more fully elucidated by the identification of 97 and 203 secreted proteins, respectively. Mapping of more than 80 *N*-linked glycosylation sites on adipocytokines from the cell lines further defines this proteome. Importantly, adipocytokines that are modulated when cells are shifted from insulin responsive to insulin resistant conditions are determined. By the use of two protocols for inducing insulin resistance, classical hyperglycemia with chronic insulin exposure and pharmacological elevation of *O*-GlcNAc levels, several proteins are identified that are regulated in a similar fashion under both conditions including HCNP, Quiescin Q6, Angiotensin, lipoprotein lipase, matrix metalloproteinase 2, and slit homologue 3. Detection of these potential prognostic/diagnostic biomarkers for metabolic syndrome, type II diabetes, and the resulting complications of both diseases further establishes the central role of the *O*-GlcNAc modification of intracellular proteins in the pathophysiology of these conditions.

O-GLCNAC MODIFICATIONS REGULATE CELL SURVIVAL AND EPIBOLY DURING ZEBRAFISH DEVELOPMENT[2]

I assisted Dr. Daniel Webster with most of the biochemistry studies in her dissertation work, and eventually was asked to perform all the biochemistry experiments

[2] Webster, D.M., Teo, C.F., Sun, Y., Wloga, D., Gay, S., Klonowski, K.D., Wells, L., and Dougan. S.T. 2009, *BMC Dev. Biol.*, **9**, 28.

reported in this paper upon her graduation. My scientific contributions include (1) performed immunoblot analyses to evaluate global *O*-GlcNAc level on zebrafish (zf) embryos that have been manipulated to overexpression or knock-down of zfOGTs, (2) overexpressed zfOGTs in *E. coli* and measured their enzymatic activities, and (3) demonstrated for the first time that OCT4, a key regulator of pluripotency in embryonic stem cells, is *O*-GlcNAc modified using the classical immunoprecipitation/western blot analyses. Meanwhile, I was participated in the writing of the corresponding sections in the manuscript.

Abstract

BACKGROUND: The post-translational addition of the monosaccharide *O*-linked beta-*N*-acetylglucosamine (*O*-GlcNAc) regulates the activity of a wide variety of nuclear and cytoplasmic proteins. The enzymes *O*-GlcNAc Transferase (Ogt) and *O*-GlcNAcase (Oga) catalyze, respectively, the attachment and removal of *O*-GlcNAc to target proteins. In adult mice, Ogt and Oga attenuate the response to insulin by modifying several components of the signal transduction pathway. Complete loss of ogt function, however, is lethal to mouse embryonic stem cells, suggesting that the enzyme has additional, unstudied roles in development. We have utilized zebrafish as a model to determine role of *O*-GlcNAc modifications in development. Zebrafish has two ogt genes, encoding six different enzymatic isoforms that are expressed maternally and zygotically. RESULTS: We manipulated *O*-GlcNAc levels in zebrafish embryos by overexpressing zebrafish ogt, human oga or by injecting morpholinos against ogt transcripts. Each of these treatments results in embryos with shortened body axes and reduced brains at 24 hpf. The embryos had 23% fewer cells than controls, and displayed increased rates of cell death as early as the mid-gastrula stages. An extensive marker analysis indicates that derivatives of three germ layers are reduced to variable extents, and the embryos are severely disorganized after gastrulation. Overexpression of Ogt and Oga delayed

epiboly and caused a severe disorganization of the microtubule and actin based cytoskeleton in the extra-embryonic yolk syncytial layer (YSL). The cytoskeletal defects resemble those previously reported for embryos lacking function of the Pou5f1/Oct4 transcription factor spiel ohne grenzen. Consistent with this, Pou5f1/Oct4 is modified by *O*-GlcNAc in human embryonic stem cells.

CONCLUSION: We conclude that *O*-GlcNAc modifications control the activity of proteins that regulate apoptosis and epiboly movements, but do not seem to regulate germ layer specification. *O*-GlcNAc modifies the transcription factor Spiel ohne grenzen/Pou5f1 and may regulate its activity.

COMBINING HIGH-ENERGY C-TRAP DISSOCIATION AND ELECTRON TRANSFER DISSOCIATION FOR PROTEIN *O*-GLCNAC MODIFICATION SITE ASSIGNMENT[3]

I prepared the proteomic sample used in this study and sent it to Dr. Rosa Viner at Thermo Fisher Scientific/Finnigan to be analyzed by the LTQ Orbitrap Velos ETD mass spectrometer.

Abstract

Mass spectrometry-based studies of proteins that are post-translationally modified by *O*-linked β-N-acetylglucosamine (*O*-GlcNAc) are challenged in effectively identifying the sites of modification while simultaneously sequencing the peptides. Here we tested the hypothesis that a combination of high-energy C-trap dissociation (HCD) and electron transfer dissociation (ETD) could specifically target the *O*-GlcNAc modified peptides and elucidate the amino acid sequence while preserving the attached GlcNAc residue for accurate site assignment. By taking advantage of the recently characterized *O*-GlcNAc-specific IgG monoclonal antibodies and the combination of HCD and ETD fragmentation

[3] Zhao, P., Viner, R., Teo, C.F., Boons, G.J., Horn, D., and Wells, L. 2011, *J. Proteome. Res*., **10(9)**, 4088-4104.

.

techniques, *O*-GlcNAc modified proteins were enriched from HEK293T cells and subsequently characterized using the LTQ Orbitrap Velos ETD (Thermo Fisher Scientific) mass spectrometer. In our data set, 83 sites of *O*-GlcNAc modification are reported with high confidence confirming that the HCD/ETD combined approach is amenable to the detection and site assignment of *O*-GlcNAc modified peptides. Realizing HCD triggered ETD fragmentation on a linear ion trap/Orbitrap platform for more in-depth analysis and application of this technique to other post-translationally modified proteins are currently underway. Furthermore, this report illustrates that the *O*-GlcNAc transferase appears to demonstrate promiscuity with regards to the hydroxyl-containing amino acid modified in short stretches of primary sequence of the glycosylated polypeptides.